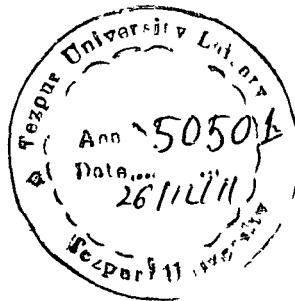


50501

CENTRAL  
TEZPUR UNI.  
Accession No. T176  
Date 28/02/13



# **DEVELOPMENT OF POLYESTER NANOCOMPOSITES**

**A THESIS SUBMITTED IN PARTIAL FULFILLMENT OF THE  
REQUIREMENTS FOR THE DEGREE OF  
Doctor of Philosophy**

By  
**Uday Konwar**

Registration Number 007 of 2010



**School of Science & Technology  
Department of Chemical Sciences  
Tezpur University  
Napaam 784028  
Assam, India**



*Dedicated to my*

*Beloved parents*

# ABSTRACT

---

## ***Background***

The polymer nanocomposites have attracted considerable attention to the researchers and industrialists due to their many new and greatly improved desirable properties over the pristine polymer by proper incorporation of a small fraction of suitable nanofillers into the polymer system. Also, these improvements are achieved without impairing the fascinating properties such as light weight characteristic, flexibility, transparency etc. of the pristine polymers. Although, the research on polymer nanocomposites have progressed considerably fast within a short span of time by the help of nanoscience and nanotechnology, however, researchers are still in search of the answers of some fundamental questions that are yet to decipher.

Again, among the different types of polymers, polyester is one of the attractive polymers with high significance and interest, demanding the popularity in a diversified field of applications such as coatings, paints, varnish, fibers, composites, biomaterials and many other niches. The factors behind the popularity of polyester thermoset are as follows. It is a single-pack system i.e. stable in the 'can' for a long time. The raw materials and processing costs are relatively low compared to other synthetic resins. It possesses high order of durability, excellent pigment dispersion quality, high gloss accompanied by exceptional toughness and adhesion. It is compatible with many other resins that are used in surface coating industry. Its structure and properties can be tailored by varying the selection of raw materials depending upon the cost and availability.

Further, the polymer science has forward a significant growth in the field of non-linear highly branched polymers over the last two decades. These polymers possess unique architectural features and have large number of surface functionalities with low viscosity. The highly branched polymers have the feasibilities of industrial production due to their easy preparative process. Thus the utilization of highly branched polyesters as the matrices for preparation of different polymer nanocomposites is worth thinking and can be investigated for the same.

Again the uses of renewable natural resources to replace petroleum derived ones are increasing continuously in different industrial fields including polymers. This is due to awareness to the environmental and ecological issues, such as volatile organic compound (VOC) emissions and recycling or waste disposal problems, spiraling rise in



prices and high rate of depletion of the stocks. In this context, vegetable oil is one of such renewable resources which possess excellent properties for utilization in the production of different polymeric materials such as polyester, epoxy, poly(ester amide), polyurethane etc. Vegetable oils can play an important role not only for edible purposes but for many industrial applications too. These oils have a number of advantages like physical and chemical stability, aptitude to facile chemical modification, reduced toxicity, reduced risk for handling and transportation, possibility of recycling, renewability and biodegradability, at the same time available in large quantities in relatively low and stable prices, and are susceptible to agricultural diversification and environmentally benign in nature.

A number of seed oils are used in the synthesis of various polymeric materials. Some of the major seed oils used traditionally for preparation of polyester resins are linseed, castor, soybean, sunflower, safflower, tung, coconut etc. Non-traditional oils such as rubber seed oil, neem oil, karanja oil, jatropha seed oil, kamala seed oil, lesquerella oil, melon seed oil, apricot oil, *Annona squamosa*, African mahogany seed oil, African locust bean seed oil etc. are also used for the same purpose. *Mesua ferrea* L. is a plant available abundantly in the countries such as India, Sri Lanka, Bangladesh, Nepal, Indo-China (South East Asia), Malay Peninsula etc. This is non-drying oil and the fatty acid composition (52.3% oleic and 22.3% linoleic acids as unsaturated fatty acids and 15.9% palmitic and 9.5% stearic acids as saturated fatty acids) insisted to utilize it as raw material for the production of different industrial polymers.

### ***Scope and Objectives of the Present Investigation***

Although *Mesua ferrea* L. seed oil has tremendous potential as renewable resource based feed stock but only a few reports described its utilization in the fields of medicine, biodiesel and resinous polymeric products such as polyester, polyurethane, poly(ester amide), epoxy and recently developed thermoplastic hyperbranched polyurethane. Thus, there is no study on this oil for the development of highly branched polyester resins. Hence, the following questions may arise in this area.

- (i) Whether this oil can be used for the preparation of highly branched polyesters?
- (ii) Whether the performance characteristics of the polyester can be improved by any physical or chemical means?
- (iii) Whether the pristine polyester or modified polyester can be utilized as the matrix for the preparation of different types of nanocomposites?

(iv) Whether the incorporation of different nanofillers into the polyester matrix can lead to the genesis of advanced materials?

Under this background the main objectives of the present investigation are as follows:

- (i) To synthesize, characterize and evaluate various properties of *Mesua ferrea* L. seed oil based polyesters.
- (ii) To improve the performance of the vegetable oil based polyester by blending with other suitable commercial polymer(s).
- (iii) To improve the performance characteristics of the polyester by nanocomposites formation.
- (iv) To utilize various nanofillers for formation of different nanocomposites to achieve the desirable levels of properties.
- (v) To utilize the prepared nanocomposites as advanced materials in the field of surface coating, biodegradable biomaterial, antimicrobial materials etc.
- (vi) To use *Mesua ferrea* L. seed oil modified highly branched polyester resin for the preparation of an industrial paint.

### ***Plan of Work***

To fulfill the above objectives, the following plans of work are adopted. The plans of work for the proposed research are as follows.

- i) A state-of-art literature survey will be conducted on the field of vegetable oil based polyesters and their nanocomposites.
- ii) The highly branched polyester from vegetable oil will be synthesized by the help of literature reports.
- iii) The synthesized polyesters will be characterized by different analytical and spectroscopic techniques such as determination of acid value, saponification value, hydroxyl value, FTIR, NMR, TGA etc.
- iv) Polyester nanocomposites will be prepared by the *ex-situ* technique using vegetable oil based polyester and organophilic nanoclay/metal nanoparticles/CNT etc.
- v) The prepared nanocomposites will be characterized by UV, FTIR, XRD, TEM, SEM, rheometer etc. to study the structure, morphology and rheological behaviors.
- vi) The performance characteristics of the characterized nanocomposites will be investigated by determination of mechanical properties like tensile strength,

elongation at break, impact resistance etc.; thermal properties; chemical resistance in different chemical media etc. The special properties like biodegradation, antimicrobial test, cytocompatibility etc. will be conducted depending on requirement.

vii) The performance characteristics of the nanocomposite will be optimized by manipulation of composition of raw materials, processing parameters etc. to find out the best nanocomposite in each category.

vii) *Mesua ferrea* L. seed oil modified highly branched polyester resin will be utilized for the preparation of an industrial paint.

### ***The thesis***

**Chapter one** deals with the general introduction on polyester nanocomposites. A brief review on vegetable oil based polyester nanocomposites with special emphasis to polyester resins from vegetable oils and their nanocomposites, their importance, history, general techniques for preparation, characterization, properties and applications have been described in this chapter. This chapter also focuses the scopes and objectives along with the plans of work and methodologies of the present investigation.

**Chapter two** reports the synthesis, characterization and properties evaluation of *Mesua ferrea* L. seed oil based three highly branched polyesters using polyfunctional carboxyl or polyol compounds like trimellitic anhydride (TMA), 2,2-bis(hydroxymethyl) propionic acid (bis-MPA) and hyperbranched polyol along with the other conventional anhydrides. The linear analog of the highly branched polyester was also synthesized without tri/multifunctional compounds for comparison purpose. The synthesized resins were characterized by measurement of physical properties like acid value, iodine value, saponification value, hydroxyl value, drying time, viscosity etc. and other characterization techniques such as FTIR and <sup>1</sup>H NMR spectroscopy. All the synthesized resins were cured at different temperatures for specified period of time followed by post-curing for all the cases. Various performance characteristics of the cured polyester films such as scratch hardness, gloss, impact resistance, tensile strength, elongation at break (%) and chemical resistance in different media were determined. Thermal stabilities of the synthesized polyesters were studied by TGA technique. The chapter concludes that *Mesua ferrea* L. seed oil based polyester resins can be utilized for surface coating applications like other vegetable oil based resins. Also, they could be useful as binders for anticorrosive and non-polluting surface

coatings. Among the four polyester resins prepared from *Mesua ferrea* L. seed oil, the bis-MPA based polyester resin was found to show better properties than the others.

**Chapter three** describes the modification of bis-MPA based highly branched polyester resin by different methods such as blending with vegetable oil based epoxy, neutralization with triethylamine to form water dispersible polyester and grafting with methyl methacrylate. The characterizations and properties of these modified highly branched polyesters are also discussed in this chapter. FTIR and NMR spectroscopic techniques were utilized to characterize the modified highly branched polyesters. The various performance characteristics like tensile strength, impact resistance, hardness, thermal stability and chemical resistance in different media showed improvements over the pristine highly branched polyester resin.

**Chapter four** reports the formation of nanocomposites of organically modified montmorillonite (OMMT) and unmodified bentonite and the highly branched polyester resins of bis-MPA and hyperbranched polyol, and also all the modified highly branched polyester resins as matrices through an *ex-situ* technique. The formation of the nanocomposites was characterized by FTIR, XRD, SEM and TEM analyses. The thermal and rheological properties of the nanocomposites were also studied. The mechanical properties such as tensile strength, impact resistance, scratch hardness etc. were much improved compared to the pristine matrix system in each case. The study showed the high potentiality of the nanocomposites as advanced coating materials.

**Chapter five** demonstrates the suitability of the bis-MPA based polyester resin/clay nanocomposites as the matrix for silver nanoparticles. The formation and distribution of the silver nanoparticles were examined by FTIR, XRD, SEM and TEM analyses. The mechanical properties such as tensile strength and impact resistance were found to be improved without affecting the flexibility and elongation at break value of the pristine highly branched polyester. Excellent improvements in thermal properties were obtained in the prepared nanocomposites. The nanocomposite exhibited remarkable antimicrobial activities against Gram negative bacteria (*Escherichia coli* and *Pseudomonas aeruginosa*). Thus this chapter directed the high potential of the bis-MPA based highly branched polyester/clay silver nanocomposites as antimicrobial surface coating materials.

**Chapter six** includes the effect of insertion of modified MWCNTs in the highly branched polyester matrix of bis-MPA on various properties like mechanical, thermal, biodegradation and cytocompatibility. The homogeneous distribution of the MWCNTs

in the matrix was confirmed by FTIR, XRD, SEM and TEM analyses. The mechanical and thermal properties were much improved after nanocomposite formation compared to the pristine resin system. The biocompatibility nature in terms of non-toxicity at the cellular level and biodegradability of the nanocomposites indicate their high potentiality in biomedical applications.

**Chapter seven** reports the application of *Mesua ferrea* L. seed oil based bis-MPA containing highly branched polyester modified epoxy resin as binder material for a low volatile organic compound (VOC) containing high solid paint formulation. The highly branched low molecular weight polyester resin acts as the reactive diluent of the epoxy resin which satisfies to reduce VOC emission and produces high solid paint system. The preparation, characterization and properties of this paint are described in this chapter. Maximum part of the work was carried out in a paint industry using their set up to establish the commercial viability of the resins. The results indicate that these resins could be used for low cost deep color paints. Various parameters that reflect the performance characteristics of the test paints were found to be comparable with the standard industrial paint. The study reveals their perspectives for successful utilization as high performance paints.

**Chapter eight**, the last chapter of the thesis includes the concluding remarks, highlights of the findings and future scopes of the present investigation. The major achievements of the present investigation are as follows-

- (i) A low cost non-edible vegetable oil, *Mesua ferrea* L. seed oil was successfully utilized for the first time to prepare highly branched polyesters.
- (ii) The synthesized highly branched polyesters were successfully characterized by the conventional analytical and spectroscopic techniques.
- (iii) The modification of the highly branched polyester resin by different methods such as blending with vegetable oil based epoxy, neutralization with triethylamine to form water reducible polyester and grafting with methyl methacrylate significantly improved the properties especially mechanical properties, thermal stability and chemical resistance.
- (iv) The nanocomposites of highly branched polyester resins, the modified highly branched polyester resins and nanoclay (OMMT and bentonite) were successfully prepared by *ex-situ* techniques. The prepared nanocomposites exhibited noticeable improvements in performance characteristics.

(v) The bis-MPA based highly branched polyester is good matrix for the preparation of silver nanocomposites. The well dispersed and highly stable silver nanoparticles based nanocomposites showed better properties than the pristine system. The silver nanocomposites also exhibited adequate antimicrobial property.

(vi) The bis-MPA based highly branched polyester/MWCNTs nanocomposites showed excellent improvements in the properties like mechanical, thermal and rheological behavior. They also showed higher biodegradation and more cytocompatibility compared to the pristine system.

(vii) The different nanocomposites have the high potential to be used as advanced surface coating materials, highly thermo-stable materials, biodegradable biomaterials.

(viii) The bis-MPA based highly branched polyester showed high potentiality to be used as binder for epoxy based industrial paint.

## DECLARATION

---

I do hereby declare that the thesis entitled "*Development of Polyester Nanocomposites*", submitted to the Department of Chemical Sciences, Tezpur University, is a record of original research work carried out by me. All sources of assistance have been assigned due acknowledgment. I also declare that neither this work as a whole nor a part of it has been submitted to any other University or Institute for any other degree, diploma or award.

Place: Tezpur University, Tezpur

*Uday Konwar*  
(Uday Konwar)

Date: 12/04/11



**TEZPUR UNIVERSITY**

Ph: 03712-267004

(A Central University established by an Act of Parliament) 03712-267005

NAPAAM, TEZPUR-784028

Fax: 03712-267006

DISTRICT: SONITPUR:: ASSAM:: INDIA

03712-267005

E-mail: [nkarak@tezu.ernet.in](mailto:nkarak@tezu.ernet.in)

---

## CERTIFICATE

This is to certify that the thesis entitled "*Development of Polyester Nanocomposites*" submitted to the Tezpur University in the Department of Chemical Sciences under the School of Science & Technology, in partial fulfillment for the award of the Degree of Doctor of Philosophy in Science, is a record of research work carried out by Uday Konwar under my personal supervision and guidance.

All helps received by him from various sources have been duly acknowledged.

No part of this thesis has been reproduced elsewhere for award of any other degree.

Place: Tezpur University

Date:

*Niranjan Karak*  
(Dr. Niranjan Karak) 12/04/11

Professor & Head

Department of Chemical Sciences  
School of Science & Technology





**TEZPUR UNIVERSITY**

Ph: 03712-267004

(A Central University established by an Act of Parliament) 03712-267005

NAPAAM, TEZPUR-784028

Fax: 03712-267006

DISTRICT: SONITPUR:: ASSAM :: INDIA

03712-267005

---

## **CERTIFICATE**

This is to certify that the thesis entitled "*Development of Polyester Nanocomposites*" submitted to the Tezpur University in the Department of Chemical Sciences under the School of Science and Technology, in partial fulfillment for the award of the Degree of Doctor of Philosophy in Science, has been examined by us on ..... and found to be satisfactory.

The committee recommends for the award of the degree of Doctor of Philosophy.

Principal Supervisor

External Examiner

Date:

Date:

# PREFACE

---

The development of polymer nanocomposites has opened up a new avenue for advanced polymeric materials and leads to the genesis of a new era in Material Science. Again, the petroleum based raw materials are replaced by the renewable resource based feed stocks in the production of different polymers are attracting the researchers all around. *Mesua ferrea* L. seed oil is one of such renewable resources with ample potential to design various types of industrial polymers. The hyperbranched polymers with novel and inimitable architectural features and high surface functionalities with low viscosity and high solubility have also attracted a considerable attention.

Thus the foremost objective of this thesis is to utilize this vegetable oil in the development of hyperbranched polyesters and their different nanocomposites. The thesis describes the synthesis, characterization, property and application of *Mesua ferrea* L. seed oil based highly branched polyesters. Attempts have also been made to modify the highly branched polyesters by different approaches to improve their performance characteristics. The properties of the pristine highly branched polyester and their modified polyesters were further enhanced by formation of clay nanocomposites by using *ex-situ* techniques. One of these highly branched polyesters was also exploited as the matrix for different nanofillers such as multiwalled carbon nanotubes and silver nanoparticles. The prepared nanocomposites exhibited high potential to be applicable in a spectrum of applications such as advanced thin film materials, highly thermo-stable materials, antimicrobial surface coating materials and biodegradable biomaterials. This highly branched polyester was also utilized as the binder as well as reactive diluent for an epoxy resin to prepare an industrial paint.

Date: 12/04/2011

Place: Napaam, Tezpur

Uday Konwar  
(Uday Konwar)

# CONTENTS

---

<i>Content</i>	<i>Page No.</i>
Abstract	i
Declaration	viii
Certificate of Supervisor	ix
Certificate of Examiners	x
Preface	xi
Contents	xii
List of Abbreviations and Symbols	xix
List of Tables	xxi
List of Figures	xxii
List of Schemes	xxvi
Acknowledgement	xxvii

## CHAPTER 1

### General Introduction

1.1. Introduction	1
1.2. Background	3
1.3. Polymer Nanocomposites	4
1.3.1. Materials	5
1.3.1.1 Polyester	5
1.3.1.2 Nanofillers	11
1.3.2. Methods	15
1.3.2.1. Solution Technique	15
1.3.2.2. <i>In-situ</i> Polymerization Technique	16
1.3.2.3. Melt Mixing Technique	17
1.3.2.4. Template Synthesis	18
1.3.2.5. Sol-Gel Technique	18
1.3.3. Characterization	19
1.3.3.1. Polyester Matrix	19
1.3.3.2. Nanocomposites	21
1.3.4. Properties	25
1.3.4.1. Mechanical	25

1.3.4.2. Barrier	27
1.3.4.3. Thermal	28
1.3.4.4. Flame Retardancy	28
1.3.4.5. Rheological	29
1.3.4.6. Optical	30
1.3.4.7. Electrical	30
1.3.4.8. Biodegradation	30
1.3.5. Applications	31
1.4. Vegetable Oil Based Highly Branched Polyester Nanocomposites:	34
A Short Review	
1.4.1. Introduction	34
1.4.2. Background	35
1.4.3. Materials	35
1.4.3.1. Vegetable Oils	36
1.4.3.2. Preparation of Polyester from Vegetable Oils	41
1.4.3.3. Preparation of Hyperbranched Polyester from Vegetable Oil	44
1.4.3.4. Preparation of Nanocomposites from Vegetable Oil	45
1.4.4. Characterization	46
1.4.5. Properties	48
1.4.6. Applications	50
1.5. Scope and Objectives of the Present Investigation	51
1.6. Plan of Work	52
References	

## **CHAPTER 2**

### **Synthesis, Characterization and Properties of *Mesua ferrea* L. Seed Oil Based Polyester Resins**

2.1. Introduction	66
2.2. Experimental	67
2.2.1. Materials	67
2.2.2. Instruments and Methods	71
2.2.2.1. Synthesis of <i>Mesua ferrea</i> L. Seed Oil Based Polyester Resins	73
2.2.2.2. Curing of TMAP Resins	75
2.2.2.3. Curing of HBPE, PE and LPE Resins	76

2.3. Results and Discussion	76
2.3.1 Resinification of TMAP Resins	76
2.3.2. Resinification of HBPE, PE and LPE Resins	80
2.3.3. Characterization of the Polyester Resins	82
2.3.3.1. Physical Properties	82
2.3.3.2. FTIR and <sup>1</sup> H NMR Spectroscopic Studies	83
2.3.4. Rheological Behaviors	87
2.3.5. Curing Study for the Polyester Resins	88
2.3.6. Coating Performance	89
2.3.7. Chemical Resistance	89
2.4. Conclusions	90
References	

## **CHAPTER 3**

### **Modification of bis-MPA Based Highly Branched Polyester Resin**

3.1. Introduction	93
3.2. Experimental	95
3.2.1. Materials	96
3.2.2. Instruments and Methods	97
3.2.2.1. Preparation of HBPE	98
3.2.2.2. Preparation of Vegetable Oil Based Epoxy Resin	98
3.2.2.3. Modification of HBPE by Blending with Epoxy Resin	98
3.2.2.4. Modification of HBPE by Triethylamine (Water Dispersible HBPE)	99
3.2.2.5. Preparation of Water Dispersible HBPE Films	99
3.2.2.6. Modification of HBPE by Grafting with Methylmethacrylate	99
3.2.2.7. Curing of Acrylate Modified HBPE	100
3.3. Results and Discussion	100
3.3.1. Modification of HBPE	100
3.3.1.1. Formation of HBPE/Epoxy Blends	100
3.3.1.2. Preparation of Water Dispersible HBPE	101
3.3.1.3. Preparation of Acrylate Modified HBPE	101
3.3.2. FTIR Study for Resins and Blends	102
3.3.2.1. HBPE/Epoxy Blends	102

3.3.2.2. Water Dispersible HBPE	103
3.3.2.3. Acrylate Modified HBPE	103
3.3.3. NMR Study for Acrylate Modified HBPE	103
3.3.4. Curing Study	104
3.3.4.1. HBPE/Epoxy Blends	104
3.3.4.2. Water Dispersible HBPE	105
3.3.5. Performance Study	105
3.3.6. Chemical Resistance	107
3.3.7. Thermal Properties	108
3.4. Conclusions	110
References	

## CHAPTER 4

### *Mesua ferrea* L. Seed Oil Based Polyester/Clay Nanocomposites

4.1. Introduction	114
4.2. Experimental	115
4.2.1. Materials	115
4.2.2. Instruments and Methods	116
4.2.2.1. Preparation of HBPE and Its Nanocomposites	117
4.2.2.2. Preparation of LPE and Its Nanocomposites	117
4.2.2.3. Preparation of PE and Its Nanocomposites	118
4.2.2.4. Preparation of HBPE/Epoxy Blend and Its Nanocomposites	118
4.2.2.5. Preparation of Water Dispersible HBPE and Its Nanocomposites	118
4.2.2.6. Preparation of Acrylate Modified HBPE and Its Nanocomposites	119
4.2.2.7. Bacterial Media	119
4.2.2.8. Bacterial Strains	119
4.3. Results and Discussion	120
4.3.1. Formation of Nanocomposites	120
4.3.2. Characterization of Nanocomposites	122
4.3.2.1. FTIR Study	122
4.3.2.2. XRD Study	126
4.3.2.3. SEM Study	130
4.3.2.4. TEM Study	133
4.3.3. Rheological Behaviors	137

4.3.4. Curing Studies of the Nanocomposites	143
4.3.5. Performance Characteristics of the Nanocomposites	144
4.3.6. Thermal Properties	150
4.3.7. Chemical Resistance	154
4.3.8. Biodegradation Studies	156
4.4. Conclusions	160
References	

## **CHAPTER 5**

### **HBPE/Clay Silver Nanocomposites**

5.1. Introduction	165
5.2. Experimental	167
5.2.1. Materials	167
5.2.2. Instruments and Methods	167
5.2.2.1. Preparation of HBPE/Clay Nanocomposites	168
5.2.2.2. Preparation of Silver Nanocomposites	168
5.2.2.3. Preparation of Nanocomposite Films	168
5.2.2.4. Preparation of Culture Media	169
5.2.2.5. Antibacterial Assessment	169
5.3. Results and Discussion	170
5.3.1. Formation of HBPE/Clay Silver Nanocomposites	170
5.3.2. Characterization of the Nanocomposites	170
5.3.2.1. UV-Vis Spectroscopy	170
5.3.2.2. XRD Study	172
5.3.2.3. SEM Study	173
5.3.2.4. TEM Study	173
5.3.2.5. FTIR Study	174
5.3.3. Rheological Behaviors	175
5.3.4. Curing Studies of HBPE/Clay Silver Nanocomposites	176
5.3.5. Performance Characteristics	176
5.3.6. Thermal Properties	178
5.3.7. Antibacterial Properties	179
5.4. Conclusions	181
References	

## **CHAPTER 6**

### ***Mesua ferrea* L. Seed Oil Based HBPE/MWCNTs Nanocomposites**

6.1. Introduction	185
6.2. Experimental	186
6.2.1. Materials	186
6.2.2. Instruments and Methods	187
6.2.2.1. Purification and Modification of MWCNTs	188
6.2.2.2. Preparation of HBPE/MWCNTs Nanocomposites	188
6.2.2.3. Fabrication of Nanocomposites into Thin Films and Their Curing	188
6.2.2.4. Preparation of Bacterial Culture Media	189
6.2.2.5. Bacterial Strains	189
6.2.2.6. Cytotoxicity by Hemolytic Activity Assay	189
6.3. Results and Discussion	190
6.3.1. Purification and Modification of MWCNTs	190
6.3.2. Preparation of HBPE/MWCNTs Nanocomposites	191
6.3.3. Solvent Dispersibility	191
6.3.4. Characterization of Nanocomposites	192
6.3.4.1. FTIR Study	192
6.3.4.2. XRD Study	193
6.3.4.3. SEM Study	194
6.3.4.4. TEM Study	195
6.3.5. Performance Characteristics of the Nanocomposites	195
6.3.6. Thermal Properties	197
6.3.7. Biodegradation Study	198
6.3.8. Cytotoxicity Study	200
6.4. Conclusions	201
References	

## **CHAPTER 7**

### **HBPE Modified Epoxy Based Industrial Paint**

7.1. Introduction	205
7.2. Experimental	207
7.2.1. Materials	207
7.2.2. Instruments and Methods	207



7.2.2.1. Preparation of HBPE	208
7.2.2.2. Preparation of Paints	208
7.2.2.3. Preparation of Test Panels	209
7.3. Results and Discussion	210
7.3.1. Paint Preparation	210
7.3.2. Physical Properties	210
7.3.3. Rheological Behaviors	211
7.3.4. Morphological Study	212
7.3.5. Performance Characteristics	213
7.3.6. Thermal Study	216
7.4. Conclusions	217
References	

## **CHAPTER 8**

### **Conclusions and Future Directions**

8.1. Summary and Conclusions	220
8.2. Future Directions	222

<b>List of Publications</b>	223
-----------------------------	-----

## LIST OF ABBREVIATIONS AND SYMBOLS

---

$A_w$	atomic weight
b.p.	boiling point
$\text{cm}^3$	cubic centimeter
cm	centimeter(s)
$^{\circ}\text{C}$	degree centigrade
DSC	differential scanning calorimetry
FTIR	Fourier transform infrared
$F_w$	Formula weight
g	gram(s)
GPC	gel permeation chromatography
h	hour(s)
K	Kelvin
kN	kilo-Newton
kV	kilo-volt
L	liter(s)
lb	pound(s)
m	meter(s)
mA	mili ampere
min	minute(s)
mL	mili liter(s)
mm	mili meter(s)
mol	mole
m.p.	melting point
$M_w$	molecular weight
N	Newton
NMR	nuclear magnetic resonance
nm	nano meter(s)
OD	optical density
OMMT	organically modified montmorillonite
Pa	Pascal
Pas	Pascal second
phr	parts per hundred

ppm	parts per million
RBC	red blood cell
rpm	rotation per minute
s	second(s)
SEM	scanning electron microscope
TEM	transmission electron microscopy
$T_{\text{end}}$	endset of thermal degradation temperature
$T_g$	glass transition temperature
$T_i$	initial thermal degradation temperature
$T_{\text{on}}$	onset of thermal degradation temperature
TGA	thermogravimetric analysis
TMS	tetramethyl silane
UTM	universal testing machine
UV	ultraviolet
v	volume
wt.	weight
XRD	X-ray diffraction
$\mu\text{g}$	micro gram(s)
$\mu\text{m}$	micro meter(s)
$\mu\text{M}$	micro molar(s)
$\mu\text{L}$	micro liter(s)
%	percentage
$\eta_{\text{inh}}$	inherent viscosity
$\lambda_{\text{max}}$	wavelength maximum
$\theta$	scattering angle

# LIST OF TABLES

---

- Table 1.1: Different polyhydric alcohols with their structures and a few physical properties
- Table 1.2: Different polybasic acids with their physical properties
- Table 1.3: Chemical structure and physical properties of a few fatty acids present in vegetable oils
- Table 1.4: A few important vegetable oils used to prepare polyester with their physical properties and major fatty acids contents
- Table 2.1: Some technical specifications of epoxy resin and hardener
- Table 2.2: Composition of the reactants
- Table 2.3: Extent of reaction ( $p$ ), average degree of polymerization ( $DP$ ) and second order rate constant [ $k$ ] at the onset of gelation ( $t_{onset}$ )
- Table 2.4: Physical properties of polyester resins
- Table 2.5: Coating performance characteristics of the polyester resins
- Table 2.6: Chemical resistance of the polyester resin films
- Table 3.1: Technical specifications of MF resin
- Table 3.2: Composition of HBPE/epoxy resin blends
- Table 3.3: Formulation for water dispersible HBPE film
- Table 3.4: The main FTIR bands and the corresponding functional groups of epoxy resin
- Table 3.5: The performance characteristics of HBPE/epoxy blends, water dispersible HBPE and acrylate modified HBPE films
- Table 3.6: Chemical resistance of the HBPE/epoxy blends, water dispersible HBPE and acrylate modified HBPE films
- Table 4.1: Performance characteristics of HBPE and its nanocomposites
- Table 4.2: Performance characteristics of LPE and its nanocomposites
- Table 4.3: Performance characteristics of PE and its nanocomposites
- Table 4.4: Performance characteristics of HBPE/epoxy blend and its nanocomposites
- Table 4.5: Performance characteristics of water dispersible HBPE and its nanocomposites
- Table 4.6: Performance characteristics of acrylate modified HBPE and its nanocomposites
- Table 4.7: Chemical resistance of HBPE and its nanocomposites

- Table 4.8: Chemical resistance of LPE and its nanocomposites
- Table 4.9: Chemical resistance of PE and its nanocomposites
- Table 4.10: Chemical resistance of HBPE/epoxy blend and its nanocomposites
- Table 4.11: Chemical resistance of water dispersible HBPE and its nanocomposites
- Table 4.12: Chemical resistance of acrylate modified HBPE and its nanocomposites
- Table 5.1: Performance characteristics of the HBPE/clay silver nanocomposites
- Table 5.2: Chemical resistance of the HBPE/clay silver nanocomposites
- Table 5.3: Antimicrobial activity of HBPE/clay silver nanocomposites
- Table 6.1: Performance characteristics of HBPE/MWCNTs nanocomposites
- Table 7.1: Formulations for the test paint
- Table 7.2: Physical parameters of the HBPE and paints (standard and test)
- Table 7.3: Performance characteristics of test and standard paints

## **LIST OF FIGURES**

---

- Fig. 1.1: Different types of polymer/clay nanocomposites
- Fig. 1.2: Different types of nanofillers
- Fig. 1.3: Structure of 2:1 phyllosilicates
- Fig. 1.4: Structures of (a) SWCNT, (b) MWCNT and (c) cellulose chain
- Fig. 1.5: Different fields of applications of polymer nanocomposites
- Fig. 1.6: Structure of triglyceride
- Fig. 2.1: Variation of acid value with time for pre-polyesterdiol
- Fig. 2.2: Variation of acid value with time for TMAP
- Fig. 2.3: Plot of  $(1-p)^{-1}$  versus time for pre-polyesterdiol
- Fig. 2.4: Plot of  $(1-p)^{-1}$  versus time for TMAP
- Fig. 2.5: FTIR spectrum of HBPE
- Fig. 2.6: FTIR spectrum of PE
- Fig. 2.7: FTIR spectrum of LPE
- Fig. 2.8:  $^1\text{H}$  NMR spectrum of HBPE
- Fig. 2.9:  $^1\text{H}$  NMR spectrum of PE
- Fig. 2.10:  $^1\text{H}$  NMR spectrum of LPE
- Fig. 2.11: Rheological behaviors of the TMAPs
- Fig. 3.1: Structure of epichlorohydrin

Fig. 3.2: Structure of PTSA

Fig. 3.3: Structure of TEA

Fig. 3.4: Structure of HMMA

Fig. 3.5: Structure of MMA

Fig. 3.6: Structure of BPO

Fig. 3.7: FTIR spectrum of PEB1

Fig. 3.8: FTIR spectrum of water dispersible HBPE

Fig. 3.9: FTIR spectrum of acrylate modified HBPE

Fig. 3.10: <sup>1</sup>H NMR spectrum of the acrylate modified HBPE

Fig. 3.11: TGA thermograms for the HBPE/epoxy blends

Fig. 3.12: TGA thermogram for water dispersible HBPE

Fig. 3.13: TGA thermograms for HBPE1 and acrylate modified HBPE

Fig. 4.1: FTIR spectra for (a) HBPE, (b) PENC1, (c) PENC2.5 and (d) PENC5

Fig. 4.2: FTIR spectra for (a) LPE, (b) LPENC1, (c) LPENC2.5 and (d) LPENC5

Fig. 4.3: FTIR spectra for (a) PEB1, (b) BNC1, (c) BNC2.5 and (d) BNC5

Fig. 4.4: FTIR spectra for (a) water dispersible HBPE, (b) WBPENC1, (c) WBPENC2.5 and (d) WBPENC5

Fig. 4.5: XRD diffractograms for (a) HBPE, (b) PENC1, (c) PENC2.5, (d) PENC5 and (e) OMMT

Fig. 4.6: XRD diffractograms for (a) LPE, (b) LPENC1, (c) LPENC2.5, (d) LPENC5 and (e) OMMT

Fig. 4.7: XRD diffractograms for (a) PE, (b) PNC1, (c) PNC2.5, (d) PNC5 and (e) OMMT

Fig. 4.8: XRD diffractograms for (a) PEB1, (b) BNC1, (c) BNC2.5, (d) BNC5 and (e) OMMT

Fig. 4.9: XRD diffractograms for (a) PANC5, (b) PANC2.5, (c) PANC1, (d) acrylate modified HBPE and (e) OMMT

Fig. 4.10: XRD diffractograms for (a) water dispersible HBPE, (b) WBPENC1, (c) WBPENC2.5, (d) WBPENC5 and (e) bentonite

Fig. 4.11: SEM micrographs for (a) HBPE, (b) PENC1, (c) PENC2.5 and (d) PENC5

Fig. 4.12: SEM micrographs for (a) LPE, (b) LPENC1, (c) LPENC2.5 and (d) LPENC5

Fig. 4.13: SEM micrographs for (a) PE, (b) PNC1, (c) PNC2.5 and (d) PNC5

Fig. 4.14: SEM micrographs for (a) PEB1, (b) BNC1, (c) BNC2.5 and (d) BNC5

- Fig. 4.15: SEM micrographs for (a) water dispersible HBPE, (b) WPENC1, (c) WPENC2.5 and (d) WPENC5
- Fig. 4.16: SEM micrographs for (a) acrylate modified HBPE, (b) PANC1, (c) PANC2.5 and (d) PANC5
- Fig. 4.17: TEM micrographs for (a) PENC1, (b) PENC2.5 and (c) PENC5
- Fig. 4.18: TEM micrographs for (a) LPENC1 and (b) LPENC2.5
- Fig. 4.19: Representative TEM micrograph for PE nanocomposite (PNC2.5)
- Fig. 4.20: TEM micrographs for (a) BNC1 and (b) BNC2.5
- Fig. 4.21: TEM micrographs for (a) WPENC1, (b) WPENC2.5 and (d) WPENC5
- Fig. 4.22: Representative TEM micrograph for acrylate modified HBPE nanocomposite (PANC2.5)
- Fig. 4.23: Rheological behaviors of HBPE nanocomposites
- Fig. 4.24: Rheological behaviors of LPE nanocomposites
- Fig. 4.25: Rheological behaviors of PE nanocomposites
- Fig. 4.26: Rheological behaviors of water dispersible HBPE nanocomposites
- Fig. 4.27: Rheological behaviors of acrylate modified HBPE nanocomposites
- Fig. 4.28: TGA thermograms for HBPE nanocomposites
- Fig. 4.29: TGA thermograms for LPE nanocomposites
- Fig. 4.30: TGA thermograms for PE nanocomposites
- Fig. 4.31: TGA thermograms for HBPE/epoxy blend nanocomposites
- Fig. 4.32: TGA thermograms for water dispersible HBPE nanocomposites
- Fig. 4.33: TGA thermograms for acrylate modified HBPE nanocomposites
- Fig. 4.34: Growth of (a) *Pseudomonas aeruginosa*, PN8A1, (b) *Pseudomonas aeruginosa*, vs1 and (c) *Bacillus subtilis*, MTCC73 on HBPE nanocomposites
- Fig. 4.35: SEM micrographs for (a) HBPE, (b) PENC1, (c) PENC2.5 and (d) PENC5 after biodegradation by *Bacillus subtilis*, MTCC73
- Fig. 4.36: Growth of (a) *Pseudomonas aeruginosa*, SD2, (b) *Pseudomonas aeruginosa*, SD3 and (c) *Bacillus subtilis*, MTCC736 on HBPE nanocomposites
- Fig. 4.37: SEM micrographs for (a) HBPE, (b) PENC1, (c) PENC2.5 and (d) PENC5
- Fig. 5.1: Silver nanoparticles (A) and silver salt solution before reduction (B) in nanocomposite
- Fig. 5.2: UV-visible spectra for silver nanoparticles against time during reduction
- Fig. 5.3: TEM micrographs for (a) PENCAG1, (b) PENCAG3 and (c) PENCAG5

- Fig. 5.4: XRD diffractograms for (a) PENCAg0, (b) PENCAg1, (c) PENCAg3 and (d) PENCAg5
- Fig. 5.5: SEM micrographs for (a) PENCAg0, (b) PENCAg1, (c) PENCAg3 and (d) PENCAg5
- Fig. 5.6: Bar diagram for size distributions of silver nanoparticles
- Fig. 5.7: FTIR spectra for (a) PENCAg0, (b) PENCAg1, (c) PENCAg3 and (d) PENCAg5
- Fig. 5.8: Variation of shear viscosity of silver nanocomposites against (a) time at constant stress and temperature, (b) temperature under constant stress and (c) shear rate under constant temperature
- Fig. 5.9: TGA thermograms for (a) PENCAg0, (b) PENCAg1, (c) PENCAg3 and (d) PENCAg5
- Fig. 6.1: Stability of neat MWCNTs in (a) DMF, (b) HBPE, and modified MWCNTs in (c) DMF (d) HBPE nanocomposites
- Fig. 6.2: FTIR spectra of (a) MWCNTs and (b) modified MWCNTs
- Fig. 6.3: FTIR spectra of (a) HBPE, (b) PCNTC0.5, (c) PCNTC1 and (d) PCNTC2
- Fig. 6.4: XRD diffractograms for (a) HBPE, (b) PCNTC0.5, (c) PCNTC1, (d) PCNTC2 and (e) MWCNTs
- Fig. 6.5: SEM micrographs for A. HBPE, B. PCNTC0.5, C. PCNTC1 and D. PCNTC2
- Fig. 6.6: TEM micrographs for A. PCNTC1 and B. PCNTC2
- Fig. 6.7: TGA thermograms for (a) HBPE, (b) PCNTC0.5, (c) PCNTC1, (d) PCNTC2 and (e) modified MWCNTs
- Fig. 6.8: Bacterial growth of *Pseudomonas aeruginosa* with strains (a) PN8A1 and (b) vs1, and *Bacillus subtilis* with strain (c) MTCC73 on nanocomposites
- Fig. 6.9: SEM micrographs for (a) HBPE, (b) PCNTC0.5, (c) PCNTC1 and (d) PCNTC2 after biodegradation
- Fig. 6.10: Bar diagram showing cytotoxicity test results for the nanocomposites
- Fig. 7.1: Variation of shear viscosity against time at constant stress and temperature for (a) test and (b) standard paints
- Fig. 7.2: Variation of shear viscosity against shear rate at constant temperature for (a) test and (b) standard paints
- Fig. 7.3: SEM micrographs for (a) test and (b) standard paints
- Fig. 7.4: TGA thermograms for (a) test and (b) standard paints



# LIST OF SCHEMES

---

Scheme 1.1: Formation of polyester

Scheme 1.2: General scheme of the formation of vegetable oil based polyester resin

Scheme 2.1: Possible reaction scheme for synthesis of TMAP

Scheme 2.2: Possible reaction scheme for synthesis of HBPE

Scheme 2.3: Possible reaction scheme for synthesis of PE

Scheme 2.4: Possible reaction scheme for preparation of LPE

Scheme 4.1: Possible interactions in HBPE nanocomposites

Scheme 4.2: Possible interactions in LPE nanocomposites

Scheme 4.3: Possible interactions in water dispersible HBPE nanocomposites

Scheme 6.1: Possible interactions of MWCNTs with polyester, epoxy and hardener system

Scheme 7.1: Flow sheet diagram for the manufacturing process of the paint

Scheme 7.2: Possible curing reaction mechanisms of the paints

# ACKNOWLEDGMENT

---

*It is my greatest pleasure to express my gratitude to large numbers of people who have directly or indirectly influenced and encouraged me over the course of my studies and my life in general.*

*First of all, I would like to express my deep sense of gratitude and indebtedness to my research guide Dr. Niranjana Karak, Professor and Head, Department of Chemical Sciences, Tezpur University for his invaluable guidance, support, advice and a wonderful accompany throughout my Ph.D. work. His dedication towards research and indomitable spirit would ever remain as a source of inspiration for me.*

*Words fall short as I extend my gratitude to Dr. M. Mandal, Associate Professor, Department of Molecular Biology and Biotechnology, Tezpur University for his cooperation during the course of my bio-related laboratory work.*

*It is my pleasant duty to acknowledge with thanks the co-operation and support extended to me by the authority of Tezpur University and entire community of the Department of Chemical Sciences, for allowing me to use the administrative and technical facilities required for my research work.*

*It is my greatest pleasure to acknowledge the present and former Heads of the Department, Prof. N. Karak, Prof. T. K. Maji, Dr. R.K. Dutta and Prof. N. S. Islam (Dean, Research and Development) for giving me the opportunity to work on my topic and valuable advises throughout my stay at Tezpur University.*

*I would also like to express my sincere gratitude and humble respect to my doctoral research committee members Prof. S. K. Dolui and Dr. R. Borah for their timely help and advises.*

*I am immensely grateful to Prof. R.C. Deka, Dr. A.K. Phukan, Dr. A.J. Thakur, Dr. P. Puzari, Dr. G.V. Karunakar and Mr. K.K. Bania faculty members of Department of Chemical Sciences, Tezpur University for valuable suggestions and advices.*

*My heartfelt thanks go to my senior lab-mates Dr. Nandini Dutta, Dr. Jyotishmoy Borah, Dr. Sibdas Singha Mahapatra, Dr. Suvangshu Dutta and Dr. Harekrishna Deka for their manifold help and active co-operation over all these years. I would also like to thank my junior group members Gautam Das, Buddhadeb Roy, Rocktopal Konwarh, Sujata Pramanik, Shaswat Barua, Hemjyoti Kalita and Beauty Das for their constant inspiration and help during my Ph.D. work.*

*I would like to offer my sincere thanks to Dr. Biren Gohain, Dr. Binoy Saikia, Mr. Nipu Dutta, Mr. Raju K. Borah, Mr. Sankur Phukan, Mr. Rajen Borah, Mr. Biraj borah, Mr. Arup Chakrabarty, Dr. Kishor K. Baruah, Mr. Ratan Baruah and Mr. Jayanta Bora for instrumental and experimental helps. IIT Guwahati, NEHU Shillong and other institutions are highly acknowledged for their help in analyzing and testing works.*

*I would like to thank also the office staffs of Department of Chemical Sciences, Tezpur University, Mr. Prafulla Nath, Ms Babita Das and Mr. Hemanta Gogoi for their kind help during my Ph.D. work.*

*I wish to thank all my friends (research scholar) for their help and support during the course of my work.*

*I am also grateful to CSIR, New Delhi for financial support to me as SRF.*

*I take this opportunity to express my sincere gratitude to Mrs. Susmita Karak for her great affection, which I continue to enjoy during my stay at Tezpur University.*

*Finally, I owe heartfelt gratitude to my parents and all my family members for their blessings, support and constantly inspiring me to carry out my research work to completion. I am thankful to all my relatives and well-wisher for their encouragement. The endless love of them will always be in my heart that will inspire me in every step of my future life.*

Place : Tezpur University, Tezpur

Date : 12/04/2011

*Uday Konwar*  
(Uday Konwar)

# CHAPTER 1

---

## General Introduction

### 1.1. Introduction

Nanoscience and technology have colossal contribution in the materials science of 21<sup>st</sup> century in developing promising high performance advanced polymeric materials for today's society. They opened up a new avenue of structure-property tailoring in the domain of polymers for multifaceted advanced applications. They engraved the polymer nanocomposites an inimitable position in the niche of advanced materials. The low levels of desired properties of pristine polymers have coerced to modify them through different approaches. However, the filled polymer and conventional polymer composite systems encompass some demerits like causing processing difficulties and increasing density. Also, the properties improvements are not on top of things in many cases which limit their advanced applications.<sup>1</sup>

Thus, the development of polymer nanocomposites have attracted a great deal of interest to the material scientists as a way to enhance the properties of polymers or to get material with intrinsically new set of properties and hence, extends their utility in different field of applications.<sup>2</sup> The polymer nanocomposites are the combination of two or more phases containing different compositions or structures, where at least one of the phases is in the nanoscale regime.<sup>1</sup> A very small amounts (within 5 wt.%) of nanofillers with high aspect ratios, are reinforced into the polymers which enhanced the mechanical strength, thermal, gas barrier, flame retardant, biodegradability etc.<sup>3-8</sup> properties remarkably. The value of polymer nanocomposites technology is neither solely based on the mechanical enhancement of the neat polymers nor the direct replacement of the conventional filled or composite technology.<sup>9,10</sup> Rather, its importance comes for providing value-added properties that are not present in the neat polymers, without sacrificing their inherent processability, light weight and transparency (if any) characteristics.

---

Parts of this work are accepted for publication as book chapter in the book "*Developments in Nanocomposites*" edited by Kar K.K.; Hodzic, A. (ISBN: 978-981-08-3711-2, Research Publishing Services, Innovative Partners for Publishing Solutions, Singapore, 2011)

## Chapter 1

Different polymeric systems are in so far used as matrices to fabricate the polymer nanocomposites. Polyester is an attractive polymeric system with high industrial significance and interest. They are the polycondensation products of dihydric or polyhydric alcohols/phenols and dibasic or polybasic acids/anhydrides comprising with ester functional groups in their backbones. The term polyester is a broad one, and includes saturated polyester plasticizers such as poly(propylene adipate), polyester fiber forming compounds such as poly(ethylene terephthalate) and polyesters modified by fatty acids/drying or non-drying oils used in paints and varnish industry.<sup>11</sup> The chemistry of the structural units connecting the ester groups can be varied over an immensely covering everything from labile biomedical matrices to liquid crystals including, fibers and heat resistant polyesters.<sup>12</sup> However, the term polyester is used as the vegetable oil modified unsaturated polyester resin in the present thesis.

Further, the highly branched polymers are applied into various fields of advanced polymeric materials in much significant manner over the conventional linear polymers.<sup>13,14</sup> This is due to their intrinsic characteristics like highly compact structure, narrow size distribution and large numbers of terminal functional groups with highly active surface functionality. The hyperbranched polymers fall into the major class of polymer architecture known as dendritic polymers. They exhibit three-dimensional (3D) globular and spherical like structural architectures<sup>15</sup> and are closely related to highly branched macromolecules with significantly less regular branched structures that accommodate certain numbers of structural defects. However, they have almost equal potential for many applications as they have almost similar properties like dendrimers, the other class of dendritic polymer. The most important advantage of these is their simple preparation by single step or one pot processes of  $AB_X$  ( $X \geq 2$ ),  $A_2 + B_3$  and  $A_2 + BB_2$  etc. types of monomers.<sup>16</sup> This allows their large scale production, which makes them less expensive and hence likely to have great potential for commercialization. The hyperbranched polymers show unique properties like low melt and solution viscosity, high solubility and reactivity, easy modification to optimize the properties for special applications etc. as they possess unusual structural features with confined geometry.<sup>17</sup> Thus the use of highly branched polyesters as the matrices is gaining interest in the field of polymer nanocomposites.

Again, for sustainable development, the uses of renewable natural resources are increasing continuously in different industrial fields including polymers because of their potential substitution capabilities to petrochemical derivatives. This is due to

## Chapter 1

awareness to the environmental and ecological issues, recycling or waste disposal problems, spiraling rise in prices and high rate of depletion of the stocks.<sup>18-20</sup> In this context, vegetable oil is one of such renewable resources which possesses excellent properties for utilization in the production of different polymeric materials such as polyester, epoxy, poly(ester amide), polyurethane etc.<sup>21-24</sup> Vegetable oils can play an important role not only for edible purposes but also for industrial applications such as surface coatings including paints, varnishes etc. printing inks, soaps, shampoos, shoe polishes, cosmetics, pharmaceuticals, lubricants, emulsifiers, plasticizers, multipurpose additives, biodiesels etc.<sup>25-28</sup> These oils have a number of advantages like physical and chemical stability, aptitude to facile chemical modification, reduced toxicity, reduced risk for handling and transportation, possibility of recycling, renewability and biodegradability, and at the same time available in large quantities in relatively low and stable prices, and are susceptible to agricultural diversification and environmentally benign in nature.<sup>29-33</sup>

Thus the last decade has seen a growing interest in the use of the abundant and cheap vegetable oils for production of polymers, which are generally prepared from petrochemicals. The vast forest resources and farm lands yield varieties of oil-bearing seeds. Among them, about 350 oil bearing crops are identified so far. A number of seed oils are used in the synthesis of various polymeric resins like polyester, epoxy, polyurethane, poly(ester amide) etc. Some of the major seed oils used traditionally for preparation of polyester resins are linseed, castor, soybean, sunflower, safflower, tung, coconut etc. Non-traditional oils such as rubber seed oil,<sup>34</sup> neem oil,<sup>29</sup> karanja oil,<sup>35,36</sup> jatropha seed oil,<sup>37</sup> kamala seed oil,<sup>38</sup> lesquerella oil,<sup>39</sup> melon seed oil,<sup>40</sup> apricot oil,<sup>41</sup> *Annona squamosa*,<sup>42</sup> African mahogany seed oil,<sup>43</sup> African locust bean seed oil<sup>44</sup> etc. are also used for the same purpose. Therefore, vegetable oil based highly branched polyester nanocomposites are the present interest of research.

### 1.2. Background

The term “nanocomposite” is first proposed by Theng in 1970.<sup>45</sup> Before this Hess and Parker proposed a stable dispersion of metallic cobalt particles with uniform size (1-100 nm) in polymer solutions in 1966.<sup>46</sup> Although research on polymer/clay intercalation can be traced back to before the 1980s, these developments should not be taken into account in the history of polymer nanocomposites as the work did not result in dramatic improvement in the physical and engineering properties of polymers. The

era of polymer/clay nanotechnology can truly be said to start with Toyota's work<sup>47</sup> on the exfoliation of clay in nylon-6 in the latter part of the 1980s and the beginning of the 1990s. It is this work that demonstrates a significant improvement in a wide range of engineering properties by reinforcing polymers with nanometer scale clay. Since then, extensive research in this field is carried out globally by different researchers. At present, development is widened into almost every polymer like epoxies, unsaturated polyester, poly( $\epsilon$ -caprolactone), poly(ethylene oxide), silicone rubber and other rubber, polystyrene, polyimide, polypropylene, poly(ethylene terephthalate), polyurethane etc.<sup>48</sup>

The history of polyester production dates back to 1847 when Barzelius prepared polyglycerol tartarate by the reaction of glycerol with tartaric acid.<sup>49</sup> The film forming capabilities and properties of the condensation products of polyhydric alcohols and polybasic acids are first demonstrated by the General Electric Co. during 1912-1915.<sup>50</sup> In 1921 Kienle modified glyptal by vegetable oils. Kienle and Hovey's oil-modified polyester resins result a US patent 1,893,873 in the year 1933. This achievement is the root cause of the phenomenal acceptance of polyester resins as surface coatings. In 1935, when Kienle's patent is declared invalid, then the field of polyester manufacture became accessible to all.<sup>49</sup>

### 1.3. Polymer Nanocomposites

A nanocomposite is the product of combination of at least two dissimilar components with a distinct interface, where one of them must have at least one dimension in the nanometer size range (1–100 nm). Further, a polymer nanocomposite is a bi- or multiphase material in which disperse phase (nanofiller) is distributed at the nanolevel in the polymeric matrix. It can broadly be divided into three categories depending on the dimension of nanofillers.

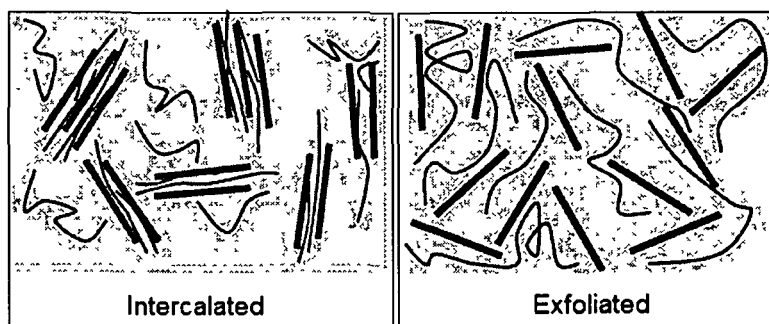
The first category has all three dimensions of the nanofiller (iso-dimensional nanofiller) present in the matrix are within 100 nm. Different nanofillers that fall in this category are spherical silica, silica or titania oxides, metal nanoparticles etc. The nanocomposites which have nanofillers with two dimensions are in the nanometer scale and the third dimension is larger, forming an elongated structure belongs to the second category. Nanotubes or nanofibers/whiskers/nanorods are the examples of this category of nanofillers. The third type of nanocomposites includes the nanofiller which are characterized by only one dimension in nanometer scale such as nanolayers, nanosheets

etc. This particulate is present in the form of sheets of one to a few nanometer thick and hundred to thousand nanometers long. The extensively studied polymer/layered silicates and polymer/layered double hydroxide (LDH) nanocomposites represent this category.

Again depending on the nature of the components used (layered silicate, organic cation and polymer matrix), extent of interactions between nanofillers and polymer, and the method of preparation; different structures/morphologies of nanocomposites can be obtained. These are as follows.

(a) *Intercalated nanocomposites*: When one or more than one extended polymer chain is inserted in a regular fashion between the layers/sheets/bundle of tubes of nanofillers resulting in a well-ordered multilayer morphology that are built up with alternating polymer and nanofiller layers, the obtained nanocomposites can be called as intercalated nanocomposites (Fig. 1.1).

(b) *Exfoliated nanocomposites*: When the individual layer/sheet/bundle of tubes of nanofillers is uniformly dispersed in a continuous polymer matrix, an exfoliated or delaminated structure (Fig. 1.1) is obtained. The exfoliated nanocomposites are preferred polymer nanocomposites as the improvements of properties are much higher than that of intercalated nanocomposites.



*Fig. 1.1: Different types of polymer/clay nanocomposites*

### **1.3.1. Materials**

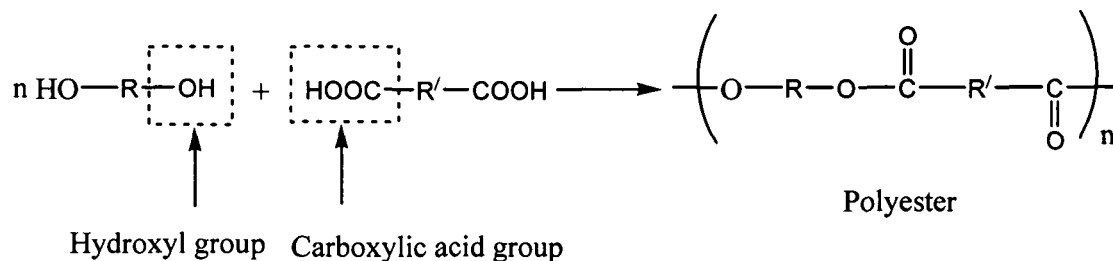
For the development of polyester nanocomposites, polyester is used as the matrix and nanoclay, metal nanoparticles and carbon nanotubes are used generally as the nanofillers. Therefore in this section the discussion is restricted for these materials only.

#### **1.3.1.1. Polyester**

Polyester is being used as matrix for the preparation of both conventional composites as well as nanocomposites. The polyesters are usually synthesized by direct esterification



of the carboxyl groups of polybasic acids with hydroxyl groups of polyhydric alcohols through polycondensation reaction (Scheme 1.1) as stated earlier. The details of polyester are discussed in the short review of vegetable oil based polyester nanocomposites in the later part of this chapter.



**Scheme 1.1:** Formation of polyester

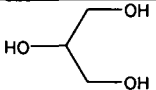
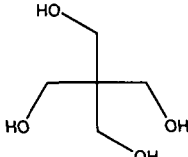
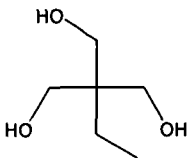
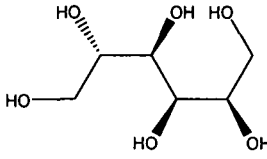
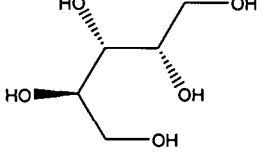
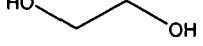
A brief description on different polyhydric alcohols, polybasic acids that are used for the preparation of polyester is presented below.

### *Polyhydric Alcohols*

Glycerol, a trihydric-alcohol generally obtained from vegetable oils is one of the polyhydric alcohol components of polyester resins. Its popularity is due to high availability as well as adaptability to many technical variations involved in the production of resins.<sup>51,52</sup> The highly functional penta-erythritol is the second most widely used polyhydric alcohol for polyester resins. It is especially useful in long oil polyester resins. In the synthesis of polyester the high functionality of penta-erythritol can be reduced,<sup>51,49,53</sup> by using low functionality polyhydric alcohols such as glycol, glycerol etc. large amount of fatty acids, formaldehyde, monobasic acids like benzoic acid, rosin etc. Trimethylol propane (TMP) is another important polyhydric alcohol used to prepare polyester resins. But due to the steric hindrance present in its structure the rate of esterification reaction is slow.<sup>52</sup> It is also used for the synthesis of hyperbranched polyester resin.<sup>54</sup> Linear dihydric alcohols are also used in the preparation of polyester. As a substitute for glycerol and penta-erythritol, the use of sorbitol and xylitol is also reported.<sup>55,56</sup> Glycol glycoside can also be used as a polyhydric alcohol in polyester synthesis.<sup>57</sup> The use of polystyrene glycol as a partial substitute of glycerol led to the formation of polyester resin, which possesses better physical and chemical resistance than conventional styrenated polyesters.<sup>58</sup> Aurelian et al.<sup>59</sup> used 1,1'-isopropylidene bis(4-cyclohexanol) (I), bisphenol-A bis(2-hydroxyethyl) ether (II), bisphenol-A bis(2-hydroxypropyl) ether (III) and ethylene glycol (IV) separately for the preparation of polyesters resins and observed that polyesters from (I),

(II) and (III) had higher viscosities than (IV). Drying time and hardness for coatings from (III) polyesters are comparable to those for (IV) polyesters, but drying time is reduced and hardness increased for (I) and (II) polyester coatings. The use of polyentaerythritol in the synthesis of binder for baking primer is also reported in literature.<sup>60</sup> A few polyhydric alcohols with their structures and physical properties are given in Table 1.1.

*Table 1.1: Different polyhydric alcohols with their structures and a few physical properties*

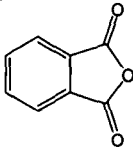
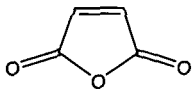
Name	Structure	Melting point (°C)	Boiling point (°C)	Density (g/cm <sup>3</sup> )
Glycerol		17.8	290	1.26
Pentaerythritol		260.5	276	1.40
Trimethylol propane		58	160	1.08
Sorbitol		95	296	1.49
Xylitol		92-96	216	1.52
Ethylene glycol		-12.9	197.3	1.11

### *Polybasic Acids*

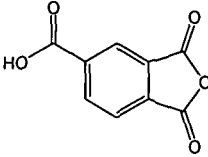
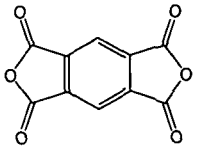
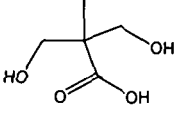
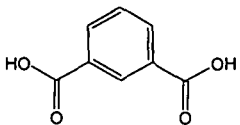
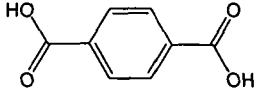
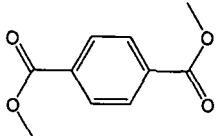
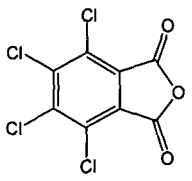
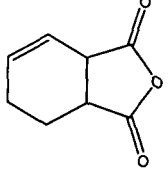
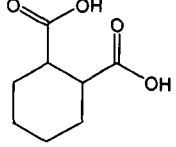
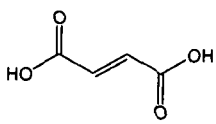
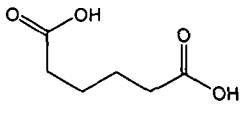
One of the most dominant dibasic acids/anhydrides used in the preparation of polyester is phthalic anhydride (PA). It is available at low price in addition to its other advantages like easy to handle, quite stable at cooking temperature of polyester, stable to UV radiation, reduces the reaction time as less amount of water is evolved etc.<sup>61,52</sup> Isophthalic acid (IPA) is the second most widely used dibasic acid. The IPA based polyesters are more hydrolytic resistant than the PA based polyesters in the pH range of

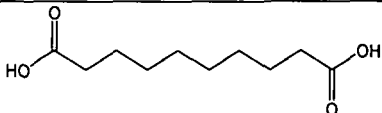
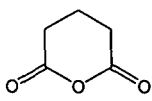
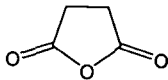
4-8 which is the most important range for exterior durability.<sup>52</sup> IPA is used to make tougher, fast drying and more chemical resistant coatings. Terephthalic acid (TPA) is also used for polyester preparation. Again the better solubility and low melting point of the dimethyl ester of TPA make it suitable than TPA in some esterification reactions.<sup>51,49</sup> The chlorine containing materials like tetrachloro phthalic anhydride and chlorendic anhydride are used to make flame retardant polyester resin.<sup>62</sup> Tetrachloro phthalic anhydride gives polyester resins, which are more water and alkali resistant than phthalic anhydride based polyester resin. Tetrahydro and hexahydrophthalic acids are suggested as components for polyester resin formulation with low viscosity. Maleic anhydride and fumaric acid are used frequently in the preparation of polyester in limited amounts with phthalic anhydride. Maleic anhydride and fumaric acid have also been utilized for waterborne coatings.<sup>30,33,63</sup> If flexibility and plasticization properties are required, then dibasic saturated acids with long hydrocarbon chains such as adipic, sebacic and azelaic acids are used.<sup>53,50</sup> Trimellitic anhydride (TMA), 2,2-bis(hydroxymethyl) propionic acid (bis-MPA) and pyromellitic anhydrides are also used for waterborne polyesters.<sup>51,64,65</sup> bis-MPA is reported to be used for the synthesis of hyperbranched polyester resin. Glutaric and succinic anhydrides<sup>66</sup> have also been reported for the preparation of low viscosity oil modified polyester resin. El-Hai et al. reported<sup>67</sup> that the use of 3,3'-methylene bis(salicylic acid) as a partial replacement of phthalic anhydride in polyesters formulation led to significant improvement in hardness, gloss and alkali resistance. Volozhin et al.<sup>68</sup> prepared polyester coatings using bicycle [2.2.2] oct-5-ene-2,3-dicarboxylic acid, the coatings showed high impact strength, flexural strength, heat resistance and resistance to water. The use of benzophenone tetracarboxylic dianhydride for polyester resin preparation has also been reported.<sup>69</sup> A few polybasic acids with their structures and physical properties are given in Table 1.2.

**Table 1.2: Different polybasic acids with their physical properties**

Name	Structure	Melting point (°C)	Boiling point (°C)	Density (g/cm <sup>3</sup> )
Phthalic anhydride		131	295	1.53
Maleic anhydride		52.8	202	1.48

## Chapter 1

Trimellitic anhydride		163	240	1.67
Pyromellitic anhydride		283-286	397-400	1.68
2,2-bis(hydroxymethyl)propionic acid		189-190	> 200	-
Isophthalic acid		347	100	1.53
Terephthalic acid		300	402	1.52
Dimethyl terephthalate		140-142	288	-
Tetrachlorophthalic anhydride		255-257	371	1.49
Tetrahydrophthalic anhydride		102	195	1.4
Hexahydrophthalic acid		220-221	339	1.31
Fumaric acid		287	355	1.63
Adipic acid		152.1	337.5	1.36

Sebacic acid		131-134.5	294.4	1.21
Glutaric anhydride		50-55	150	-
Succinic anhydride		119-120	261	4.16

### Monobasic Acids

The monobasic acids used sometimes in preparation of polyester resins are benzoic acid, *p*-*tert*-butylbenzoic acid, rosin (abietic acid), levopimaric acid etc. along with the naturally occurring fatty acids.<sup>49,50</sup> Using mixture of benzoic acid and *p*-*tert*-butylbenzoic acid, polyester resins with reduced drying time and very good chemical resistance are obtained.<sup>70</sup> In short oil polyester resin preparation benzoic acid is used to regulate the optimum level of polymerization.<sup>71</sup> The use of rosin for water thinnable polyester emulsions is also reported.<sup>72</sup> Other monobasic acids such as pelargonic acid, perfluoropelargonic acid, lauric acid, lactic acid, iso-octanoic acid, iso-decanoic acid and versatic acid etc. are also used.<sup>49,73,74</sup> The cardanoxo acetic acid rendered better hardness, flexibility and chemical resistance in linseed oil-phthalic acid-glycerol based polyester resin compared to linseed oil polyester resin without cardanoxo acetic acid.<sup>75</sup>

### Catalysts

Both acid and base are used to catalyze an alcoholysis reaction. Base catalysts are much more efficient than the acid catalysts.<sup>76</sup> A few base catalysts used are metal hydroxides, metal oxides, metal salts of weak acids. Oxides, alkoxides of lead, lithium, calcium, tin, zinc etc. are commercially used catalyst in alcoholysis.<sup>77</sup> Carbonates and alcoholates are also used as most effective catalysts.<sup>78</sup> In many cases, sodium and potassium alkoxides of specific alcohols are also preferred. Lead compounds are found to be the most efficient catalysts followed by naphthenates of lanthanum, calcium, cerium and lithium salts on alcoholysis of soybean oil with equimolar amounts of pentaerythritol. Gupta et al.<sup>79</sup> carried out a general study to determine the rate and extent of alcoholysis of refined soybean oil, linseed oil, dehydrated castor oil with polyhydric alcohols e.g. neopentyl glycol, glycerine and pentaerythritol in presence of catalyst such as LiOH, Ca(oct)<sub>2</sub>, PbO, MeONa, DBTO (di-butyl tin oxide) at temperature 200-240 °C and

observed that at a constant temperature and at a fixed concentration of the catalyst, the rate of alcoholysis follows the order  $\text{LiOH} > \text{PbO} > \text{DBTO} > \text{MeONa} > \text{Ca}(\text{oct})_2$  and extent of alcoholysis (monoglyceride/triglyceride ratio) follows the order  $\text{DBTO} > \text{Ca}(\text{oct})_2 > \text{MeONa} > \text{PbO} > \text{LiOH}$ . In the case of castor oil, both the glycerolysis rate and the equilibrium glyceride content varied in the order  $\text{LiOH} > \text{CaO} > \text{PbO}$ . The use of organotin catalysts<sup>80</sup> (e.g. Fascat 4350) for the preparation of oil modified polyester resin reduces the cooking time, and generates haze free resin with improved color when compared to lithium neodecanoate catalyst. Athawale et al.<sup>81</sup> prepared modified castor oil based polyester resins by chemoenzymatically using enzyme catalyst, Lipozyme IM 60 (lipase from the fungus *Mucor miehei* immobilized on micro-porous anion exchange resin). The chemoenzymatically synthesized polyester resins showed light color, good reverse impact strength, excellent chemical resistance and storage stability compared to the conventional ones. The use of Porcine pancreatic lipase<sup>82</sup> in the synthesis of coconut oil based polyester resin is reported which lead to the synthesis of more controlled polyester resin structure than the conventional coconut oil based polyester resin.

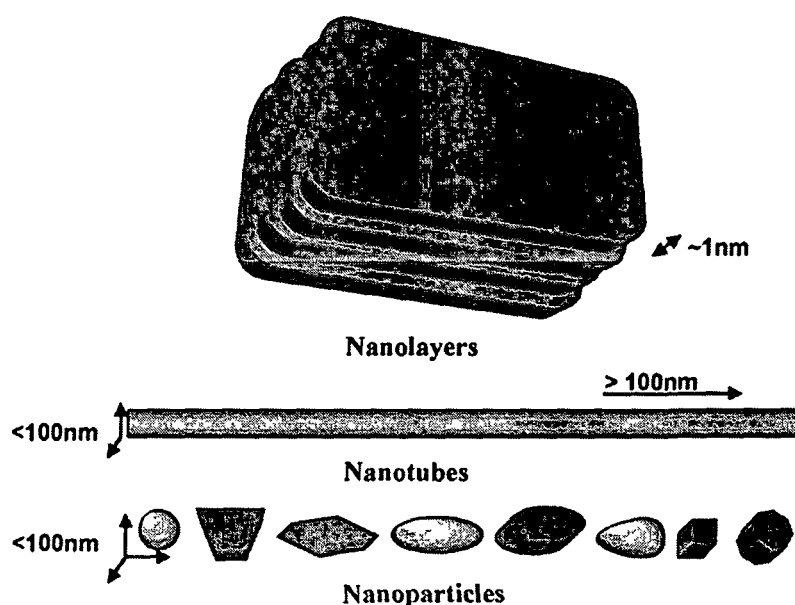
### *1.3.1.2. Nanofillers*

The fillers that have one or more dimensions within 100 nm are known as the nanofillers (Fig. 1.2). The specific surface area of the materials increases with the decrease in grain size, which results markedly different physico-chemical properties that are dominated by the physics of the bulk materials. The nanofillers generally used in the preparation of nanocomposites to enhance the desired performance of pristine polymer systems are divided into three types depending on the dimensions of the fillers and are discussed briefly below.

### *Nanolayers*

This type has only one dimension in the nanometer range. They possess a platelet like structure in the form of sheets or layers. The lateral dimension may be in the range of several hundred nanometers to microns, while the thickness is usually less than 100 nm. There is a vast array of both natural and synthetic-layered crystalline fillers that are intercalated by the polymer under suitable conditions. Examples of possible layered nanofillers, which are candidates for preparing polymer nanocomposites are element (graphite), oxides {graphite oxide,  $\text{V}_6\text{O}_{13}$ ,  $\text{HTiNbO}_5$ ,  $\text{W}_{0.2}\text{V}_{2.8}\text{O}_7$ }, phyllosilicates

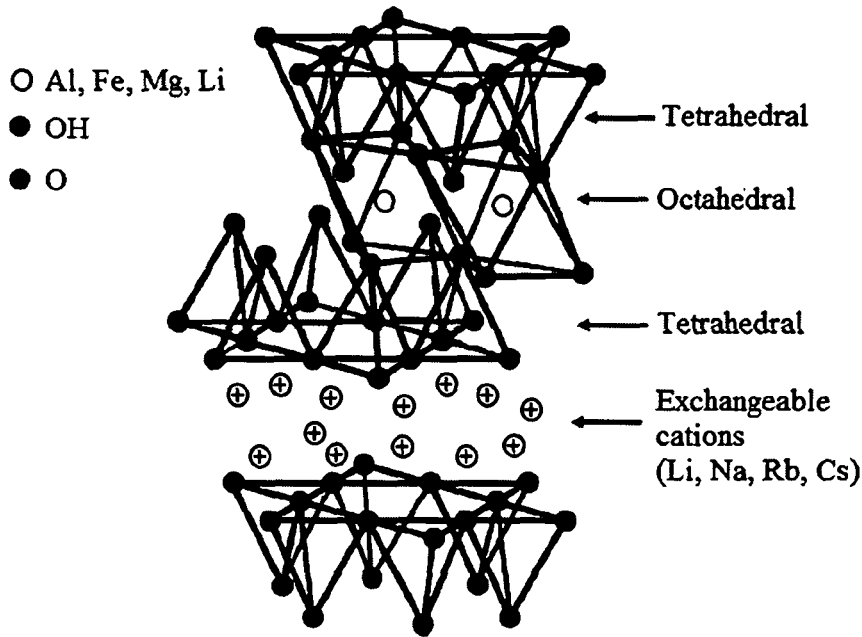
{kaolinite, dickite, nacrite, halloysite, chrysotile, antigorite, lizardite, montmorillonite, bentonite, nontronite, beidellite, hectorite, colknskonite, pyrophyllite, talc, vermiculite, illite, glauconite, muscovite, celadonite, phlogopite, taenolite, margarite (brittle mica), palygorskite, sepiolite, clinochlore}, layered silicic acids {kanemite, makamite, octosilicate, magadite, kenyaite, layered organo-silicates}, mineral-layered hydroxides {brucite ( $\text{Mg}(\text{OH})_2$ ), gibbsite ( $\text{Al}(\text{OH})_3$ )}, layered double hydroxides (LDH)  $\{\text{M}_6\text{Al}_2(\text{OH})_{16}\text{CO}_3n\text{H}_2\text{O}$  (M: Al, Zn)}, layered aluminophosphates {berlinite, vantasselite ( $\text{Al}_4(\text{PO}_4)_3(\text{OH})_3 \cdot 9\text{H}_2\text{O}$ )}, metal ( $\text{M}^{4+}$ ) phosphates  $\{\text{M}^{4+}$ : Zr, Ti or Sn;  $\text{Zr}(\text{HPO}_4)\}$ , chlorides  $\{\text{FeCl}_3, \text{FeOCl}, \text{CdI}_2, \text{CdCl}_2\}$ , metal chalcogenides  $\{(\text{PbS})_{18}(\text{TiS}_2)_2, \text{TiS}_2, \text{MoS}_2, \text{MoS}_3\}$ , cyanides  $\{\text{Ni}(\text{CN})_2\}$ .



*Fig. 1.2: Different types of nanofillers*

Among these nanolayers, clay minerals based on phyllosilicates have extensively been used for last two decades, most probably because the starting clay materials are easily available and because their intercalation chemistry has been studied for a long time. In the family of phyllosilicates, 2:1 type layered silicates are most popular both in industries and in academia. Their crystal structure consists of layers made up of two tetrahedrally coordinated silicon atoms fused to an edge-shared octahedral sheet of either aluminum or magnesium hydroxide (Fig. 1.3). The layer thickness is around 1 nm and the lateral dimensions of these layers may vary from 30 nm to several microns or larger, depending on the particular layered silicate. These layers are attracted by van der Waals forces. Stacking of the layers leads to a regular van der Waals gap between the layers called the interlayer or gallery. Isomorphic substitution within the layers (for example,  $\text{Al}^{3+}$  is replaced by  $\text{Mg}^{2+}$  or  $\text{Fe}^{2+}$ , or  $\text{Mg}^{2+}$  is

replaced by  $\text{Li}^+$ ) generates negative charges that are counterbalanced by alkali and alkaline earth cations ( $\text{Na}^+$ ,  $\text{K}^+$ ,  $\text{Ca}^{2+}$  and  $\text{Mg}^{2+}$ ) situated inside the galleries. These natural clay minerals are hydrophilic in nature.<sup>83</sup>



*Fig. 1.3: Structure of 2:1 phyllosilicates*

To render layered silicates miscible with hydrophobic polymeric matrices, one must convert the hydrophilic silicate surface to an organophilic one by ion-exchange reactions with cationic surfactants including primary, secondary, tertiary and quaternary alkylammonium or alkylphosphonium cations. Alkylammonium or alkylphosphonium cations in the organosilicates lower the surface energy of the inorganic host and improve the wetting characteristics of the polymer matrix and result in a larger interlayer spacing. Additionally, the alkylammonium or alkylphosphonium cations can provide functional groups that can react with the polymer matrix, or in some cases initiate the polymerization of monomers to improve the strength of the interface between the inorganic and the polymer matrix.<sup>84</sup> These organophilic montmorillonite (OMMT) clays whose surface energy is lowered and are more compatible with organic polymers may intercalate under well defined conditions by the polymer chains.

### *Nanotubes*

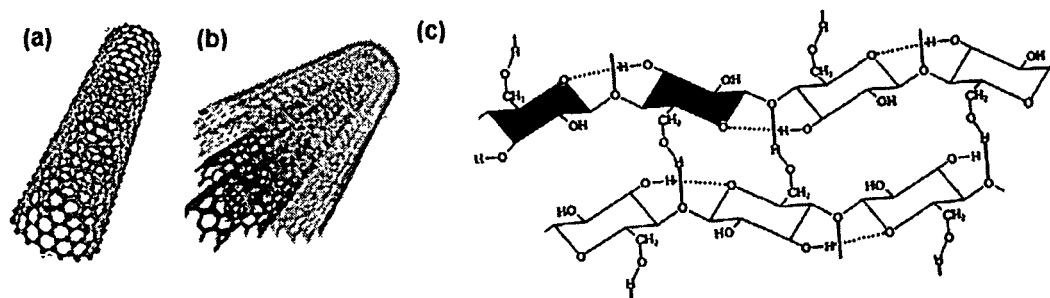
The second type of nanofillers has two dimensions in the nanometer scale while the third dimension is a few hundred nanometers in size. They possess an elongated structure. They are found in cylindrical or tubular form and are known as nanotubes or



nanofibers/whisker/nanorods. Carbon nanotubes and nanocellulose fibers, cellulose whiskers belong to this category.

Carbon nanotubes (CNTs) are allotropes of carbon, with nanometer sized diameter and micrometer-sized length (where the length to diameter ratio exceeds 1000). The atoms are arranged same manners as in graphite. The structure of CNTs consists of enrolled cylindrical graphitic sheet (called graphene) where each carbon atom is  $sp^2$  hybridized and covalently bonded to three neighboring carbon atoms that are rolled up into a seamless cylinder with diameter of the order of nanometer.<sup>85</sup> There are two types of CNTs: multi-walled carbon nanotubes (MWCNTs) and single-walled carbon nanotubes (SWCNTs) (Fig. 1.4). The former consists of two or more concentric cylindrical shells of graphene sheets coaxially arranged around a central hollow core with interlayer separations as in graphite. In contrast, SWCNT comprises a single graphene cylinder. Both SWCNTs and MWCNTs have physical characteristics of solids and are micro-crystals with high aspect ratios. The atomic arrangements, diameter and length of the nanotubes, morphology or nanostructure predict the properties of the carbon nanotubes. Carbon nanotubes are the strongest and stiffest materials yet discovered in terms of tensile strength and elastic modulus respectively. This strength results from the covalent  $sp^2$  bonds formed between the individual carbon atoms. They also show high optical, electrical and thermal properties. The strong interfacial adhesion between CNTs and polymer matrix is improved by the modification of CNTs, which leads to well dispersed and a stable nanocomposites with enhanced properties.<sup>86</sup>

Another type of tube-like nanoscale particles is a biopolymer, cellulose, which is a linear condensation polymer, consists of  $\beta$ -1-4-linked D-anhydroglucopyranose units (Fig. 1.4). Depending on the sources, degree of polymerization (DP) ranges from 2500 to 15,000. The inter- and intra-molecular hydrogen bonds result the linearity, the stiffness, the rigidity, strength and ultimately to form thread-like material called microfibrils that are apparently bound to form natural fibers. They are often referred to as cellulosic fibers, related to the main chemical component cellulose, or as lignocellulosic fibers, since the fibers usually contain a natural polyphenolic polymer, lignin also, in their structure. After defibrillation, they are mostly produced as stiff rodlike particles called whiskers or nanofibers.<sup>87</sup> Generally, their geometrical characteristics depend on the origin of cellulose microfibrils and acid hydrolysis process conditions such as time, temperature and purity of materials.



**Fig. 1.4:** Structures of (a) SWCNT, (b) MWCNT and (c) cellulose chain

### *Nanoparticles*

The different metal nanoparticles like silver, copper, magnetic iron etc. and spherical silica where all the three dimensions are in nanometer scale are the examples of this class. The nanoparticles are also often named as equi-axed or nanogranules or nanocrystals. They have different shapes depending on their sizes and the same nanoparticles may have different shape, size and behavior.

Nanoparticles are generally thermodynamically unstable. To produce stable nanoparticles, they must be arrested during the preparation either by adding surface protecting reagents, such as organic ligands or inorganic capping materials, or by placing them in an inert environment such as an inorganic matrix or polymers. In general, the nanoparticles are obtained by different routes such as sol process, chemical precipitation, sol-gel process, hydrothermal/solvothermal synthesis, reaction in confined space, pyrolysis, vapor deposition etc. However, for preparing monodisperse nanostructures, the process requires a single, temporally short nucleation event followed by slower growth on the existing nuclei.<sup>88</sup>

### **1.3.2. Methods**

The preparative techniques of polymer nanocomposite are mainly classified into three categories. These are namely solution, *in-situ* polymerization and melt-mixing techniques. All these techniques are discussed briefly in this section.

#### *1.3.2.1. Solution Technique*

In solution technique, a solvent or a solvent mixture swells and disperses the nanofillers into the polymer solution and then the solvent(s) is evaporated from this combined homogeneously dispersed mixture or the mixture is precipitated out in a non-solvent. Depending on the interaction of the solvent and the nanofiller, the nanofillers may be

delaminated in an adequate solvent due to weak van der Waals force that stacks the layers or tubes or particles together. Then, the polymer chains adsorb onto the delaminated individual nanofillers. Depending on the interactions between polymer and nanofillers the resultant structure may be either intercalated or exfoliated.

During solvent evaporation or precipitation, if the nanofillers do not reassemble or the polymer chains do not allow them to come closer the resultant composites will be exfoliated nanocomposites. In general, after solvent evaporation, the nanofillers reassemble to reform the stack with polymer chains sandwiched in between and forming a well-ordered structure. In the inter-gallery space, the adsorbed polymer chains do not coil but remain in almost fully extended state. Thus, after solvent evaporation, generally an intercalated nanocomposite is formed. For the overall process, in which polymer is exchanged with the previously intercalated solvent in the gallery, a negative variation in the Gibbs free energy is required. The driving force for the polymer intercalation into nanofillers from solution is the entropy gained by desorption of solvent molecules, which compensates for the decreased entropy of the confined, intercalated chains.<sup>89</sup> Using this method, intercalation only occurs for certain polymer/solvent pairs. This method is good for the intercalation of polymers with little or no polarity into layered structures, and facilitates production of thin films with polymer-oriented clay intercalated layers. However, from industrial point of view, this method involves the copious use of organic solvents, which is usually environmentally not acceptable as well as economically prohibitive. Nevertheless it is an attractive route for water soluble polymers, as water is used as solvent in that case.

### *1.3.2.2. In-situ Polymerization Technique*

*In-situ* polymerization involves inserting of a polymer precursor between nanofillers followed by expanding and dispersing of the nanofillers into the polymer matrix by the polymerization process. The nanofillers is swollen within the liquid monomer (or a pre-polymer solution) so as the polymer formation can occur in between the intercalated nanofillers. Polymerization can be initiated either by heat or radiation, or by the diffusion of a suitable initiator or catalyst inside the nanofillers before the swelling step by the monomer. Polymerization produces long-chain polymers within the nanofillers. Under the used conditions in which intra- and extra-gallery polymerization rates are properly balanced, the nanofillers are delaminated and the resulting material possesses a disordered structure.<sup>90</sup> The driving force of this technique is related to the secondary

interactions of the monomers. In the swelling state due to the high surface energy, the nanomaterials attract the monomer molecules so that they diffuse between the layers or tube structure of nanomaterials. After reaching the equilibrium the diffusion of the monomer is stop and the nanomaterials are swelled. During polymerization, the polymer chains start to grow within the nanomaterials and ultimately resulted the exfoliated structure.

It is easier to break up the agglomerates by this technique, using a high shear device and to achieve more uniform mixing of nanomaterials in the monomer, because of low viscosity of the monomer or pre-polymer compared to polymer as in other techniques. In addition, the low viscosity and diffusivity result in a high rate of monomer or pre-polymer diffusion into the interlayer of clay region. Furthermore, it is possible to control nanocomposite morphology through the combination of reaction conditions and nanofiller surface modification. This method is capable of producing well-exfoliated nanocomposites and has been applied to a wide range of polymer systems. This technique is suitable for polymer manufacturers to produce clay/polymer, metal/polymer nanocomposites in polymerization process itself. This technique is particularly useful for thermosetting polymers. *In-situ* polymerization is the first reported method to prepare the polymer/clay nanocomposites.

### *1.3.2.3. Melt Mixing Technique*

This process involves mixing of the polymer and nanofillers above the softening point or at processing temperature of the polymer under shear. Under these conditions and if the layer surfaces are sufficiently compatible with the chosen polymer, the polymer can crawl into the interlayer space and form either an intercalated or an exfoliated nanocomposite depending on the degree of penetration of the polymer chains in-between the nanofillers.<sup>83,90</sup> While heating, the polymer chains can diffuse in between the nanofillers. Although there is an entropy loss associated with the confinement of a polymer melts by the formation of nanocomposite, this process is allowed because there is an entropy gain associated with the layer separation.

The melt mixing method may not be as efficient as that of *in-situ* polymerization and solution technique and often produces partially exfoliated structures. But at the same time, this approach can be applied by the polymer processing industry to produce nanocomposite based on traditional polymer processing techniques, such as extrusion and injection molding. In addition, the absence of a

solvent makes direct melt intercalation an environmentally sound and an economically favorable method for industries. Thus this technology has an ample contribution in spreading up the process for commercial production of polymer nanocomposite.

Besides the above methods there are other techniques too, which are used sometimes to prepare polymer nanocomposites. Among these template synthesis and sol-gel process are the most important and hence discussed briefly.

### *1.3.2.4. Template Synthesis*

In this technique, the nanomaterials are synthesized in the presence of the polymer matrix. It is also called as *in-situ hydrothermal crystallization*.<sup>88</sup> Here, the nanofillers are synthesized from precursor solution using polymers as template. This technique is widely used for the synthesis of LDH based nanocomposites but is far less developed for layered silicates. Though this technique presents high potential route for the dispersion of the nanofillers in a one-step process, without needing the presence of the onium ion, in the polymer matrices at nanometer scale, however it suffers from some drawbacks. The synthesis process generally requires the use of high temperatures, which may degrade the polymers. The silicate materials generated by the self-assembly process have also the tendency to aggregate.

### *1.3.2.5. Sol-Gel Technique*

The sol-gel technique is based on inorganic polymerization reactions. It is a wet chemical technique, also known as chemical solution deposition. It involves four steps: hydrolysis, polycondensation, drying and thermal decomposition. The precursors of the metal or non-metal alkoxides are hydrolyzed using water or alcohols according to the hydrolysis process.<sup>91</sup> Most of the colloidal nanocomposites are prepared by this technique, where the silica precursors are precipitated in controlled manner onto the polymer core particles to form silica coated hybrid colloids. Polymer latexes are commonly used as colloidal templates and therefore the surface modification of the polymer particles is carried out to increase the chemical affinity with the shell. The conditions of the sol-gel reactions employed have a dramatic effect on the structure of the inorganic network formed, which makes it difficult to control the size and arrangement of the inorganic domain in the hybrid materials at the molecular level. The limitation in the selection of polymers and the severe difficulty in synthesizing hybrid

materials with stable quality and high reliability are a bottleneck in the stable supply and industrial application development of hybrid material products.

Besides these, large varieties of other techniques are also employed for the preparation of polymer nanocomposites. These include cryogenic ball milling, thermal spraying, plasma induced polymerization, evaporation of elemental metal with its deposition on polymeric matrices, thermal decompositions of metal ions using different procedures etc. However, to achieve the uniform distribution of the nanoparticles through these techniques is very difficult and thus they are not used, in general.

### 1.3.3. Characterization

#### 1.3.3.1. Polyester Matrix

Polyesters are being characterized by the conventional analytical and spectroscopic techniques similar to the other polymers. Different physical properties like iodine value, acid value, saponification value, hydroxyl value, viscosity, volatile matter content, specific gravity etc. are determined by using the standard techniques.<sup>92</sup> Structural confirmation, molecular weight determination, rheological behavior and thermal characterization are generally done by techniques like Fourier transform infrared (FTIR)/nuclear magnetic resonance (NMR), gel permeation chromatography (GPC) analysis, rheometer/dynamic mechanical analyzer (DMA) studies and thermogravimetric analysis (TGA)/differential scanning calorimetry (DSC)/thermo-mechanical analyzer (TMA) respectively.<sup>93-97</sup> Crystallinity and morphology in certain cases are characterized by X-ray diffractometer (XRD) and scanning electron microscopy (SEM) respectively.

#### *Analytical Techniques*

Hydroxyl value of a polymer is a measure of the hydroxyl content and is defined as the numbers of milligram of KOH equivalent to the hydroxyl content of one gram of the polymer.<sup>92</sup> Determination of physical property like iodine value indicates the degree of unsaturation present in the resin, which implies their drying ability by the conventional drying techniques. Similarly, the results of acid value, saponification value, hydroxyl value and viscosity<sup>98</sup> indicate the level of free  $-\text{COOH}$  groups, molecular weight (chain length), free  $-\text{OH}$  groups and processibility respectively. The extent of reaction in the preparation of polyester resin is monitored by determination of acid value at various time intervals of the resinification reaction.<sup>99</sup>

### *Spectroscopic Techniques*

FTIR technique<sup>93</sup> is largely used to determine the functional groups present in the structure like carboxyl group, ester group, hydroxyl group, unsaturation, aromatic ring etc. The curing reactions of palm oil based polyester and melamine-formaldehyde resin blends is studied by FTIR technique.<sup>100</sup> The significant reduction of the absorbance bands of -OH and  $>NCH_2OCH_3$  and formation of methylene ether linkages with time at constant temperature is utilized for this purpose. The photoacoustic Fourier transform infrared spectroscopy has also been utilized for *in-situ* measurements of the curing processes in polyester based on soybean fatty acids.<sup>101</sup> FTIR spectroscopy is also utilized for the determination of the oil content in oil modified orthophthalic polyester resins.<sup>102</sup> Even miscibility of chlorinated polypropylene with polyester resin in the specified mixing ratios is studied by FTIR spectra.<sup>103</sup>

<sup>1</sup>H NMR can play an important role to understand the actual structures of a range of polyester binders and their precursors, the drying oil, polyhydric alcohol and aromatic acids being used.<sup>104</sup> In general, <sup>1</sup>H NMR indicates the presence of different types of protons like carboxylic, hydroxyl, ester, carbonyl, hydrocarbons of saturated and unsaturated, aliphatic, aromatic etc.<sup>97</sup> This spectroscopic technique is also used for fast qualitative and quantitative determination of fatty acids in polyester resins. In addition to structural identification of the oil, the <sup>1</sup>H NMR spectra provided quantitative determination of the oil, the phthalic anhydride and polyhydric alcohol components in the polyester resins.<sup>105</sup> Similarly <sup>13</sup>C NMR technique<sup>93</sup> is utilized to find out the presence of chemically different carbon atoms in aromatic, aliphatic, unsaturated, saturated hydrocarbons, in ester, carboxyl group etc. It is also used to measure the extent of reaction in polyesters as the degree of curing of the resins affects the resolution of the spectrum.<sup>106</sup> Spyros reported<sup>107</sup> the application of advanced 1D and 2D <sup>1</sup>H and <sup>13</sup>C NMR techniques for the characterization of various polyester resins used in the coating industry. 2D NMR allows the spreading of chemical shift information in two dimensions, so much more for polyesters exhibiting complex 1D NMR spectra with broad and/or featureless peaks.

### *Other Techniques*

The molecular weight and its distribution of oil modified polyesters are generally determined by GPC technique. The use of GPC analysis for monitoring the formation

of di- and mono-glyceride, and di- and mono-trimethylol propane esters has also been reported.<sup>108</sup>

The thermal characterizations of the resin are generally carried out by TGA and DSC techniques. By TGA technique along with the thermostability of the resins in different environment, the pattern of degradation, kinetics of degradation, char residue etc. are determined.<sup>95,96</sup> Whereas DSC technique is most widely used to get the information about the phase change, different chemical changes like degradation, cross-linking etc.<sup>95,96</sup> The kinetic of cross-linking reactions is also determined by DSC technique. The nature of curing reaction of polyesters based on dehydrated castor oil fatty acid and melamine-formaldehyde resin mixture<sup>109</sup> is studied by DSC. The use of DSC is also reported for the determination of optimum curing temperature for mixture of polyester and melamine-formaldehyde resins and for measurement of peroxides formed in order to monitor drying extent of polyester resins.<sup>110</sup>

In addition to the above techniques, scanning electron microscopy (SEM) is utilized to study the morphology of the blends of polyesters with other resins and compounded polyesters (paints), which indicate the dispersibility, compatibility of different components present in the system.<sup>111</sup> Aurelia et al.<sup>112</sup> reported the study of morphology of polyester and melamine-formaldehyde resins and their mixtures with clay by using transmission electron microscopy (TEM). Atomic force microscopy (AFM) is used to study the surface structure of polyesters.<sup>113</sup>

#### *1.3.3.2. Nanocomposites*

The microscopic structure of polymers is often studied by X-ray techniques and neutron scattering. The XRD technique is based on the elastic scattering of X-rays from the structures that have long-range order, and it is an efficient analytical technique used to identify and characterize crystalline materials. Due to its ease of use and availability, XRD is most commonly used to probe the nanocomposite structure and occasionally to study the kinetics of polymer melt intercalation.<sup>114</sup> This technique allows the determination of the spaces between structural layers of the silicate by utilizing Bragg's law:  $2d\sin\theta = n\lambda$ , where  $\lambda$  corresponds to the wave length of the X-ray radiation used in the diffraction experiment,  $d$  is the spacing between diffracted lattice planes and  $\theta$  is the measured diffraction angle or glancing angle in case of polymer/clay nanocomposites. By monitoring the position, shape and intensity of the basal reflections from the distributed silicate layers, the nanocomposite structure can be identified. For the



nanolayered silica nanocomposites, XRD is commonly performed to analyze the degree of orderness of the nanocomposites. The absence of such a peak is not conclusive evidence for a highly exfoliated structure; many more factors must be considered to interpret XRD patterns. If the sensitivity or counting time of the scan is low then an existing peak may not be seen. When the nanofillers are internally disordered or not well aligned to one another, the peak intensity will be low and may appear to be completely absent.<sup>115</sup>

WAXRD involves measuring scattering intensity at scattering angles  $2\theta > 5^\circ$ , where SAXRD patterns are recorded at very low angles (typically  $< 5^\circ$ ). In this angular range, information about the shape and size of the in-homogeneities are obtained. The scattering methods can also give geometrical descriptions of the structures using the concept of fractal geometry because random processes of polymerization or aggregation usually result in formation of fractal objects.<sup>116</sup>

Neutron scattering is preferred sometimes due to the extended  $q$ -range (with respect to standard X-ray laboratory sources), giving access to length scales between several thousand angstroms. SANS measurements made on the polymer-grafted particles led to an understanding of the system behavior during the polymerization procedure. These observations permit improvement of the synthetic conditions to get a better dispersion of the particles and a better control of the polymerization process. The SANS technique is well suited for the size range of interest, and due to the unique possibility of contrast variation, it is able to highlight independently the contributions of the polymer layer and of the silica beads or aggregates.

TEM, SEM and AFM are three powerful microscopy techniques used to observe the morphology of nanocomposites. In TEM a beam of electrons is transmitted through an ultrathin specimen and carries information about the inner structure of the specimen. It is difficult to receive details of some samples due to low contrast resulting from weak interaction with the electrons; this can partially be overcome by the use of stains such as phosphotungstic acid and  $\text{RuO}_4$ . Sometimes the organic components of the sample would be decomposed by the electron beam; this can be avoided using cryogenic microscopy (cryo-TEM), where the specimen is measured at liquid nitrogen or liquid helium temperature under a frozen state. High resolution TEM (HRTEM) can afford a much closer look at the samples.<sup>116</sup> The recent application of electron energy loss spectroscopy imaging techniques to TEM (ESI-TEM) can provide information on the composition of polymer surfaces. This is a powerful technique for the

## Chapter 1

characterization of colloidal nanocomposite particles.<sup>117</sup> This technique enables the spatial location and concentration of the ultrafine silica sol within the nanocomposite particles to be determined. Combined TEM and SAXS investigations are shown to be important tools in gaining complete information about the morphology of the materials. TEM analysis gave visible information on the extent of particle separation in the nanocomposites depending on the surface modification over a broad scale range including especially large sized aggregates. On the other hand, SAXS analysis enabled acquisition of more detailed information about size distributions of primary particles and “mean” size aggregates in the real nanosize range below 20 nm.

The scanning electron microscope (SEM) is a type of electron microscope that creates images by the electrons emitted when the primary electrons coming from the source strike the surface and are in-elastically scattered by atoms in the sample. SEM images have a characteristic 3D appearance and are therefore useful for judging the surface structure of the sample. Besides the emitted electrons, X-rays are also produced by the interaction of electrons with the sample. These can be detected in a SEM equipped for energy-dispersive X-ray (EDX) spectroscopy.<sup>116</sup> The fracture surface is very dense. Both the SEM and EDX Si-mapping results indicated the homogeneous dispersion of the silica in the polymer matrix.

AFM is an effective tool to characterize nanocomposites by providing the morphological information. The AFM consists of a sharp tip (10-20 nm diameter) attached to a stiff cantilever. The tip is brought close to the surface and the sample is scanned beneath the tip. The tip moves in response to tip-surface interactions and this movement is measured by focusing a laser beam onto the back of the cantilever and detecting the position of the reflected beam with a photodiode.<sup>116</sup>

Ultraviolet (UV) visible spectrophotometer is another very important tool for characterization of nanocomposites. This is specially used for metal/polymer nanocomposites. The formation of metal nanoparticles from its precursor compounds can be easily detected by UV-visible spectroscopic measurement in a suitable solvent/solvent mixture. Different nanometals have unique characteristic spectrum of individual metal.

The <sup>1</sup>H NMR technique allows measurement of the total topological constraint density (such as entanglements or cross-links) in polymeric systems. By comparing the transverse magnetization relaxation of reinforced and non-reinforced matrices, one can estimate the topological constraints density at the particle/matrix interface.<sup>116</sup>

## Chapter 1

Characterization of polymer/layered silicate nanocomposites by  $^{13}\text{C}$  solid-state nuclear magnetic resonance ( $^{13}\text{C}$  NMR) is also proposed. van der Hart et al.<sup>118</sup> first used this technique as a tool for gaining greater insight about the morphology, surface chemistry, and to a very limited extent, the dynamics of exfoliated polymer clay nanocomposites. They are especially interested in developing NMR methods to quantify the level of clay exfoliation, a very important facet of nanocomposite characterization. The main objective in solid-state NMR measurement is to connect the measured longitudinal relaxations of proton (and  $^{13}\text{C}$  nuclei) with the quality of clay dispersion.

Some authors also used Fourier transform infrared spectroscopy (FTIR) to elucidate the structure of the nanocomposites. FTIR may be able to identify differences between the bonding in a mixture and the bonding in a related nanocomposite, but as these variations are minute, even when intercalation has taken place. However, FTIR is an unreliable method of characterization in most of the cases.<sup>90</sup>

Gas transport in polymers is known to be strongly dependent on the amount of free volume in the polymer matrix. Positron annihilation lifetime spectroscopy (PALS) is a technique that probes the free volume cavities by measuring the lifetime of *ortho*-positronium (*o*-Ps) before annihilation in the free volume regions of the polymer. The lifetime of *o*-Ps (normally 2-5 ns) is a direct measure of the free volume size.<sup>116</sup>

Differential scanning calorimetry (DSC) provides further information concerning intercalation. The intercalated chains of the polymer create many interactions with the host species greatly and thereby reduce their rotational and translational mobility.<sup>90</sup> The situation is similar to that in a reticulated polymer, where restrictions on its mobility increase its glass transition temperature ( $T_g$ ). A similar increase is anticipated to occur in a nanocomposite due to elevation of the energy threshold needed for the transition. This effect is readily detected by DSC. In addition to being an interesting analytical datum, the considerable increase in  $T_g$  is an important property of these materials that enables them to be employed at higher temperatures compared with the original polymer and thus extends their fields of application.<sup>119</sup>

The rheometric study and dynamic mechanical analysis (DMA) are utilized to measure the viscous and elastic components of polymer nanocomposite in terms of storage ( $G'$ ) and loss modulus ( $G''$ ), which in turn help in determination of state of dispersion of nanofillers in matrix. The well dispersed nanofillers caused shifting of  $G'$  and  $T_g$  values of the nanocomposite. They also measure the stiffness of nanocomposite quantitatively.

## Chapter 1

Dynamic light scattering (DLS) and disk centrifuge photosedimentometry (DCP) are also sometime used to unveil the structural aspect as well as conformation of the nanocomposites. X-ray photoelectron spectroscopy (XPS) is a surface analytical technique for assessing surface compositions. The XPS data combined with TEM studies of the ultra-microtomed particles can shed further light on particle morphology. The other techniques such as determination of mechanical properties, chemical resistance, flame retardancy, barrier property etc. are same as that of the conventional polymer composites.

### *1.3.4. Properties*

Nanocomposites consisting of a polymer and small amount ( $\leq 5$  wt.%) of nanofiller frequently exhibit remarkably improved properties as compared to those of pristine polymers. The improvements include increased mechanical strength and modulus, thermal properties, decreased gas permeability and flammability, increased biodegradability of biodegradable polymer etc. The main reason for these improved properties in nanocomposites is the strong interfacial interaction between the polymer matrix and the nanofillers. Therefore, the researchers are being attracted in this field to design high performance polymeric materials with the help of nanotechnology. Various properties of polymer nanocomposites are briefly presented here.

#### *1.3.4.1. Mechanical*

The mechanical properties of polymer nanocomposites are the most important amongst the other properties. With the addition of nanofillers to the polymers the mechanical properties improved tremendously over the pristine polymer.<sup>120</sup> The tensile strength generally increases with the increase in amount of nanofiller. However the values generally decreased at high level of nanofiller loading (nanoclay  $> 5$  wt.%). This mechanical property is dependent on the structure of the nanocomposite such as the extent of dispersion of nanofillers in the matrix i.e. the intercalation or exfoliation or agglomeration state of nanofillers. The exfoliation or delamination configuration is of particular interest because it maximizes the polymer-nanofiller interactions making the entire surface of nanofillers available for the polymer. The exfoliated nanocomposites give better mechanical properties than intercalated ones. The enhancement of this property of polymer nanocomposites is attributed to the high rigidity and aspect ratio together with the good affinity between polymer and the nanofiller. The complete

## Chapter 1

dispersion of nanofillers in a polymer matrix optimizes the number of available reinforcing elements for carrying an applied load and deflecting cracks. The coupling between the tremendous surface area of the nanofiller and the polymer matrix facilitates stress transfer to the reinforcement phase and thereby improving the mechanical properties.<sup>121</sup> High amount of nanofillers leads to agglomeration of the nanofillers and deterioration of the property. On the other hand, the elongation at break values of nanocomposites generally decreases but sometimes it remains constant or even increased. The increased restricted movement of polymer chains is attributed to the decrease of elongation at break but the increase of elongation at break value may be due to formation of nanodomain shear zones under stress and strain, and plasticization effect. Impact resistance is another important mechanical property for many end applications of polymers. It is a combined effect of flexibility and strength of the materials. Hardness of polymer nanocomposites is important from application point of view as it refers to the resistant to change of shape when force is applied. There are three major types of hardness viz. scratch hardness, indentation hardness and rebound hardness. The hardness of polymer nanocomposite depends on type of nanofillers and the interfacial interactions between fillers and polymer chains.<sup>116</sup>

Dynamic mechanical analysis (DMA) measures the dynamic mechanical properties of polymer nanocomposites. It determines response of a material to a cyclic deformation (usually tension or three-point bending type deformation) as a function of the temperature. DMA results are expressed by three main parameters: (i) the storage modulus ( $E'$  or  $G'$ ), correspond to the elastic response of the deformation; (ii) the loss modulus ( $E''$  or  $G''$ ), correspond to the plastic response of the deformation and (iii)  $\tan\delta$ , that is, the  $E''/E'$  (or  $G''/G'$ ) ratio, useful for determining the occurrence of molecular mobility transitions such as the glass transition temperature.<sup>83</sup> In the case of nanocomposites, the main conclusion derived from dynamic mechanical studies is that the storage modulus increases upon dispersion of a nanofillers into a polymer matrix. This increase is generally higher above the glass transition temperature than below this transition and for exfoliated nanocomposite structures than intercalated ones. This is probably due to the creation of a three-dimensional network structure interconnected with nanofillers, strengthening the material through mechanical percolation. Above the glass transition temperature, when materials become soft, the reinforcement effect of the nanofillers become more prominent and thereby restricts the movement of the polymer chains. This results in the observed enhancement of  $G'$ . Enhancement of the

loss modulus ( $G''$ ), is also reported for nanocomposites. However this aspect of dynamic mechanical performance is far less discussed in the literature. Finally, the  $\tan\delta$  values are affected in different ways by nanocomposite formation, depending on the polymer matrix. It depends not only on the dispersion state of nanofillers but also on the type of matrix used.

### *1.3.4.2. Barrier*

Generally, polymer nanocomposites are characterized by very strong enhancements of their barrier properties. The dramatic improvement of barrier properties can be explained by the concept of tortuous path. While impermeable nanofillers are incorporated into a polymer, the permeating molecules are forced to wiggle around them in a random walk, and hence diffuse by a tortuous pathway. The tortuosity factor is defined as the ratio of the actual distance that the penetrant must travel to the shortest distance that it would travel in the absence of barriers.<sup>90</sup> A sheet-like morphology is particularly efficient at maximizing the path length, due to the large length-to-width ratio, as compared to other filler shapes. The different polymer nanocomposites show enhanced barrier property to various gases, liquids, water vapor and other small molecules. Improvements in capability of the polymer nanocomposite based membranes for gas separation have also been achieved.

Although a decrease of diffusivity is a well-established result of formation of nanocomposite, contradictory results are reported concerning the saturation uptake values of various solvents or gases. Increases of the saturation uptake level are usually attributed to clustering phenomena.<sup>90</sup> It is worth noticing, however, that in nanocomposites the co-existence of phases with different permeabilities can cause complex transport phenomena. On the one hand, the nanofillers mainly organophillic nanoclay gives rise to superficial adsorption and to specific interactions with the solvents. In turn, the polymer phase can be considered, in most cases, as a two-phase, crystalline-amorphous system. The crystalline regions are being generally impermeable to penetrant molecules. The presence of the silicate layers may be expected to cause a decrease in permeability, due to the more tortuous path for the diffusing molecules that must bypass impenetrable platelets.<sup>122</sup> Simultaneously, the influence of changes in matrix crystallinity and chain mobility, induced by the presence of the filler, should always be taken into consideration.<sup>123</sup>

### *1.3.4.3. Thermal*

Thermal properties are the properties of materials that changes with temperature. They are studied by thermal analysis techniques, which include DSC, TGA, DTA, TMA, DMA/DMTA, dielectric thermal analysis etc. TGA/DTA and DSC are the two most widely used methods to determine the thermal properties of polymer nanocomposites. TGA can demonstrate the thermal stability, the onset of degradation and the percent nanofillers incorporated in the polymer matrix.<sup>116</sup> DSC can be efficiently used to determine the thermal transition behavior of polymer nanocomposites. Furthermore, the coefficient of thermal expansion (CTE), which is the criterion for the dimensional stability of materials, can be measured with TMA. In addition, thermomechanical properties measured by DMA/DMTA are very important to understand the viscoelastic behavior of the nanocomposites. The storage modulus ( $G'$ ), loss modulus ( $G''$ ) and  $\tan \delta$  ( $G''/G'$ ) are three important parameters of dynamic mechanical properties that can be used to determine the occurrence of molecular mobility transitions, such as glass transition temperature,  $T_g$ . Dielectric thermal analysis is also useful to understand the viscoelastic behavior of the nanocomposites. Generally, the incorporation of nanometer-sized nanofillers into the polymer matrix can enhance thermal stability by acting as a superior insulator and mass transport barrier to the volatile products generated during decomposition. Meanwhile, the incorporation of nanometer-sized inorganic particles such as silica is very effective in decreasing the CTE of the polymer matrix.<sup>116</sup>

### *1.3.4.4. Flame Retardancy*

Polymer nanocomposites are emerged as one of the most promising developments in the area of flame retardancy, appearing to offer significant advantages over conventional formulations like regulatory concerns about the human and environmental contamination caused by the toxic chemicals, which are evolved during the combustion of halogens; high levels of loading; additional costs; processing difficulties; deterioration of polymer mechanical properties etc. A flame retardant is used to make materials harder to ignite by slowing decomposition and increasing the ignition temperature. It functions by a variety of methods such as absorbing energy away from the fire or preventing oxygen from reaching the fuel.<sup>116</sup> The flammability behavior of polymer is defined on the basis of several processes or parameters, such as burning rates, spread rates, ignition characteristics etc. There are several standard methods to test the flame retardancy of polymer nanocomposites. Among them the following are

## Chapter 1

the five main types: ignitability tests (or UL94); flame spread tests; limiting oxygen index (LOI); heat release tests (cone calorimeter), smoke and toxicity tests. The other useful indicator at the research and development stage is char yield obtained from thermal gravimetric analysis (TGA) under either air or nitrogen atmosphere. Thick char becomes a good thermal insulating layer, which undergoes slow oxidative degradation and prevents heat to reach to the remaining polymer. Lewin pointed out that the char obtained in the intumescent systems are different from the char from TGA. The former are prepared at lower temperatures and are not fully pyrolyzed or oxidized, their rate of formation is high and involves thermo-oxidation though they serve the same purpose, namely acting as barriers to the passage of molten polymer and generated gases.<sup>124</sup>

The improved flame retardancy of nanocomposite is described on the basis of formation of char residue. This effectively reduces the amount of flammable small molecules into vapor phase and decreases the heat release rate. The char also holds the material structural integrity and thereby preventing fire spreading. The char creates a protective layer that impedes oxygen penetration and creates an insulating layer between heat and fuel. Synergistic effect on enhancing flame retardancy can also be achieved by incorporation of atoms like phosphorus, sulfur, nitrogen, metal/metalloid etc. into polymer precursor along with nanofillers.

### *1.3.4.5. Rheological*

Rheology is the study of the deformation and flow of matter under the influence of an applied stress. The measurement of rheological properties is helpful to predict the physical properties of polymer nanocomposites as well as useful for processing.<sup>116</sup> The measurement of the rheological properties of any polymeric material is crucial to gain fundamental understanding of the processibility of that material and is usually conducted by either dynamic oscillatory shear or steady shear measurements. In case of polymer nanocomposites, the study of rheological properties is instructive for two reasons: first, these properties are indicative of melt processing behavior in unit operations, such as injection molding. Second, since the rheological properties of particle-filled materials are sensitive to the structure, particle size, shape and surface characteristics of the dispersed phase, rheology potentially offers a means to assess the state of dispersion in nanocomposites, directly in the melting state. Thus, rheology can be envisaged as a tool that is complementary to traditional methods of materials characterization. It is generally established that when nanocomposites are formed, the



viscosity at low shear rates increases with nanofiller concentration.<sup>90</sup> Very often, solid-like behavior is observed, which is attributed to the physical jamming or percolation of the randomly distributed nanofillers, at surprisingly low volume fraction, due to their anisotropy. On the other hand, at high shear rates, shear thinning behavior is usually observed. It has been suggested that this is the result of the alignment of nanofillers towards the direction of flow at high shear rates.<sup>125</sup> Such observations support the percolation argument used in the case of nanocomposite rheological behavior under low shear.

### *1.3.4.6. Optical*

The polymer nanocomposites containing polymers with optically active functional group or material show different interesting optical properties.<sup>126</sup> These include transparency, refractive index, fluorescence, luminescence, non-linearity etc. In polymer nanocomposite, the nano-sized fillers enhance the optical properties while the polymer matrix acts as stabilizer to the particle size and growth of the fillers. The nanocomposites for the transparent pristine polymers remain as optically clear since no marked decreased in clarity is observed due to the dispersed nanofillers in the polymer matrix.

### *1.3.4.7. Electrical*

Electrical properties of polymers include several electrical characteristics that are commonly associated with dielectric properties and electrical conducting properties. Electrical properties of polymers are expected to be different when the fillers get to the nanoscale for several reasons. First, quantum effects begin to become important, because the electrical properties of nanoparticles can change compared with the bulk. Second, as the particle size decreases the inter-particle spacing decreases for the same volume fraction. Therefore, percolation can occur at lower volume fractions.<sup>116</sup> In addition, the rate of resistivity decrease is lower than in micrometer scale fillers. This is probably due to the large interfacial area and high interfacial resistance. Battisti et al.<sup>127</sup> reported the electrically conductive thermosetting polyesters nanocomposites based on carbon nanotubes. They determined electrical properties of the nanocomposites by AC impedance spectroscopy and DC conductivity measurements.

### *1.3.4.8. Biodegradation*

Another interesting and exciting aspect of polymer nanocomposites is their significant improvement of biodegradability often reported by the formation of nanocomposite. The improved biodegradability of the nanocomposites may be attributed to catalytic role of the nanofillers in biodegradation process. A typical biodegradation process involves four main steps viz. water absorption, ester cleavage and formation of oligomeric fragments, solubilization of oligomeric fragments, and ultimately removal of soluble oligomers by microorganisms.<sup>128</sup> Therefore any factor which influences the hydrolysis tendency may control the biodegradation process. In case of polymer/clay nanocomposites the terminal hydroxyl group of silicate layers is one of the reasons for improvement of biodegradation ability of polymers.

### ***1.3.5. Applications***

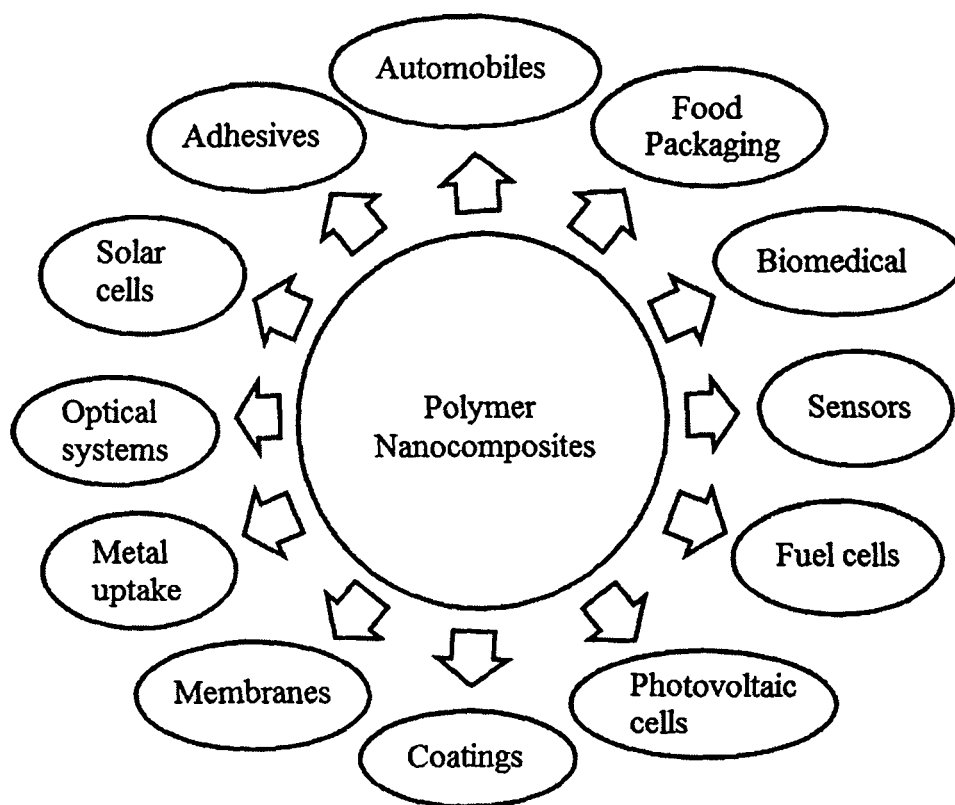
Polymer nanocomposites represent an exciting and promising alternative to the pristine polymer or conventional composites or filled systems owing to the dispersion of nanofillers and their markedly improved performance in mechanical, thermal, barrier, optical, electrical, and other physical and chemical properties. These unique properties of polymer nanocomposites provide with myriad of applications in different fields. This results a strong interest and investment of fund by many companies in developing polymer nanocomposites for their products. A few applications of polymer nanocomposites are shown in Fig. 1.5.

Today, polymer nanocomposites offer their high performance with significant weight reduction, reduced materials density and high fuel efficiency to afford materials for transport industries such as automotive and aerospace. The first commercial product of polymer nanocomposites is the timing-belt cover made from nylon-6 nanocomposites in Toyota Motors in early 1990s. Such timing-belt cover exhibited good rigidity, excellent thermal stability and no wrap.<sup>90</sup> Besides, it is also used as engine cover, oil reservoir tank and fuel hoses in the automotive industry because of their remarkable increase in heat distortion temperature and enhanced barrier properties together with their improved mechanical properties. It is now believed that polymer nanocomposites can be utilized as potential materials in various vehicles for external and internal parts such as mirror housings, door handles and under-the-hood parts. The weight advantage of polymer nanocomposites could have a significant impact on environmental protection and material recycling. Polyester nanocomposites have also their own niche in automotive industries.

## Chapter 1

The excellent barrier properties of polymer nanocomposites resulted considerable enhancement of shelf-life for many types of packaged food. Also the optical transparency of polymer nanocomposite film make them acceptable widely in packaging industries as wrapping films and beverage containers, such as processed meats, cheese, confectionery, cereals, fruit juice and dairy products, beer and carbonated drinks bottles.<sup>129</sup> For example, Bayer has recently developed a new grade of plastic films for food packaging which are made from nylon-6/clay based exfoliated nanocomposites.

On the other hand, enormous amounts of large varieties of plastics used today are produced mostly from fossil fuels and after their useful service life they are discarded in the environment. These plastics do not degrade spontaneously and thus are treated by incineration, resulting in large amounts of carbon dioxide or even more toxic gases.<sup>130</sup> Therefore, there is an urgent need for the development of environment-friendly polymer materials that would not involve the use of toxic or noxious components in their manufacture and could allow degradation via a natural process specifically in some applications such as composting, packaging, agriculture and hygiene. To meet such a goal, various biodegradable polymers have recently been reported to be used in the manufacturing of polymer nanocomposites.



*Fig. 1.5: Different fields of applications of polymer nanocomposites*

## Chapter 1

The combination of hardness, scratch resistance and flexibility is a highly desired feature in many surface coating applications. Many reports are found which have developed the polymer nanocomposites for coating purposes. Polyester nanocomposites with different type of nanofillers such as nanoclay, metals nanoparticles etc. are used to obtain highly hydrophobic, antimicrobial, flame retardant, high performance and thermostable surface coatings. Besides surface coating materials the polymer nanocomposites are also used as adhesive and sealant. Very recently Fogelstrom et al.<sup>131</sup> introduced montmorillonite in hyperbranched polyester resin to design hard and flexible coatings which showed enhanced surface hardness, scratch resistance and flexibility as well as excellent chemical resistance and adhesion. Composites with gel coats are an essential part of many aspects of life today; from bathroom units to boats; from cultured marble to airplane structures; from windmills to automotive parts. Gel coat imparts good surface finish and bears better hardness, scratch resistance, and resistance to corrosion and water absorption to the composites. It is expected that the incorporation of nanoclay in gel coat would lead to an improvement in the properties, which will make the material viable in high-loading environment. Jawahar et al.<sup>132</sup> reported the nanocomposite gel coat system using unsaturated polyester resin with aerosil and CaCO<sub>3</sub> powders and organoclay.

Another most demanding application of polymer nanocomposites is their biomedical applications. They are now used as biosensors as well as medical implants. The property enhancement, especially on heat responsivity, swelling-deswelling rate and molecular diffusion, is expected to extend the nanocomposites to such applications as artificial muscles and rapid actuators.<sup>129</sup>

Polymer nanocomposites open a promising route to novel organic-inorganic materials with peculiar electrical properties. The remarkable electrochemical behavior of conducting polymers associated with nanomaterials attracts potential applications such as modified electrodes biosensors, solid-state batteries, smart windows and other electrochemical devices. Recently Kawasaki<sup>133</sup> et al. used fluorine-based polyester as matrix for carbon nanotubes to prepare nanocomposites which can be used optical fields because of their high thermostability, transparency, refractive index and low birefringence.

The sensor technology is highly utilizing the advantages of nanotechnology.<sup>134</sup> The polymer nanocomposites are utilized for sensitivity of gas, humidity, toxic chemicals, metals etc. The factors like accuracy of sensitivity, selectivity,

reproducibility, scanning time etc. are dependent directly on the sensing capability of the membrane.

### **1.4. Vegetable Oil Based Highly Branched Polyester Nanocomposites: A Short Review**

#### ***1.4.1. Introduction***

The production, use and disposal of technical products have strong impact on the ecological, economic and social sectors of sustainable development. Thus, there is a growing urgency to develop novel and innovative technologies which can influence prosperity, consumption patterns, lifestyles, social relations and cultural developments as well as should have major importance for the sustainable development of mankind's.<sup>135-137</sup> In recent days the renewable resources become indispensable due to the continuous exhaustion of oil reserves, dwindling prices of petroleum based products, the threat of global warming and stringent environmental rules and regulations, waste disposal and risk to the aquatic life systems. They can provide an interesting sustainable platform to substitute partially, or even in some cases fully, petroleum-based polymers through designing bio-based polymers which can contend or even surpass the existing petroleum-based materials on a cost-performance basis with significant eco-friendliness.<sup>138</sup> Various renewable resources introduced into the act are biomass or plant derived resources like starch, cellulose and lignin, lipids (triacylglycerols, phospholipids, sterols etc.), proteins, sea resources, vegetable oils and other agricultural components. Among them, the vegetable oils have the tremendous attention to the researchers as well as to the industrialists. This is due to its various advantages like easy availability in large quantities with varieties of compositions and structures, relatively low cost, easy handling, reducing green house gases and overall environmental benignness. This resulted increasing demand of vegetable oils in production of non-food value added products such as paints and coatings, shampoos, soaps, cosmetics, lubricants, emulsifiers, plasticizers, biodiesels, pharmaceuticals etc.<sup>139</sup> The structural composition of vegetable oil has also tempted the scientists to make use of it to develop different polymeric materials. The reported literature described the use of different vegetable oils such as castor, sunflower, soybean, linseed, tobacco seed, tung etc. to prepare different types of polyesters.

Polymer systems are widely used due to their unique attributes: ease of production, light weight, and often ductile in nature. However, polymers have lower

modulus and strength as compared to metals and ceramics. Further, the vegetable oil based polymers have much lower mechanical strength than that of conventional petroleum based polymers. Therefore, there is constantly a need for stronger, lighter, less expensive and more versatile polymeric systems to meet the demands of many industrial consumers. In the last two decades there is a continuous increase of research for improvement of the properties of materials by employing nanometric engineered structures i.e. nanomaterials with inherent high surface area/volume ratio. Therefore the development of polymer nanocomposites has attracted much attention in recent years due to their dramatic improvements in their desired properties at relatively low loadings of nanofillers and without the property trade-offs commonly that are encountered in conventional microcomposite systems. This is mainly due to their extremely small interparticles distance and the interaction lies between the interface of polymer and fillers in nano scale.<sup>140</sup> The polymer nanocomposites are also extending the applications of physics, chemistry, biology, engineering and technology into previously unapproached infinitesimal length scales.<sup>141</sup> Now, at nanoscale one enters a world where physics and chemistry meet and develop novel properties of matter.

### ***1.4.2. Background***

The first vegetable oil based resins are reported by Kienle and Hovey in 1925<sup>142</sup>, though potentiality of vegetable oil is first reported by Kane in 1911.<sup>143</sup> Since the first report of vegetable oil based polyester, different types of vegetable oils are being used for manufacturing of polyesters. Hyperbranched polyester resins are studied first by Benthem<sup>144</sup> in the year of 2000 and latter on by Manczyk and Szewczyk<sup>145</sup> in 2002. They mainly prepared these resins to obtain low viscosity with rapid air drying. The common part in this work is that the hydroxyl groups at the outer periphery are modified with different fatty acids. In 2006, Bat et al.<sup>146</sup> modified this hyperbranched polyester with castor and linseed oil fatty acids. Very recently in 2010 Murillo et al.<sup>147</sup> prepared hyperbranched polyester resins based on tall oil fatty acids. The amalgamation of peculiar structural characteristic of hyperbranched polymer and the benefit of green vegetable oils in the field of polymer nanocomposites are described below.

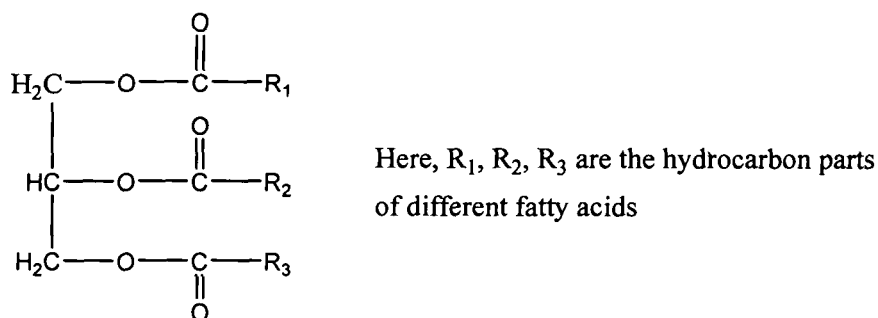
### ***1.4.3. Materials***

The significances of the polyester nanocomposites are enhanced when the matrix is vegetable oil based polyester. The triglyceride moiety of the vegetable oil enhanced the

structural and physical properties in the polyester matrix. The vegetable oil based polyester possesses properties like good flexibility, high gloss, good toughness and adhesion etc. Most importantly, as one of the raw materials is renewable natural resource and available in large quantity, so the overall cost of the raw materials and processing are also relatively lower as compared to the petroleum based polyester. Again these materials are also environment friendly and biodegradable in nature.

#### 1.4.3.1. Vegetable Oils

Vegetable oils are commonly known as fixed oils. They are non-volatile and unstable at high temperature compared to mineral oils found in petroleum fractions, obtained from mines. They possess different degrees of unsaturation. They have fixed composition and boiling point (b.p.). While the essential oils found in the stems, leaves, flowers, fruits etc. of plants are volatile. Vegetable oils are mainly constituted of triglycerides or triacylglycerols (95–98%) and complex mixtures of minor compounds (2–5%) of a wide range of chemical nature.<sup>148</sup> The main groups of minor constituents present in vegetable oil are: fatty alcohols, wax esters, hydrocarbons, tocopherols and tocotrienols, phenolic compounds, volatiles, pigments, minor glyceridic compounds, phospholipids and triterpenic acids. Triglycerides are esters of three molecules of fatty acids and one of glycerol and contain substantial amounts of oxygen in their structures (Fig. 1.6). The fatty acids vary in their carbon chain length and in the number of double bonds. Different types of vegetable oils contain different types of fatty acids which lead to a great variety of triglycerides in vegetable oils. Depending on the fatty acid distribution, different vegetable oils possess different physical and chemical properties. The saturated fatty acids such as arachidic, lauric, palmitic, stearic etc. and oleic, linoleic, linolenic etc. as unsaturated fatty acids are generally found in different triglycerides. Some vegetable oils also contain ricinoleic, myristic, behenic, capric, caproic, eleostearic, erucic, licanic, isanic, caprylic etc. fatty acids.



**Fig. 1.6:** Structure of triglyceride

## Chapter 1

Besides the regular carboxylic, saturated or unsaturated moieties, these fatty acids contain some special functionalities like ketonic, hydroxyl, epoxy, triene etc. The structures and physical properties like density, boiling point (b.p.) and melting point (m.p.) of some important fatty acids<sup>143</sup> are given in Table 1.3. The fatty acid composition of the vegetable oils is fixed and acts as its “finger print” (Table 1.3) that can be used to differentiate the vegetable oils from one another.

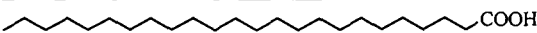
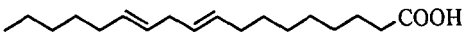
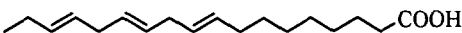
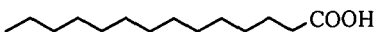
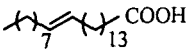
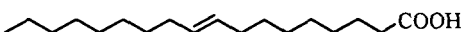
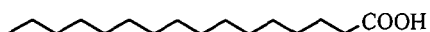
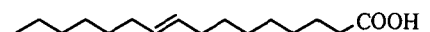
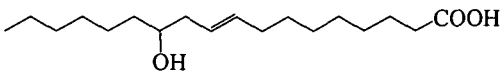

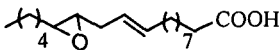
The vegetable oils may be of different types depending on the film forming ability, edibility (or toxicity) and yellowing tendency (linolenic acid content). The iodine value i.e. the unsaturation content measures the film forming ability of a vegetable oil.

**Table 1.3: Chemical structure and physical properties of a few fatty acids present in vegetable oils**

Name of fatty acid	Structure	Density (g/cm <sup>3</sup> ) at 25 °C	m.p. (°C)	b.p. (°C)
Arachidic		0.8240	74-76	328
Behenic		0.822	75-80	306
Capric		0.888	31-32	269
Caproic		0.92	-3	202
Caprylic		0.910	16-17'	237
Eleostearic		0.924	48	390.6
Erucic		0.891	28-32	386.1
Eicosenoic		0.895	25-32	430.5
Gadoleic		1.01	-	161-162
Heptadecan- -oic		0.853	59-61	227
Heptadecen- -oic		0.902	-	388.3
Isanic		0.930	39.5	-
Lauric		0.880	44-46	299
Licanic		-	75	-



## Chapter 1

Lignoceric		0.879	74-78	306
Linoleic		0.9	-5	229
Linolenic		0.914	-11	230-232
Myristic		0.862	58.8	250
Nervonic		0.918	42-44	398
Oleic		0.895	13-14	360
Palmitic		0.853	63-64	351
Palmitoleic		-	33	162
Ricinoleic		0.94	5.5	245
Stearic		0.83- 0.94	66-70	365-370
Vernolic		-	23-25	-

The oils are generally classified as drying, semi-drying and non-drying depending upon the unsaturation present. In general, the oils with iodine value greater than 150 are termed as drying oils (linseed, perilla, tung, oiticica, walnut etc. oils), in between 120-150 are termed as semi-drying (safflower, sunflower, soybean, watermelon, rubber seed, nigerseed, tobacco seed etc. oils) and under 120 are called as non-drying oils (castor, cottonseed, coconut, rapeseed, olive, karanja, ground nut, sesame, rice bran etc. oils).

However for non-conjugated oils, the drying rates are more closely related to the average number of methylene groups adjacent to two double bonds per oil molecule ( $f_n$ ) instead of their iodine values. Oil with  $f_n$  value  $> 2.2$  is said to be a drying oil, whereas oil with  $f_n$  value less than 2.2 is semi-drying. This method cannot be used to classify conjugated systems, though this method is superior and more reliable than the conventional iodine value method.<sup>149</sup>

The non-conjugated oils can also be classified based on their drying index values which is defined as, Drying index = % linoleic acid + 2 × (% linolenic acid). Oils are said to be drying when drying index is greater than 70.<sup>150</sup>

Again, depending on the linolenic acid content the vegetable oils are industrially classified as yellowing or non-yellowing. Generally, the drying oils are yellowing and semi-drying and non-drying oils are non-yellowing.

Based on edibility which depends on odor, taste and toxicity the vegetable oils may be edible and non-edible. Cotton seed, peanut, olive, mustard, corn etc. oils include as the edible oils while perilla, castor, tung, oiticicca oils falls into the non-edible category. Some oils are used for dual purpose such as sunflower, safflower, rapeseed, soybean etc.<sup>150</sup> A few important vegetable oils used to prepare polyester are given in Table 1.4 with their physical properties and major fatty acids contents.

### *Extraction and Purification of Vegetable Oils*

The oils are extracted from the seeds by using four general methods like mechanical pressing, solvent extraction, enzymatic process and high pressure CO<sub>2</sub> extraction process.<sup>150</sup> The mechanical pressing method involves hydraulic pressing or screw pressing of the pretreated seeds to squeeze out the oil from the protein meal of the seeds. In solvent extraction technique, the oil is isolated by using a soxhlet apparatus, where the pretreated seeds are immersed in a suitable solvent system for a considerable period at 60-80 °C and then the oil is separated by distillation. However, the process involves loss of solvent. In the enzymatic process, the pretreated seeds are boiled in water and mixed with a suitable enzyme viz. cellulase,  $\alpha$ -amylase, protease etc. which digest the solid material from the seed. The oil is then extracted by liquid-liquid centrifugal method. Finally in the high pressure CO<sub>2</sub> method, the pretreated seeds are mixed with CO<sub>2</sub> under high pressure, which dissolves the oil. Then the pressure is released which makes liquid CO<sub>2</sub> gaseous and hence the oil gets separated. The yields of the last two methods viz., enzymatic and high pressure CO<sub>2</sub> method are quite high and hence are adopted largely in commercial scale. In order to avoid the hydrolysis of the oil to free fatty acids by moisture present in the atmosphere, the extracted oil is kept at low temperature. Again, care should be taken during storage and handling to minimize the chances of contamination by oxygen. The best way to keep the oil without losing quality and stability is under nitrogenous atmosphere.<sup>143,150</sup>

The crude oil obtained after extraction generally contains certain impurities consisting of phosphatides, gums, resins, free fatty acids and colored substances. Before utilization of the vegetable oils for industrial and edible purposes, they should be refined in order to remove the impurities. Dirt's can be removed by settling or by simple filtration technique.<sup>143</sup> Gums are removed by degumming which exploits the affinity of phosphatides towards water by converting them to hydrated gums by

treatment with water, salt solution, acid etc. As a result, gums coagulate and are separated by a centrifugal separator.<sup>150</sup>

**Table 1.4:** *A few important vegetable oils used to prepare polyester with their physical properties and major fatty acids contents*

Name of oil	Major fatty acids (% of total)	Saponification value (mg KOH/g)	Iodine value (gI <sub>2</sub> /100 g)
Linseed oil	Linolenic (50-61)/ linoleic (13-15)	192-195	175-204
Castor oil	Ricinoleic (80-90)/ linoleic (3-4)	180	82-88
Tung oil	Elaeostearic (77-88)/ oleic (4-10)	193	155-175
Soybean oil	Linoleic (54.5)/ oleic (22.3)	189-195	125-140
Sunflower oil	Linoleic (69)/ oleic (18.3)	188-194	119 - 135
Safflower oil	Linoleic (75)/ oleic (14)	135-190	140-150
Tobacco seed oil	Linoleic (66-76)/ oleic (17-27)	193	135
Oiticica oil	Licanic (73-76)/ linoleic (8-10)	150	179-218
Perilla oil	Linolenic (46.5)/ linoleic (37)	182-205	192-208
Coconut oil	Lauric (48.2)/ myristic (16.6)	252-284	8-10
Rubber seed oil	Linoleic (39.6)/ oleic (24.6)	192	155

The alkali refining technique is a complete refining process which removes free fatty acid contents and causes effective color removal without excessive saponification of the oil and without loss of oil by emulsification.<sup>92,143</sup> In this technique, a very dilute caustic soda solution is used in sufficient quantity to neutralize the free fatty acids. The quantity of caustic soda required depends upon the type of oil, the impurities present and the final color required.<sup>143</sup> Sometimes, acid refining technique is also used although color removal in the process is not suitable as in alkali refining technique. In this process, the cold oil is stirred with concentrated sulphuric acid solution. On settling, the impurities are drawn off and the oil is washed to make free from impurities. As a finishing step of the refining process, bleaching should be done for partial or complete removal of color.<sup>150</sup> Bleaching can be done either by chemical or by physical means. The chemical method is disadvantageous as the oil suffers oxidation during the process. However, in the physical method, the oil is heated with an adsorbent such as fullers earth, activated carbon, silica, bentonite etc. in the absence of oxygen. The process is

generally carried out at about 110 °C with 0.2-2.5% solution of the adsorbent for duration of ca. 30-60 min.<sup>143</sup>

### *1.4.3.2. Preparation of Polyester from Vegetable Oils*

The vegetable oil based polyesters are mainly prepared by using four methods viz. (1) Monoglyceride/alcoholysis, (2) Fatty acid, (3) Acidolysis and (4) Fatty acid/oil. However out of these fatty acid and monoglyceride processes are most commonly used commercial methods.

#### *Monoglyceride/Alcoholysis Process*

This process is most widely used for preparation of polyester. To overcome the incompatibility of virgin vegetable oil with the directly prepared polyester, the monoglyceride process is developed where the triglyceride oils are reacted with glycerol in presence of a catalyst at temperature of 225-250 °C. The extent of alcoholysis is usually checked by solubility of the monoglyceride formed in methanol under ambient conditions. There are two other methods, one is to observe solubility of phthalic anhydride in the alcoholysis product and the other is to determine the electrical conductivity of the monoglyceride formed.<sup>51,143</sup> The alcoholysis actually results an equilibrium mixtures of monoglyceride, diglyceride, unchanged triglyceride and free glycerol. Generally, 51% monoglyceride, 40% di-glyceride, 4% triglyceride and 5% free glycerol is an acceptable composition. The high amount of monoglyceride leads to the polyesters that have superior properties. Different methods such as thin layer chromatography, gas chromatography, HPLC etc. are used to measure alcoholysis compositions.<sup>143</sup> Mandik et al.<sup>151</sup> used GPC to determine the concentration of different glycerides for linseed oil. The properties of resulting resin depend on the degree of alcoholysis. Under the influence of heat and catalyst, the polyhydric alcohols undergo inter-etherification, which results in loss of available hydroxyl group and the formation of higher functional polyhydric alcohols. Oxygen seems to retard the alcoholysis reaction, as it is found that the reaction time is almost doubled when the alcoholysis is carried out in the absence of a blanket of inert atmosphere.<sup>143</sup> Traces of water present have shown to decrease the rate and the extent of monoglyceride formation from castor oil.<sup>143</sup> Choudhury<sup>152</sup> performed glycerolysis for a number of oils and it is shown that the yield of monoglyceride is not dependent on the fatty acid composition of the oil but depends on the solubility of glycerol in the oil, which is more or less dependent upon temperature. Pintile studied the alcoholysis of oils and observed that the highest

monoglyceride content of the final product is 54-55% and the lowest diglyceride content is 23-24%.<sup>143</sup> Sathyanarayana et al.<sup>153</sup> carried out alcoholysis of linseed oil with glycerol and characterized the partial glyceride formed by thin layer chromatography-flame ionization detector and <sup>1</sup>H NMR. They found  $\alpha$ -monoglyceride as the predominant product, the concentration of which increased with the decrease in oil length. Igwe et al.<sup>154</sup> showed that the alcoholysis reactions of rubber seed and linseed oils are found to be similar, same in the case of melon and soybean oils. This similarity indicates that rubber seed oil and melon seed oil can replace linseed and soybean oils in the synthesis of oil modified polyester resins.

After formation of monoglycerides, the polybasic acids and the rest of polyhydric alcohols are added and the polycondensation is carried out at temperature 220-255 °C to obtain polyester of desired acid value.<sup>52</sup> A general scheme of the formation of vegetable oil based polyester resin is shown in Scheme 1.2.

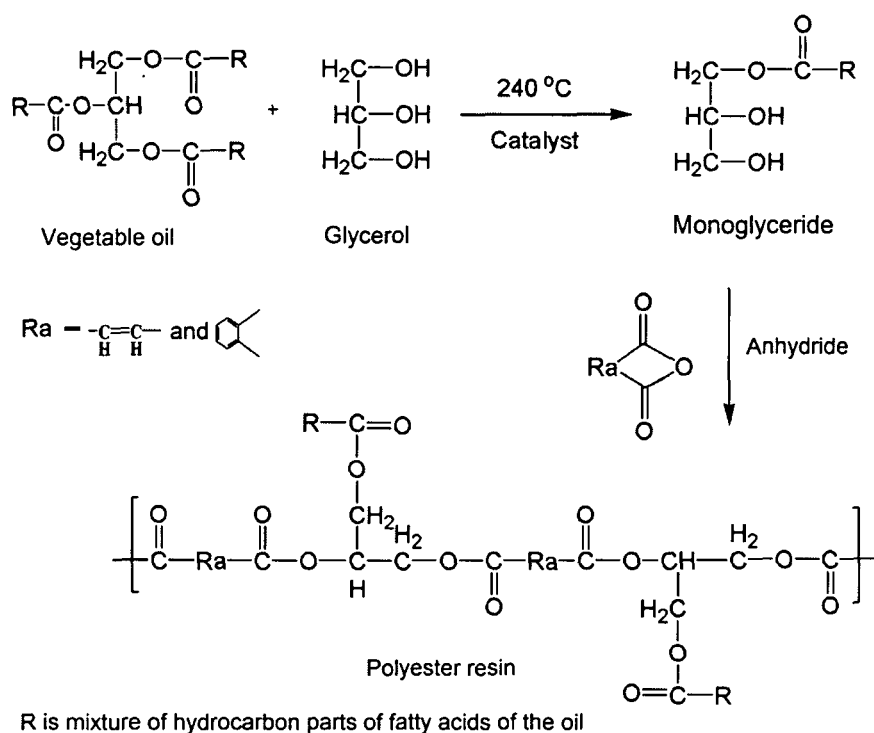
### *Fatty Acid Process*

In the fatty acid process, polyhydric alcohol, dibasic acid and monobasic acids are reacted simultaneously at temperature of 220-260 °C until the desired degree of polymerization is reached which is followed by measurement of acid value and viscosity. The process allows greater formulation freedom since any polyhydric alcohol or its blend can be used, and the fatty acids that are not available as glycerides, such as pelargonic acid, 2-ethylhexanoic acid, tall oil fatty acids etc. can be used as special fatty acids.<sup>49,53</sup>

The fatty acid process is modified by Kraft by 'high polymer technique'.<sup>50,53</sup> In this modified process the dibasic acid and the polyalcohols are precondensed with a portion of the monobasic acids (fatty acids). When acid value becomes low, the remaining portion of fatty acids is added to complete the polycondensation. Polyester prepared by this technique is light in color and more viscous than those prepared from conventional fatty acid method. The fatty acid process has many advantages<sup>51,52,143</sup> over the monoglyceride process like, any polyhydric alcohol can be used, product can be tailor made, no catalyst is required which reduces the risk of discoloration and oxidation, more reproducible process as the monoglyceride formation is not controlled fully, reduced processing time etc. However, the fatty acid process has some disadvantages<sup>51,52,143</sup> over the monoglyceride process. The fatty acids are more expensive than triglyceride oil, more corrosive than oil and need corrosion resistant

## Chapter 1

equipment for storage, often have higher melting point than oils which require preheating equipment to facilitate handling them as liquids, more susceptible to discoloration during storage etc.



**Scheme 1.2:** General scheme of the formation of vegetable oil based polyester resin

### Acidolysis Method

This method is converse of the alcoholysis process where the oil is subjected to acidolysis in the presence of acids in first stage of the process. In the second stage the condensation reaction is completed by reacting with the polyhydric alcohol. This reaction occurs at high temperature without a catalyst and its use is limited to polybasic acids, such as isophthalic and terephthalic acids, which do not sublime and are quite insoluble in the monoglyceride until considerable esterification has occurred.<sup>49,53,143</sup> At the high processing temperature, side reaction like dimerization of the oils is unavoidable, which leads to discoloration of polyester resin.<sup>51</sup> Carlston<sup>155</sup> studied the acidolysis of vegetable and marine oils with three isomers of phthalic acid and it is found that orthophthalic acid dehydrates to anhydride before any interchange occurs, but isophthalic and terephthalic acids are heat stable and react easily with oils at 280-300 °C. Isophthalic acid reacts more rapidly than terephthalic acid. Commercial use of the acidolysis reaction in polyester resin manufacture is economically attractive as no catalyst is required.

### *Fatty Acid-Oil Process*

This process involves the direct reaction of fatty acid, oil, polyhydric alcohol and dibasic acid. The ratio of fatty acid to oil must be such that a homogeneous reaction mixture results. This process has a cost advantage over fatty acid process and results high viscosity polyester, if the fatty acid represents 60-65% of the total fatty acids and oil. Heat polymerized oil yields even higher viscosity polyester resin than the other normal oil.<sup>49,53,143</sup>

During esterification stage of polyester resin manufacturing, water is evolved as a by-product. Since esterification is an equilibrium reaction, the evolved water must be removed to force the reaction towards completion. The fusion and solvent techniques are used in order to remove water.

### *Fusion Technique*

In fusion technique all the reactants (in case of oil after monoglyceride process) are processed together at the reaction temperature, in a stream of inert gas (N<sub>2</sub> or CO<sub>2</sub>) which remove water of esterification and prevent aerial oxidation.<sup>50,51,53</sup> At high temperature the volatile reactants may be lost. The quantities lost must be considered when basic components are added. Fusion process is often acceptable for polyester containing a high percentage of oil. The equipment cost is comparatively low in fusion process and no water condenser is required.

### *Solvent Technique*

In solvent technique, the polycondensation is carried out in the presence of aromatic solvent (usually xylene), which is immiscible in water and capable of forming azeotropic mixture with it. Solvent is commonly used in amount from 3-10% of the batch. Solvent method is generally used for preparation of short oil polyester resin. Advantages of solvent process<sup>53,143</sup> are i) reaction time is short as water formed is removed rapidly, ii) extent and rate of reaction can be determined easily, iii) better color and batch-to-batch reproducibility is obtained, iv) uniform molecular distribution of the product is obtained, v) losses of phthalic anhydride by sublimation is reduced, vi) solvent provides protection against attack by atmospheric oxygen etc.

#### *1.4.3.3. Preparation of Hyperbranched Polyester from Vegetable Oil*

As stated earlier hyperbranched polyesters (HBPs) composed of branched structures adopt compact conformations with large numbers of surface reactive groups and preferred over the conventional linear analogs in many aspects. One important feature of these HBPs is their high solubility in common solvents (e.g., DMF, DMSO, acetone etc.), which makes them ideal for the development of hyperbranched polyester nanostructures, such as polymeric nanoparticles, by the solvent diffusion method. There is no report found for the preparation of hyperbranched polyester using vegetable oil directly. However, the utilization of fatty acids from vegetable oil is reported very recently in the synthesis of hyperbranched polyester.<sup>147</sup> Murillo et al.<sup>147</sup> emphasized on the synthesis and characterization of hyperbranched polyester resins (HBR) based on tall oil fatty acids (TOFA). HBR are synthesized from fourth generation hydroxylated hyperbranched polyester (HBP1–4) and TOFA by esterification reaction between acid groups of TOFA and OH groups of HBP1–4 using acid catalyst. Bař et al.<sup>146</sup> studied the synthesis of hyperbranched polyester resins based on a hydroxylated hyperbranched polyester obtained from dipentaerythritol and 2,2-bis(hydroxymethyl) propanoic acid and posterior modification with castor oil fatty acids, linseed oil fatty acids and benzoic acids. They found that the hardness of the resins increased with fatty acids and linseed oil fatty acids contents but the hardness did not change with benzoic acid content.

#### *1.4.3.4. Preparation of Nanocomposites from Vegetable Oil*

Haq et al.<sup>156</sup> reported the bio-based nanocomposites of blends of petroleum and vegetable oil based resins and nanoclay which lead to enhancement of material properties. An array of 12 nanocomposites with up to 30% epoxidized methyl linseedate (EML) and up to 5 wt.% nanoclay in unsaturated polyester are manufactured using a solution technique. The developed eco-friendly bio-based nanocomposites exhibit good stiffness–toughness balance along with improvements in other mechanical properties, thereby showing potentiality in structural applications.

Alam et al.<sup>157</sup> reported the corrosion-resistance performance of soybean oil polyester, containing polyaniline/ferrite nanocomposite. The corrosion-protective performance is evaluated in terms of physico-mechanical properties, corrosion rate, and SEM studies. The polyaniline/ferrite nanocomposite coatings are found to show a far superior corrosion resistance performance compared to that of a pure PANI/ polyester system.



## Chapter 1

Dhoke et al.<sup>158</sup> also studied the effect of nano-Al<sub>2</sub>O<sub>3</sub> on the corrosion, mechanical, and optical properties of polyester based waterborne coating prepared by using high mechanical mixing. They found that addition of small concentration of nano-Al<sub>2</sub>O<sub>3</sub> can improve the corrosion resistance, UV resistance, scratch resistance, and abrasion resistance of the coating as compared to the pristine system.

Effect of nano-ZnO addition on the silicone-modified polyester-based waterborne coatings on its mechanical and heat-resistance properties are also investigated by Dhoke et al.<sup>159</sup> and found that the heat-resistance and mechanical properties of the coating improved significantly as a function of nano-ZnO content.

Bal et al.<sup>160</sup> prepared the nanocomposites of coconut oil based polyester resins with organoclay using *in-situ* method and the prepared nanocomposites are cured with different ratios of melamine-formaldehyde and urea-formaldehyde resins. The film properties of the resins such as drying degree, hardness, adhesion strength, abrasion resistance, water, acid, alkali, solvent resistance, and resistance to environmental conditions are investigated and found to be improved.

Bhanvase et al.<sup>161</sup> also investigated the effect of polyaniline-nano CaCO<sub>3</sub> on mechanical and anticorrosion performance of soybean oil based polyester resin. The nanocomposite is prepared by *in-situ* method using ultrasound and improvement in mechanical and anticorrosion properties is found.

Unsaturated polyester clay nanocomposites prepared by high mechanical mixing method are also reported.<sup>162</sup> Bio-based nanocomposites from functionalized plant oils and layered silicate are reported by Lu et al.<sup>163</sup> The nanocomposites are prepared by *in-situ* methods and often an intercalated or exfoliated structure is formed. Because triglyceride based monomers optionally have polar groups such as hydroxyl and carboxylic acid groups, these molecules are favored in the formation of a possible exfoliated structure. Triglycerides also offer the ability to control the number of polar groups through chemical modifications. In the report of Jiratumnukul et al.<sup>164</sup> the enhancement of properties is observed by the incorporation of organophillic montmorillonite into polyester coating by the high speed disperser.

### **1.4.4. Characterization**

Characterization of the vegetable oil based polyester nanocomposites are done by the similar methods as discussed in the sub-section 1.3.3.2. XRD technique is widely used to characterize the vegetable oil based polymer nanocomposites too. The shifting of the

diffraction peak for the [001] plane of nanoclay towards low angle value reveals the intercalation of clay galleries by the polyester chains. Again the disappearance of this peak also roughly offers an idea on the formation of the exfoliated structure, though that has to be confirmed by TEM study. In case of polymer/metal nanoparticles nanocomposites new desired peaks appeared which confirmed the formation of nanocomposites.

In the FTIR spectra of vegetable oil based polyester nanocomposites, besides the characteristic bands for the nanoclays, the bands for fatty acids are also obtained. The bands for ester carbonyl  $\text{-C=O}$ , ether oxygen  $\text{-C-O-C-}$  etc. as well as bands for stretching vibration of  $\text{Si-O}$ ,  $\text{Al-O}$  and  $\text{Si-O-Si}$  for nanoclay are observed in the FTIR spectra of vegetable oil based polyester/clay nanocomposites. Again for other types of metal nanoparticles the bands for metal oxides or metal hydroxides are obtained. For example, titanium oxide shows band for  $\text{Ti-OH}$  groups in different co-ordinations. The zirconia presents bands at  $3771\text{ cm}^{-1}$  to terminal  $\text{Zr-OH}$  groups and at  $3671\text{ cm}^{-1}$  to bridging or triple-bridging  $\text{OH}$  groups. Magnesium oxide shows weak adsorption band in the  $\text{OH}$  stretching region at  $3750\text{ cm}^{-1}$ . Also in case of nanoparticles some bands are obtained at low frequency due to the fundamental skeletal vibrations, whose position mostly depends on the weight of the metal element and on the nature of the bond.<sup>165</sup> For example band is found near  $1250\text{ cm}^{-1}$  for silica and silica-alumina, near  $1000\text{ cm}^{-1}$  for alumina and titania, near  $800\text{ cm}^{-1}$  for zirconia and  $700\text{ cm}^{-1}$  for magnesia.

The surface morphology of the vegetable oil based polyester nanocomposites is characterized by SEM technique. The dispersion pattern of different nanomaterials in the polyester matrix is observed from the SEM micrographs. TEM is used to get direct qualitative information of structure, morphology and spatial distribution of the various nanofillers as well as the defect structure of the polyester nanocomposites.

TGA and DSC techniques are used to characterize the thermal properties of vegetable oil based polyester nanocomposites in a similar manner as they are used for other polymer nanocomposites. Higher thermal stability compared to the pristine polyester matrix is reported by several authors after formation of nanocomposites by incorporation of nanoclay. This high thermal stability is attributed to the nanoclay which acts as a thermal insulator and mass transport barrier to the volatile products produced during decomposition by providing tortuous path way to escape. Similarly the melting enthalpy ( $\Delta H_m$ ) and  $T_g$  are also enhanced after nanocomposite formation.

DMA (DMTA) and TMA analyses are used to analyze the structure and morphology by determining the transitions and relaxations (variation of  $G'$  and  $G''$  with temperature).

### **1.4.5. Properties**

Vegetable oil based polyester nanocomposites exhibited equivalent or even better properties in some cases than the petroleum based polyester nanocomposites. The properties as described in Section 1.3.4. are also valid for vegetable oil based polyester nanocomposites.

The incorporation of nanofillers results in the improvement of mechanical properties in terms of tensile strength, scratch resistance, impact strength, toughness etc. of vegetable oil based polyester nanocomposites. While the elongation at break value decrease in general though it may increase in some cases. The decreased value is due to the imposed restricted chain motion in general. On the other hand, the increasing trend in elongation at break values with the increase of clay loadings is observed by Li.<sup>4</sup> The vegetable oil based polyester exhibited enhanced flexibility and it retains in the nanocomposites. The presence of long chain of fatty acid in the vegetable oil may be attributed to this flexibility in the nanocomposites.

The incorporation of nano-ZnO particles in the polyester coatings enhances the abrasion resistance and impact resistance. This is due to strong interfacial surface interaction between nano-ZnO and the base matrix.<sup>159</sup> The physico-mechanical properties like cross-cut adhesion, gloss and impact resistance of oil based polyester resin are improved by the incorporation of polyaniline-nano  $\text{CaCO}_3$  particles. An electrochemical measurement of the same nanocomposites shows that corrosion current decreased from 0.89 to  $0.03 \mu\text{A}/\text{cm}^2$ , when polyaniline-nano  $\text{CaCO}_3$  nanohybrid is added into neat coatings.<sup>161</sup> A positive shift of electrochemical corrosion also indicates that the nanocomposite acts as an anticorrosive additive to polyester coating.

The thermal stability of vegetable oil based polyester is improved with the incorporation of different nanofillers like nanoclay, nanometal, carbon nanotubes etc. These nanofillers are well-dispersed in the polyester matrix and hinder the diffusion of volatiles and assist the formation of char after thermal decomposition.

A significant improvement of biodegradation is observed for the vegetable oil based polyester/clay nanocomposites. Different mechanisms are put forward for biodegradation, though exact pathway is not still confirmed. Silver nanoparticles

containing vegetable oil based polyester nanocomposites exhibited antimicrobial activity. Vegetable oil based polyesters are known for their biocompatibility and hence its nanocomposites. The cytocompatibility of polyester nanocomposites can be checked from the study of the red blood cell (RBC) hemolysis inhibition capacity. Further the bacterial degradation of the same is also tested conveniently by broth culture technique where the nanocomposites are exposed to microbial degradation.

The rheological study of vegetable oil based highly branched polyester showed shear thinning behavior with the incorporation of nanomaterials. The interaction between nanofillers and the polyester chains restricted the chains to relax. The high shear rates cause a break down in network structure and the nanomaterials do increasingly align in parallel. This results the orientation of the nanomaterials in the flow direction, and contributes shear thinning behavior in the nanocomposites. Because of this shear thinning behavior, the nanocomposites can be processed in the melt state using the conventional equipment available in a manufacturing line. Also pronounced shear thinning has been found to be a characteristic feature of truly nano dispersed composites.

Alam et al.<sup>166</sup> prepared nanostructured PANI soybean oil polyester nanocomposites and found enhancement of electrical conductivity even at lower loading of nanostructured PANI. The conductivity of the composites is found to be  $1.7 \times 10^{-4}$ ,  $2.3 \times 10^{-3}$ ,  $2.4 \times 10^{-3}$  S/cm for 0.5, 1.0, and 2.0 wt.% of PANI, respectively. The PANI chains physically cross-link with the polyester segments through hydrogen bonding and results intense conformational changes which provides the path for the charge conduction.

The metal nanocomposites have catalytic activity due to the high surface area of the nanoparticles, which can effectively catalyzed reactions where the matrix acts as support. Karak et al.<sup>167</sup> explored the catalytic activity of the sunflower oil based hyperbranched polyurethane/silver nanocomposite in the reduction of 4-nitrophenol to 4-aminophenol. Similarly vegetable oil based highly branched polyester/silver nanocomposites can also be checked to proof its potentiality as catalyst.

The vegetable oil based polyesters exhibit poor alkali resistance as they are susceptible to hydrolysis due to the presence of ester bonds. However, the addition of the nanofillers and formation of a suitable blend enhanced the alkali resistant to the nanocomposites.

### 1.4.6. Applications

Vegetable oil based polyester nanocomposite is gaining vast popularity due to its diversified field of potential application. Polyester itself is a unique class of material as used in different field of applications. The reasons for the popularity of polyesters are: excellent surface appearance, cost, versatility, relatively inexpensive in terms of raw material and manufacturing cost and since they are readily soluble in the less expensive solvents.<sup>143</sup> Whilst other polymers may offer improved properties in specific areas, polyester resins have the widest spectrum of acceptable properties in terms of surface coating usage. They can be easily pigmented and are compatible with most of the other binders used in surface coatings e.g. nitrocellulose, polyurethanes, amino resins, phenolics epoxy etc. In addition they are tolerant of most substrates and are easily modified for specialist applications.<sup>143</sup>

Vegetable oil based polyester nanocomposites can be used as a direct substituent's of petroleum based polyester nanocomposites in the field of surface coatings. Improvement of thermal, mechanical and morphological properties of soybean oil polyester upon reinforcement with nanostructured PANI reported by Alam et al.<sup>166</sup> exhibits potential application of the nanocomposites as a corrosion protective coating material. The nanocomposite coating provides space for a variety of modifications of its physical structure, making it more malleable and adaptable for many application processes, including spraying, dipping or spin coating.<sup>166</sup>

Even though vegetable oil based other polymer nanocomposites like polyurethane, epoxy etc. nanocomposites have different fields of applications, the vegetable oil based polyester nanocomposites are yet to be developed for applications other than in surface coating industries though a few literatures are found now-a-days. Ashraf et al.<sup>168</sup> described the use of linseed oil based poly(urethane amide)/PNA nanocomposites in anti-static and corrosive-protective coatings. Linseed oil based polyurethane/silica nanocomposites are used in thermal resistant protective coatings and paints.<sup>169</sup> Castor oil modified polyhydric alcohol based polyurethane/nano-hydroxyapatite with tunable biodegradable properties is reported to be utilized in biomedical implants and tissue engineering.<sup>170</sup> Epoxy modified *Mesua ferrea* oil based biocompatible and biodegradable polyurethane nanocomposites hold the immense potential as biomaterials.<sup>171</sup> Vegetable oil based hyperbranched and linear polyurethane/silver nanocomposites can also be utilized as heterogeneous catalyst.<sup>167</sup> Liu et al.<sup>172</sup> developed epoxidized soybean oil-based green nanocomposites which can

be used as promising alternative materials to petrochemical polymers. Uyama et al.<sup>173</sup> developed green nanocomposites from epoxidized soybean oil and organically modified clay which are highly expected to be a new class of biodegradable polymers and coating materials from inexpensive renewable resources, contributing to global sustainability. Very recently, Jaffar Al-Mulla et al.<sup>174</sup> prepared new biopolymer nanocomposites of blend of polylactic acid/epoxidized soybean oil with fatty nitrogen compound modified MMT. The prepared nanocomposites showed potentialities in textile industries, automotive and clinical uses, as well represent a good candidate to produce disposable packaging.

### **1.5. Scope and Objectives of the Present Investigation**

It is found from the main features of the foregoing discussion that many vegetable oils are widely used as starting raw materials for preparation of many industrial polymers instead of petroleum based products. Again vegetable oils are environment friendly as they are biodegradable and obtained from nature. *Mesua ferrea* L. (Nahar) is a widely grown plant in India which produces high oil content (70-75 wt.%) seeds. Besides India (mainly North-East region, Karnataka, Kerala, Tamil Nadu, West-Bengal, Uttar Pradesh etc.) it is also available in other countries like Sri Lanka, Bangladesh, Nepal, Indo-China (South East Asia), Malay Peninsula etc. The oil possesses both saturated and unsaturated fatty acids. Also there are literatures on the utilization of this oil in the fields of medicine, biodiesel and polymers. However, there is no report on the utilization of this oil in the field of highly branched polyester and its nanocomposites, to our knowledge, even though they may have many advantages. So, it appears that there is a lack of systematic and comprehensive study on the utilization of this oil in the field of highly branched polyester and its nanocomposites. Hence, the following questions may arise in this area.

- (i) Whether this oil can be used for the preparation of highly branched polyester?
- (ii) Whether the performance characteristics of the polyester can be improved by any physical or chemical means?
- (iii) Whether the pristine polyester or modified polyester can be utilized as the matrix for the preparation of different types of nanocomposites?
- (iv) Whether the incorporation of different nanofillers into the polyester matrix can lead to the genesis of advanced materials?

## Chapter 1

Under this background the main objectives of the present investigation are as follows:

- (i) To synthesize, characterize and evaluate various properties of *Mesua ferrea* L. seed oil based highly branched polyesters.
- (ii) To improve the performance of the vegetable oil based polyester by blending with other suitable commercial polymers.
- (iii) To improve the performance characteristics of the polyester by the formation of nanocomposites.
- (iv) To utilize various nanofillers for formation of different types nanocomposite to achieve desirable levels of properties.
- (v) To utilize the prepared nanocomposites as advanced materials in the field of surface coating, biodegradable biomaterial, antimicrobial materials etc.
- (vi) To use *Mesua ferrea* L. seed oil modified polyester resin for the preparation of an industrial paint.

### 1.6. Plan of Work

To fulfill the above objectives, the following plans of work are adopted. The plans of work for the proposed research are as follows.

- i) A state-of-art literature survey on the field of vegetable oil based polyesters and their nanocomposites.
- ii) The highly branched polyester from vegetable oil will be synthesized by the help of literature reports.
- iii) The synthesized polyesters will be characterized by different analytical and spectroscopic techniques such as determination of acid value, saponification value, hydroxyl value, FTIR, NMR, TGA etc.
- iv) Polyester nanocomposites will be prepared by the *ex-situ* technique using vegetable oil based polyester and organophilic nanoclay/metal nanoparticles/CNT etc.
- v) The prepared nanocomposites will be characterized by UV, FTIR, XRD, TEM, SEM, rheometer etc. to study the structure, morphology and rheological behavior.
- vi) The performance characteristics of the characterized nanocomposites will be investigated by determination of mechanical properties like tensile strength, elongation at break, impact resistance etc.; thermal properties; chemical resistance in different chemical media etc. The special properties like biodegradation,

antimicrobial test, cytocompatibility etc. will be conducted depending on requirement.

vii) The performance characteristics of the nanocomposite will be optimized by manipulation of composition of raw materials, processing parameters etc. to find out the best nanocomposite in each category.

vii) *Mesua ferrea* L. seed oil modified polyester resin will be utilized for the preparation of an industrial paint.

## References

1. Karak, N. Polymer (epoxy) clay nanocomposites. *J. Polym. Mater.* **23**, 1-20 (2006)
2. Ahmadi, S.J.; Huang, Y.D.; Li, W. Synthetic routes, properties and future applications of polymer-layered silicate nanocomposites. *J. Mater. Sci.* **39**, 1919-1925 (2004)
3. Jia, Q.M.; Zheng, M.; Chen, H.X.; Shen, R.J. Synthesis and characterization of polyurethane/epoxy interpenetrating network nanocomposites with organoclays. *Polym. Bullet.* **54**, 65-73 (2005)
4. Li, J. High performance epoxy resin nanocomposites containing both organic montmorillonite and castor oil-polyurethane. *Polym. Bullet.* **56**, 377-384 (2006)
5. Jia, Q.; Shan, S.; Wang, Y.; Gu, L.; Li, J. Tribological performance and thermal behavior of epoxy resin nanocomposites containing polyurethane and organoclay. *Polym. Adv. Technol.* **19**, 859-864 (2008)
6. Lei, Z.; Yang, Q.; Wu, S.; Song, X. Reinforcement of polyurethane/epoxy interpenetrating network nanocomposites with an organically modified palygorskite. *J. Appl. Polym. Sci.* **111**, 3150-3162 (2009)
7. Rana, S.; Karak, N.; Cho, J.W.; Kim, Y.H. Enhanced dispersion of carbon nanotubes in hyperbranched polyurethane and properties of nanocomposites. *Nanotechnology* **19**, 495707 (8pp) (2008)
8. Turunc, O.; Kayaman-Apohan, N.; Kahraman, M.V.; Menciloglu, Y.; Gungor, A. Nonisocyanate based polyurethane/silica nanocomposites and their coating performance. *J. Sol. Gel Sci. Technol.* **47**, 290-299 (2008)
9. Usuki, A.; Hasegawa, N.; Kato, M. Polymer-clay nanocomposites. *Adv. Polym. Sci.* **179**, 135-195 (2005)



10. Haq, M.; Burgueño, R.; Mohanty, A.K.; Misra, M. Hybrid bio-based composites from blends of unsaturated polyester and soybean oil reinforced with nanoclay and natural fibers. *Compos. Sci. Technol.* **68**, 3344-3351 (2008)
11. Parkyn, B. Chemistry of polyester resin. *Composites* **3**, 29-33 (1972)
12. Edlund, U.; Albertsson, A.C. Polyesters based on diacid monomers. *Adv. Drug Delivery Rev.* **55**, 585-609 (2003)
13. Voit, B.I. Hyperbranched polymers: A chance and a challenge. *C. R. Chimie* **6**, 821-832 (2003)
14. Pang, K.; Kotek, R.; Tonelli, A. Review of conventional and novel polymerization processes for polyesters. *Prog. Polym. Sci.* **31**, 1009-1037 (2006)
15. Gao, C.; Yan, D. Hyperbranched polymers: From synthesis to applications. *Prog. Polym. Sci.* **29**, 183-275 (2004)
16. Gao, C.; Yan, D.Y.; Tang, W. Hyperbranched polymers made from A<sub>2</sub>-and BB'<sub>2</sub>-type monomers 3. Polyaddition of n-methyl-1,3-propanediamine to divinyl sulfone. *Macromol. Chem. Phys.* **202**, 2623-2629 (2001)
17. Yates, C.R.; Hayes, W. Synthesis and applications of hyperbranched polymers. *Eur. Polym. J.* **40**, 1257-1281 (2004)
18. Ahmed, S.; Ashraf, S.M.; Naqvi, F.; Yadav, S.; Hasnat, A. A polyesteramide from Pongamia glabra oil for biologically safe anticorrosive coating. *Prog. Org. Coat.* **47**, 95-102 (2003)
19. Aigbodion, A.I.; Pillai, C.K.S.; Bakare I.O.; Yahaya, L.E. Synthesis, characterization and evaluation of heated rubber seed oil and rubber seed oil-modified alkyd resins as binders in surface coatings. *Indian J. Chem. Technol.* **8**, 378-384 (2001)
20. Derksen, J.T.P.; Cuperus, F.P.; Kolster, P. Paints and coatings from renewable resources. *Ind. Crop. Prod.* **3**, 225-236 (1995)
21. Dutta N.; Karak N.; Dolui, S.K. Synthesis and characterization of polyester resins based on Nahar seed oil. *Prog. Org. Coat.* **49**, 146-152 (2004)
22. Das, G.; Karak, N. Epoxidized *Mesua ferrea* L. seed oil-based reactive diluent for BPA epoxy resin and their green nanocomposites. *Prog. Org. Coat.* **66**, 59-64 (2009)
23. Mahapatra, S.S.; Karak, N. Synthesis and characterization of polyesteramide resins from Nahar seed oil for surface coating applications. *Prog. Org. Coat.* **51**, 103-108 (2004)

24. Deka, H.; Karak, N. Bio-based hyperbranched polyurethane/clay nanocomposites: Adhesive, mechanical, and thermal properties. *Polym. Adv. Technol.* (doi:10.1002/pat.1603) (2010)
25. Aigbodion, A.I.; Pillai, C.K.S. Preparation, analysis and applications of rubber seed oil and its derivatives in surface coatings. *Prog. Org. Coat.* **38**, 187-192 (2000)
26. Sabin, P.; Mlayah, B.B.; Delmas, M. Offset printing inks based on rapeseed oil and sunflower oil. Part II: Varnish and ink formulation. *J. Am. Oil Chem. Soc.* **74**, 1227-1233 (1997)
27. Joseph, R.; Alex, R.; Vinod, V.S.; Premalatha, C.K.; Kuriakose, B. Studies on epoxidized rubber seed oil as plasticizer for acrylonitrile butadiene rubber. *J. Appl. Polym. Sci.* **89**, 668-673 (2003)
28. Ramadhas, A.S.; Jayaraj, S.; Muraleedharan, C. Use of vegetable oils as IC engine fuels-a review. *Renew. Energy* **29**, 727-742 (2004)
29. Malik, S.M. Neem oil studies in performance of alkyd-amino combinations based on neem oil as a film forming material. *Paintindia* **52**, 41-52 (2002)
30. Ikhuoria, E.U.; Aigbodion, A.I.; Okieimen, F.E. Preparation and characterization of water-reducible alkyds with fumarized rubber seed oil. *Prog. Org. Coat.* **52**, 238-240 (2005)
31. Blayo, A.; Gandini, A.; Le Nest, J.F. Chemical and rheological characterization of some vegetable oils derivatives commonly used in printing inks. *Ind. Crop. Prod.* **14**, 155-167 (2001)
32. Carrick, L.L. Vegetable oil paints. *J. Am. Oil Chem. Soc.* **27**, 513-522 (1950)
33. Kim, J.; Kim, D.N.; Lee, S.H.; Yoo, S.H.; Lee, S. Correlation of fatty acid composition of vegetable oils with rheological behaviour and oil uptake. *Food Chem.* **118**, 398-402 (2010)
34. Aigbodion, A.I.; Okieimen, F.E.; Obazee E.O.; Bakare, I.O. Utilization of maleinized rubber seed oil and its alkyd resin as binder in water-borne coatings. *Prog. Org. Coat.* **46**, 28-31 (2003)
35. Shende, P.G.; Dabhade, S.B. *Polymers Synthesis and Applications in Proceedings of the National Seminar on Polymers*, edited by Vohra, D.K.; Singh, D.; Singh, P. Vol 104, (Allied Publishers Ltd., 1997)
36. Chahande, P.P.; Gogte, B.B. Ecofriendly primers based on very short oil novel alkyd. *Paintindia* **57**, 61-64 (2007)
37. Mondhe, O.P.S.; Rao, J.T. Studies on *Jatropha Curcas* seed oil incorporated alkyd

- dyes. II. Preparation and application of azo alkyd dyes. *Colourage* **40**, 51-53 (1993)
38. Kulkarni, R.D.; Gogte, B.B. "SORBO" alkyd emulsion paste for primers & synthetic enamels. *Paintindia* **44**, 41-45 (1994)
39. Thames, S.F.; Yu H.; Wang, M.D. Air-dry primer coatings from dehydrated lesquerella oil. *Ind. Crop. Prod.* **6**, 169-175 (1997)
40. Igwe, I.O.; Ogbobe, O. Studies on the properties of polyesters and polyester blends of selected vegetable oils. *J. Appl. Polym. Sci.* **75**, 1441-1446 (2000)
41. Abd El-Aal, M.H.; Khalil, M.K.M.; Rahma, E.H. Apricot kernel oil: Characterization, chemical composition and utilization in some baked products. *Food Chem.* **19**, 287-298 (1986)
42. Panda, S.; Kar, A. *Annona squamosa* seed extract in the regulation of hyperthyroidism and lipid-peroxidation in mice: Possible involvement of quercetin. *Phytomedicine* **14**, 799-805 (2007)
43. Ajiwe, V.I.E.; Okeke, C.A.; Agbo, H.U. Extraction and utilization of *Azelaia Africana* seed oil. *Bioresour. Technol.* **53**, 89-90 (1995)
44. Aigbodion, A.I.; Okieimen, F.E. An investigation of the utilization of African locustbean seed oil in the preparation of alkyd resins. *Ind. Crop. Prod.* **13**, 29-34 (2001)
45. Theng, B.K.G. Interactions of clay minerals with organic polymers: Some practical applications. *Clay Miner.* **18**, 357-362 (1970)
46. Hess, P.H.; Parker, P.H.J. Polymers for stabilization of colloidal cobalt particles. *J. Appl. Polym. Sci.* **10**, 1915-1927 (1966)
47. Kojima, Y. *et al.* Sorption of water in nylon 6-clay hybrid. *J. Appl. Polym. Sci.* **49**, 1259-1264 (1993)
48. Paul, D.R.; Robeson, L.M. Polymer nanotechnology: Nanocomposites. *Polymer* **49**, 3187-3204 (2008)
49. Paul, S. *Surface Coatings Science & Technology*, 2<sup>nd</sup> edn. (John Wiley & Sons, New York, 1997)
50. Stoye, D.; Freitag, W. (Eds.), *Resins for Coatings Chemistry* (Hanser Publishers, New York, 1996)
51. Malshe, V.C.; Sikchi, M. *Basics of Paint Technology*, Part I, 1<sup>st</sup> edn. (UICT Mumbai, 2004)
52. Wicks, Z.W.; Frank, J.; Jones, N.; Pappas, S.P. *Organic Coatings Science and Technology*, 2<sup>nd</sup> edn. (John Wiley & Sons, New Jersey, 1999)

53. Mark, H.F.; Bikales, N.M.; Overberger, C.G.; Menges, G. *Encyclopedia of Polymer Science and Engineering*, Vol. 1 (Wiley Interscience, New York, 1985)
54. Zhang, X. Synthesis and characterization of hyperbranched polyesters based on isophthalic acid and trimethylolpropane. *J. Macromol. Sci. Part A: Pure Appl. Chem.* **48**, 128-134 (2011)
55. Hajek, K. Verwendung von sorbit and xylit zur synthese von alkydharzen. *Farbe und Lack* **83**, 798-804 (1977)
56. Bagchi, D.; Malakar, R.K. Sorbitol as an alkyd ingredient. *J. Coat. Technol.* **58**, 51-57 (1986)
57. Mckillip, W.J.; Kellan, J.N.; Impola, C.N.; Buckney, R.W.; Otey, F.H. Glycol glycosides in alkyds. *J. Paint Technol.* **42**, 312-319 (1970)
58. Chandra, S.; Pasari, S. Synthesis of styrenated alkyds. *J. Sci. Ind. Res.* **41**, 248-257 (1982)
59. Aurelian, B.; Rom, B. Effects of cycloaliphatic and alkylarylic glycols on the relations between the chemical structure and the properties of fatty acid modified isophthalic alkyd resins. *Farbe und Lack* **79**, 413-419 (1973)
60. Pakulin, V.V.; Bulatov, M.A.; Spasskii S.S., Kruglikov, A.A. Synthesis and properties of modified alkyd resins made from polyepentaerythritols. *Lakokrasochnye Materialy i lkh Primenenie* **2**, 23-25 (1973)
61. Golding, B. *Polymers and Resins* (D. Van Nostrand Company Inc., New Jersey, 1959)
62. Bhandari, S.; Chandra, S. Chlorinated resins and polymers: A survey of the present state. *Prog. Org. Coat.* **23**, 155-182 (1993)
63. Aigbodion, A.I.; Okieimen, F.E.; Ikhuoria, E.U.; Bakare I.O.; Obazee, E.O. Rubber seed oil modified with maleic anhydride and fumaric acid and their alkyd resins as binders in water-reducible coatings. *J. App. Polym. Sci.* **89**, 3256-3259 (2003)
64. Angiolini, L.; Greci, V.; Salatelli, E. Improving waterborne alkyd resins with fatty acids. *Ind. Paint Powder* **80**, 27-30 (2004)
65. Odian, G. (Ed.), *Principles of Polymerization*, 3<sup>rd</sup> edn. (John Wiley & Sons, New York, 1991)
66. Aydin, S.; Akcay, H.; Özkan, E.; Güner, F.S.; Erciyes, A.T. The effects of anhydride type and amount on viscosity and film properties of alkyd resin. *Prog. Org. Coat.* **51**, 273-279 (2004)

67. El-hai, F.A.; Sabbah, I.A.; Nasar, A.M.; Abdel-Rehim, N.S. High performance alkyd resin compositions for coating. *Int. J. Polym. Mater.* **53**, 871-878 (2004)
68. Volozhin, A.I.; Lopatik, D.V.; Solntsev, A.P.; Radkevich, S.E. Modified alkyd resins obtained from bicycle [2.2.2.] oct-5-ene-2,3-dicarboxylic acid anhydride, pentaerythritol, and trimethylolpropane. *Seryya Khimichnykh Navuk* **2**, 89-91 (1973)
69. Belorossova, Z.P.; Buntova, V.I.; Izyummov, V.N. Alkyd resins made from benzophenonetetracarboxylic dianhydride. *Lakokrasochnye Materialy i Ikh Primenenie* **1**, 4-7 (1973)
70. Zuckert, B. Aqueous emulsion of air drying and stoving alkyd resins and process for producing said resins. *US patent* 4333865 (1980)
71. Phate, B.W.; Gogte, B.B. Wall finishes based on novel short oil rosinated alkyd. *Paintindia* **55**, 71-76 (2005)
72. Gangotri, L.T. Water thinnable alkyd emulsions. *Paintindia* **53**, 33-36 (2003)
73. Yakovlev, A.D. *et al.* Alkyd resin-based compositions for coatings on wet surfaces. *RU Pat.* 2200176 (2003)
74. Chatfield, H.W. *Varnish Constituents*, 3<sup>rd</sup> edn. (Leonard Hill Limited, London, 1953)
75. Madhusudhan, V.; Murthy, B.G.K. Polyfunctional compounds from cardanol. *Prog. Org. Coat.* **20**, 63-71 (1992)
76. Tawn, A.R.H. Metal-drier catalysis. *J. Oil Col. Chem. Assoc.* **39**, 223-232 (1956)
77. Gryglewicz, S. Alkaline-earth metal compounds as alcoholysis catalysts for ester oils synthesis. *Appl. Catal., A* **192**, 23-28 (2000)
78. Brown, R.S.; Neverov, A.A. Metal-catalyzed alcoholysis reactions of carboxylate and organophosphorus esters. *Adv. Phys. Org. Chem.* **42**, 271-331 (2007)
79. Gupta, S.; Samuel, K.S.; Belgaonkar, V.H. Alcoholysis of vegetable oils and its effect on alkyd synthesis. *Paintindia* **43**, 17-21 (1993)
80. Mahendra, D.; Chang, X.; Victor, P. *Proceedings of the international waterborne, high solids and powder coatings symposium* **30**, 423-424 (2003)
81. Athawale, V.D.; Joshi, K.R. A comparative study on coating properties of chemoenzymatically synthesised and conventional alkyd resins. *Paintindia* **51**, 47-50 (2001)

82. Kumar, G.S.; Ghogare A.; Mukesh, D. Synthesis of alkyds involving regioselective lipase-catalyzed transesterification in organic media. *J. Appl. Polym. Sci.* **63**, 35-45 (1997)
83. Alexandre, M.; Dubois, P. Polymer-layered silicate nanocomposites: Preparation, properties and uses of a new class of materials. *Mater. Sci. Eng. R* **28**, 1-63 (2000)
84. Ray, S.S.; Bousmina, M. Biodegradable polymers and their layered silicate nanocomposites: In greening the 21st century materials world. *Prog. Mater. Sci.* **50**, 962-1079 (2005)
85. Grobert, N. Carbon nanotubes-becoming clean. *Mater. Today* **10**, 28-35 (2007)
86. Spitalsky, Z.; Tasis, D.; Papagelis, K.; Galiotis, C. Carbon nanotube-polymer composites: Chemistry, processing, mechanical and electrical properties. *Prog. Polym. Sci.* **35**, 357-401 (2010)
87. Tasis, D.; Tagmatarchis, N.; Bianco, A.; Prato, M. Chemistry of carbon nanotubes. *Chem. Rev.* **106**, 1105-1136 (2006)
88. Kumar, A.P.; Depan, D.; Tomer, N.S.; Singh, R.P. Nanoscale particles for polymer degradation and stabilization-Trends and future perspectives. *Prog. Polym. Sci.* **34**, 479-515 (2009)
89. Vaia, R.A.; Giannelis, E.P. Lattice of polymer melt intercalation in organically modified layered silicates. *Macromolecules* **30**, 7990-7999 (1997)
90. Pavlidou, S.; Papaspyrides, C.D. A review on polymer-layered silicate nanocomposites. *Prog. Polym. Sci.* **33**, 1119-1198 (2008)
91. Tanahashi, M. Development of fabrication methods of filler/polymer nanocomposites: with focus on simple melt-compounding-based approach without surface modification of nanofillers. *Materials* **3**, 1593-1619 (2010)
92. Oil and Colour Chemist's Association of Australia, *Surface Coatings*, Vol. 1 (Chapman and Hall, London, 1981)
93. Silverstein, R.M.; Bassler G.C.; Morrill, T.C. *Spectroscopic Identification of Organic Compounds*, 5<sup>th</sup> edn. (John Wiley & Sons, New York, 1991)
94. Kemp, W. *Organic Spectroscopy*, 3<sup>rd</sup> edn. (ELBS, Hampshire, 1991)
95. Crompton, T.R. *Analysis of Polymers* (Pergamon Press, New York, 1989)
96. Hunt, B.J.; James, M.I. (Eds.), *Polymer Characterization* (Blackie Academic & Professional, New York, 1993)
97. Ibbett, R.N. (Ed.), *NMR Spectroscopy of Polymers* (Blackie Academic & Professional, New York, 1993)

98. Jaisankar, S.N.; Lakshminarayana, Y.; Radhakrishnan, G.; Ramasami, T. Modified castor oil based polyurethane elastomers for one shot process. *Polym. Plast. Technol. Eng.* **35**, 781-789 (1996)
99. Aigbodion, A.I.; Okieimen, F.E. Kinetics of the preparation of rubber seed oil alkyds. *Eur. Polym. J.* **32**, 1105-1108 (1996)
100. Gan, S.N.; Tan, B.Y. FTIR studies of the curing reactions of palm oil alkyd melamine enamels. *J. Appl. Polym. Sci.* **80**, 2309-2315 (2001)
101. Salazar-Rojas, E.M.; Urban, M.W. Curing of non-pigmented alkyd coatings detected by in-situ photoacoustic Fourier transform infrared spectroscopy (PA FTIR). *Prog. Org. Coat.* **16**, 371-386 (1989)
102. Vance, J.A.; Brakke, N.B.; Quinney, P.R. Determination of oil content in oil modified o-phthalic polyester resins by infrared spectrometry. *Anal. Chem.* **51**, 499-501 (1979)
103. Zhong-lei, F.; Da-zhuang, L.; Gen-suo, Z. IR studies on chlorinated polypropylene/alkyd resin blends. *Guangpuxue Yu Guangpu Fenxi* **23**, 611-612 (2003)
104. Marshall, G.L.; Lander, J.A. Characterisation of cured alkyd paint binders using swollen state <sup>13</sup>C-NMR. *Eur. Polym. J.* **21**, 959-966 (1985)
105. Haken, J.K.; Iddamalgoda, P.I. Analysis of polyesters and alkyd resins. *Prog. Org. Coat.* **19**, 193-225 (1991)
106. Marshall, G.L. A <sup>13</sup>C-NMR study of stoving alkyd systems. *Eur. Polym. J.* **22**, 217-230 (1986)
107. Spyros, A. Characterization of unsaturated polyester and alkyd resins using one- and two-dimensional NMR spectroscopy. *J. Appl. Polym. Sci.* **88**, 1881-1888 (2003)
108. Thames, S.F.; Yu, H.; Wang, M.D. Air-dry primer coatings from dehydrated lesquerella oil. *Ind. Crop. Prod.* **6**, 169-175 (1997)
109. Filipovic, J.M.; Velickovic, J.S.; Batalovic, Z.U.; Trifunovic, M.D. Kinetics of the curing process of alkyd-melamine resin systems. *Thermochim. Acta* **149**, 341-348 (1989)
110. Mallegol, J.; Gonon, L.; Commereuc, S.; Verney, V. Thermal (DSC) and chemical (iodometric titration) methods for peroxides measurements in order to monitor drying extent of alkyd resins. *Prog. Org. Coat.* **41**, 171-176 (2001)

111. Athawale, V.D.; Chamankar, A.V.; Athawale, M. Alkyd-ketonic blends for coatings applications. *Paintindia* **50**, 39-46 (2000)
112. Aurelia, I.; Constanta, I.; Camelia, M. Morphology of a synthetic alkyd melamine resin system. *Seria Chimie si Midiului* **46**, 274-279 (2001)
113. Wang, C.; Jones, F.N. Stability and film properties of tung oil modified soybean alkyd emulsion. *J. Appl. Polym. Sci.* **78**, 1698-1706 (2000)
114. Vaia, R.A.; Jant, K.D.; Kramer, E.J.; Giannelis, E.P. Microstructural evolution of melt intercalated polymer-organically modified layered silicates nanocomposites. *Chem. Mater.* **8**, 2628-2635 (1996)
115. Morgan, A.B.; Gilman, J.W. Effects of organoclay Soxhlet extraction on mechanical properties, flammability properties and organoclay dispersion of polypropylene nanocomposites. *J. Appl. Polym. Sci.* **87**, 2313-2320 (2003)
116. Zou, H.; Wu, S.; Shen, J. Polymer/silica nanocomposites: Preparation, characterization, properties and applications. *Chem. Rev.* **108**, 3893-3957 (2008)
117. Amalvy, J.I.; Percy, M.J.; Armes, S.P.; Leite, C.A.P.; Galembeck, F. Characterization of the nanomorphology of polymer-silica colloidal nanocomposites using electron spectroscopy imaging. *Langmuir* **21**, 1175-1179 (2005)
118. VanderHart, D.L.; Asano, A.; Gilman, J.W. NMR measurements related to clay dispersion quality and organic-modifier stability in nylon-6/clay nanocomposites. *Macromolecules* **34**, 3819-3822 (2001)
119. Zanetti, M.; Lomakin, S.; Camino, G. Polymer layered silicate nanocomposites. *Macromol. Mater. Eng.* **279**, 1-9 (2000)
120. Crosby, A.J.; Lee, J.Y. Polymer nanocomposites: The "nano" effect on mechanical properties. *Polym. Rev.* **47**, 217-229 (2007)
121. LeBaron, P.C.; Wang, Z.; Pinnavaia, T.J. Polymer-layered silicate nanocomposites: An overview. *Appl. Clay Sci.* **15**, 11-29 (1999)
122. Osman, M.A.; Mittal, V.; Lusti, H.R. The aspect ratio and gas permeation in polymer-layered silicate nanocomposites. *Macromol. Rapid Commun.* **25**, 1145-1149 (2004)
123. Becker, O.; Varley, R.J.; Simon, G.P. Thermal stability and water uptake of high performance epoxy layered silicate nanocomposites. *Eur. Polym. J.* **40**, 187-195 (2004)



124. Lu, S.Y.; Hamerton, I. Recent developments in the chemistry of halogen-free flame retardant polymers. *Prog. Polym. Sci.* **27**, 1661-1712 (2002)
125. Cho, J.W.; Paul, D.R. Nylon 6 nanocomposites by melt compounding. *Polymer* **42**, 1083-1094 (2001)
126. Beecroft, L.L.; Ober, C.K. Nanocomposite materials for optical applications. *Chem. Mater.* **9**, 1302-1317 (1997)
127. Battisti, A.; Skordos, A.A.; Partridge, I.K. Percolation threshold of carbon nanotubes filled unsaturated polyesters. *Compos. Sci. Technol.* **70**, 633-637 (2010)
128. Liu, J.W.; Zhao, Q.; Wan, C.X. Research progresses on degradation mechanism *in vivo* and medical applications of polylactic acid. *Space Med. Med. Eng.* **14**, 308-312 (2001)
129. Zeng, Q.H.; Yu, A.B.; Lu (Max), G.Q.; Paul, D.R. Clay-based polymer nanocomposites: Research and commercial development. *J. Nanosci. Nanotechnol.* **5**, 1574-1592 (2005)
130. Bordes, P.; Pollet, E.; Avérous, L. Nano-biocomposites: Biodegradable polyester/nanoclay systems. *Prog. Polym. Sci.* **34**, 125-155 (2009)
131. Fogelstrom, L.; Malmstrom, E.; Johansson, M.; Hult, A. Hard and flexible nanocomposite coatings using nanoclay-filled hyperbranched polymers. *Appl. Mater. Interfaces* **2**, 1679-1684 (2010)
132. Jawahar, P.; Balasubramanian, M. Preparation and properties of polyester-based nanocomposite gel coat system. *J. Nanomater.* **21656**, 1-7 (2006)
133. Kawasaki, S.; Yamada, M.; Kobori, K.; Jin, F.; Takata, T. High dispersion ability of fluorene-based polyester as a polymer matrix for carbon nanotubes. *J. Appl. Polym. Sci.* **118**, 2690-2695 (2010)
134. Rajesh, Ahuja, T.; Kumar, D. Recent progress in the development of nano-structured conducting polymer/nanocomposites for sensor applications. *Sens. Actuators B: Chem.* **136**, 275-286 (2009)
135. de Espinosa, L.M.; Meier M.A.R. Plant oils: The perfect renewable resource for polymer science? *Eur. Polym. J.* doi:10.1016/j.eurpolymj.2010.11.020 (2011)
136. Narodslawsky, M.; Niederl-Schmidinger, A.; Halasz, L. Utilising renewable resources economically: New challenges and chances for process development. *J. Cleaner Prod.* **16**, 164-170 (2008)
137. Fleischer, T.; Grunwald, A. Making nanotechnology developments sustainable: A role for technology assessment? *J. Cleaner Prod.* **16**, 889-898 (2008)

138. Miyagawa, H.; Misra, M.; Drzal, L.T.; Mohanty, A.K. Novel biobased nanocomposites from functionalized vegetable oil and organically-modified layered silicate clay. *Polymer* **46**, 445-453 (2005)
139. Tao, B.Y. *Bioprocessing for Value-Added Products from Renewable Resources: New Technologies and Applications*, edited by Yang, S.T. Chapter **24**, 611-627 (Elsevier, 2007).
140. Raman, N.; Sudharsan, S.; Pothiraj, K. Synthesis and Structural Reactivity of inorganic-organic hybrid Nanocomposites: A review. *J. Saudi Chem. Soc.* doi:10.1016/j.jscs.2011.01.012 (2011)
141. Kumar, A.P.; Depan, D.; Tomer, N.S.; Singh, R.P. Nanoscale particles for polymer degradation and stabilization-Trends and future perspectives. *Prog. Polym. Sci.* **34**, 479-515 (2009)
142. Bringi, N.V. (Ed.), *Non-Traditional Oil Seeds and Oils in India* (Oxford & IBH Publishing Co. Pvt. Ltd., New Delhi, 1987)
143. Dutta, N. *Development of Polyester Resins from Mesua ferrea L. Seed Oil* (PhD Thesis, Tezpur University, India, 2006)
144. van Benthem, R.A.T.M. Novel hyperbranched resins for coating applications. *Prog. Org. Coat.* **40**, 203-214 (2000)
145. Manczyk, K.; Szewczyk, P. Highly branched high solids alkyd resins. *Prog. Org. Coat.* **44**, 99-109 (2002)
146. Bat, A.; Gunduz, G.; Kisakurek, D.; Akhmedov, I.M. Synthesis and characterization of hyperbranched and air drying fatty acid based resins. *Prog. Org. Coat.* **55**, 330-336 (2006)
147. Murillo, E.A.; Vallejo, P.P.; López, B.L. Synthesis and characterization of hyperbranched alkyd resins based on tall oil fatty acids. *Prog. Org. Coat.* **69**, 235-240 (2010)
148. Cert, A.; Moreda, W.; Perez-Camino, M.C. Chromatographic analysis of minor constituents in vegetable oils. *J. Chromatogr. A* **881**, 131-148 (2000)
149. Hayes, D.G. Enzyme-Catalyzed modification of oilseed materials to produce eco-friendly products. *J. Am. Oil Chem. Soc.* **81**, 1077-1103 (2004)
150. Dutta, S. *Development of Mesua ferrea L. Seed Oil Based Polyurethane Resins* (PhD Thesis, Tezpur University, India, 2009)
151. Mandik, A.; Tutalkova, A.; Makes, J. Investigation of alcoholysis by GPC. *Farbe und Lack* **83**, 186-192 (1977)

## Chapter 1

152. Roy Choudhury, R.B. The preparation and purification of monoglycerides I. Glycerolysis of oils. *J. Am. Oil Chem. Soc.* **37**, 483-486 (1960)
153. Sathyanarayana, M.N.; Kishanprasad, V.S.; Rao, T.C.; Sampathkumaran, P.S.; Gedan, P.H. Compositional analysis of partial glycerides. *Paintindia* **44**, 31-36 (1994)
154. Igwe I.O.; Ogbobe, O. Studies on the alcoholysis of some seed oils. *J. Appl. Polym. Sci.* **78**, 1826-1832 (2000)
155. Carlston, E.F. Acidolysis of vegetable and marine oils with phthalic acids. *J. Am. Oil Chem. Soc.* **37**, 366-371 (1960)
156. Haq, M.; Burgueño, R.; Mohanty, A.K.; Misra, M. Bio-based polymer nanocomposites from UPE/EML blends and nanoclay: Development, experimental characterization and limits to synergistic performance. *Compos Part A: Appl. Sci. Manuf.* **42**, 41-49 (2011)
157. Alam, J.; Riaz, U.; Ashraf, S.M.; Ahmad, S. Corrosion-protective performance of nano polyaniline/ferrite dispersed alkyd coatings, *J. Coat. Technol. Res.* **5**, 123-128 (2008)
158. Dhoke, S.K.; Sinha, T.J.M.; Khanna, A.S. Effect of nano- $\text{Al}_2\text{O}_3$  particles on the corrosion behavior of alkyd based waterborne coatings. *J. Coat. Technol. Res.* **6**, 353-368 (2009)
159. Dhoke, S.K.; Bhandari, R.; Khanna, A.S. Effect of nano-ZnO addition on the silicone-modified alkyd-based waterborne coatings on its mechanical and heat-resistance properties. *Prog. Org. Coat.* **64**, 39-46 (2009)
160. Bal, A.; Guclu, G.; Acar, I.; Iyim, T.B. Effects of urea formaldehyde resin to film properties of alkyd-melamine formaldehyde resins containing organo clay. *Prog. Org. Coat.* **68**, 363-365 (2010)
161. Bhanvase, B.A.; Sonawane, S.H. New approach for simultaneous enhancement of anticorrosive and mechanical properties of coatings: Application of water repellent nano  $\text{CaCO}_3$ -PANI emulsion nanocomposite in alkyd resin. *Chem. Eng. J.* **156**, 177-183 (2010)
162. Mironi-Harpaz, I.; Narkis, M.; Siegmann, A. Curing of styrene-free unsaturated polyester alkyd and development of novel related clay nanocomposites. *Macromol. Symp.* **242**, 201-207 (2006)

163. Lu, J.; Hong, C.K.; Wool, R.P. Bio-based nanocomposites from functionalized plant oils and layered silicate. *J. Polym. Sci. Part B: Polym. Phys.* **42**, 1441-1450 (2004)
164. Jiratumnukul, N.; Pruthipaitoon, S.; Pitsaroup, T. Nanocomposite Alkyd Coatings. *J. Appl. Polym. Sci.* **102**, 2639-2642 (2006)
165. Riccio, M. *et al.* An IR study of the chemistry of triethoxysilane at the surface of metal oxides. *Colloids Surf., A* **294**, 181-190 (2007)
166. Alam, J.; Riaz, U.; Ahmad S. Nanostructured polyaniline reinforced sustainable resource (soy oil alkyd) based composites. *Polym. Compos.* **31**, 32-37 (2010)
167. Karak, N.; Konwarh, R.; Voit, B. Catalytically active vegetable-oil-based thermoplastic hyperbranched polyurethane/silver nanocomposites. *Macromol. Mater. Eng.* **295**, 159-169 (2010)
168. Ashraf, S.M.; Ahmad, S.; Riaz, U. Development of novel conducting composites of linseed-oil-based poly(urethane amide) with nanostructured poly(1-naphthylamine). *Polym. Int.* **56**, 1173-1181 (2007)
169. Akram, D.; Ahmad, S.; Sharmin, E.; Ahmad, S. Silica reinforced organic-inorganic hybrid polyurethane nanocomposites from sustainable resource. *Macromol. Chem. Phys.* **211**, 412-419 (2010)
170. Dong, Z.; Li, Y.; Zou, Q. Degradation and biocompatibility of porous nano-hydroxyapatite/polyurethane composite scaffold for bone tissue engineering. *Appl. Surf. Sci.* **255**, 6087-6091 (2009)
171. Dutta, S.; Karak, N.; Saikia, J.P.; Konwar, B.K. Biocompatible epoxy modified bio-based polyurethane nanocomposites: Mechanical property, cytotoxicity and biodegradation. *Bioresour. Technol.* **100**, 6391-6397 (2009)
172. Liu, Z.; Erhan, S.Z. Green composites and nanocomposites from soybean oil. *Mater. Sci. Eng. A* **483-484**, 708-711 (2008)
173. Uyama, H. *et al.* Green nanocomposites from renewable resources: Plant oil-clay hybrid materials. *Chem. Mater.* **15**, 2492-2494 (2003)
174. Jaffar Al-Mulla, E.A.; Suhail, A.H.; Aowd, S.A. New biopolymer nanocomposites based on epoxidized soybean oil plasticized poly(lactic acid)/fatty nitrogen compounds modified clay: Preparation and characterization. *Ind. Crop. Prod.* **33**, 23-29 (2011)

## CHAPTER 2

---

### Synthesis, Characterization and Properties of *Mesua ferrea* L.

#### Seed Oil Based Polyester Resins

##### 2.1. Introduction

The declining of petroleum oil reserves, dwindling price of petroleum products and the stringent environment concerns drive the polymer industries to opt the ecologically acceptable feed stocks for the development of polymeric materials. In this regard, renewable natural bio-resources are now greatly being favored in the production of varieties of industrial products including polymeric materials in preference to petroleum based products because of the biodegradability and environmental friendly characteristics of the former.<sup>1-3</sup> Among the different types of such renewable resources, vegetable oils represent one of the most environmentally benign and abundant biological feed stocks and thereby expected to be an alternative viable raw materials for production of valuable industrial products including polymers.<sup>3</sup> The products based on vegetable oils play important roles for many industrial applications such as surface coatings, paints, varnishes, printing inks, soaps, shoe polishes, cosmetics, pharmaceuticals, multipurpose additives etc.

The vegetable oil used for the present investigation was obtained from *Mesua ferrea* L. seed plant available in different countries especially in India. The seeds contain exceptionally large amount of oil (75%). The oil contains oleic (52.3%) and linoleic (22.3%) acids as unsaturated, and palmitic (15.9%) and stearic acids (9.5%) as saturated fatty acids.<sup>4</sup> This fatty acid composition indicates its potentiality as feedstock in the development of different types of industrially important polymers. This has already been proved by the preparation of various types of polymers like polyester, polyurethane, poly(ester amide), epoxy etc. from the same laboratory.<sup>5-7</sup> Among the above resins, polyester resins have many advantages over other industrially used resins for different applications and also oil modified polyester resins have been used in

---

Parts of this work are published in (i) *Polym. Plast. Technol. Eng.* **48**, 970-975 (2009)

(ii) *Polym. Degrad. Stab.* **94**, 2221-2230 (2009)

(iii) *Int. J. Polym. Mater.* (In press)

(iv) *Polym. J.* (On line)

surface coating industry for a long time.<sup>8</sup> A number of both traditional and non-traditional vegetable oils including *Mesua ferrea* L. seed oil are being utilized for the preparation of polyesters.<sup>5,9-11</sup>

Again, the unique structural characteristics of hyperbranched polymers have drawn a significant attention for the utilization of such materials in different advanced applications.<sup>12</sup> The single step one pot polymerization technique has paved the way for large scale production of the hyperbranched polymers with low polydispersity index at a reasonable cost.<sup>13</sup> The hyperbranched polymer possesses higher solubility, lower hydrodynamic diameter and lower melt as well as solution viscosity than its linear analog.<sup>14</sup> This is due to the compact, non-entangled, globular and highly branched structure with large numbers of active surface functionalities of the hyperbranched polymer. Therefore hyperbranched polymers have many advantages over their linear analogs. The use of polyfunctional acids or polyols and their derivatives like trimellitic anhydride (TMA), 2,2-bis(hydroxymethyl) propionic acid (bis-MPA) and hyperbranched polyol may generate highly branched structures of the synthesized resins, if gelation can be avoided during the resinification reactions. In the present investigation, the highly branched polyesters were synthesized by polycondensation of vegetable oil based hydroxyl or carboxyl terminated pre-polymer and TMA or bis-MPA or bisphenol-S with hyperbranched polyether polyol of bisphenol-A and cyanuric chloride using a three-stage single pot resinification technique. The pre-polymer and the conventional linear polyester of the oil were prepared by the conventional glycerolysis process followed by polycondensation with phthalic and maleic anhydrides. Therefore in this chapter, the synthesis, characterization and properties of *Mesua ferrea* L. seed oil modified highly branched and linear polyesters are discussed.

## 2.2. Experimental

### 2.2.1. Materials

The *Mesua ferrea* L. seed oil used in the present investigation was extracted from the matured seeds collected from Sivasagar, Assam, India. The seeds were obtained from the Nahar plant, which is a large tree with a conical crown and is about 3-15 m in height. It is found in different countries like India, Sri Lanka, Bangladesh, Nepal, Indochina (South-East Asia), Malay Peninsula etc. In India<sup>15,16</sup> it is mainly found in North-East region, West Bengal, Karnataka, Kerala etc. The oil is slightly viscous

liquid and brown in color and has a characteristic smell. The tree bears flowers between April and July, and fruits between October and November. The average yield of seeds per tree is around 10-15 kg per annum. The oil content is about 70-75%. The availability of Nahar seeds in India per year is 5,690 tonnes.<sup>17</sup> The oil was extracted from the dried powdered seeds by solvent soaking technique using petroleum ether (Merck, India) as the solvent. The oil was purified by degumming with water followed by alkali refining technique using 0.01% aqueous NaOH solution, and then washed with distilled water followed by drying under vacuum.<sup>18</sup>

Glycerol was obtained from Merck, India with density 1.26 g/mL, maximum sulphated ash 0.005% and minimum assay 99%. Other impurities present are glycerol tributyrate 0.05%, chloride 0.0001%, sulphate 0.0005% and heavy metals 0.0002%. Glycerol is used as a prochiral building block in organic synthesis. It is generally used in the production of hydrogen gas, citric acid, propylene glycol, acrolein, ethanol, epichlorohydrin for epoxy synthesis etc. It is also used in pharmaceutical and medical applications. In the present investigation, it was used as a triol (alcoholizing reagent) for converting triglyceride ester of *Mesua ferrea* L. seed oil into monoglyceride. It was used after drying under vacuum.

Lead mono-oxide (PbO) was obtained from Loba Chemie, India with minimum assay 99%, and maximum limit of impurities chloride 0.02%, copper 0.005% and iron 0.01%. It is generally used in lead paints, lead-acid batteries, vulcanization of rubber and as catalysts in many organic condensation reactions. Herein, it was used as a catalyst for trans-esterification reaction of triglyceride with glycerol. It was utilized as received.

Phthalic anhydride (PA) obtained from Merck, India with melting range 129-132 °C, sulphated ash 0.005%, minimum assay 99.5% etc. was used as received.

Maleic anhydride (MA) was obtained from Merck, Germany with melting range 51-53 °C, maximum sulphated ash 0.05% and minimum assay 99.5%. It was used without further purification.

Trimellitic anhydride (TMA) was obtained from Merck, Germany. It has a melting point (m.p.) of 165 °C, a boiling point (b.p.) of 390 °C, and a molecular weight of 192.13 g/mol. It is a highly reactive chemical and is a starting material for a variety of organic chemical products. TMA is used in the synthesis of plasticizers that are in turn compounded with polyvinyl chloride (PVC) to make flexible plastic products such as automotive dashboards and coatings for electrical wire and cable. It is used as a

## Chapter 2

reactant of polyester resins, which was mainly employed in powder coatings and the products used in military, industrial and aerospace applications. It is also used for a variety of purposes including as an epoxy curing agent, textile sizing agent, rubber curing accelerator, electrostatic toner binder, and vinyl cross-link agent.

2,2-Bis(hydroxymethyl) propionic acid (bis-MPA) was obtained from Merck, Germany. It is a white crystalline material and is a trifunctional compound of neopentyl structure containing two primary hydroxyl groups and one tertiary carboxyl group. It is used in polyurethane dispersions, photographic chemicals, printing inks, waterborne alkyds and polyesters, conventional alkyds and polyesters, chemical building block etc. It has a hydroxyl value of 810-860 mg KOH/g and acid value of 405-425 mg KOH/g. Its m.p. is 180 °C and molecular weight is 134.13 g/mol.

Bisphenol-A (BPA) was obtained from Burgoyne India, Mumbai. It was recrystallized from toluene before use. The m.p. of the purified compound is 157 °C and molecular weight is ( $M_w$ ) 228.29 g/mol.

4,4'-Sulfonyl diphenol (BPS) was obtained from Aldrich Chemie, Germany. The compound has m.p. 245 °C, purity 98% and molecular weight ( $M_w$ ) 250.27 g/mol. It was used as received. This compound is generally used in preparation of thermostable epoxy resin as an aromatic diol. Here it is used as a thermostable aromatic diol ( $A_2$  monomer).

Cyanuric chloride (CYC) was purchased from Merck, Germany. It has m.p. 144-147 °C, purity 99% and molecular weight ( $M_w$ ) 184.41 g/mol. It was used after recrystallization in chloroform. It is mainly used as an intermediate for manufacturing agrochemical, dyestuffs, optical brighteners, tanning agents, softening agents, pharmaceutical building block for plastics and additives. Here it was used as an  $A_3$  monomer.

Sodium metal (Na) was obtained from Merck, Germany. It has atomic weight ( $A_w$ ) 22.9 g/mol and purity 98.8% with chloride (0.01%), silica (0.002%), calcium (0.1%) and iron (0.01%) as impurities. It was kept in paraffin oil and used as received after cutting into small pieces.

Magnesium turning (Mg-turning) was purchased from SRL, Mumbai. It has atomic weight ( $A_w$ ) 24.31 g/mol and purity 99.8% with maximum 0.05% iron as impurity. It was purified by thorough washing with dilute HCl followed by washing with distilled water. The process is repeated for several times until the turning became



shining. Finally it was washed with acetone and dried under vacuum at 45 °C for 4-5 h. The dried turnings were used in the same day.

Calcium oxide (CaO) was obtained from S.D. Fine Chem. Ltd., Mumbai. Its molecular weight ( $M_w$ ) is 56.08 g/mol and purity is 95% after ignition. The loss on ignition is 10% and impurities present are generally chloride (0.1%), sulfate (0.5%), iron (0.1%) and lead (0.02%). It was used as received.

Methyl-ethyl ketone peroxide (MEKP) and cobalt octate were obtained from Kumud enterprise, Kharagpur. MEKP is a clear liquid with density of 1.053 g/mL and cobalt octate is 2% solution of cobalt octate in cyclohexanone.

Styrene was obtained from Merck, Germany of density 0.906 g/ml, assay  $\geq$  99%. It contained tertiary butyl catecol as inhibitor. Styrene was used after removal of the inhibitor by washing with 4% alkali solution followed by washing with distilled water and then drying.

Bisphenol-A based epoxy resin (Araldite LY 250) and poly(amido amine) hardener (HY 840) were obtained from Hindustan Ciba Geigy Ltd. and used as received. The specifications of epoxy resin and hardener are given in Table 2.1.

**Table 2.1:** Some technical specifications of epoxy resin and hardener

Name	Araldite LY 250 (Ciba Geigy)	Hardener HY 840 (Ciba Geigy)
Viscosity at 25 °C (mPas)	450-650	10000-25000
Epoxy equivalent (g/eq)	182-192	—
Epoxy content (eq/kg)	5.2-5.5	—
Amine value (eq/kg)	—	6.6-7.5
Density at 25 °C (g/cm <sup>3</sup> )	1.15	0.98

Methanol (CH<sub>3</sub>OH) was obtained from Merck, India. It has molecular weight 58.0 g/mol, purity  $\geq$  99.5%, density 0.971 g/mL and b.p. 56-57 °C. It is used as a solvent and also as a reagent to prepare sodium methoxide. Super dry methanol was used for this purpose, which was obtained as follows. An amount of about 4 g of purified dry Mg-turnings was taken in a 1000 mL single neck round bottom flask. A pinch of iodine was added into it and heated for 2-3 min. About 50 mL of distilled methanol was added into the above mixture. The flask was then fitted with a reflux condenser along with a guard tube containing anhydrous calcium chloride. The mixture was refluxed until the color of the iodine disappeared. Then about 600 mL of distilled

methanol was added in the flask and it was refluxed until the color of the solution became milky white. This was then distilled. The distillate obtained was the super dry methanol and kept in an amber bottle using 4A type molecular sieves.

Xylene from Merck, India was used as a solvent after simple distillation. It has molecular weight 106.17 g/mol, purity  $\geq 98.0\%$ , density 0.86 g/cm<sup>3</sup> at 20 °C and b.p. 137-143 °C.

*N,N'*-Dimethylformamide (DMF) was purchased from Merck, India. It was used as a solvent after drying over CaO (Merck, India) and distilled under reduced pressure. It has molecular weight 73.09 g/mol, purity  $\geq 98.0\%$ , density 0.94 g/cm<sup>3</sup> and b.p. 153 °C.

*N,N'*-Dimethylacetamide (DMAc) was purchased from Merck, India. Its purity is 99.5% with 0.1% water and 0.12% free acid as impurities. The density of it is 0.938-0.942 g/mL at 25 °C and b.p. is 165-167 °C. It was purified by the following procedure. About 500 mL of DMAc was taken in a round bottom flask and 20 g of powder calcium oxide was added into it. The solution was kept for overnight. Then it was filtered and distilled under reduced pressure. This distillate obtained was kept in an amber bottle with 4A type molecular sieves.

Acetone was obtained from Merck, India. It has molecular weight ( $M_w$ ) 32.05 g/mol, purity  $\geq 99\%$  with water  $\leq 0.2\%$ , density 0.791-0.892 g/mL at 25 °C and b.p. 64-65 °C. It was used as received.

Toluene was obtained from Merck, India. Its purity is 99.0% with 0.04% water, 0.003% non-volatile matter and 0.0005% sulfur compounds (CS<sub>2</sub>) as impurities. The molecular weight ( $M_w$ ) is 92.14 g/mol, density is 0.860-0.866 g/mL at 25 °C and b.p. is 110-111 °C. It was purified by distillation before use.

Molecular sieve of 4A type was obtained from Merck, India. They often consist of alumino-silicate minerals, clays, porous glasses, microporous charcoals, zeolites, active carbons or synthetic compounds that have porous structure through which small molecules can diffuse. Its equilibrium capacity for water at 30 °C and 75% relative air humidity is  $\geq 20\%$  and bulk density is 650-700 g/cm<sup>3</sup>. It was used as received to trap trace amount of moisture present in solvents.

### **2.2.2. Instruments and Methods**

FTIR spectra of the polyester resins were recorded in a FTIR spectrophotometer (Impact-410, Nicolet, USA) using KBr pellet. <sup>1</sup>H NMR spectra were recorded in a

Varian 400 MHz NMR spectrometer (Australia) using  $\text{CDCl}_3$  and or deuterated dimethylsulphoxide ( $d_6$ -DMSO) as the solvents and tetramethylsilane (TMS) as the internal standard.

The different physical properties such as acid value, saponification value, iodine value, hydroxyl value, drying time etc. of the polyester resins were determined by the standard methods<sup>19,20</sup> as reported earlier.

The rheological study of the polyester resins was done by using CVO100 Rheometer (Malvern, UK). The relationships of viscosity versus time and viscosity versus temperature were measured at constant stress (200 Pa) under single shear. The variation of shear viscosity with temperature was carried out in the range of 25-100 °C at shear stress of 70 Pa. Thickness of the cured polyester films was measured by the Pentest, coating thickness gauge (Sheen Instrument Ltd., Model 1117, UK). The coating performance of the cured films was evaluated by the determination of various mechanical properties. The mechanical properties such as tensile strength and elongation at break were measured with the help of Universal Testing Machine, UTM (Zwick, Z010, Germany) with a 10 kN load cell and crosshead speed of 50 mm/min. Impact resistance was determined by falling weight impact tester (SC Dey, Kolkata) as per the standard falling weight (ball) method (standard ASTM D 1037). In this test a weight of 850 g was allowed to fall on the film coated on a mild steel plate from minimum to maximum falling heights. The maximum height was taken as the impact resistance up to which the film was not damaged. Gloss characteristic of the cured films was evaluated<sup>21</sup> using a glossmeter (Minigloss meter, Sheen, UK) over cured resin coated on mild steel plates at an angle of incidence of 60°. Scratch hardness of the cured films was measured by using scratch tester, Model no. 705, (Sheen Instrument Ltd., UK) with stylus accessory and a travel speed of 30-40 mm/s. The chemical resistance tests were performed in a number of different chemical media as per the ASTM D 543-67 standard procedure<sup>22</sup> by taking weighted amount of cured polyester resin films in 250 mL beakers containing 150 mL of the individual chemical medium for specified periods. The chemical resistance was determined by making observations of visual changes in the films after the specified time.

Swelling test was done by immersing weighted amount of the cured films in xylene. After 48 h, the weight of the swelled films was taken. Swelling value (%) was determined by differences in weight between the dried film and the swelled film as

follows: Swelling (%) =  $[(W_s - W_d)/W_d] \times 100$  where,  $W_s$  and  $W_d$  are the weight of the swelled film and the dried film respectively.

### 2.2.2.1. Synthesis of *Mesua ferrea* L. Seed Oil Based Polyester Resins

#### Preparation of Monoglyceride of the Oil

A three-neck round bottom flask equipped with a mechanical stirrer, a thermometer, a nitrogen gas inlet and a dropping funnel, was flushed with nitrogen and charged with 34.73 g (0.04 mol) of *Mesua ferrea* L. seed oil, 7.36 g (0.08 mol) of glycerol and 0.017 g (0.05 wt.% with respect to the oil) of lead mono-oxide under continuous stirring. The mixture was then heated upto  $(225 \pm 5)^\circ\text{C}$  and continues until the monoglyceride was formed. This was confirmed by checking its solubility in methanol (monoglyceride: methanol = 1: 3 v/v) at ambient temperature.

#### Synthesis of Trimellitic Anhydride Based Highly Branched Polyester Resin (TMAP)

The monoglyceride prepared by the above method was cooled to near about  $100^\circ\text{C}$ , and then 0.02 mol (1.96 g) of MA and 0.06 mol (8.89 g) of PA were added in the reaction mixture. The mixture was heated to  $(225 \pm 5)^\circ\text{C}$  for 3 h with vigorous stirring without using any solvent to form the pre-polyesterdiol. Again the reaction mixture was cooled to room temperature. Then, 25 g of this pre-polyesterdiol in 36 mL DMF solvent, and 2.5 g TMA in 5 mL DMF were taken in a three neck round bottom flask with the same arrangements as described in the preparation of monoglyceride under the nitrogen atmosphere with constant stirring. The mixture was slowly heated to  $(225 \pm 5)^\circ\text{C}$  and continued for 2 h at this temperature. The reaction was monitored by acid value determination. Similarly, resins of different compositions (Table 2.2) were prepared by changing proportion of pre-polyesterdiol and TMA.

**Table 2.2:** Composition of the reactants

Reactants (g)	TMAP5	TMAP10	TMAP15
Pre-polyesterdiol	25	25	25
TMA	1.25	2.5	3.75

#### Synthesis of 2,2-Bis(hydroxymethyl) Propionic Acid Based Highly Branched Polyester Resin (HBPE)

The monoglyceride prepared by the above method was cooled to  $100^\circ\text{C}$ , and 0.064 mol (6.27 g) of MA and 0.096 mol (14.22 g) of PA were added to the reaction mixture.

## Chapter 2

The mixture was again heated to (220–230) °C for 1 h with vigorous stirring using xylene as the solvent to avoid gelation. This product was treated as pre-polymer. Again the reaction mixture was cooled to room temperature and then 20 g of pre-polymer and 3.35 g (0.025 mol) of bis-MPA in 25 mL DMF solvent were taken in a three-neck round bottom flask with the same arrangements as described above under the N<sub>2</sub> atmosphere with constant stirring. The mixture was heated for 2.5 h at 150 °C followed by increasing of temperature up to 220 °C to complete the condensation and removal of the solvent. The reaction was monitored by the determination of acid value of the aliquots taken out time to time from the reaction mixture.

### *Synthesis of Hyperbranched Polyether Core Containing Polyester Resin (PE)*

#### Preparation of Sodium Methoxide

In a completely dried 100 mL three neck round bottom flask fitted with a water condenser and a nitrogen inlet about 50 mL ‘super dry’ methanol was taken. The reaction flask was placed in an ice-water bath to maintain the temperature of the reaction, 0-5 °C. About 10 g of pure and dry sodium metal as small pieces was added very slowly with vigorous stirring in the flask. After completion of addition the reaction mixture was refluxed for 2 h. Finally the excess methanol was removed by vacuum distillation. A white powder of sodium methoxide was obtained, which was stored in a dessicator.

#### Preparation of Sodium Salt of Bisphenol-A

In a completely dried 100 mL three neck round bottom flask fitted with a water condenser and a nitrogen inlet, the reaction flask was placed in a water bath. An exactly weighted amount of sodium methoxide was placed into the flask. Sodium methoxide was dissolved in a minimum volume of ‘super dry’ methanol. To the above solution, a clear solution of BPA (weight is half-equivalent to sodium methoxide) in ‘super dry’ methanol was added very slowly with the help of pressure equalizing funnel at room temperature. After the completion of addition, the reaction mixture was refluxed for 3 h. Finally the methanol was removed by vacuum distillation and an off white powder of sodium salt of diol was obtained, which was stored in a dessicator.

#### Preparation of Hyperbranched Polyether (HBE)

The HBE was prepared as reported earlier.<sup>23</sup> Briefly, in DMAc solution of sodium salt

of BPA (6.034 g, 0.022 mol), CYC (2.73 g, 0.0148 mol) solution of the same solvent was added drop-wise under the nitrogen atmosphere with constant stirring at room temperature ( $\sim 27$  °C) for 2 h. Then, the reaction was allowed to continue for 2 h at 70 °C followed by heating at  $137 \pm 2$  °C for another 8 h. The sticky mass was obtained from the filtrate of the reaction mixture in ice cooled water and purified by re-precipitation technique using acetone and water. The sticky product was finally washed with toluene to remove any unreacted CYC and dried under vacuum at 60 °C for two days. The yield of the product was 65%.

### Synthesis of Hyperbranched Polyether Core Containing Polyester Resin (PE)

At first a carboxyl terminated pre-polymer was prepared using the same method as described earlier. Briefly, 0.12 mol (42.09 g) of monoglyceride was reacted with 0.064 mol (6.27 g) of MA and 0.096 mol (14.22 g) of PA to prepare the carboxyl terminated pre-polymer. Then, 15.65 g of this pre-polymer was reacted with 2.5 g (0.01 mol) of BPS and 0.25 g of HBE (10% with respect to BPS) in DMF (25 ml) at 145-150 °C for 3.5 h under the nitrogen atmosphere with continuous stirring. The temperature of the reaction was then raised slowly to 220 °C and finally cooled to room temperature to obtain the desired viscous resin. The yield obtained for the product was about 90-95%.

### *Preparation of Linear Polyester Resin (LPE)*

The LPE was prepared by using similar method as described earlier<sup>5</sup> with little variation in composition. Briefly, a three necked round bottom flask equipped with a mechanical stirrer, a thermometer, a nitrogen gas inlet and a dropping funnel was charged with 0.12 mol (42.09 g) of *Mesua ferrea* L. seed oil based monoglyceride, 0.048 mol (4.706 g) of MA and 0.072 mol (10.664 g) of PA under the blanket of nitrogen with constant stirring. 20 mL of xylene was used to facilitate proper mixing of the components. The mixture was heated to (220-230) °C and the reaction was monitored by the determination of acid value at an interval of  $\frac{1}{2}$  h. The resinification reaction was stopped after 1.5-2 h when the acid value had reached to 10-15 mg KOH/g.

### 2.2.2.2. *Curing of TMAP Resins*

A homogeneous mixture of resin with 30 phr of styrene as the reactive diluent, 4 phr of MEKP as the initiator and 2 phr cobalt octate as the activator was prepared in a glass

breaker at room temperature by ultrasonication for 20 min. The coating was prepared at ambient temperature on commercially available mild steel strips 150 mm × 100 mm × 1.44 mm for gloss, scratch hardness and impact test and 75 mm × 25 mm × 1.39 mm glass strips for chemical resistance test, using above resin mixture. The coating thickness was measured by Pentest, coating thickness gauge (model 1117, Sheen Instrument Ltd., U.K.). Thickness of these coatings was found to be 25–35 μm. The uniformly coated plates were cured by heating in an oven at a definite temperature for specific period of time. The curing time was estimated based on the hard drying time of the casted thin film of resins on glass plates. The hard drying time was determined as the minimum time required for curing the film.

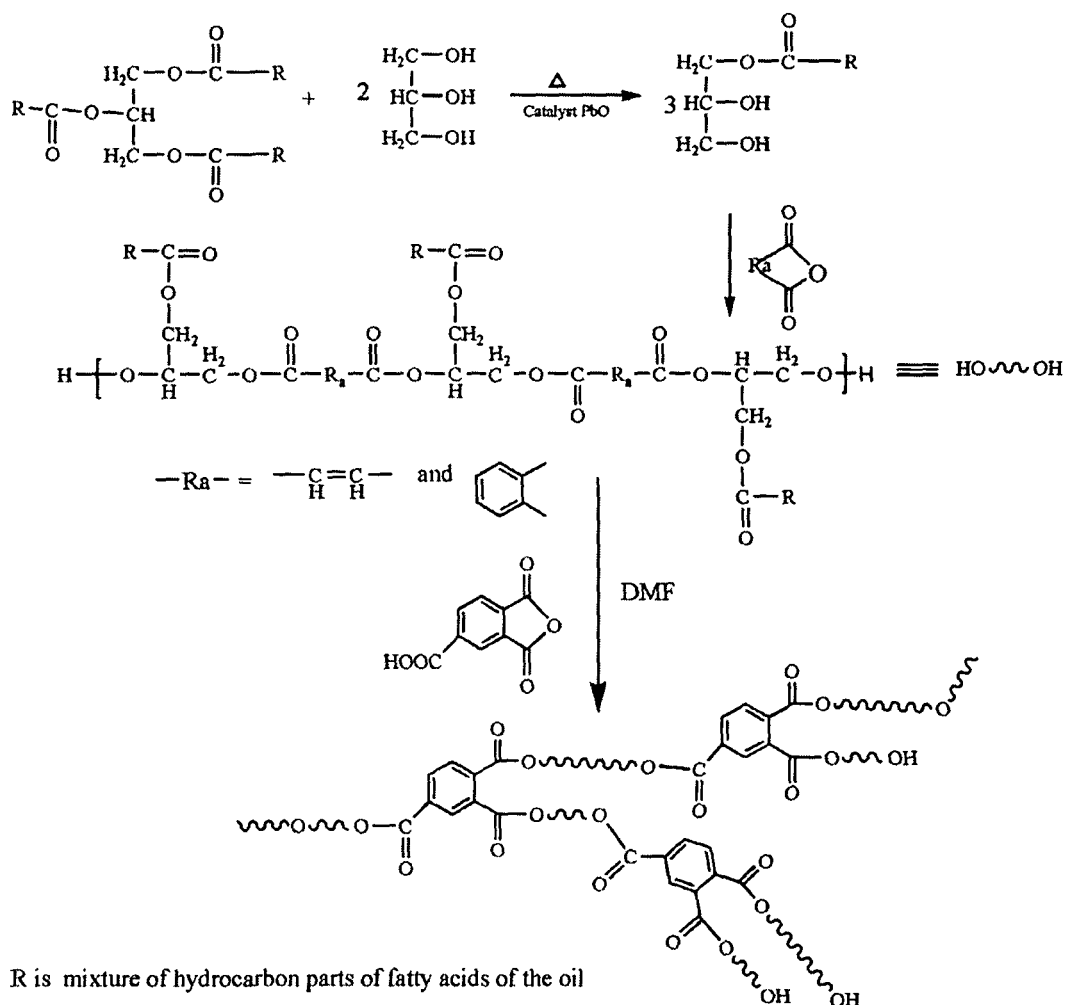
### *2.2.2.3. Curing of HBPE, PE and LPE Resins*

Polyester resin (HBPE or PE or LPE) and BPA based epoxy resin (at 60:40 weight ratio) were mechanically mixed with minimum amount of xylene and 25% poly(amido amine) hardener (with respect to epoxy resin) applying high shear mixing for 30 min. After getting a homogeneous mixture it was degassed under vacuum to remove the entrapped air bubbles and the solvents. Then the mixture was cast on mild steel and glass plates, similar to as mentioned above and dried under vacuum in dessicator for overnight at room temperature. The films were then allowed to cure at 120 °C for further study.

## **2.3. Results and Discussion**

### *2.3.1 Resinification of TMAP Resins*

In the present investigation, the *Mesua ferrea* L. seed oil based highly branched polyester resins were synthesized through three-stage single pot process of resinification technique by avoiding gelation. Here, in the first two stages no solvent was used but in the last stage DMF was employed as a suitable solvent (Scheme 2.1). The last step of the reaction generates highly branched structure of the resin through the well-known  $A_2 + B_3$  reaction mechanism. In this stage gel formation may be encountered under uncontrolled reaction conditions such as high temperature, low agitation speed and use of no solvent. However, in this case no gel product was formed as reaction was controlled by slow addition and use of dilute solution of the reactants.



**Scheme 2.1:** Possible reaction scheme for synthesis of TMAP

During resinification reaction both at pre-polymer stage as well as at the final stage i.e. esterification by TMA, the changes of acid values with the increase of the reaction time are shown in Fig. 2.1 and Fig. 2.2. The extent of reaction,  $p$  and average degree of polymerization,  $DP$  with respect to the acid value were calculated using the following equation in both the cases.<sup>24,25</sup>

$$p = C_0 - C_t / C_0 \quad (2.1)$$

where  $C_0$  is the acid value at zero reaction time and  $C_t$  is the acid value after time  $t$ , respectively. The average degree of polymerization,  $DP$  is given by  $DP = (1 - p)^{-1}$

From Fig. 2.1 it was observed that the acid value decreases with the increase of reaction time. The decrease in acid value was more rapid during the early stage of resinification reaction though at the later stage of reaction, the rate of decrease of acid value became slow. The change of acid value is due to the fact that the primary hydroxyl groups of monoglyceride react much faster with anhydride than the secondary hydroxyl groups. Thus it is believed that rapid decrease in acid value at the early stage



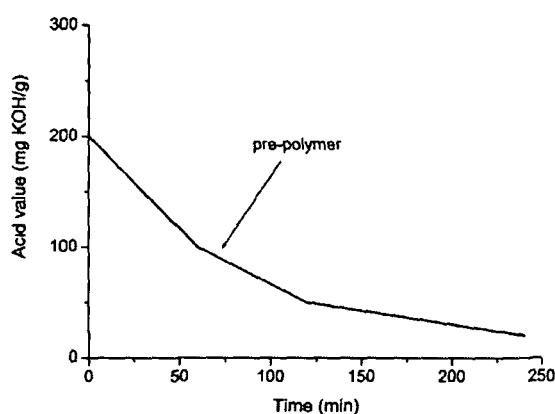
of polycondensation reaction corresponds to the reaction of primary hydroxyl groups, while the slower rate is due to the reaction of less reactive secondary hydroxyl groups.

The change of acid value of the TMAP (Fig. 2.2) is due to the fact that the hydroxyl groups of pre-polyesterdiol react faster rate with TMA at the early stage as the concentration of reactants are high. Thus the initial decrease in acid value at the early stage of polycondensation reaction corresponds to the esterification reaction where more numbers of acid groups are consumed by the hydroxyl groups. The period when change in acid value during polycondensation reaction is slow, probably then the branching of resin has started to form a three-dimensional structure. Thus, it may also be inferred that reaction, probably crosslinking started slowly.<sup>24,25</sup>

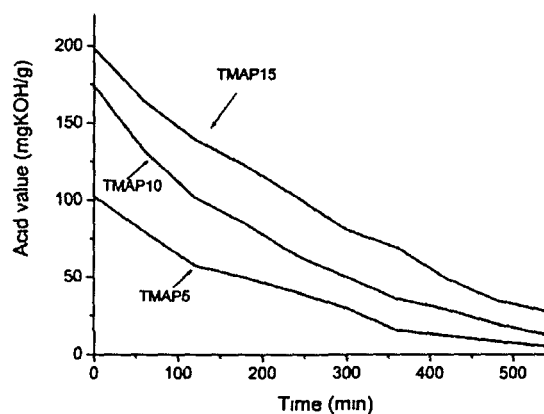
The polycondensation reactions can be considered as equivalent as essentially they are the reaction between functional groups, so their rate of reaction can be expressed as a second-order rate law.

$$(1-p)^{-1} = C_0kt + 1 \quad (2.2)$$

where  $C_0$  is the initial concentration of reactant,  $t$  is the time of reaction,  $p$  is the extent of reaction and  $k$  is the rate constant of the reaction. Here the acid value is substituted for concentration. Thus the plot of  $(1-p)^{-1}$  versus time should be linear, if the rate constant  $k$  is constant throughout the reaction, which is observed in case of pre-polyester (Fig. 2.3). But the plot (Fig. 2.4) shows a non-linear variation, which indicates the change of rate during resinification reaction.



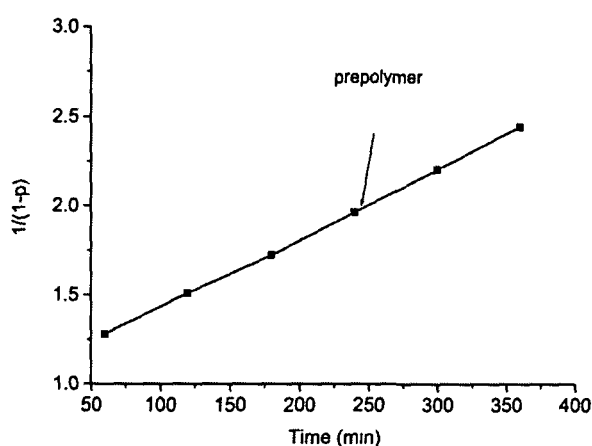
**Fig. 2.1:** Variation of acid value with time for pre-polyesterdiol



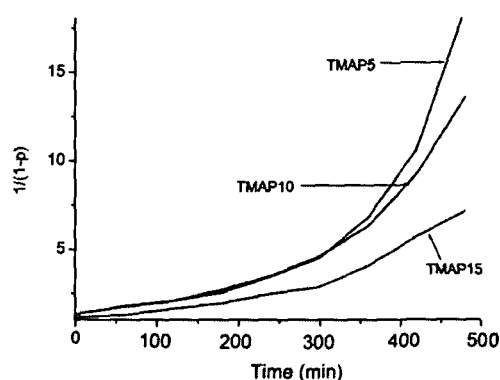
**Fig. 2.2:** Variation of acid value with time for TMAP

Even though, initially the variation of  $(1-p)^{-1}$  versus time is linear for the polyester at the final stage, but after a certain point it deviates from linearity. The similar observation was also reported in preparation of different oil modified simple polyester resins.<sup>24,25</sup> This trend of variation may be due to the fact that the first linear

portion is considered to represent time of formation of linear chains, but the second non-linear portion may represent onset period of branching that is three dimensional architecture formation of the resin, which is very significant in this case. The extent of reaction and the average degree of polymerization were calculated for the resin at the point of deviation from linearity and are given in Table 2.3. The result indicates that the extent of reaction at this region is about 90%. Although this result is little higher than the value (75-80%) obtained by reaction of PA with glycerol but is much higher than results reported for African locustbean and rubber seed oil modified polyester resins.<sup>24,26</sup> The average degree of polymerization value indicates the formation of chains with relatively medium molecular weight at that point and also cross-linking started at the same time. The second order rate constant value of the resin (Table 2.3) obtained from the linear portion of the plot indicates that the rate of resinification reaction depends on the ratio of reactants used in the formulation. From this study, it is cleared that the preparation of polyester resin is relatively easier in this case without gel formation using the tri-functional TMA.



**Fig. 2.3:** Plot of  $(1-p)^{-1}$  versus time for pre-polyesterdiol



**Fig. 2.4:** Plot of  $(1-p)^{-1}$  versus time for TMAP

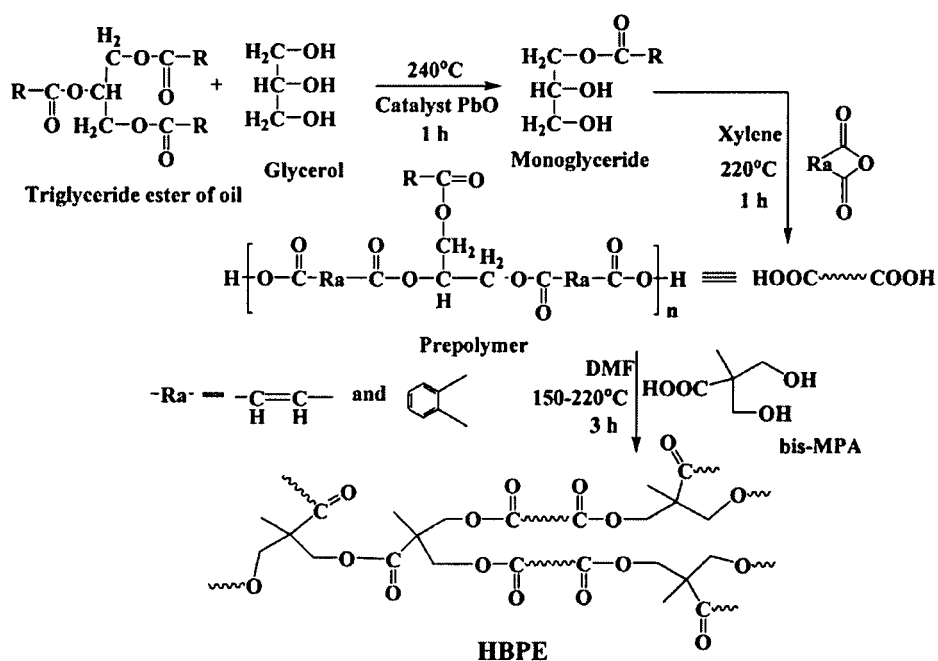
**Table 2.3:** Extent of reaction ( $p$ ), average degree of polymerization ( $DP$ ) and second order rate constant [ $k$ ] at the onset of gelation ( $t_{onset}$ )

Parameter	TMAP5	TMAP10	TMAP15
$t_{onset}$ (min)	450	390	300
$p$ (%)	94.6	92.6	85.9
$DP$	18.5	13.5	7.1
$k$ [ $g$ ( $mg$ KOH) $^{-1}$ $min^{-1}$ ]	$4.56 \times 10^{-5}$	$6.2 \times 10^{-5}$	$4.39 \times 10^{-5}$

### 2.3.2. Resinification of HBPE, PE and LPE Resins

The HBPE (Scheme 2.2) of the oil was prepared by alcoholysis followed by polycondensation reaction in a three step single pot reaction. In the first step, triglyceride ester of oil was converted to monoglyceride which was then treated with excess amount of MA and PA to form carboxyl terminated pre-polyester. This carboxyl terminated pre-polyester was treated with bis-MPA in the third step, where DMF was used as solvent to avoid gelation during resinification, as bis-MPA is a trifunctional reactant. The  $-\text{COOH}$  group of the pre-polyester and also bis-MPA reacts with the  $-\text{OH}$  group of bis-MPA to form HBPE. DMF used during resinification was automatically removed from the product by evaporation under the used reaction conditions and the resin with  $\sim 100\%$  solid content was obtained. Thus this technique is unique of its own as the resin obtain was a high solid content resin without employing any extra step.

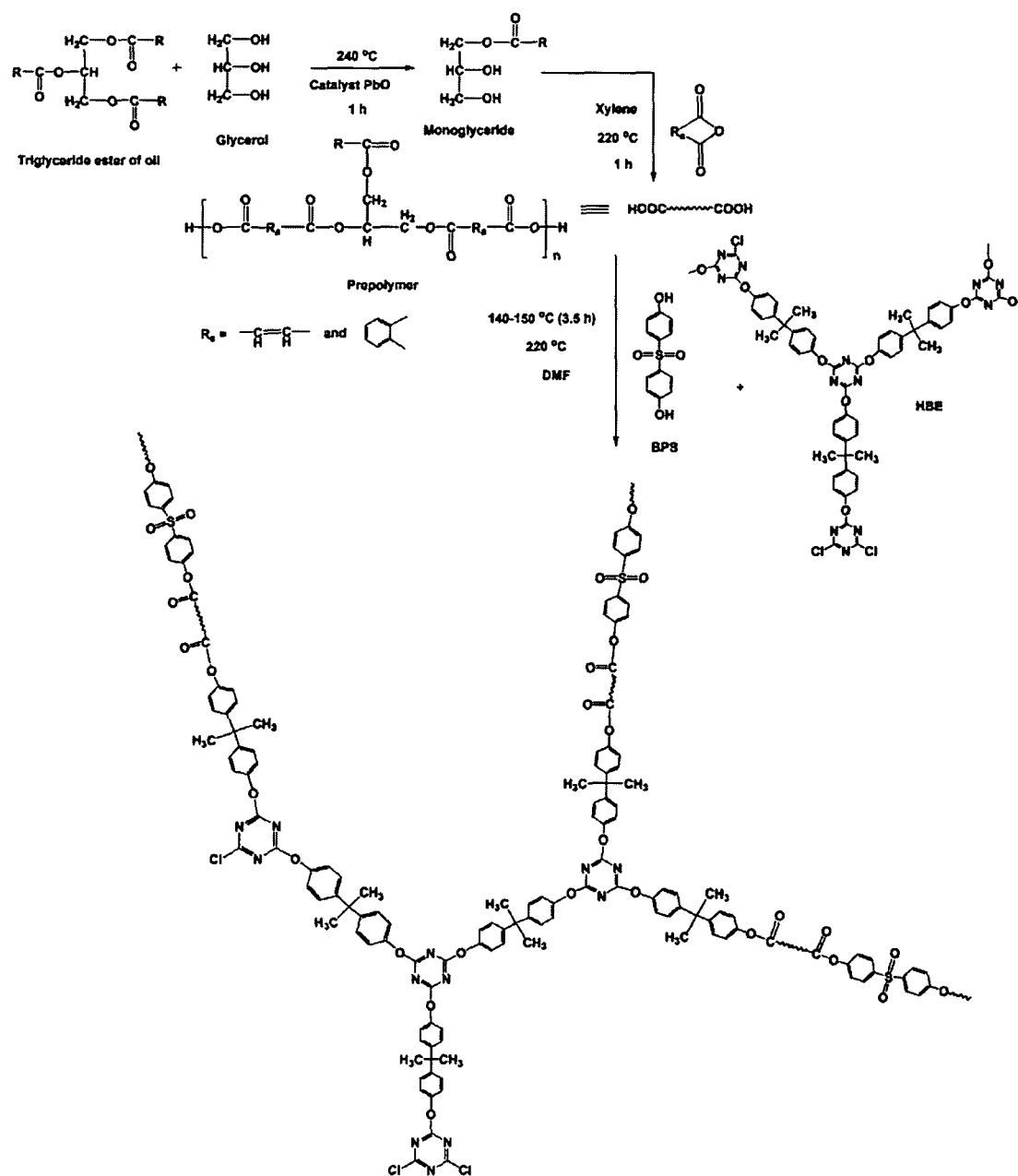
The PE was prepared from the carboxyl terminated pre-polyester of *Mesua ferrea* L. seed oil, BPS and HBE (Scheme 2.3). The HBE was used as a core molecule to enhance different properties of the polyester like good processability, thermal stability and chemical resistance due to its hyperbranched structure with s-triazine moiety. The renewable resource based pre-polyester provides the effects of structure and composition of the oil, whereas BPS helps in thermostability and rigidity of the polyester. The high yield of the resin (90-95%) may be attributed to the use judicious amount of solvent which facilitates homogenization of the reactants.



Scheme 2.2: Possible reaction scheme for synthesis of HBPE

## Chapter 2

The LPE was prepared from the *Mesua ferrea* L. seed oil by alcoholysis which was followed by polycondensation reaction with 60:40 ratio of saturated acid anhydride (PA) and unsaturated acid anhydride (MA). First the triglyceride ester of the oil was converted to monoglyceride by reacting with glycerol. The hydroxyl group of this monoglyceride reacts with carboxyl ester group of both MA and PA to form the polyester resin. The schematic representation of the reaction is shown in Scheme 2.4. The extent of reaction was monitored by measurement of acid values at different intervals and the reaction was stopped at the desired level of acid values. High yield of the resin was found (85-90%) and may be due to the use of little amount of solvent which facilitates in homogenization of the reactants.



**Scheme 2.3:** Possible reaction scheme for synthesis of PE



slow, the branching of HBPE had started to form a three-dimensional structure. The formation of sufficient number of ester linkages in HBPE was supported by saponification value (Table 2.4). Lower level of unsaturation in HBPE compared to the used oil<sup>5</sup> (89.26 g I<sub>2</sub>/100 g) was indicated by the iodine value (Table 2.4), which is due to polymerization of the monomers through cyclization which are supported by the results reported by others.<sup>31</sup> Further, improved solubility and low viscosity support the formation of highly branched structure of the resin.

Table 2.4 showed the moderate acid value of LPE which decreased with the increase of reaction time during resinification. The moderate acid value supports the adequate reactivity of the resin for paint and coating applications. The saponification value of LPE supports the formation of sufficient number of ester linkages in the resin. Lower level of unsaturation in LPE compared to the used oil (89.26 g I<sub>2</sub>/100 g) was indicated by the iodine value, which is due to polymerization of the monomers through cyclization as mentioned earlier.<sup>31</sup>

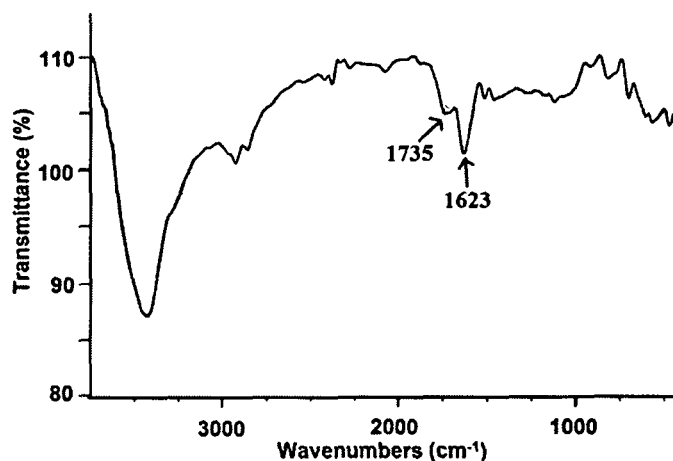
*Table 2.4: Physical properties of polyester resins*

Property	TMAP5	TMAP10	TMAP15	HBPE	LPE
Color	Dark brown	Dark brown	Dark brown	Dark Brown	Dark brown
Acid value (mg KOH/g)	5.5	12.7	27.8	10.66	13.2
Saponification value (mg KOH/g)	320	400	513	280.5	270.43
Iodine value (g I <sub>2</sub> /100 g)	51	43	39	43.34	52.10
Viscosity ( $\eta_{inherent}$ in 0.5% DMF at 25 °C)	0.22	0.26	0.31	48.02 <sup>a</sup>	64.52 <sup>a</sup>
Solubility	DMF, DMSO, THF, xylene, acetone etc.	DMF, DMSO, THF, xylene, acetone etc.	DMF, DMSO, THF, xylene, acetone etc.	DMF, DMSO, THF, xylene, acetone etc.	DMF, THF, xylene, acetone etc.

<sup>a</sup> Viscosity in Pas, determined by rheological study

### 2.3.3.2. FTIR and <sup>1</sup>H NMR Spectroscopic Studies

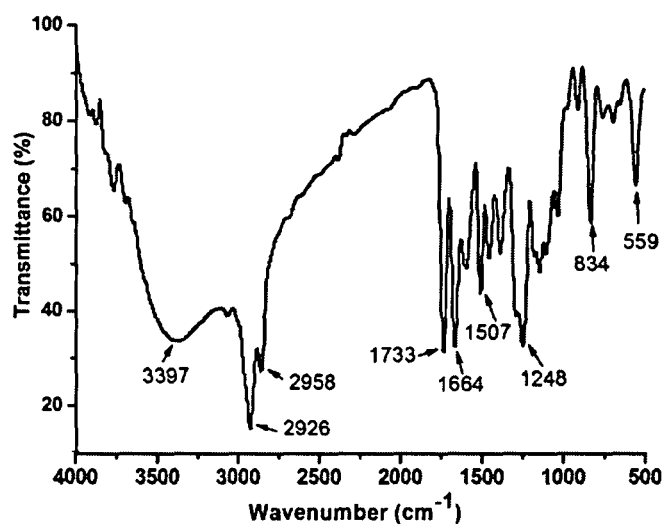
The presence of important linkages such as ester group, olefinic double bond etc. of HBPE was confirmed by FTIR analysis, which indicated polycondensation esterification reaction. It was noticeable from the Fig. 2.5 that the C=O band of the HBPE was found at  $\sim 1734\text{-}1736\text{ cm}^{-1}$ , which is different from the oil<sup>5</sup> ( $1747\text{ cm}^{-1}$ ), indicating certain influences around the carbonyl group. Also, the bands for unsaturation of fatty acid moiety and MA moiety at  $\sim 1620\text{-}1625\text{ cm}^{-1}$ , and aromatic PA moiety at  $\sim 700\text{ cm}^{-1}$ , were observed in the resin.



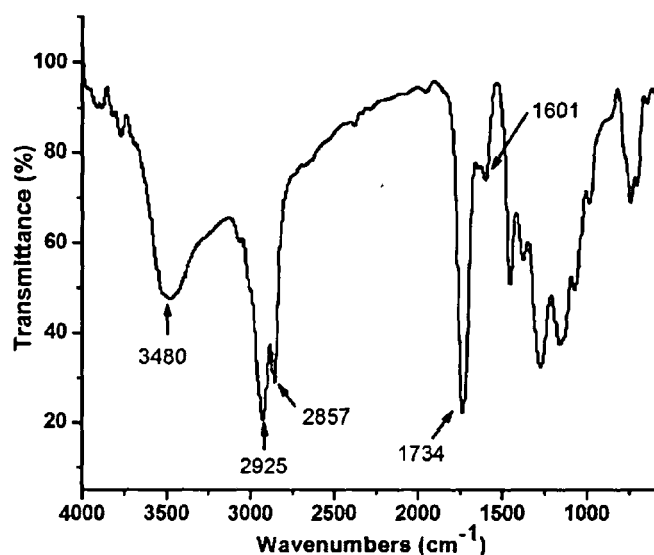
*Fig. 2.5: FTIR spectrum of HBPE*

The FTIR spectrum of PE (Fig. 2.6) indicated the presence of important linkages such as ester groups ( $1733\text{ cm}^{-1}$ ) and olefinic double bonds. The other characteristic bands present in the HBE are the bands for phenyl group and methyl group of the BPA moiety appeared at  $1507, 834$  and  $559\text{ cm}^{-1}$ , respectively and aromatic ether linkage at  $1248\text{ cm}^{-1}$  etc. These revealed the formation of polyester resin through the reaction of acid groups of the pre-polyester with the -OH groups of BPS and HBE. Band for unsaturation of MA moiety at  $1645\text{ cm}^{-1}$  was also observed in the resin. The band appeared at  $3397\text{ cm}^{-1}$  indicates the presence of hydroxyl group in polyester resin. The bands at  $2926\text{ cm}^{-1}$  and  $2858\text{ cm}^{-1}$  represent the aliphatic -C-H symmetric and asymmetric stretching of polyester resin respectively.

The FTIR spectrum of the LPE (Fig. 2.7) indicated the presence of important linkages such as ester groups, olefinic double bonds and other characteristic bands which reveal the formation of polyester resin through ester linkage of the oil with the anhydrides. The resin showed C=O band at  $1734\text{ cm}^{-1}$ . Bands for unsaturation of aromatic PA moiety at  $1601\text{ cm}^{-1}$  and MA moiety at  $1645\text{ cm}^{-1}$  were also observed in this resin. The band appeared at  $3480\text{ cm}^{-1}$  indicates the presence of hydroxyl group in polyester resin. The bands at  $2925\text{ cm}^{-1}$  and  $2857\text{ cm}^{-1}$  represent the aliphatic C-H symmetric and asymmetric stretching of the polyester resin, respectively.



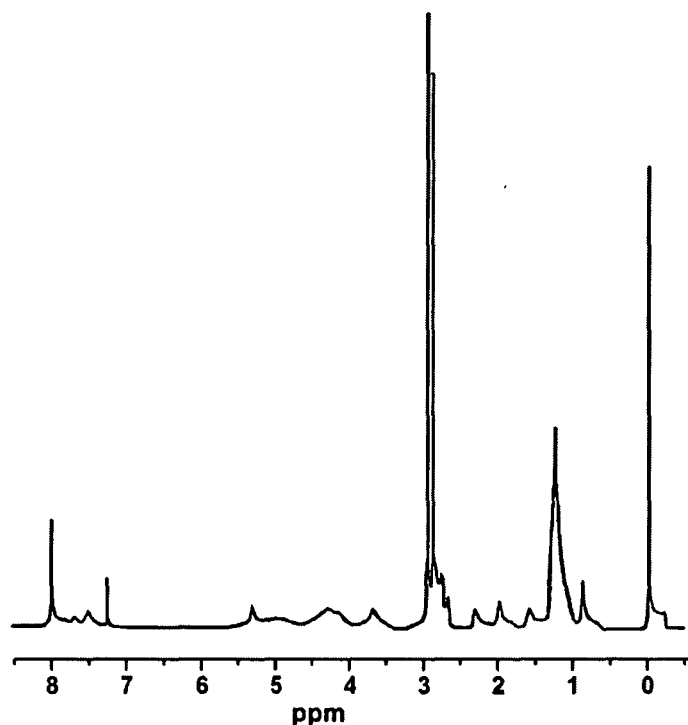
*Fig. 2.6: FTIR spectrum of PE*



*Fig. 2.7: FTIR spectrum of LPE*

From  $^1\text{H}$  NMR spectrum of HBPE (Fig. 2.8), the presence of following protons was confirmed. Peaks at  $\delta = 0.80\text{-}0.85$  ppm are for terminal methyl group of the fatty acid chains and  $\delta = 1.55\text{-}1.60$  ppm is due to protons of  $-\text{CH}_2-$  group attached next to the above terminal methyl group. The protons of all the internal  $-\text{CH}_2-$  groups present in the fatty acid chains indicated by the peak at  $\delta = 1.23$  ppm. The peaks for protons of unsaturated carbons appeared at  $\delta = 5.20\text{-}5.31$  ppm. The  $-\text{CH}_2-$  protons attached with the double bonds were found at  $\delta = 1.9\text{-}2.0$  ppm, whereas the protons for  $-\text{CH}_2-$  attached with ester groups were observed at  $\delta = 2.2\text{-}2.3$  ppm. The aromatic protons appeared at  $\delta = 7.25\text{-}8.0$  ppm and the peaks at  $\delta = 2.74\text{-}2.94$  ppm are for protons attached with ester group directly linked with aromatic moiety. However, because of presence of other unseparable compounds in the oil, it is difficult to determine the degree of branching for the resin.

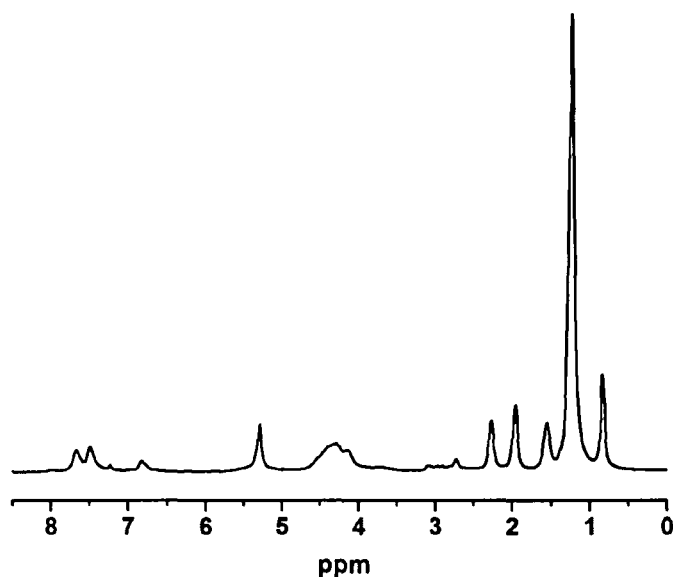




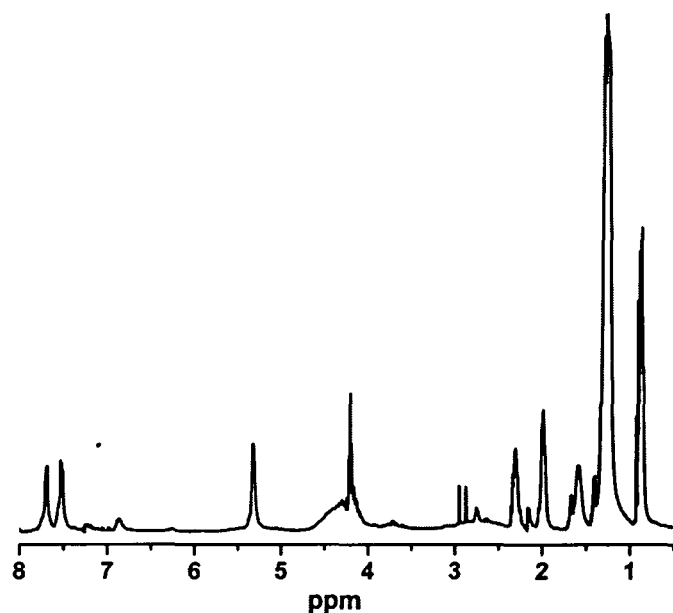
*Fig. 2.8: <sup>1</sup>H NMR spectrum of HBPE*

The <sup>1</sup>H NMR spectrum of the PE is shown in (Fig. 2.9). Along with the peaks obtained for the HBE the other peaks observed for different environment of protons are as follows. The peaks for the protons of terminal methyl group of the fatty acid chains were found at  $\delta = 0.89-0.92$  ppm. The peaks for protons of  $-\text{CH}_2-$  moiety attached next to the terminal methyl group appeared at  $\delta = 1.60$  ppm. The peaks observed at  $\delta = 1.25-1.29$  ppm are due to the protons of all the internal  $-\text{CH}_2-$  groups present in the fatty acids chains. For the protons of unsaturated carbons the peaks appeared at  $\delta = 5.33$  ppm. The aromatic protons of PA and protons for MA unit were found at  $\delta = 7.54-7.71$  ppm and at  $\delta = 2.00-2.33$  ppm respectively. However, as the structure is very complex, so it is really difficulty to assign the exact structure of the hyperbranched polyester.

Different environments of proton were observed from the <sup>1</sup>H NMR spectrum of the LPE (Fig. 2.10). The protons of terminal methyl group of the fatty acid chains were found at  $\delta = 0.89-0.92$  ppm. Proton signal of  $-\text{CH}_2-$  group attached next to the terminal methyl group appeared at  $\delta = 1.60$  ppm. The peaks observed at  $\delta = 1.25-1.29$  ppm are due to the protons of all the internal  $-\text{CH}_2-$  groups present in the fatty acids chains. The peaks for protons of unsaturated carbons appeared at  $\delta = 5.33$  ppm. The aromatic protons of PA and protons for MA unit were found at  $\delta = 7.54-7.71$  ppm and at  $\delta = 2.00-2.33$  ppm respectively.



*Fig. 2.9: <sup>1</sup>H NMR spectrum of PE*



*Fig. 2.10: <sup>1</sup>H NMR spectrum of LPE*

#### **2.3.4. Rheological Behaviors**

The rheological behaviors like variations of viscosity with time, temperature and shear rate of the TMAPs are shown in Fig. 2.11. From these figures, it was observed that the viscosity remains constant with respect to time and shear stress though the same decreases with the increase of temperature for all the cases. These results indicated that the physical structure of the polymers remains intact with the variation of time at constant shear stress or even with table of shear (change of shear value), though the viscosity decreases due to increase of kinetic energy of the molecules with the increase

of temperature. In all cases, the viscosity value increased with the increase of TMA, which is due to increase in chance of crosslinking during polymerization reaction, though the probability of branch formation also increases with the same, which decreases the viscosity. So the overall effect of TMA on viscosity of the TMAPs was not so significant (Fig. 2.11). These rheological behaviors indicated the significance of highly branched structure of the resins. These resins exhibited much improved flow behavior (viscosity – 10 Pas) compared to conventional similar polyester of the same oil (viscosity – 410 Pas).<sup>5</sup>

### 2.3.5. Curing Study for the Polyester Resins

The curing time of the TMAPs decreased with the increase of TMA in the system, which may be due to the increase of branching due to formation of compact structure and increase of number of crosslinking sites in each molecule (Table 2.5). This value is much lower compared to the conventional similar type polyester resin of the oil.<sup>5</sup> Non-drying oil based polyester resin requires long time for hard drying due to the crosslinking reaction which occurs through radical reactions by absorbing oxygen from the atmosphere. The drying time of the polyester resin improved significantly by using epoxy resin as curing agent along with poly(amido amine) hardener. This is due to high

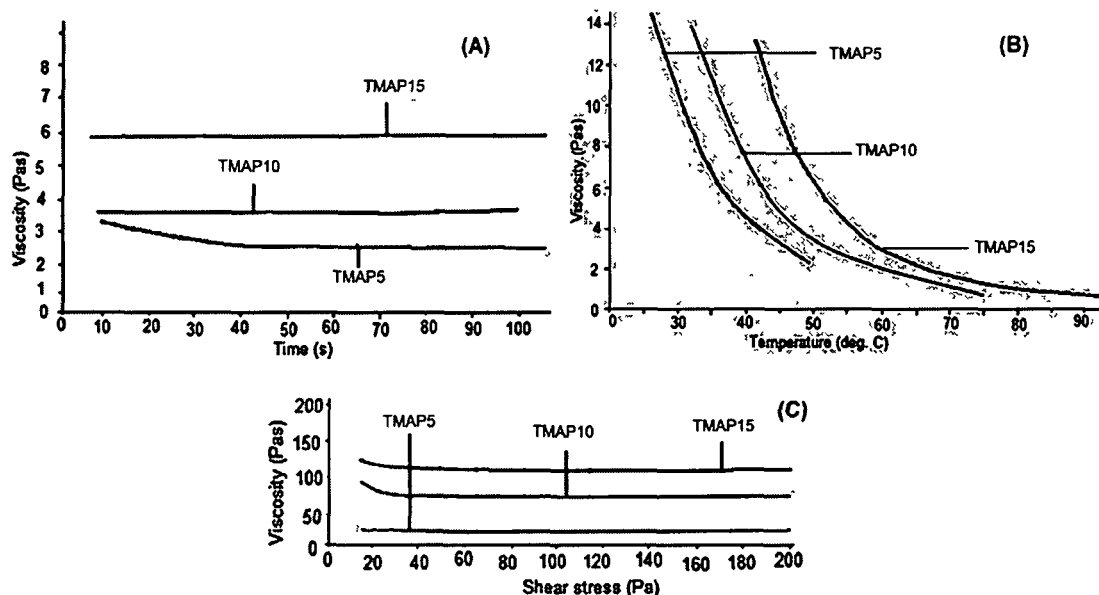


Fig. 2.11: Rheological behaviors of the TMAPs

curing rate of epoxy resin by the hardener. Also, there is a possibility of crosslinking reactions of hydroxyl/epoxide of epoxy resin and amine groups of the hardener with the hydroxyl/ester groups of polyester resin. Thus, the HBPE, PE and LPE were cured in 3 h, 1 h 20 min and 4 h at 120 °C, respectively.

### 2.3.6. Coating Performance

The different coating characteristics like gloss, impact resistance and scratch hardness of the synthesized polyester resins are shown in Table 2.5. The polyester resins possess very good gloss property, which is due to the presence of the rigid aromatic moiety in the polymer chain and adequate crosslinking density. The gloss value of TMAP marginally increased with the amount of TMA may be due to the enhancement of dimensional stability through the formation of more branched compact structure. The scratch hardness and the impact resistance of the synthesized TMAP resins increased with the increase of the amount of the TMA. The increase of scratch hardness may again be due to increase of rigidity and branching in the structure, whereas the impact may be due to increase of strength and molecular weight of the resin (increase of saponification value, Table 2.4). In case of HBPE, PE and conventional LPE, along with the above mentioned properties the other mechanical properties like tensile strength and elongation at break values were also measured and are shown in Table 2.5. But, for TMAP resins the tensile strength and elongation at break values were not able to determine due to the inability to peel out the cured films from the coated strips.

**Table 2.5:** Coating performance characteristics of the polyester resins

Property	TMAP5	TMAP10	TMAP15	HBPE	LPE	PE
Gloss at 60 °	80.2	83	84.4	98	78	83
Scratch hardness (kg)	1	1.5	2	7	6	8
Impact resistance (cm)	50	55	62	80	55	>100
Tensile strength (N/mm <sup>2</sup> )	-	-	-	2.68	5.66	5.46
Elongation at break (%)	-	-	-	24	31.7	102.21
Curing time (h at 150 °C)	7	6	5.5	3 <sup>a</sup>	4 <sup>a</sup>	1.33 <sup>a</sup>
Swelling (%) in xylene	32.5	33.8	34.4	33.8	36.22	35.26

a: Curing temperature is 120 °C

### 2.3.7. Chemical Resistance

Table 2.6 shows the chemical resistance of the polyester resins in different chemical media. The results showed that the resins were unaffected and highly resistant to dilute HCl, aqueous NaCl solution and distilled water. However, they are affected to varying degrees by alkali. The poor resistance of the polyester resins to alkali is explained on the basis of that they are essentially consisted of ester groups. This is supported by the results of other vegetable oil based-polyester resins.

**Table 2.6: Chemical resistance of the polyester resin films**

Types of media	TMAP5	TMAP10	TMAP15	HBPE	PE	LPE
5 wt.% aqueous NaOH	P	P	F	F	F	PO
25 wt.% aqueous HCl	E	E	E	E	E	G
25 wt.% aqueous NaCl	E	E	E	E	E	G
Distilled water	E	E	E	E	E	E

P= Poor, PO= Peeled off, G= Good, F= fair and E= Excellent

## 2.4. Conclusions

From this study, it can be concluded that the renewable *Mesua ferrea* L. seed oil has tremendous potential for the preparation of conventional linear as well as highly branched polyester resins. These prepared resins can be utilized for surface coating applications like other vegetable oil based resins. The cured resins exhibited good coating performance characteristics such as good gloss, adequate hardness and strength along with high chemical resistance to dilute HCl, aqueous NaCl salt solution and distilled water. So they could be useful as binders for anticorrosive and non-polluting surface coatings. Again, among the four polyester resins prepared from *Mesua ferrea* L. seed oil, the bis-MPA based polyester resin (HBPE) showed better properties than the others. Hence this resin can be suggested for industrial applications.

## References

1. Tsujimoto, T.; Uyama, H.; Kobayashi, S. Green nanocomposites from renewable resources: Biodegradable plant oil-silica hybrid coatings. *Macromol. Rapid Commun.* **24**, 711-714 (2003)
2. Shogren, R.L.; Petrovic, Z.; Lui, Z.; Erhan, S.Z. Biodegradable behavior of some vegetable oil-based polymers. *J. Polym. Environ.* **12**, 173-178 (2005)
3. Syed, H.; Nitin, V.P. Renewable materials in surface coatings. *Paintindia* **56**, 81-86 (2006)
4. Konwer, D.; Taylor, S.E.; Gordon, B.E.; Otvos, J.W.; Calvin, M. Liquids from *Mesua ferrea* L. seed oil. *J. Am. Oil Chem. Soc.* **66**, 223-226 (1989)
5. Dutta, N.; Karak, N.; Dolui, S.K. Synthesis and characterization of polyester resins based on Nahar seed oil. *Prog. Org. Coat.* **49**, 146-152 (2004)

6. Dutta, S.; Karak, N. Synthesis, characterization of poly(urethane amide) resins from Nahar seed oil for surface coating applications. *Prog. Org. Coat.* **53**, 147-152 (2005)
7. Mahapatra, S.S.; Karak, N. Synthesis and characterization of polyesteramide resins from Nahar seed oil for surface coating applications. *Prog. Org. Coat.* **51**, 103-108 (2004)
8. Malshe, V.C.; Sikchi, M. *Basics of Paint Technology, Part I.* 1<sup>st</sup> edn. (UICT, Mumbai, 2004)
9. Igwe, O.; Ogbobe, O. Studies on the properties of polyesters and polyester blends of selected vegetable oils. *J. Appl. Polym. Sci.* **75**, 1441-1446 (2000)
10. Phate, B.W.; Gogte, B.B. Wall finishes based on novel short oil rosinated alkyd. *Paintindia* **55**, 71-76 (2005)
11. Piotr, P.; Dorota, A.; Gabriel, R.; Ryszard, O. Unsaturated polyester resins modified with vegetable oil and dicyclopentadiene. *Polimery* **49**, 767-773 (2004)
12. Karak, N.; Maiti, S. *Dendrimers and Hyperbranched Polymers—Synthesis to Applications* (MD publication Pvt. Ltd., New Delhi, 2008)
13. Scholl, M.; Kadlecova, Z.; Klok, H.A. Dendritic and hyperbranched polyamides. *Prog. Polym. Sci.* **34**, 24-61 (2009)
14. Gao, C.; Yan, D. Hyperbranched polymers: From synthesis to applications. *Prog. Polym. Sci.* **29**, 183-275 (2004)
15. Bringi N.V. (Ed) *Non-Traditional Oil Seeds and Oils in India* (Oxford & IBH Publishing Co. Pvt. Ltd., New Delhi, 1987)
16. Dennis, T.J.; Kumar, K.A. Constituents of *Mesua ferrea*. *Fitoterapia* **69**, 291-304 (1998)
17. Banerji, R.; Mishra, G.; Nigam, S.K. Non-edible oil seeds potential raw material for industry. *J. Sci. Ind. Res.* **42**, 686-693 (1983)
18. Carr, R.A. Refining and degumming systems for edible fats and oils. *J. Am. Oil Chem. Soc.* **55**, 765-771 (1978)
19. Oil and Colour Chemist's Association of Australlia, *Surface Coatings* Vol. 1, (Chapman and Hall, London, 1981)
20. Sharma, B.K. *Industrial Chemistry* 10<sup>th</sup> edn. (GOEL Publisher, Meerut, 1999)
21. Indian Standard, *Methods of Sampling and Test for Paints, Varnishes and Related Products* 101 (Part 4/Sec 4), (1988)

## Chapter 2

22. Annual Handbook of ASTM Standard, *The American Society for Testing Materials* (Philadelphia, 1973)
23. Borah, J.; Karak, N. Synthesis and characterization of a novel hyperbranched polyether. *Polym. Int.* **53**, 2026-2030 (2004)
24. Aigbodion, A.I.; Okieimen, F.E. Kinetics of the preparation of rubber seed oil alkyds. *Eur. Polym. J.* **32**, 1105-1108 (1996)
25. Dutta, N.; Karak, N.; Dolui, S.K. Stoving paint from *Mesua ferrea* L. seed oil based short oil polyester and MF resins blend. *Prog. Org. Coat.* **58**, 40-45 (2007)
26. Aigbodion, A.I.; Okieimen, F.E. An investigation of the utilisation of African locustbean seed oil in the preparation of alkyd resins. *Ind. Crop. Prod.* **13**, 29-34 (2001)
27. Silverstein, R.M.; Bassler, G.C.; Morrill, T.C. *Spectroscopic Identification of Organic Compounds* 6<sup>th</sup> edn. (Wiley, New York, 1998)
28. Dyer, J.R. *Applications of Absorption Spectroscopy of Organic Compounds* (Prentice Hall of India, New Delhi, 1991)
29. Kemp, W. *Organic Spectroscopy* 3<sup>rd</sup> edn. (Palgrave, New York, 1991)
30. Smith, P.B. *et al.* Analysis of synthetic polymers and rubbers. *Anal. Chem.* **71**, 61R-80R (1999)
31. Aigbodion, A.I.; Okieimen, F.E.; Obazee, E.O.; Bakare, I.O. Utilisation of maleinized rubber seed oil and its alkyd resin as binders in water-borne coatings. *Prog. Org. Coat.* **46**, 28-31 (2003)

## CHAPTER 3

---

# Modification of bis-MPA Based Highly Branched Polyester Resin

### 3.1. Introduction

In recent days the significance of environmental friendly materials for industrial appliance has become exceedingly apparent with increasing emphasis on ecological issues, waste disposal and depletion of non-renewable resources.<sup>1</sup> Polymers from renewable resources can form a dais to replace/substitute petroleum-based polymers through inventive design of new bio-based polymers that can contend or even surpass the existing petroleum-based materials from the social and environment viewpoints along with the cost performance.<sup>2</sup> The environment is being besieged by non-biodegradable petroleum-based polymeric materials. The decline of petroleum-based resources for the polymer industry has enforced to explore the naturally available renewable assets as alternating raw materials.<sup>2</sup> New environmental regulations, societal concerns, and a mounting environmental consciousness right through the world have triggered the exploration for new opportunities for developing environmental friendly materials.<sup>3</sup> The current interest in inexpensive, environmental friendly polymeric materials has encouraged the development of such materials from readily available, renewable economical natural resources.<sup>4</sup>

Among these, vegetable oils have drawn immense attention because of their advantages like easy availability, sustainability, versatility in structure and properties, relatively low and stable cost and also they are biodegradable as well as eco-friendly in nature.<sup>5</sup> Keeping in mind to this, we use renewable *Mesua ferrea* L. seed oil as the starting material. As already mentioned in Chapter 2, it is largely available in different parts of the world particularly in the North-East region of India. It has exceptionally high oil content (70%), possessing both saturated and unsaturated long chain fatty acid in its structure. The oil has already been exploited in the synthesis of different types of polymers from the same laboratory.<sup>6-9</sup> Vegetable oil based polyester resins encompass a wide range of industrial relevance such as industrial finishes and maintenance,

---

Parts of this work are published in (i) *J. Appl. Polym. Sci.* (On line)

(ii) *J. Polym. Environ.* (On line)

Parts of this work are communicated



architectural uses, paints and surface coatings etc.<sup>10</sup> These resins have a number of advantages including versatility in structure and properties, overall low cost, ease of applications etc.<sup>11</sup> However, they endure from some decisive drawbacks such as long drying time, low mechanical properties, alkali resistance, low hardness etc.<sup>12</sup> So, to improve those drawbacks of polyester resins, blending with other suitable resins such as epoxy resin, amino resin, silicone resin, ketonic resin etc. can be performed, as polyester resins have good compatibility with a wide variety of other resins.<sup>13</sup> The better compatibility comes from the relatively low viscosity of resin and from the structure of resin that contains a relatively polar and aromatic backbone as well as aliphatic side chains with low polarity.<sup>14</sup> Blending technique may be used effectively to improve the inferior properties of both the components. Miscible polymer blends produce a new improved material from the less superior individual components, but well-established miscible polymer blends are very rare to get.<sup>15,16</sup> However, semi-miscible blends with uniform distribution of components are also improving properties to an acceptable range.<sup>17</sup> Again, due to compact three-dimensional structure with high surface functionality and lack of restrictive interchain entanglements, the highly branched polymers show low melting point and solution viscosity than their linear analogs.<sup>18</sup> Also, due to their high density of tailorable end groups on the surface, they can effectively function as blend components with other polymers.

Epoxies obtained from vegetable oils are marked by good adhesion, flexibility and corrosion resistance properties.<sup>19</sup> These attributes of oil based epoxies render them suitable for versatile applications as plasticizers, diluents and corrosion protective coatings. Thermoset epoxy resins are widely used in coatings, adhesives, moulding compounds and in polymer composites, due to their superior thermo-mechanical properties and excellent processability.<sup>20</sup> However, the use of thermosetting materials is often limited owing to a toughness problem. Therefore, the bulk amounts of epoxies, when used, are usually blended with tougheners, mostly rubber particles, used as second phase in the resin system. However, these particles always affect the processability of the system. Due to the flexibility present in the structure of vegetable oil based epoxy it can be used as one of the blend components in this study. It also has large numbers of epoxy and hydroxyl groups, which may take part in crosslinking reactions with oil modified polyester resin. Besides blends of natural polymers<sup>21</sup> so far no report has been found on the utilization of vegetable oil based resins as the sole blend components. Due to the presence of long chain fatty acids in the vegetable oil,

the used blend components have advantages like ease of processability and compatibility. Again, due to the enhancement of properties like mechanical, thermal, barrier properties etc. even at low concentrations, the nanocomposites of such blends have drawn the attention to the researchers.

Again, due to the added advantages like low volatile organic components, reduced odor, decreased flammability, improved safety and easier cleanup with water, the water soluble or water dispersible polymers are commercially interested because of their ability to alter the properties of aqueous systems. This motivated the researchers to concentrate more on the development of polymeric materials that are water soluble or dispersible as well as environment friendly. The most common way to solubilize or disperse an organic polymer into water is to introduce some highly hydrophilic polar functional groups like carboxylic acid group, sulphonic acid group and tertiary amine group into the polymer.<sup>22,23</sup> Polyester resins are the most popular material for many applications, where water is the best suitable solvent or medium.

Acrylic polymers possess excellent durability, hardness and alkali resistance which make them very useful for coatings, papers and textile finishes, cement additives, and other applications.<sup>24</sup> To improve the performance of acrylic polymers with respect to toughness, flexibility, abrasion resistance, and film-forming properties considerable effort has been devoted to combine the polyesters and acrylics into hybrid by blending.<sup>25</sup> Thus the modification of polyester resin by acrylic polymers will present a good balance between the application properties of the polyester resins and those of the acrylic polymers. Generally, polyester resin and acrylic polymer do not form a compatible blend. Therefore, to obtain a stable blend, the acrylic polymer should be chemically linked by grafting to polyester resin. This is possible through radical addition of acrylic monomer to the carbon-carbon double bonds of the polyester. The acrylic monomers, initiators and reaction conditions play important roles in such grafting processes.<sup>26</sup>

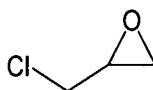
Therefore the present chapter describes the modification of the bis-MPA based highly branched polyester resin (HBPE) by different methods such as blending with vegetable oil based epoxy, neutralization with triethylamine to form water reducible polyester and grafting with methyl methacrylate. The characterizations and properties of these modified HBPEs are also discussed here.

### 3.2. Experimental

### 3.2.1. Materials

*Mesua ferrea* L. seed oil, glycerol, PA, MA, bis-MPA, xylene, DMF, BPS, BPA, epoxy resin, poly(amido amine), MEKP and cobalt octate were of same specifications as described in Chapter 2, section 2.2.1.

Epichlorohydrin (Fig. 3.1) was obtained from Merck, India and was used as received. It is a colorless liquid with a pungent, garlic-like odor, insoluble in water, but miscible with most polar organic solvents. It is a highly reactive compound and is used in the production of glycerol, plastics, epoxy glues and resins, and elastomers. Its molecular weight is 92.52 g/mol. It has density of 1.18 g/cm<sup>3</sup>. Its melting and boiling points are -25.6 °C and 117.9 °C respectively. It was used for the preparation of vegetable oil based epoxy resin.



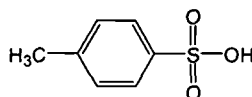
**Fig. 3.1:** Structure of epichlorohydrin

Partially n-butylated (60% solid content) melamine-formaldehyde (MF) resin was received from Asian Paints India Ltd., Mumbai and was used as received. The technical specifications of MF resin are as given in Table 3.1.

**Table 3.1:** Technical specifications of MF resin

Properties	Values
Application viscosity at 25 °C (GP-02)	20-25 s
Non-volatile matter (%)	60±2
Density at 25 °C	1.2
Thinning with xylene: n-butanol	90:10 (v/v)

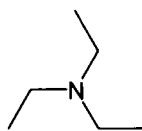
*p*-Toluene sulfonic acid (PTSA, Fig. 3.2) was obtained from Loba Chemie, India. The compound has melting point (m.p.) 100-105 °C, minimum assay 98.0%, maximum sulfated ash 0.2% and molecular weight (M<sub>w</sub>) 190.21 g/mol. It was used as received.



**Fig. 3.2:** Structure of PTSA

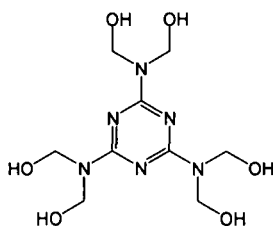
Triethylamine (TEA, Fig. 3.3) obtained from Merck, India was used without further purification. Its molar mass is 101.19 g/mol and has density of 0.7255 g/cm<sup>3</sup>. Its m.p. is -114.7 °C and b.p. is 88.7 °C.

## Chapter 3



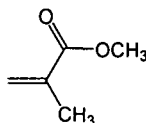
**Fig. 3.3:** Structure of TEA

Hexamethylol melamine (HMMA, Fig. 3.4) was used as a co-crosslinking agent. It is also known as 2,4,6-tris(dihydroxymethylamino)-1,3,5-triazine. Its molecular weight is 306.27 g/mol and melting point is 163-164 °C.



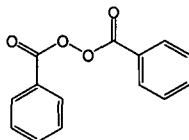
**Fig. 3.4:** Structure of HMMA

Methyl methacrylate (MMA, Fig. 3.5) as received from Merck, India is a colorless liquid and was used after purification by vacuum distillation. Its molecular weight is 100.12 g/mol and has density of 0.94 g/cm<sup>3</sup>. Its melting point and boiling points are -48 °C and 101 °C respectively.



**Fig. 3.5:** Structure of MMA

Benzoyl peroxide (BPO, Fig. 3.6) was obtained from Merck, India and was used as the catalyst for the polymerization of MMA. Mostly, benzoyl peroxide is used as a radical initiator to induce polymerization. Other major applications include as antiseptic and bleaching compound. It is a white solid. Its molecular weight is 242.23 g/mol. Its density is 1.334 g/cm<sup>3</sup> and melting point is 103–105 °C.



**Fig. 3.6:** Structure of BPO

### 3.2.2. Instruments and Methods

The FTIR and NMR analyses were carried out using same instruments and methods as described in Chapter 2, section 2.2.2. The measurements of impact resistance, scratch hardness, tensile strength, elongation at break (%), gloss, chemical resistances, percent of swelling and curing time were determined by the same way as mentioned in Chapter

2, section 2.2.2. The thermal analysis was done by TGA, (Shimadzu, TG 50, USA) with a nitrogen flow rate of 30 mL/min and heating rate of 10 °C/min. Ultrasonicator (Heishler, 200S, Germany) was used to mix the bis-MPA based highly branched polyester (HBPE) with epoxy resin at 60% of amplitude and a half cycle for 10 min.

The isolation and purification of the oil was performed exactly the same ways as described in Chapter 2, section 2.2.1. Monoglyceride of *Mesua ferrea* L. seed oil was prepared by glycerolysis process as described in Chapter 2, section 2.2.2.1. Hexamethylol melamine was prepared as per the reported method.<sup>27</sup>

### 3.2.2.1. Preparation of HBPE

The HBPE was prepared by the same method as described in Chapter 2, section 2.2.2.1. Briefly, 0.12 mol (42.09 g) of monoglyceride, 0.064 mol (6.27 g) of MA and 0.096 mol (14.22 g) of PA were reacted to form the carboxyl terminated pre-polyester. An amount of 20 g of this pre-polyester was then reacted with 3.35 g (0.025 mol) of bis-MPA to obtain the desired HBPE resin.

### 3.2.2.2. Preparation of Vegetable Oil Based Epoxy Resin

The vegetable oil based epoxy resin was prepared by the reported method from the same laboratory.<sup>28</sup> Briefly, monoglyceride of *Mesua ferrea* L. seed oil, epichlorohydrin, BPA and BPS were reacted together by maintaining the mole ratio of 1:8:2:1 at (110±5) °C for 8 h in slightly alkaline medium. After completion of the reaction the product was separated in a separating funnel, washed with brine solution and distilled water. Then the mass was vacuum dried to obtain the product with 80-90% yield. This *Mesua ferrea* L. seed oil based epoxy resin (epoxy equivalent = 447 g/eq and hydroxy value = 250 mg KOH/g) was used as one of the blend components.

### 3.2.2.3. Modification of HBPE by Blending with Epoxy Resin

HBPE and vegetable oil based epoxy resin were placed in a vacuum oven at 50 °C prior to the preparation of blends to remove entrapped air or moisture or volatiles. HBPE and epoxy resins were mixed in predetermined ratios of 30/70, 40/60, 50/50 and 60/40 (w/w) to obtain the blends PEB1, PEB2, PEB3 and PEB4 respectively along with the required amount of poly(amido amine) hardener (Table 3.2). The hardener was added in each case by maintaining the ratio of epoxy to hardener 2:1 (w/w). Each of these samples was mixed under continuous agitation by mechanical stirring for 30 min.

Blends were left at ambient temperature for 24 h, under observation. No visual phase separation was observed indicating proper mixing with good interactions between the two constituents. Then the mixture was cast on mild steel plates (150 mm × 50 mm × 1.60 mm) and glass plates (75 mm × 25 mm × 1.75 mm), and dried under vacuum in a dessicator for overnight at ambient temperature which were then allowed to cure at 120 °C for further study.

**Table 3.2:** *Composition of HBPE/epoxy resin blends*

Sample code	HBPE (g)	Epoxy resin (g)	Hardener (g)
PEB1	30	70	35
PEB2	40	60	30
PEB3	50	50	25
PEB4	60	40	20

#### 3.2.2.4. *Modification of HBPE by Triethylamine (Water Dispersible HBPE)*

The HBPE with large numbers of functionality and excess of free carboxylic acid groups was prepared as followed. First, a carboxyl terminated pre-polyester was prepared by the same method as described in Chapter 2, section 2.2.2.1. This was followed by reaction of 15 g of this pre-polymer with 1.285 g (0.0095 mol) of bis-MPA to form the HBPE with free carboxyl groups. The resultant HBPE was then neutralized with calculated quantity of TEA by refluxing at 140 °C for 3-4 h to get the water dispersible HBPE. The amount required for complete neutralization was calculated on equivalent basis.

#### 3.2.2.5. *Preparation of Water Dispersible HBPE Films*

The calculated amount of water dispersible HBPE, water, THF, TEA, MF resin, HMMA and PTSA were mixed (Table 3.3) by vigorous mechanical stirring for 30 min followed by ultrasonication for another 30 min. The pH was maintained at 8.3. After being sonicated the mixture was degassed under vacuum until it was completely bubble free. Then the mixture was cast on mild steel plates (150 mm × 50 mm × 1.60 mm) and glass plates (75 mm × 25 mm × 1.75 mm). The cast films were dried under vacuum in dessicator for overnight at room temperature and allowed to cure at 140 °C for further study.

#### 3.2.2.6. *Modification of HBPE by Grafting with Methylmethacrylate*

A three-neck 100 mL round-bottom flask equipped with an inert gas inlet, a thermometer and a mechanical stirrer was used. The HBPE (15 g) and purified MMA monomer (10 g) were added into the flask after purging with nitrogen under continuous stirring until a homogenous solution was obtained. BPO (0.08 g) was then added. The reaction mixture was left under a constant nitrogen purge and continuous stirring for 24 h at 90-100 °C.

**Table 3.3: Formulation for water dispersible HBPE film**

<i>Water dispersible HBPE</i>							
Material	Water dispersible HBPE	Water	TEA	HMMA	MF resin	THF	PTSA
Amount (g)	10	10	0.5	0.6	2.4	2	0.06

#### 3.2.2.7. Curing of Acrylate Modified HBPE

MEKP (8 wt.% of MEKP solution with respect to resin) and cobalt-octate (4 wt.% cobalt-octate solution with respect to resin) were mixed with the acrylate modified HBPE by vigorous mechanical stirring and the mixture was degassed for 30 min under vacuum to make it completely bubble free. After complete removal of the solvent and the bubbles, the mixture was then cast on mild steel plates (150 mm × 50 mm × 1.60 mm) and glass plates (75 mm × 25 mm × 1.75 mm). The films were then dried under vacuum in dessicators for overnight at room temperature and allowed to cure at 150 °C for further study. The HBPE was also cured by using MEKP and cobalt octate similar to the method mentioned above. The HBPE film cured by MEKP and cobalt octate is coded as HBPE1.

### 3.3. Results and Discussion

#### 3.3.1. Modification of HBPE

##### 3.3.1.1. Formation of HBPE/Epoxy Blends

Blends of HBPE and epoxy resins were prepared at different compositions (Table 3.2) under mechanical agitation in the absence of any solvent. As there is no visible phase separation between HBPE and epoxy resins in the prepared blends even after sufficient time of storing, so it may be concluded that components are completely miscible with each other along with the hardener. This is attributed to the strong intermolecular interactions in the form of H-bonding and polar-polar interactions between the components through the ester, epoxide etc. groups. Such good miscibility between the

components eventually has positive effect on the entanglement of the chains and formation of network structures.

#### *3.3.1.2. Preparation of Water Dispersible HBPE*

The HBPE of the oil was prepared by alcoholysis followed by polycondensation reaction in a three step single pot reaction which has already been discussed in Chapter 2, section 2.2.2.2. However to make this resin as water dispersible the process was slightly modified. Briefly in the first step, triglyceride ester of oil was converted to monoglyceride which was then treated with excess amount of MA and PA to form carboxyl terminated pre-polyester. This pre-polyester was treated with bis-MPA in the third step of resinification, in such a way that some excess amount of free carboxylic acid groups should present in the HBPE. The  $-\text{COOH}$  groups of the pre-polymer and also bis-MPA reacted with the  $-\text{OH}$  groups of bis-MPA to form the HBPE. Then free carboxylic acid groups present in the HBPE were neutralized with TEA to form an ammonium salt, which resulted the water dispersible HBPE. The amount of TEA required for complete neutralization was calculated on equivalent basis depending on the acid value of the HBPE. The acid value of the resin was found to 62.06 mg KOH/g, so amount of TEA required for 100 of HBPE is 11.19 g. After complete neutralization of the free carboxylic acid groups, the resulted water dispersible HBPE was found to be well-dispersed in aqueous medium.

#### *3.3.1.3. Preparation of Acrylate Modified HBPE*

The HBPE was modified with MMA to obtain a combination of superior properties from the individual components. The desirable application and wetting properties of polyesters can be preferentially combined with strength, toughness and durability of the acrylic resins. The monomer MMA was polymerized in the presence of HBPE using BPO (0.8% with respect to MMA) as the initiator for modification of HBPE. The unsaturation present in the HBPE took part in the polymerization reaction of MMA. Although MMA was grafted onto the unsaturation site of the HBPE, but it is difficult to determine the exact degree of grafting occurring in the reaction by solvent extraction method, though the grafting was confirmed indirectly by FTIR and  $^1\text{H}$  NMR studies (discussed later). The idea behind the modification of HBPE with MMA by grafting or blend formation was to combine the fast drying of acrylics and good film properties of



the HBPE as well as to diminish the negative characters of both the resins. The blend or hybrid should be combined the major present properties of both the systems.

### 3.3.2. FTIR Study for Resins and Blends

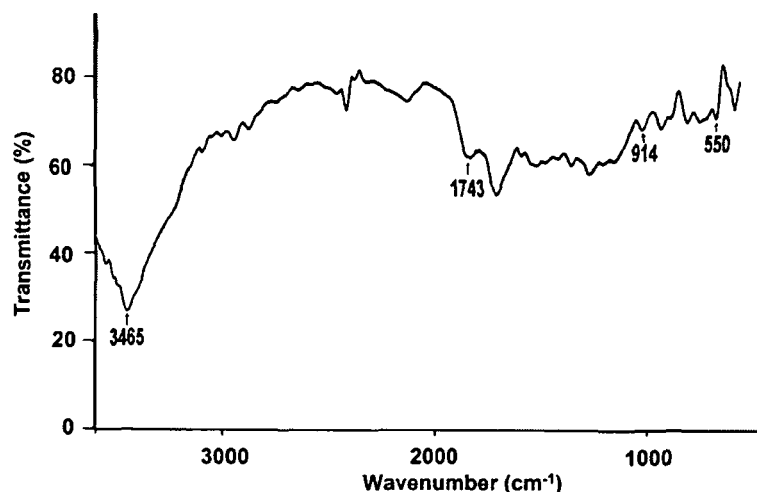
#### 3.3.2.1. HBPE/Epoxy Blends

The FTIR spectrum of the HBPE has already been discussed in Chapter 2. The important peaks for the vegetable oil based epoxy resin<sup>28</sup> are listed in Table 3.4.

From the FTIR spectrum (Fig. 3.7) of the blend (PEB1), shifting of C=O band of ester in HBPE (spectrum in Chapter 2) was observed<sup>29</sup> from 1736 to 1743  $\text{cm}^{-1}$ . This is due to the interaction of HBPE with the epoxy resin and the hardener. The band for epoxide group at 914  $\text{cm}^{-1}$  which was present in epoxy resin<sup>28</sup> with a significant intensity, decreased in intensity in the blend indicating the reaction between epoxy and curing agent.<sup>30</sup>

**Table 3.4:** The main FTIR bands and the corresponding functional groups of epoxy resin

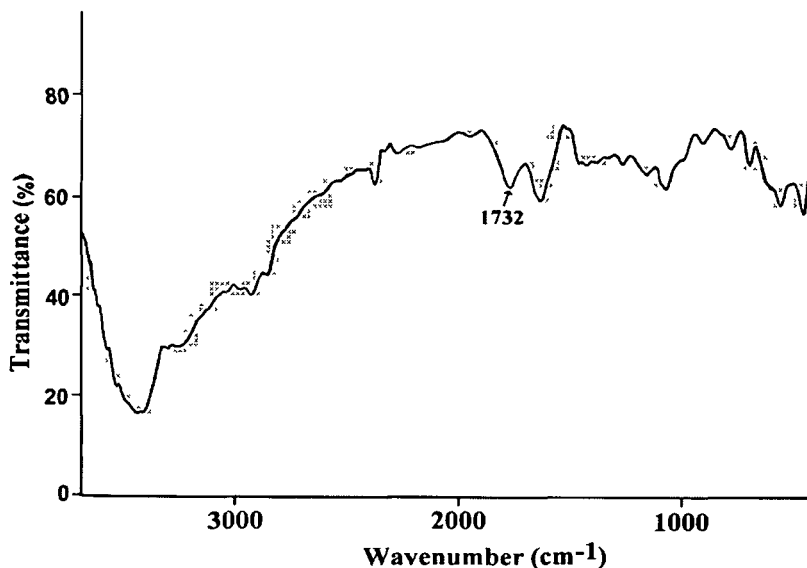
Band ( $\text{cm}^{-1}$ )	Assignment
2852-2923	Aliphatic C-H stretching vibration
3466-3675	O-H stretching vibration
1595-1610	C=C stretching vibration
1455	Aromatic C-H vibration
1163-1164	C-O-C vibration
1148-1247	Asymmetric structure of sulfone group
914	Oxirane ring (epoxy group)



**Fig. 3.7:** FTIR spectrum of PEB1

### 3.3.2.2. Water Dispersible HBPE

The FTIR spectrum of the environment friendly water dispersible HBPE is shown in Fig. 3.8. The characteristic absorbance bands appeared at  $1732\text{ cm}^{-1}$  is due to the stretching vibration of carbonyl group of polyester (C=O) and  $2925\text{-}2856\text{ cm}^{-1}$  is due to the asymmetric and symmetric stretching vibration of C-H in the FTIR spectrum of the resin.



**Fig. 3.8:** FTIR spectrum of water dispersible HBPE

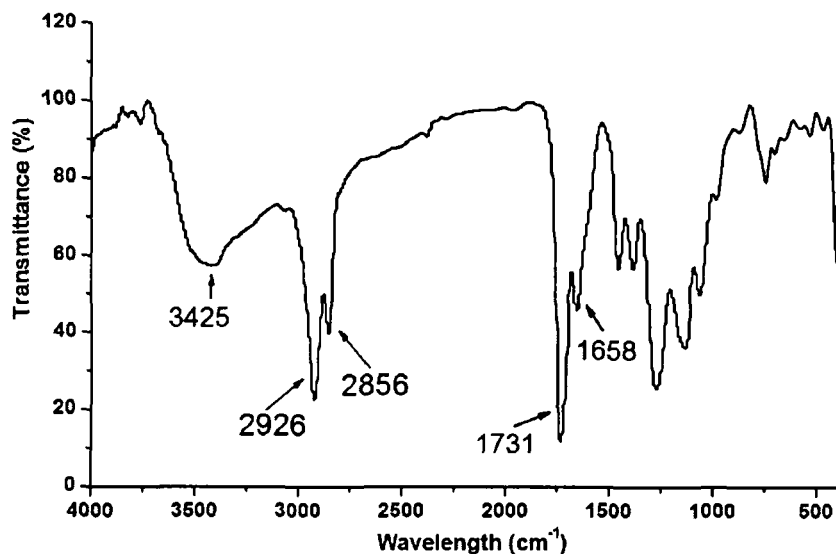
### 3.3.2.3. Acrylate Modified HBPE

Fig. 3.9 showed the FTIR spectrum of acrylate modified HBPE. The presence of important bands like C=O of ester group ( $1731\text{ cm}^{-1}$ ), C=C ( $1658\text{ cm}^{-1}$ ) etc. were observed from the spectrum. The intensity of the C=C unsaturated band in the acrylate modified HBPE decreased compared to the pristine HBPE (spectrum in Chapter 2), which again confirmed the grafting of MMA through the unsaturated site of the HBPE. The decreased in intensity of the above band was measured by calculating the ratio of the area of C=O band to that of C=C band. This ratio was found 1.39 for HBPE and 3.72 for acrylate modified HBPE. The other bands like -OH stretching frequency and -CH<sub>2</sub> asymmetric and symmetric stretching frequency were observed at 3400, 2856 and  $2926\text{ cm}^{-1}$  respectively.<sup>31</sup>

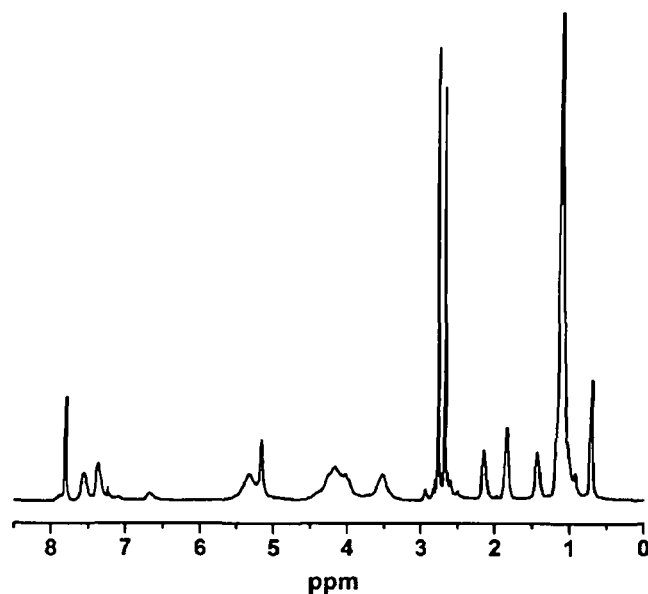
### 3.3.3. NMR Study for Acrylate Modified HBPE

Different proton environments obtained in <sup>1</sup>H NMR spectrum of the acrylate modified HBPE are shown in Fig. 3.10. The peak observed at  $\delta = 0.88\text{-}0.89\text{ ppm}$  is due to the protons of terminal methyl group of the fatty acid chains. The -CH<sub>2</sub>- protons attached

next to the above terminal methyl group were obtained at  $\delta = 1.60$  ppm. The peak for all the internal  $-\text{CH}_2-$  protons present in the fatty acids chains was observed at  $\delta = 1.27$  ppm. The peak for protons of unsaturated carbons appeared at  $\delta = 5.33$  ppm. The intensity of this peak was found to be lower than that of the pure HBPE. This is due to the involvement of the unsaturation of the HBPE in grafting of MMA. All other peaks like the aromatic protons of PA and protons for MA unit were retained at  $\delta = 7.54$ - $7.71$  ppm and at  $\delta = 2.00$ - $2.33$  ppm respectively.



*Fig. 3.9: FTIR spectrum of acrylate modified HBPE*



*Fig. 3.10: <sup>1</sup>H NMR spectrum of the acrylate modified HBPE*

### 3.3.4. Curing Study

#### 3.3.4.1. HBPE/Epoxy Blends

There is a possibility of crosslinking by the hydroxyl groups of HBPE present in the fatty acid originally or generated during crosslinking reactions with the epoxy groups of epoxy resin in the presence of amine hardener, which is an active base. Further, H-bonding between C=O of the HBPE with the -OH of epoxy resin present in the system occurred.<sup>30</sup> Also, there is a possibility of chemical reactions of hydroxyl/epoxide of epoxy resin with hydroxyl groups of HBPE, in the presence of amine hardener along with reactions of the hydroxyl/ester groups of HBPE with amine groups of the hardener.<sup>30</sup> Further, the hydroxyl groups of epoxy resin may undergo self-condensation reaction to form ether linkages. This explains the high rate of curing of epoxy resin by the amine hardener and the blend system.

### *3.3.4.2. Water Dispersible HBPE*

MF resin acts as crosslinking agent that leads to the crosslinked films via the interaction of alkoxymethyl or methylol group of MF resin and hydroxyl group of HBPE. HMMA acts as the co-crosslinking agent. It improves the effectiveness of MF resin by enhancing performance of the HBPE. THF was used as the co-solvent, which assists in removal of water in the water dispersible HBPE films. PTSA acts as the catalyst, which enhances the rate of crosslinking reactions between MF resin and HBPE. The curing mechanism associated with the oil modified HBPE and MF resins is a complex phenomenon due to the presence of a large number of functionalities such as -OH, -OR, -COOR, -COOH, >NH, -NH<sub>2</sub> etc. in the system. Thus a variety of reactions are possibly occurred between these two resins. The principal reaction occurs during the curing process between the alkoxymethyl or methylol group of amino resin and hydroxyl group of HBPE, leads to form ether linkages.<sup>32</sup>

### *3.3.5. Performance Study*

The performance characteristics like tensile strength, elongation at break, gloss, impact resistance and scratch hardness of the prepared HBPE/epoxy blends, water dispersible HBPE and acrylate modified HBPE films are given in Table 3.5.

Improvement in tensile strength of HBPE/epoxy blends was seen. This is due to the increase in the epoxy content in the blend as well as good crosslinking density in the cured blend structure as supported by swelling values (Table 3.5). The addition of vegetable oil based epoxy resin increased the flexibility of the blends as observed experimentally as enhanced elongation at break. Gloss refers to specular reflection or the

**Table 3.5:** *The performance characteristics of HBPE/epoxy blends, water dispersible HBPE and acrylate modified HBPE films*

Property	PEB1	PEB2	PEB3	PEB4	Water dispersible HBPE	Acrylate modified HBPE	HBPE1
Gloss at 60°	82	90	102	110	39	70	68
Scratch hardness (kg)	5	4.4	4	3	3.7	4	4
Impact resistance (cm)	65	50	45	45	40	55	50
Tensile strength (N/mm <sup>2</sup> )	2.7	2.04	1.96	1.78	1.96	4.53	2.25
Elongation at break (%)	52	41	30	24	51.3	47	32.4
Curing time (min at 120 °C)	80	120	180	300	90 <sup>a</sup>	330 <sup>b</sup>	300 <sup>b</sup>
Swelling (%)	28.5	30	33.4	36.2	32.5	28.5	32

Curing temperature for a: 140 °C and b: 150 °C

light reflected at the same angle as the angle of incidence. The gloss of the coated surface depends upon the amount of light absorbed or transmitted by the coating material that is influenced by the smoothness or texture of the surface. In general polyesters show good gloss and are much higher than epoxy resin. Thus epoxy resin has low gloss characteristics, which was improved by blending with HBPE in all the cases. This improvement may be due to improved compatibility of these blends and good light stability of the HBPE for which blends showed good gloss. Scratch hardness arises from the resistance of the materials to the dynamical surface deformation, i.e. ploughing, and from the interfacial friction between the indenter surface and the material.<sup>33</sup> Scratch hardness represents the response of the material under serious dynamic surface deformation that involved highly localized strain field and materials failure in plastic and/or brittle manner depending upon the nature of the scratched materials. The value of scratch hardness for HBPE/epoxy blend system increased with the increase of amount of epoxy resin (Table 3.5). This is due to the interaction of hydroxyl group of HBPE and the epoxide group of epoxy resin and also with the poly(amido amine) hardener. With the increase of epoxy resin amount the crosslinking

density of the blend system increases by the crosslinked structure of HBPE/epoxy system. The impact resistance of HBPE/epoxy blends was found to increase with epoxy content (Table 3.5). This may be due to the perfect interfacial bonding between HBPE and epoxy by the contribution of hydrogen bonding.

The performance properties of the water dispersible HBPE were found good, although they are not up to the mark to be used as high performance advanced material. The scratch hardness was good which is attributed to the decreased in flexibility of the cured films due to the presence of MF resin that may leads to self-polymerization reaction. This resulted higher degree of crosslinking, which increased the hardness of the network. The increase of hardness is also due to increase of rigid triazine moiety in the matrix. The impact resistance of the water dispersible HBPE is also good, which is due to the increase of crosslink density. However, the gloss value of water dispersible HBPE was comparatively lower than the HBPE.

The tensile strength of the HBPE was found to be increased from 2.25 to 4.53 N/mm<sup>2</sup> after acrylate modification. From Table 3.5, it was observed that the curing time of the acrylate modified HBPE was slightly higher than the unmodified HBPE<sup>1</sup>. This is due to the decrease in the level of unsaturation in the acrylate modified HBPE, since the unsaturation is the most important site for crosslinking reaction of free radical mechanism. The gloss value of the HBPE was found to increase slightly after acrylate modification.

### ***3.3.6. Chemical Resistance***

The chemical resistances of the cured HBPE/epoxy blends, water dispersible HBPE and the acrylate modified HBPE were tested in various chemical environments (Table 3.6) for 15 days at ambient temperature. All the HBPE/epoxy blends besides PEB3 and PEB4, showed relatively good alkali resistance due to the presence of more number of alkali resistant ether and amide linkages in the system. The resistivity towards all the media of all the HBPE/epoxy blends was also found to increase with the amount of epoxy resin. The resistance of the HBPE is poor toward alkali due to its hydrolyzable ester group. However this resistance was improved after modification with acrylate. The resistance of the modified HBPE was also improved towards all other media viz. dilute acid, salt and water solutions. This improved chemical resistance is due to the compact and crosslinked structure. The water dispersible HBPE films showed appreciable resistance towards dilute HCl acid, aqueous NaCl solution and distilled

water. However, due to the presence of alkali hydrolyzable ester group, the resistance towards alkali was not so good.

**Table 3.6:** Chemical resistance of the HBPE/epoxy blends, water dispersible HBPE and acrylate modified HBPE films

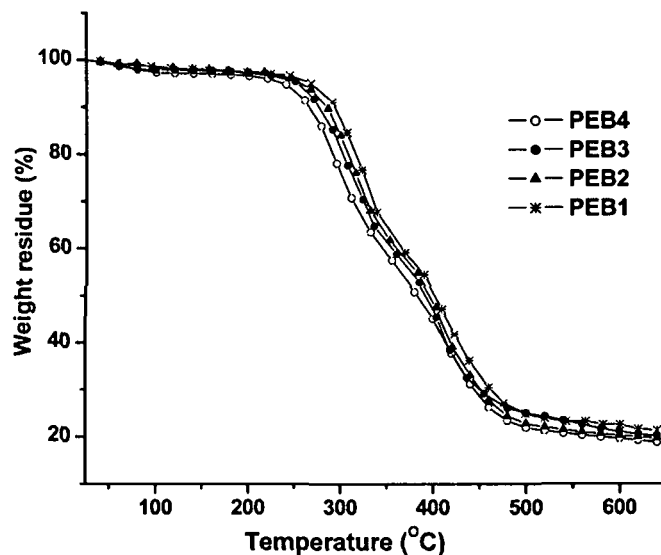
Code	5 wt.% aqueous alkali	25 wt.% aqueous HCl	25 wt.% aqueous NaCl	Distilled water
PEB1	G	E	E	E
PEB2	G	E	G	G
PEB3	PO	G	G	G
PEB4	PO	G	G	G
Water dispersible HBPE	P	A	A	G
Acrylate modified HBPE	G	E	E	E

G= Good, E= Excellent, PO= Peeled off, P= Poor, A= Average

### 3.3.7. Thermal Properties

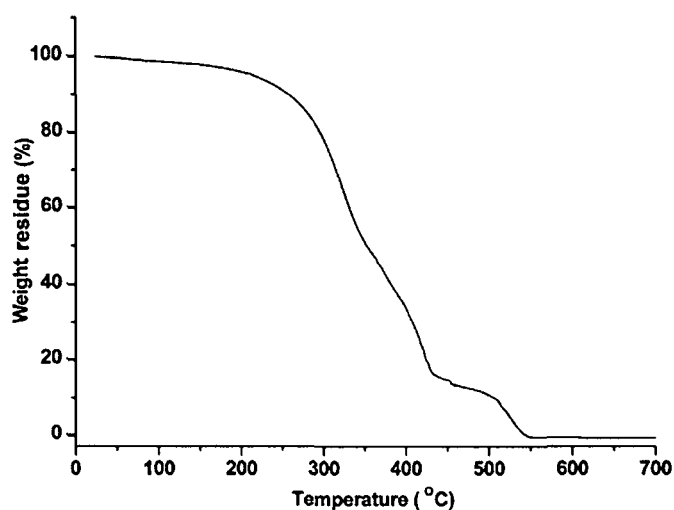
The TGA thermograms obtained for the HBPE/epoxy blends are shown in Fig. 3.11. From Fig. 3.11, it has been observed that the HBPE/epoxy blends degraded by a two step pattern. In the first step of degradation the onset ( $T_{on}$ ) and the endset ( $T_{end}$ ) thermal degradation temperatures of PEB1, PEB2, PEB3 and PEB4 were found to 273, 264, 256 and 242 °C and 378, 373, 362 and 349 °C respectively. However, in the second degradation step, the values were found to 410, 403, 400 and 393 °C and 501, 496, 477 and 469 °C respectively. Thus it was observed that with the increase of epoxy content the thermal degradation temperature of the blends also increased. The weight residue also increased with the increase of epoxy content and found 20, 19, 17 and 18% at 700 °C for the blends PEB1, PEB2, PEB3 and PEB4 respectively. This higher thermostability of blends is due to better crosslinked structure formed by crosslinking between the free hydroxyl groups present in the fatty acids of the oil originally or generated during amine crosslinking reaction as well as better physical interactions through H-bonding, polar-polar interactions etc. Thus, due to good compatibility between HBPE and epoxy resins, the thermostability of the blends got improved to a significant extent.

TGA thermogram of the water dispersible HBPE is shown in Fig. 3.12. The water dispersible HBPE is stable upto 250 °C which indicates good thermostability of the same. This good thermostability of water dispersible HBPE is due to the presence of rigid aromatic moiety in the structure.



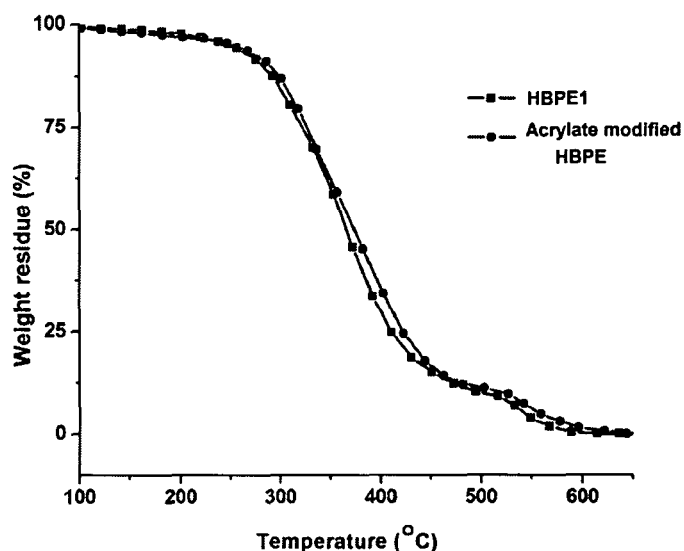
*Fig. 3.11: TGA thermograms for the HBPE/epoxy blends*

Fig. 3.13 showed the TGA thermograms of the HBPE1 and acrylate modified HBPE. From the figure we observed that the initial thermal degradation temperature ( $T_i$ ) of the polyester (HBPE1) was enhanced after modification with MMA. This good thermal stability of the acrylate modified HBPE could be attributable to the absence or reduction of unsaturation in the polyester backbone. The decomposition observed is perhaps a result of the breakdown of polyester or random scission initiated from the ester groups.



*Fig. 3.12: TGA thermogram for water dispersible HBPE*





*Fig. 3.13: TGA thermograms for HBPE1 and acrylate modified HBPE*

### 3.4. Conclusions

From this study, it can be concluded that the performance characteristics of the HBPE are well enhanced by blending with vegetable oil based epoxy resin using the solution blending technique and by modification through grafting with methylmethacrylate. In the case of HBPE/epoxy blends, the blend PEB1 exhibited the optimum film performance. The acrylate modified HBPE also showed better properties than that of the pure HBPE. The water dispersible HBPE showed desired performance properties which evaluated its suitability as a new renewable oil-based polyester system as environmental friendly aqueous processable material. The thermal properties, the thermogravimetric analysis (TGA) showed initial degradation temperature near 250 °C under the nitrogen atmosphere for all the cases indicating their high thermostability. Thus, all the results indicated the potentiality of *Mesua ferrea* L. seed oil based HBPE/epoxy blends, acrylate modified HBPE and water dispersible HBPE as surface coating materials.

### References

1. Miyagawa, H.; Mohanty, A.K.; Burgueno, R.; Drzal, L.T.; Misra, M. Development of biobased unsaturated polyester containing functionalized linseed oil. *Ind. Eng. Chem. Res.* **45**, 1014-1018 (2006)
2. Uyama, H. *et al.* Green nanocomposites from renewable resources: Plant oil-clay hybrid materials. *Chem. Mater.* **15**, 2492-2494 (2003)

3. David, S.B.; Sathiyalekshmi, K.; Raj, G.A.G. Studies on acrylated epoxidized triglyceride resin-co-butyl methacrylate towards the development of biodegradable pressure sensitive adhesives. *J. Mater. Sci. Mater. Med.* **20**, S61-S70 (2009)
4. Ahmad, S.; Ashraf, S.M.; Zafar, F. Development of linseed oil based polyesteramide without organic solvent at lower temperature. *J. Appl. Polym. Sci.* **104**, 1143-1148 (2007)
5. Uyama, H.; Kuwabara, M.; Tsujimoto, T.; Kobayashi, S. Enzymatic synthesis and curing of biodegradable epoxide-containing polyesters from renewable resources. *Biomacromolecules* **4**, 211-215 (2003)
6. Dutta, S.; Karak, N.; Saikia, J.P.; Konwar, B.K. Biodegradation of epoxy and MF modified polyurethane films derived from a sustainable resource. *J. Polym. Environ.* **18**, 167-176 (2010)
7. Deka, H.; Karak, N. Vegetable oil-based hyperbranched thermosetting polyurethane/clay nanocomposites. *Nanoscale Res. Lett.* **4**, 758-765 (2009)
8. Das, G.; Karak, N. Epoxidized *Mesua ferrea* L. seed oil-based reactive diluent for BPA epoxy resin and their green nanocomposites. *Prog. Org. Coat.* **66**, 59-64 (2009)
9. Mahapatra, S.S.; Karak, N. Synthesis and characterization of polyesteramide resins from Nahar seed oil for surface coating applications. *Prog. Org. Coat.* **51**, 103-108 (2004)
10. Ogunniyi, D.S.; Odetoye, T.E. Preparation and evaluation of tobacco seed oil-modified alkyd resins. *Bioresour. Technol.* **99**, 1300-1304 (2008)
11. Malshe, V.C.; Sikchi, M. *Basics of Paint Technology* (UICT, Mumbai, 2004)
12. Oldring, P.K.T. *Resins for Surface Coatings* (John Wiley & Sons, New York, 2000)
13. Athawale, V.D.; Chamankar, A.V. Low cost multipurpose coatings from alkyd-ketonic blends. *Paintindia* **53**, 41-48 (2003)
14. Athawale, V.D.; Chamankar, A.V.; Athawale, M. Alkyd-ketonic blends for coatings applications. *Paintindia* **50**, 39-46 (2000)
15. Cesteros, L.C.; Isasi, J.R.; Katime, I. Study of the miscibility of poly(vinyl pyridines) with poly(vinyl acetate), poly(vinyl alcohol) and their copolymers. *J. Polym. Sci. Part B: Polym. Phys.* **32**, 223-230 (1994)
16. Begawy, E.I.; Huglin, M.B. Polymer-polymer miscibility during copolymerization. *Eur. Polym. J.* **27**, 1023-1027 (1991)

17. Kim, B.K.; Oh, Y.S.; Lee, Y.M.; Yoon, L.K.; Lee, S. Modified polyacrylonitrile blends with cellulose acetate: blend properties. *Polymer* **41**, 385-390 (2000)
18. Viswanath, G.R.; Thangaraj, R.; Guhanathan, S. Thermomechanical and electrical studies on epoxy/hyperbranched polyester blends. *Int. J. Polym. Anal. Charact.* **14**, 493-507 (2009)
19. Ahmad, S.; Ashraf, S.M.; Kumar, G.S.; Hasnat, A.; Sharmin, E. Studies on epoxy-butylated melamine formaldehyde-based anticorrosive coatings from a sustainable resource. *Prog. Org. Coat.* **56**, 207-213 (2006)
20. Park, S.J.; Jin, F.L.; Lee, J.R. Thermal and mechanical properties of tetrafunctional epoxy resin toughened with epoxidized soybean oil. *Mater. Sci. Eng. A* **374**, 109-114 (2004)
21. Yu, L.; Petinakis, S.; Dean, K.; Bilyk, A.; Wu, D. Green polymeric blends and composites from renewable resources. *Macromol. Symp.* **249-250**, 535-539 (2007)
22. Bao, C.L.; Wang, L.S.; Zhang, A.Q. Synthesis and properties of waterborne hyperbranched aliphatic polyester clear coats. *J. Taiwan Inst. Chem. Eng.* **40**, 174-179 (2009)
23. Liebscher, H. Economic solutions for compliance to the new European VOC directive. *Prog. Org. Coat.* **40**, 75-83 (2000)
24. Lu, Y.; Larock, R.C. New hybrid latexes from a soybean oil-based waterborne polyurethane and acrylics via emulsion polymerization. *Biomacromolecules* **8**, 3108-3114 (2007)
25. Kukanja, D.; Golob, J.; Zupancic-Valant, A.; Krajnc, M. The structure and properties of acrylic-polyurethane hybrid emulsions and comparison with physical blends. *J. Appl. Polym. Sci.* **78**, 67-80 (2000)
26. Minari, R.J. *et al.* Molecular characterization of alkyd/acrylic latexes prepared by miniemulsion polymerization. *J. Appl. Polym. Sci.* **114**, 3143-3151 (2009)
27. Jahromi, S. The storage stability of melamine formaldehyde resin solutions: III. Storage at elevated temperatures. *Polymer* **40**, 5103-5109 (1999)
28. Das, G.; Karak, N.; Thermostable and flame retardant *Mesua ferrea* L. seed oil based non-halogenated epoxy resin/clay nanocomposites. *Prog. Org. Coat.* **69**, 495-503 (2010)
29. Prabu, A.A.; Alagar, M. Mechanical and thermal studies of intercross-linked networks based on siliconized polyurethane-epoxy/unsaturated polyester coatings. *Prog. Org. Coat.* **49**, 236-243 (2003)

### Chapter 3

30. Dutta, N.; Karak, N.; Dolui, S.K. Alkyd-epoxy blends as multipurpose coatings. *J. Appl. Polym. Sci.* **100**, 516-521 (2006)
31. Goikoetxea, M. *et al.* Polymerization kinetics and microstructure of waterborne acrylic/alkyd nanocomposites synthesized by miniemulsion. *J. Polym. Sci. Part A: Polym. Chem.* **47**, 4871-4885 (2009)
32. Vargha, V.; Kiss, G. Time-temperature-transformation analysis of an alkyd -amino resin system. *J. Therm. Anal. Calorim.* **76**, 295-306 (2004)
33. Sinha, S.K.; Song, T.; Wan, X.; Tong, Y. Scratch and normal hardness characteristics of polyamide-6/nanoclay composite. *Wear* **266**, 814-821 (2009)

## CHAPTER 4

---

### *Mesua ferrea* L. Seed Oil Based Polyester/Clay

#### Nanocomposites

##### 4.1. Introduction

From Chapter 2 it is cleared that the *Mesua ferrea* L. seed oil based HBPE, LPE and PE showed good properties. Again, the modified HBPEs discussed in Chapter 3 showed improved properties, even though the improvements were not up to the desired levels for many advanced applications. The demands of the advanced applications incline the scientists to develop the high performance polymeric materials to fulfill the requirements of materials for the society. But the development of a new high performance polymer is time consuming, laborious and involves a huge amount of cost. The formations of filled polymer and conventional polymer composite systems are two common methods to enhance the properties of polymeric materials by the inclusion of other additives and or materials. But both these techniques have some demerits like causing processing difficulties and increasing density, as a large number of different additives and or materials with high amount have to be incorporated to achieve the desired level of properties. Further in both the cases, improvements of properties are not up to the mark and thus limit their applications in different fields.<sup>1</sup> Thus, the nanotechnology brings about a revolutionary era in material science. As already mentioned in Chapter 1, the nanocomposite is one of the avant-garde genres of the composite materials, which becomes multidisciplinary in contemporary times and is challenging to the extreme.<sup>2</sup> In this domain, the polymer/clay nanocomposites are reported to be one of the best avenues to enhance the performance characteristics of the pristine polymers.<sup>3-7</sup> The high aspect ratio, stiffness, in-plane strength and at the same time ease of dispersion of the nanoclay make it a choice as nanofiller for large numbers of polymer nanocomposites. Again, the formation of an exfoliated polymer/clay nanocomposite significantly improves the properties of the pristine polymers over a

---

Parts of this work are published in (i) *Polym. Degrad. Stab.* **94**, 2221-2230 (2009)

(ii) *Polym. J.* (On line)

(iii) *Int. J. Polym. Mater.* (In Press)

(iv) *J. Appl. Polym. Sci.* (On line)

(v) *J. Polym. Environ.* (On line)

wide range, with incorporation of very low amount of nanoclay ( $\leq 5$  wt.%).<sup>8</sup> This is due to the significant change in size and shape of microphase domain in structure of the polymers, after incorporation of nanoclay.<sup>9</sup> The desired improvements of properties are obtained without affecting the density and transparency of pristine polymers, unlike the conventional filled or composite systems. Again, the degree of dispersion of the nanofillers in the polymer matrix measures the efficacy of polymer nanocomposites.<sup>10</sup> The use of ultrasound may also result the better dispersion and homogenization of nanofillers in the polymer matrices. Therefore the use of high mechanical shear force and ultrasonication may be a convenient and simple way in *ex-situ* technique to obtain suitable nanocomposites.<sup>11-12</sup>

Again among the various polymer matrices exploited, hyperbranched polyester based nanocomposites have covered a lot of research interests.<sup>13-16</sup> Further, the structural versatility of the hyperbranched polyester can be diversified by synthesizing them from bio-origins as stated in the previous chapters. The performance characteristics of the polyester can also be enhanced to a significant extent by blending with vegetable oil based epoxy resins, formation of water dispersible HBPE and modification with MMA as described in the Chapter 3. At the same time the structural confinement and the large number of surface functionality of the hyperbranched polymer may provide more sites of interaction and good stabilization to the nano reinforcing agent.<sup>17,18</sup> It is thereby expected that HBPE and its modified HBPE can bring about significant improvements in many desired properties coalescing the advantages of nanocomposites, structural beauty of hyperbranched polymers and environmentally benign vegetable oil based products by forming their nanocomposites. For comparison purpose the nanocomposites of linear polyester of the oil are also studied.

Thus in this chapter, the preparation, characterization and performance characteristics such as mechanical, thermal and rheological properties of *Mesua ferrea* L. seed oil based HBPE, LPE, PE, HBPE/epoxy blend, water dispersible HBPE and acrylate modified HBPE clay nanocomposites prepared by *ex-situ* technique are discussed.

## **4.2. Experimental**

### **4.2.1. Materials**

## Chapter 4

The necessary chemicals and solvents such as glycerol, PA, MA, bis-MPA, CYC, BPA, xylene, DMF, DMAc, epoxy resin, poly(amido amine) etc. were of same specifications as described in Chapter 2, section 2.2.1. The chemicals like BPS, epichlorohydrin, TEA, THF, MF resin, HMMA, PTSA, MMA, BPO etc. were of same specifications as described in Chapter 3, section 3.2.1. Octadecylamine modified (25-30 wt.%) montmorillonite nanoclay (OMMT, Nanomer<sup>®</sup> 1.30E) and hydrophilic bentonite nanoclay (Nanomer<sup>®</sup> PGV) were purchased from Sigma Aldrich, Germany and used without further purification. The details about nanoclay are described in Chapter 1, section 1.3.1.2.

The minerals  $(\text{NH}_4)_2\text{SO}_4$ ,  $\text{Na}_2\text{HPO}_4$ ,  $\text{KH}_2\text{PO}_4$ ,  $\text{MgSO}_4 \cdot 7\text{H}_2\text{O}$ ,  $\text{CaCl}_2 \cdot 2\text{H}_2\text{O}$ ,  $\text{FeSO}_4 \cdot 7\text{H}_2\text{O}$ ,  $\text{CuSO}_4 \cdot 7\text{H}_2\text{O}$ ,  $\text{MnSO}_4 \cdot 5\text{H}_2\text{O}$ ,  $\text{ZnSO}_4 \cdot 7\text{H}_2\text{O}$ ,  $\text{H}_3\text{BO}_3 \cdot 5\text{H}_2\text{O}$  and  $\text{MoO}_3$  used for the bacterial broth preparation were obtained from Merck, India. The bacterial strains PN8A1, vs1, SD2 and SD3 of *Pseudomonas aeruginosa*; and MTCC73 and MTCC736 of *Bacillus subtilis* along with other ingredients required for biodegradation study were obtained from the Department of Molecular Biology and Biotechnology (Department of Biotechnology, DBT Centre, Government of India), Tezpur University.

### **4.2.2. Instruments and Methods**

The FTIR and TGA analyses were carried out using the same instruments under the same conditions as mentioned in Chapter 2, section 2.2.2. and Chapter 3, section 3.2.2. respectively. The X-ray diffraction study was carried out at room temperature ( $\sim 27^\circ\text{C}$ ) by a Rigaku, Miniflex, UK, X-ray diffractometer at scanning rate of 2.0/min over the range of  $2\theta = 1-35^\circ$ . The X-ray was derived from nickel-filtered  $\text{Cu-K}\alpha$  ( $\lambda = 0.154 \text{ nm}$ ) radiation in a sealed tube operated at 40 kV and 40 mA. The surface morphology of the samples was studied by a scanning electron microscope (SEM, JEOL, JSM-6390LV, Japan) after platinum coating on the surface of the samples. The size and distribution of OMMT layers in the nanocomposites were studied by using transmission electron microscope (TEM, JEOL, JEMCXII, Japan) operated with an accelerating voltage of 100 kV, and equipped with a digital camera. The dilute polymer nanocomposite solution was transferred to a carbon-coated copper grid before analysis. The mechanical properties were tested by the same methods as stated in Chapter 2, section 2.2.2. The measurement of gloss, impact resistance, scratch hardness and chemical resistance was done according to the standard methods as mentioned earlier (Chapter 2, section 2.2.2.).

Ultrasonicator of the same specification as mentioned in Chapter 3, section 3.2.2. was used at fixed amplitudes and a half cycle for specified period of time.

*Mesua ferrea* L. seed oil was extracted from the matured seeds by the same method as described in Chapter 2, section 2.2.2. The percent of swelling of the nanocomposite films was determined with the same method as discussed in the Chapter 2, section 2.2.2.

### *4.2.2.1. Preparation of HBPE and Its Nanocomposites*

The *Mesua ferrea* L. seed oil based HBPE was prepared by using the same method as described in experimental section of Chapter 2, section 2.2.2.2. Requisite amount of OMMT (1, 2.5 and 5 wt.%) was dispersed in 1-5 mL of xylene by mechanical shearing for 30 min followed by ultrasonication for 10 min. The dispersed OMMT was then mixed with HBPE under vigorous mechanical stirring followed by ultrasonication for 30 min. Then the desired amount of BPA based epoxy resin (40 parts with respect to HBPE) and 25% poly(amido amine) hardener (with respect to epoxy resin) were mechanically mixed with the above HBPE/OMMT dispersion for 30 min using minimum amount of xylene. After homogenization the mixture was degassed for about 20 min under vacuum until it was completely bubbles free. Then the mixture was cast on different types of substrates as described in Chapter 2, section 2.2.2.1. The cast films were then dried under vacuum in dessicator for overnight at room temperature and were allowed to cure at specified temperature (120 °C) for specified period of time for further study. The curing time was estimated based on same method as described in Chapter 2, section 2.2.2.1. The cured films were denoted as PENC1, PENC2.5 and PENC5 corresponding to the OMMT content of 1, 2.5 and 5 wt.% respectively.

### *4.2.2.2. Preparation of LPE and Its Nanocomposites*

The *Mesua ferrea* L. seed oil based LPE was prepared by using the same methods as described in the experimental section of Chapter 2, section 2.2.2.1. The LPE was placed in vacuum oven at 50 °C, prior to the preparation of nanocomposites to remove entrapped volatiles. The preparative method for the nanocomposites was same as described above in the section 4.2.2.1. The nanocomposites were denoted as LPENC1, LPENC2.5 and LPENC5 corresponding to the OMMT content of 1, 2.5 and 5 wt.% respectively.



### *4.2.2.3. Preparation of PE and Its Nanocomposites*

PE was prepared by using the same methods as described in experimental section of Chapter 2, section 2.2.2.1. The nanocomposites of PE and OMMT were prepared by the same way as described above. The prepared nanocomposites were denoted as PNC1, PNC2.5 and PNC5 corresponding to the clay content of 1, 2.5 and 5 wt.% respectively, and the pristine system was denoted as PE.

### *4.2.2.4. Preparation of HBPE/Epoxy Blend and Its Nanocomposites*

Blend of HBPE and vegetable oil based epoxy was prepared by the method described in Chapter 3, section 3.2.2.3. Out of the different blend compositions the PEB1 showed the best performance and therefore it was used as the matrix for the preparation of nanocomposites. The required dose levels of OMMT (1, 2.5 and 5 wt.%) were dispersed in xylene by mechanical shearing for 30 min followed by ultrasonication for 10 min. The dispersed OMMT was then mixed with the above HBPE/epoxy blend mixture (PEB1) under vigorous mechanical stirring followed by ultrasonication for 30 min. After being sonicated, 50% poly(amido amine) hardener (with respect to epoxy resin) was mixed into the mixture and degassed for about 20 min under vacuum, until it get completely bubble free. Then the mixture was cast on mild steel and glass plates and dried under vacuum in a desiccator for overnight at room temperature. The cast films were then allowed to cure at 120 °C for further study. The prepared nanocomposites were denoted as BNC1, BNC2.5 and BNC5 corresponding to the clay content of 1, 2.5 and 5 wt.% respectively.

### *4.2.2.5. Preparation of Water Dispersible HBPE and Its Nanocomposites*

The *Mesua ferrea* L. seed oil based water dispersible HBPE was prepared by using the same method as described in experimental section of Chapter 3, section 3.2.2.4. Different doses of hydrophilic bentonite nanoclay were dispersed in water by mechanical mixing for 24 h separately. Then the calculated amount of water dispersible HBPE, water, THF, TEA, MF resin, HMMA and PTSA were mixed in the dispersed clay medium by vigorous mechanical stirring for 30 min followed by ultrasonication for another 30 min. The pH was maintained 8.3 in all the cases. After being sonication the mixture was degassed under vacuum until it was completely bubble free. Then similarly it was cast on different substrates like mild steel and glass plates as mentioned

## Chapter 4

in Chapter 2, section 2.2.2.1. and dried under vacuum in dessicator for overnight at room temperature and then they were cured at 140 °C for further study. The prepared nanocomposites were denoted as WBPENC1, WBPENC2.5 and WBPENC5 corresponding to the clay content of 1, 2.5 and 5 wt.% respectively.

### *4.2.2.6. Preparation of Acrylate Modified HBPE and Its Nanocomposites*

The acrylate modified HBPE was prepared by using the same methods as described in experimental section of Chapter 3, section 3.2.2.6. Different dose levels of OMMT were dispersed in xylene by mechanical shearing for 30 min followed by ultrasonication for 10 min. The desired amount of dispersed OMMT was then mixed with acrylate modified HBPE by mechanical stirring vigorously followed by ultrasonication for 30 min. After being sonicated, MEKP (8 wt.% MEKP solution with respect to the resin) and cobalt-octate (4 wt.% cobalt octate solution with respect to the resin) were mixed with the mixture and degassed for 30 min under vacuum to make it completely bubble free. The prepared nanocomposites were denoted as PANC1, PANC2.5 and PANC5 corresponding to the clay content of 1, 2.5 and 5 wt.% respectively.

### *4.2.2.7. Bacterial Media*

Mineral salt medium with the following composition was prepared for biodegradation study. 2.0 g of  $(\text{NH}_4)_2\text{SO}_4$ , 2.0 g of  $\text{Na}_2\text{HPO}_4$ , 4.75 g of  $\text{KH}_2\text{PO}_4$ , 1.2 g of  $\text{MgSO}_4 \cdot 7\text{H}_2\text{O}$ , 0.5 mg of  $\text{CaCl}_2 \cdot 2\text{H}_2\text{O}$ , 100  $\mu\text{g}$  of  $\text{MnSO}_4 \cdot 5\text{H}_2\text{O}$ , 70  $\mu\text{g}$  of  $\text{ZnSO}_4 \cdot 7\text{H}_2\text{O}$ , 10  $\mu\text{g}$  of  $\text{H}_3\text{BO}_3 \cdot 5\text{H}_2\text{O}$ , 100  $\mu\text{g}$  of  $\text{CuSO}_4 \cdot 7\text{H}_2\text{O}$ , 1 mg of  $\text{FeSO}_4 \cdot 7\text{H}_2\text{O}$  and 10  $\mu\text{g}$  of  $\text{MoO}_3$  were dissolved in 1.0 L of demineralized water. 3 mL of this liquid culture medium was poured into 50 mL conical test tube and they were sterilized using autoclave at 121 °C and 15 lb pressure for 15 min. The autoclaved media were then allowed to cool down to room temperature and polymer films were applied to the media under sterile condition inside a laminar air hood. Medium containing no polymer film was also cultured as negative control in each case.

### *4.2.2.8. Bacterial Strains*

Pure cultures were grown using nutrient broth at 37 °C for 18 h. 1 mL of bacterial cultures were centrifuged at 6000 rpm for 15 min at room temperature and the pellets were washed with mineral salt medium and re-suspended in 1 mL of the same medium.

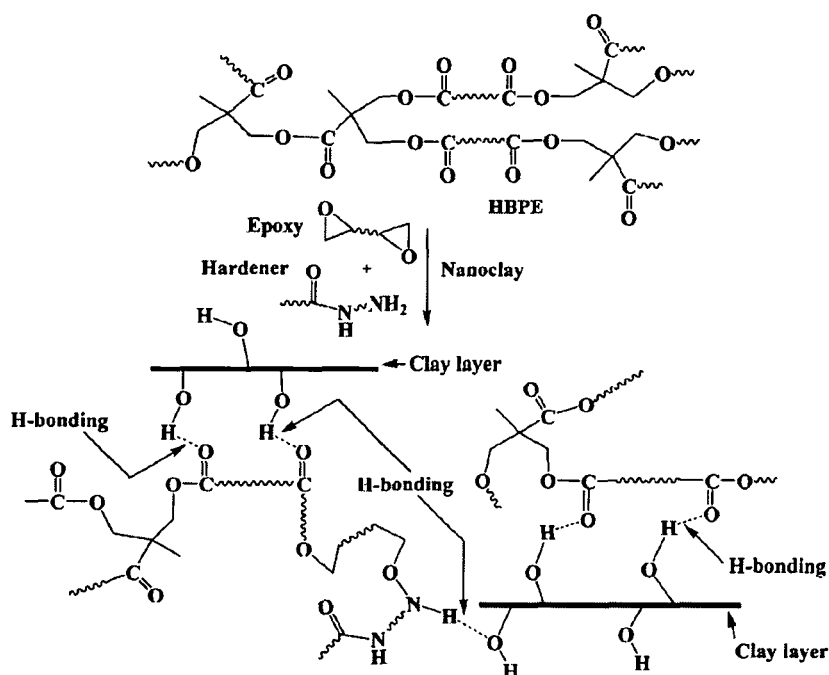
The 30  $\mu\text{L}$  of the culture medium containing  $1 \times 10^8$  / mL microbes was inoculated to the test tube containing 3 mL media for each test. The test tubes were then incubated under sterile condition at 37 °C for the degradation study. The samples were collected for spectrophotometric observation at 600 nm against blank culture media on weekly basis under sterile condition.

### 4.3. Results and Discussion

#### 4.3.1. Formation of Nanocomposites

Polymers have been frequently used as matrices for the preparation of nanocomposites, since they prevent agglomeration and settling of the nano particles. The addition of nanoclay to triglyceride-based polymers or their blends to form nanocomposites can broaden the applications of these new bio-based materials as it improves their desired properties.<sup>19-22</sup> Amongst the vast nano-reinforcements available for fabricating polymer nanocomposites, clays have been focused and studied the most, because they are naturally occurring minerals, exhibit a layered morphology with high aspect ratios, and have substantial cation exchange capacities. The processing of polymers with various reinforcing nanofillers becomes a key technology to obtain advanced materials for the next generation. Due to the low mechanical property of the vegetable oil based polyester resin, the nanocomposite fabrication has become a challenge to enhance this property along with thermal, chemical resistance etc. The state and the degree of dispersion of the OMMT in the polyester matrix played an important role to achieve the desired properties. OMMT has the tendency of self-organization to form agglomerate due to its large surface area and high activity. The polymer chains help in exfoliation or delamination of OMMT layers by diffusion and through molecular interactions. This is because the layers are stacked together by weak ionic force, which are further weakened by modification with organophilic groups.<sup>23</sup> In order to make the polymer chain molecules penetrating into the OMMT basal interspace, a strong mechanical force is commonly applied. In this study, proper dispersion of the OMMT was achieved with high shear forces by vigorous mechanical mixing and ultrasonication. Ultrasonication can produce tiny bubbles, which can collapse violently, releasing significant energy that can be used to exfoliate OMMT layers.<sup>24</sup> This prolonged force promoted the penetration of polymer chains into the galleries between the silicate layers which results the delaminated/exfoliated structure where the individual OMMT layers

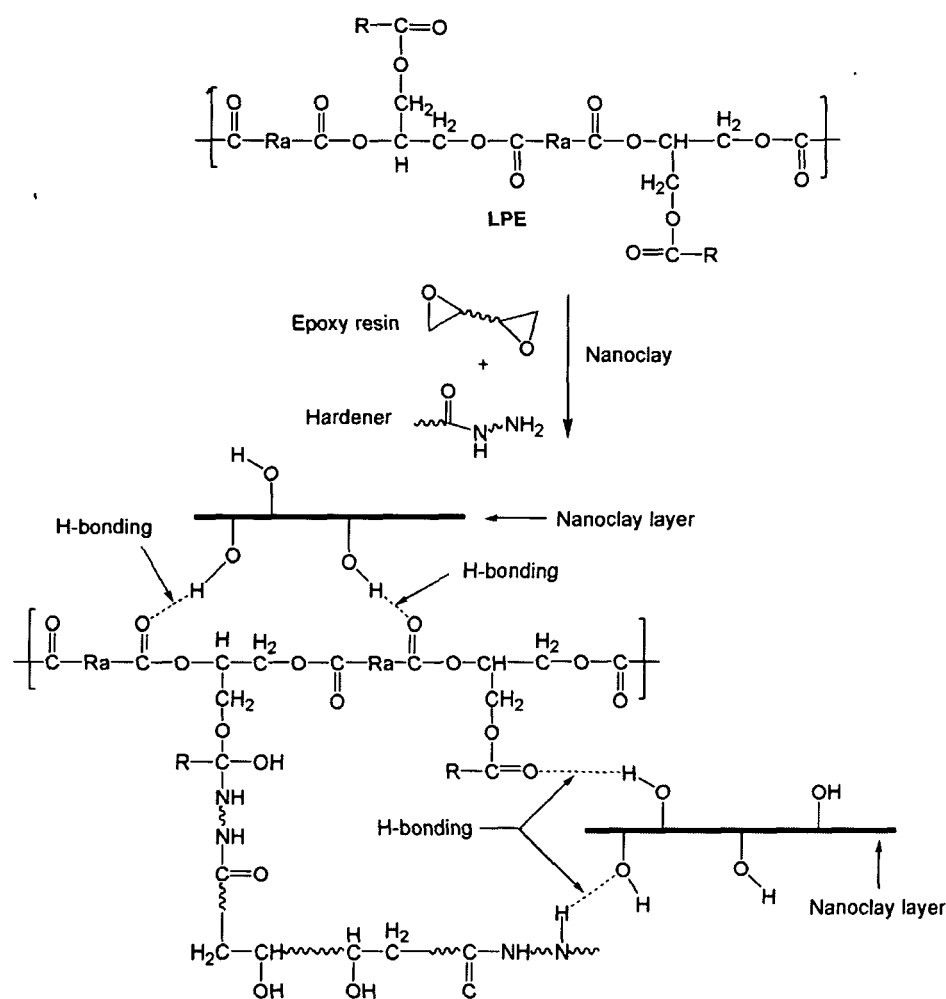
are completely separated and dispersed randomly in the polyester matrix. Here the carboxyl groups of the polyester can easily interact with the hydroxyl groups of OMMT through H-bonding or other polar-polar interactions which results a stable and well dispersed nanocomposites (Scheme 4.1 and Scheme 4.2). The confined geometry with large numbers of functional groups of HBPE helps better and stable dispersion of nanoclay compared to the same in LPE. In the blend based nanocomposites, the carboxyl groups of the polyester resin, and epoxy and hydroxyl groups of epoxy resin can easily interact with hydroxyl groups of nanoclay through H-bonding or other polar-polar interactions to form stable and well-dispersed nanocomposites.



**Scheme 4.1:** Possible interactions in HBPE nanocomposites

In the case of water dispersible HBPE nanocomposites, the hydrophilic bentonite nanoclay was dispersed in aqueous dispersion by mechanical stirring and ultrasonic agitation of the matrix. MF resin used in the formulations of nanocomposites acts as crosslinking agent that leads to the crosslinked films via the interaction of alkoxymethyl or methylol group of MF resin and hydroxyl group of polyester resin. This results the formation of ether linkage along with other interactions. HMMA acts as the co-crosslinking agent and improves the effectiveness of MF resin, thereby enhancing performance of the nanocomposites. THF was used as the co-solvent, which assists in removal of water in the nanocomposite films. PTSA acts as the catalyst, which enhances the rate of crosslinking reactions between MF resin and polyester

matrix (Scheme 4.3). The carboxyl groups of the polyester can easily interact with hydroxyl groups of nanoclay through H-bonding or other polar-polar interactions to form stable and well-dispersed nanocomposites.

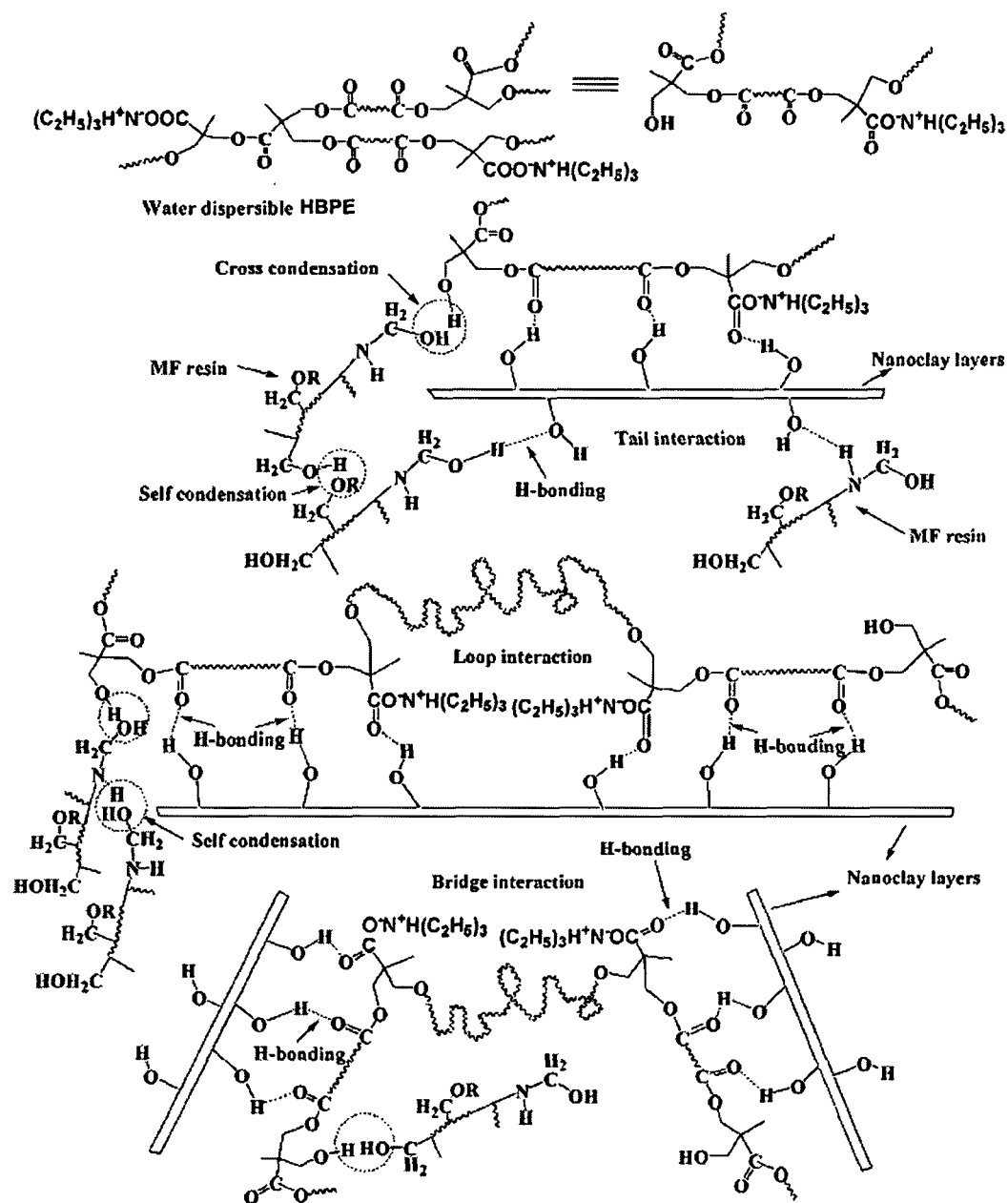


**Scheme 4.2:** Possible interactions in LPE nanocomposites

### 4.3.2. Characterization of Nanocomposites

#### 4.3.2.1. FTIR Study

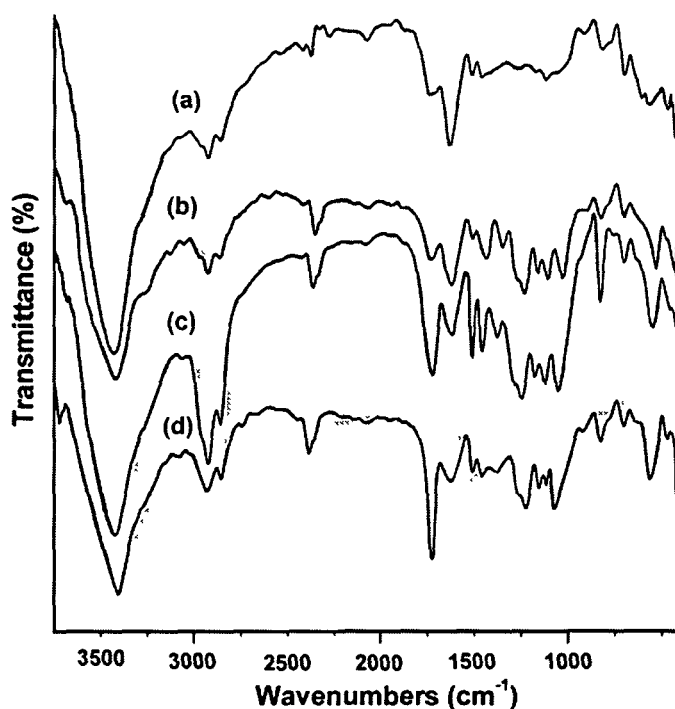
Fig. 4.1 displays the FTIR spectra of HBPE and its nanocomposites. From this figure it is observed that the HBPE and its nanocomposites show almost similar characteristic bands for the distinctive functional groups of the system. However, the difference observed in the relative intensity of the peak of C=O group ( $1735\text{ cm}^{-1}$ ) suggests that polyester segments (-COOH and -OH) interacted with the -OH groups of clay layers through H-bonding or other polar-polar interactions. The bands appeared at  $1030\text{ cm}^{-1}$



**Scheme 4.3:** Possible interactions in water dispersible HBPE nanocomposites

and  $550\text{ cm}^{-1}$  in the FTIR spectra of the clay are due to Si-O and Al-O stretching vibrations,<sup>25</sup> which increased with the clay loading. The band at  $3424\text{ cm}^{-1}$  for the -OH stretching vibration of Si-OH and Al-OH moieties located on the surface of the clay shifted to the lower wave number region ( $3420\text{-}3410\text{ cm}^{-1}$ ) after the formation of nanocomposites. This observation indicates the interactions of -OH groups of clay with the ester/ -OH groups of the polymer chain and amino groups of hardener (Scheme 4.1). The -OH stretching band was also sharpened continuously in the nanocomposites with the clay loading for the same reason. The intensity of the band at  $1629\text{-}1623\text{ cm}^{-1}$  corresponding to the H-bonded -OH bending vibration that occurs due to hydrophilic

nature of the clay is steadily minimized in the nanocomposites with clay loading.<sup>26</sup> This indicates strong interactions with the different components present in the matrix with nanoclay.

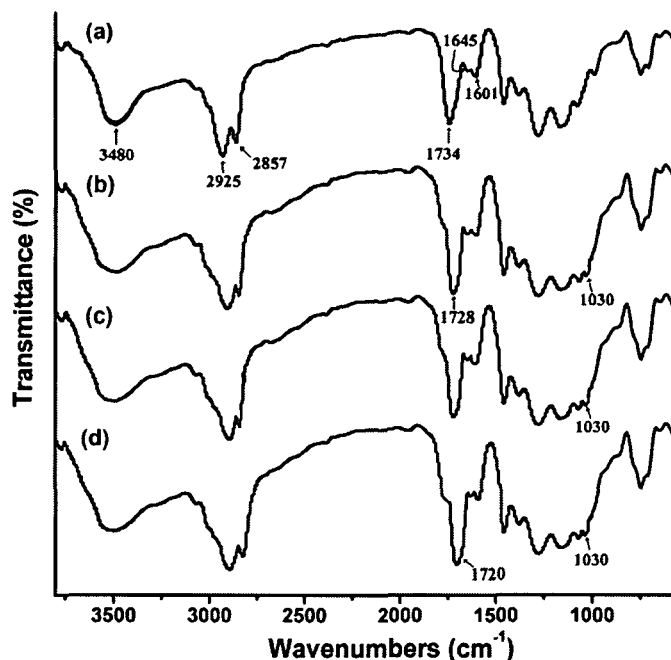


**Fig. 4.1:** FTIR spectra for (a) HBPE, (b) PENC1, (c) PENC2.5 and (d) PENC5

The characteristic FTIR absorption bands observed for the LPE nanocomposites are shown in Fig. 4.2. In the nanocomposites after incorporation of nanoclay the carbonyl stretching frequency of polyester was observed to shift towards lower value ( $1728$  to  $1720$   $\text{cm}^{-1}$ ) than the pure resin. This shifting is attributed to the interaction of polyester segments ( $-\text{COOH}$  and  $-\text{OH}$ ) with  $-\text{OH}$  group of clay through H-bonding or other polar-polar interactions (Scheme 4.2). The band due to Si-O-Si ( $1030$   $\text{cm}^{-1}$ ) stretching vibrations of nanoclay was observed to appear in the nanocomposites. The band due to  $-\text{OH}$  stretching in the polyester at  $3480$   $\text{cm}^{-1}$  became broaden with the incorporation of clay. All these results suggest strong interactions between ester/ $-\text{OH}$  groups of polyester chains with  $-\text{OH}$  group of nanoclay.

In the FTIR spectra of blend based nanocomposites (Fig. 4.3) the carbonyl stretching frequency was observed to shift towards lower value ( $1720$ - $1731$   $\text{cm}^{-1}$ ) than the blend. This shifting is attributed to the interaction of polyester segments ( $-\text{COOH}$  and  $-\text{OH}$ ) with  $-\text{OH}$  group of OMMT through H-bonding or other polar-polar interactions.<sup>27</sup> The bands due to Si-O-Si ( $1030$   $\text{cm}^{-1}$ ) and Al-O-Al ( $550$   $\text{cm}^{-1}$ ) stretching vibrations of OMMT were observed to broaden in the nanocomposites with 0-5 wt.%

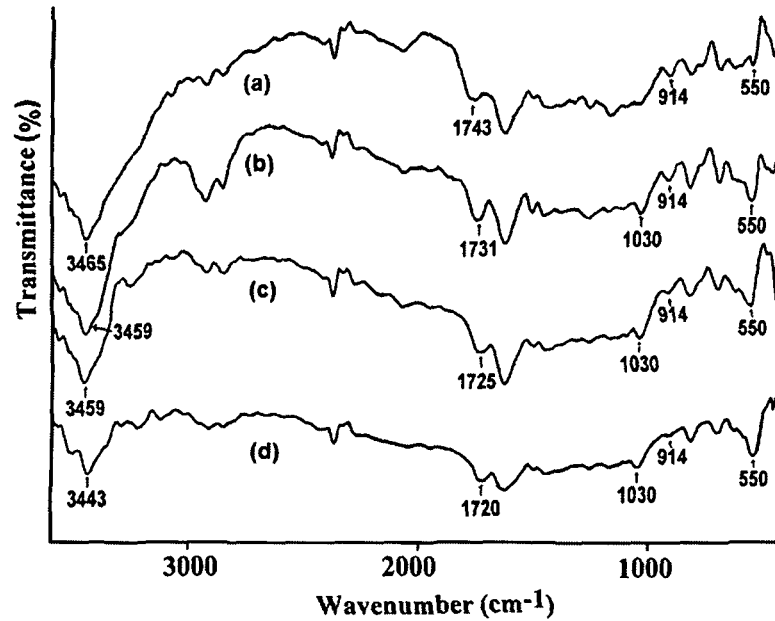
OMMT loading. Also the band at  $3465\text{ cm}^{-1}$  due to  $-\text{OH}$  stretching vibration frequency of polyester resin was shifted toward lower wave number region ( $3443\text{ cm}^{-1}$ ) after nanocomposites formation due to the overlapping with  $-\text{OH}$  group of OMMT. These results showed strong interactions between the different components present in the nanocomposite system. The interaction of ester/ $-\text{OH}$  group of polymer chains or amino group of hardener with  $-\text{OH}$  group of OMMT can be put forward for the same.



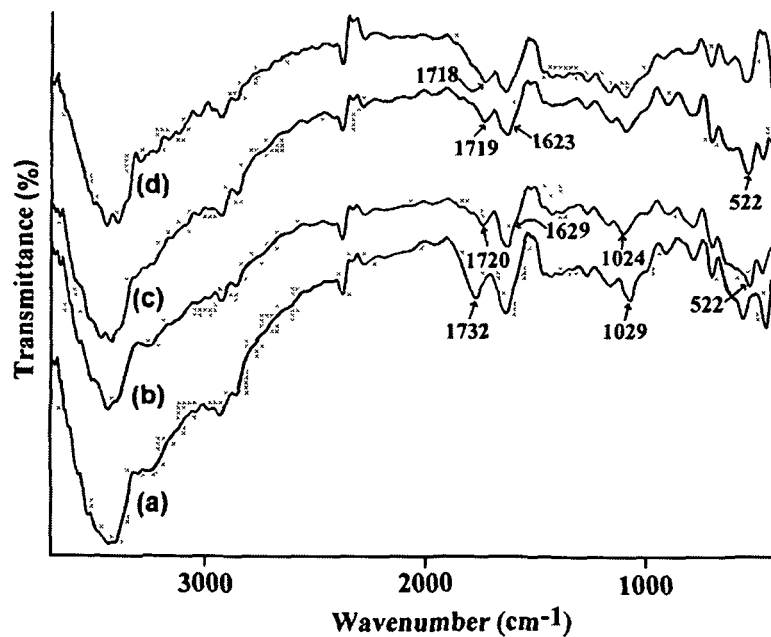
**Fig. 4.2:** FTIR spectra for (a) LPE, (b) LPENC1, (c) LPENC2.5 and (d) LPENC5

The FTIR spectra of the water dispersible HBPE nanocomposites are shown in Fig. 4.4. The characteristics absorbance bands appeared at  $1732\text{ cm}^{-1}$  due to the stretching vibration of carbonyl group of polyester ( $\text{C}=\text{O}$ ) and  $2925\text{--}2856\text{ cm}^{-1}$  due to the asymmetric and symmetric stretching vibration of  $\text{C-H}$  in the spectrum of pristine resin. After formation of nanocomposites it was observed that the carbonyl stretching vibration was shifted to lower frequencies ( $1718\text{--}1720\text{ cm}^{-1}$ ) than the pristine polyester. This shifting of frequency is attributed to the interactions of the polyester segments ( $-\text{COOH}$  and  $-\text{OH}$ ) with clay layers through H-bonding or other polar-polar interactions (Scheme 4.3). The intensity of band at  $1629\text{--}1623\text{ cm}^{-1}$ , which corresponds to the H-bonded  $-\text{OH}$  bending vibration of the nanoclay, was steadily minimized in the nanocomposites with clay loading. Also the bands appeared at  $1029$  and  $522\text{ cm}^{-1}$  due to  $\text{Si-O}$  and  $\text{Al-O}$  stretching vibrations of clay were broaden and the band appeared at  $1029\text{ cm}^{-1}$  was moved to  $1044\text{ cm}^{-1}$ .<sup>28</sup> These results showed strong interactions between the different components present in the matrix and nanoclay platelets.





*Fig. 4.3: FTIR spectra for (a) PEB1, (b) BNC1, (c) BNC2.5 and (d) BNC5*



*Fig. 4.4: FTIR spectra for (a) water dispersible HBPE, (b) WBPENC1, (c) WBPENC2.5 and (d) WBPENC5*

#### 4.3.2.2. XRD Study

XRD is a powerful tool to investigate the degree of dispersion and delamination of clay layers in the polymer matrix. The structural characterization of all the nanocomposites was performed by using XRD patterns which could allow a direct or indirect indication about the intercalation/exfoliation of the polymer chains into the clay silicate galleries. In general, the intercalated layers show intense peak in the range of  $1-10^\circ$  ( $2\theta$  value)

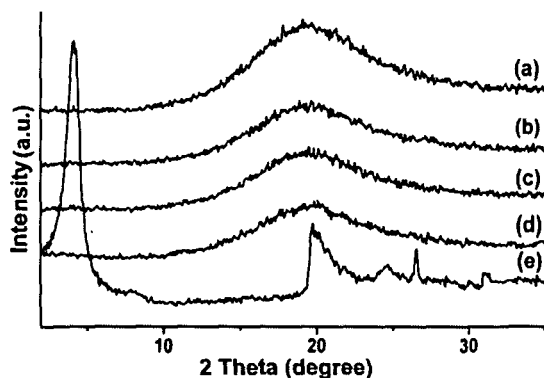
whereas exfoliated system does not show any distinct peak in that range for their loss of structural integrity. The interlayer spacing ( $d$ ) was calculated on the basis of Bragg's scattering equation (4.1) given as,

$$2d\sin\theta = n\lambda \quad (4.1)$$

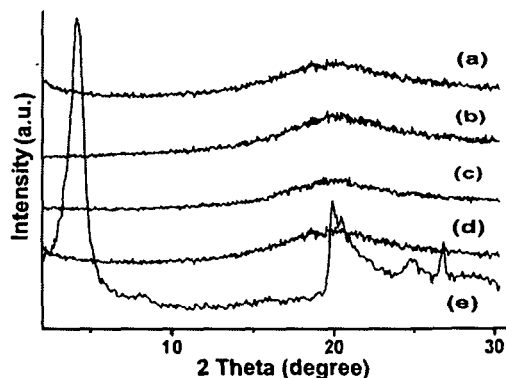
where,  $\lambda$  is the wavelength (0.154 nm) of the X-ray radiation used in the diffraction experiment of the present study,  $d$  is the spacing between the diffractive lattice plane also known as the basal spacing,  $n$  is the order of plane which is 1 in the present case and  $\theta$  is the measured half diffraction angle or glancing angle.

The XRD diffractograms of the HBPE, LPE, PE, HBPE/epoxy blend, acrylate modified HBPE and OMMT nanocomposites containing different proportions of OMMT and water dispersible HBPE/bentonite nanocomposites are displayed in Fig. 4.5, 4.6, 4.7, 4.8, 4.9 and 4.10 respectively. For octadecylamine modified OMMT clay the basal reflection peak ( $d_{001}$ ) was found at an angle  $4.17^\circ$  ( $2\theta$ ) which corresponds to  $d$ -spacing of 2.36 nm. This characteristic diffraction peak was found to disappear in the XRD diffractograms of HBPE, LPE and HBPE/epoxy blend nanocomposites with 0-5 wt.% OMMT clay in the angular range of the study ( $2\theta = 1-35^\circ$ ) suggesting the disordering and loss of structural regularity of the clay layers. Hence, possibly there was formation of an exfoliated nanocomposite structure. The disappearance of the peak due to OMMT in the nanocomposite confirms the distortion of the platy nanolayers of the clays and is feature of delamination and dispersion of the nanoclay layers within polyester matrix. The polymer sample without nanofiller showed a broad peak at  $19.8-20^\circ$  which appears due to the amorphous nature of the polyester. Although it is a common practice to define a nanocomposite as exfoliated one by the absence of peak at [001] reflection, nevertheless it is difficult to reach a final conclusion about the actual structure obtained from the XRD alone. For this one has to further confirm it by TEM studies. The absence of diffraction peaks could also be due to geometry effects or low sensitivity of the instrument at low loadings of clay.<sup>29</sup> Also, at the same time, it is worth to note that the disappearance of the characteristic peak of OMMT in the present nanocomposites is not due to the limitation of the instrument as the concentration of clay in the matrix is within the range of detection and also there is no heavy element present in the system.

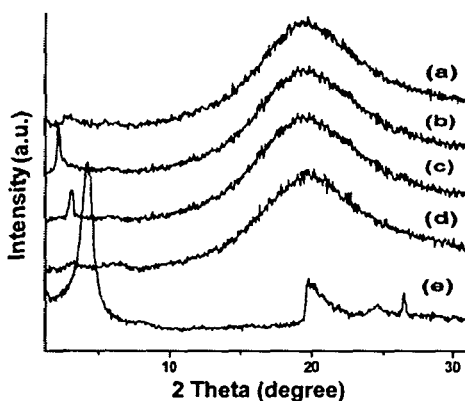
Fig. 4.7 shows the XRD diffractograms of PE/OMMT nanocomposites with 0-5 wt.% loadings. The characteristic peak of the pristine OMMT appeared at  $2\theta = 4.15^\circ$



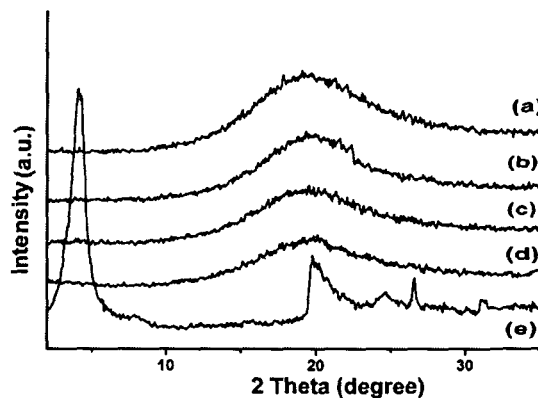
*Fig. 4.5: XRD diffractograms for (a) HBPE, (b) PENC1, (c) PENC2.5, (d) PENC5 and (e) OMMT*



*Fig. 4.6: XRD diffractograms for (a) LPE, (b) LPENC1, (c) LPENC2.5, (d) PENC5 and (e) OMMT*



*Fig. 4.7: XRD diffractograms for (a) PE, (b) PNC1, (c) PNC2.5, (d) PNC5 and (e) OMMT*



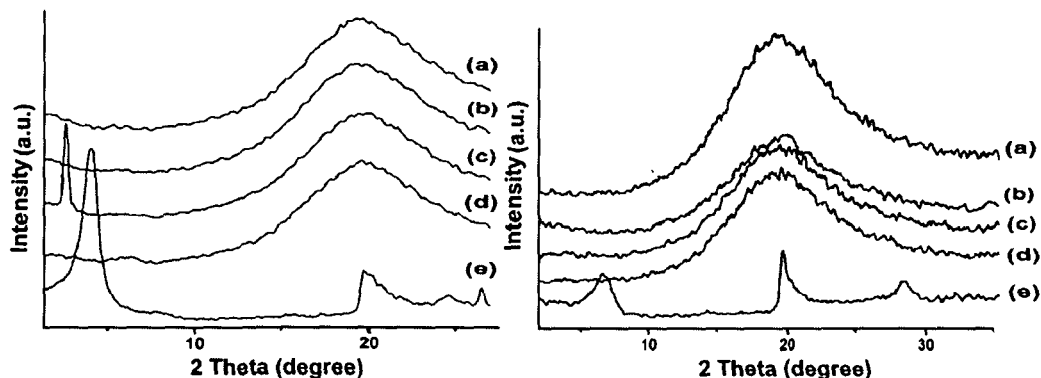
*Fig. 4.8: XRD diffractograms for (a) PEB1, (b) BNC1, (c) BNC2.5, (d) BNC5 and (e) OMMT*

with corresponding interlayer spacing  $d = 2.12$  nm, calculated from the Bragg's equation. For PNC1, this peak was shifted to  $2\theta = 3^\circ$  ( $d = 2.94$  nm) suggesting that the OMMT had swollen by the polymer chains and thereby increasing the  $d$ -spacing value. For nanocomposite PNC2.5 the above peak was further shifted towards lower angle  $2\theta = 2.12^\circ$  ( $d = 4.16$  nm). In general, a larger interlayer spacing should be advantageous in the intercalation of polymer chains. It should also lead to easier dissociation of the OMMT layers resulting in nanocomposites with better OMMT dispersions.<sup>30</sup> Thus intercalation of the OMMT layers by the polyester chains was obtained. The PNC5 showed no peak for OMMT, although a broad peak at  $2\theta = 19^\circ$  in the XRD diffractogram, which is attributed to the amorphous nature of the pristine polyester resin is present in all the nanocomposites. The absence of the characteristics peak of OMMT in the PNC5 may be due to the exfoliation of the OMMT layers by polyester

chains. This also suggested the disordering and loss of structural regularity of the OMMT layers. As already mentioned, the absence of peak at [001] reflection gives a rough idea about the exfoliated state of OMMT layer but need to further confirm by TEM studies.

Fig. 4.9 represents the XRD diffractograms of OMMT powder and that of acrylate modified polyester/OMMT nanocomposite films in the range of  $2\theta = 1-30^\circ$ . For OMMT the basal reflection peak ( $d_{001}$ ) was found at an angle  $4.17^\circ$  ( $2\theta$ ) corresponding to 2.36 nm d-spacing. This peak was shifted to  $2\theta = 2.9^\circ$  for the nanocomposite PANC1, which is attributed to the intercalation of polymer chains into the clay galleries. Further this characteristic diffraction peak was absent in the XRD diffractograms of the nanocomposites with 2.5 and 5 wt.% OMMT. Generally, an increase in d-spacing is indicative of the formation of nanocomposites, since this is confirming the polymer diffusing into the interlayer spacing of the clay. The absence of peaks may be due to exfoliation, the absence of ordering, or high order spacing between the layers. Hence, possibly an exfoliated nanocomposite structure was formed. The sample without nanofiller showed  $2\theta$  peak at  $19.8^\circ$  which is due to amorphous nature of the matrix.

Fig. 4.10 shows the patterns of XRD for the water dispersible HBPE nanocomposites with different bentonite clay contents. The hydrophilic bentonite clay shows basal reflection peak ( $d_{001}$ ) at an angle of  $6.65^\circ$  ( $2\theta$ ). In the XRD traces, the polyester nanocomposites with 1-5 wt.% bentonite clay showed no peak in the angular range of the study. The disappearance of [001] basal peak of clay in the nanocomposites may implicate homogeneous exfoliation and random dispersion of



**Fig. 4.9:** XRD diffractograms for (a) PANC5, (b) PANC2.5, (c) PANC1, (d) acrylate modified HBPE and (e) OMMT

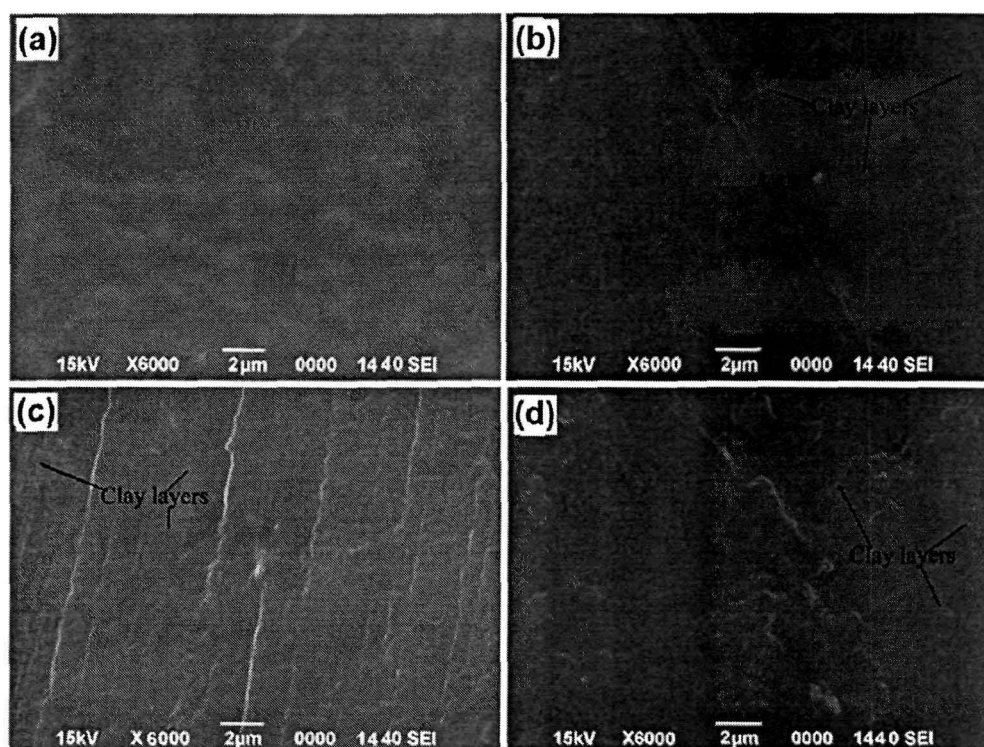
**Fig. 4.10:** XRD diffractograms for (a) water dispersible HBPE (b) WBPENC1, (c) WBPENC2.5, (d) WBPENC5 and (e) bentonite

aluminosilicate layers of clay in the polyester matrix. Thus delaminated structure of clay may be formed in the nanocomposites. In the pristine highly branched polyester resin a broad peak at  $20^\circ$  was also observed, which is due to the amorphous nature of the highly branched polyester resin.

#### 4.3.2.3. SEM Study

To validate the morphology of HBPE, LPE, PE, HBPE/epoxy blend, water dispersible HBPE and acrylate modified HBPE based nanocomposites, the nanoclay dispersion was observed from SEM micrographs which provides direct visualization of the morphology of the surface of nanocomposites films.

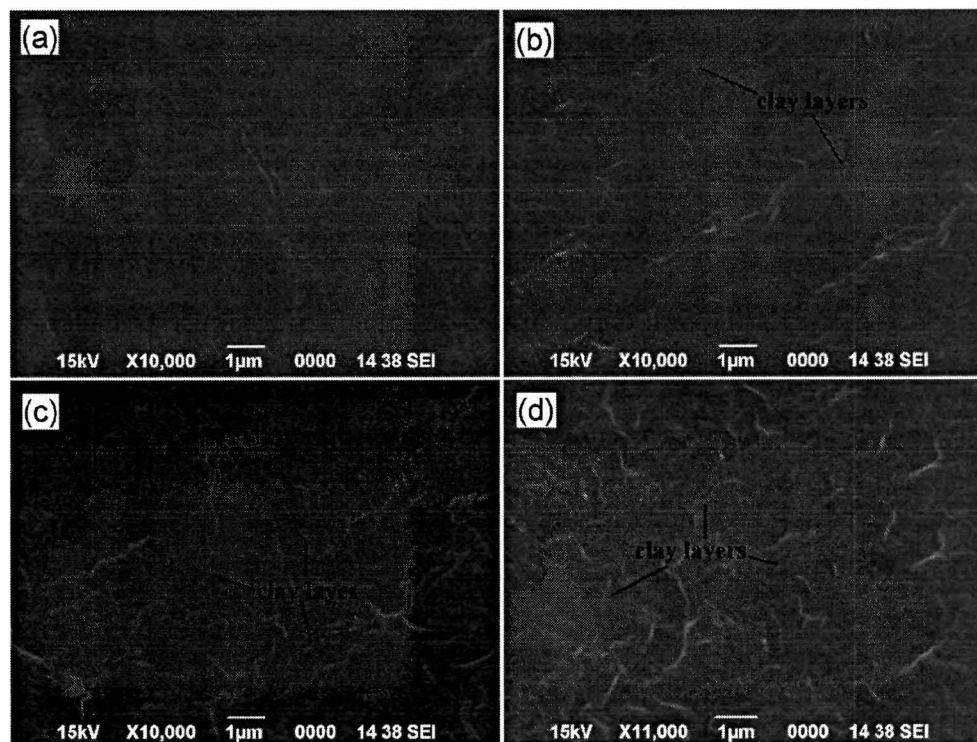
Fig. 4.11 shows SEM micrographs, where the surface for pure HBPE was smooth but rough surfaces with expanding layers or lines of clay layers for the nanocomposites were observed. This indicates the clay layers intercalated by the polymer matrix and certain amount of toughness has been induced in the matrix due to the incorporation of organoclay.



**Fig. 4.11:** SEM micrographs for (a) HBPE, (b) PENC1, (c) PENC2.5 and (d) PENC5

SEM micrographs (Fig 4.12) of the LPE nanocomposites with 0-5 wt.% OMMT showed the well distribution and dispersion of the OMMT layers throughout the polyester matrix. Uniform distribution of OMMT layers or lines with smooth surface

was observed in all the nanocomposites. Thus the results indicate that the clay layers are well-dispersed and embedded in the polyester matrix. This homogeneous distribution of the nanoclay is due to the interaction of the -OH groups of nanoclay with the ester groups of polyester through H-bonding or other polar-polar interaction (Scheme 4.1). With the increase of clay loadings, the well-dispersed layers also increase in the matrix.



**Fig. 4.12:** SEM micrographs for (a) LPE, (b) LPENC1, (c) LPENC2.5 and (d) LPENC5

In the SEM micrographs (Fig 4.13) of PE nanocomposites, wire like structures were observed which is due to OMMT layers. This OMMT layers were uniformly distributed throughout the polyester matrix in all the nanocomposites (1-5 wt.%). With the increase of OMMT loading these layers were also found to increase. This homogeneous distribution of the OMMT is attributed to the interaction of the -OH groups of OMMT with the ester groups of polyester through H-bonding or other polar-polar interactions. As the OMMT loadings increased the well-dispersed layers also increased in the matrix.

The uniform distribution of clay layers or lines with smooth surface was observed in the SEM micrographs of HBPE/epoxy blend based nanocomposites (Fig. 4.14).

This indicates that clay layers are well-dispersed and embedded in the matrix. With the increase of clay loadings, the well dispersed layers or lines also increase in the matrix.

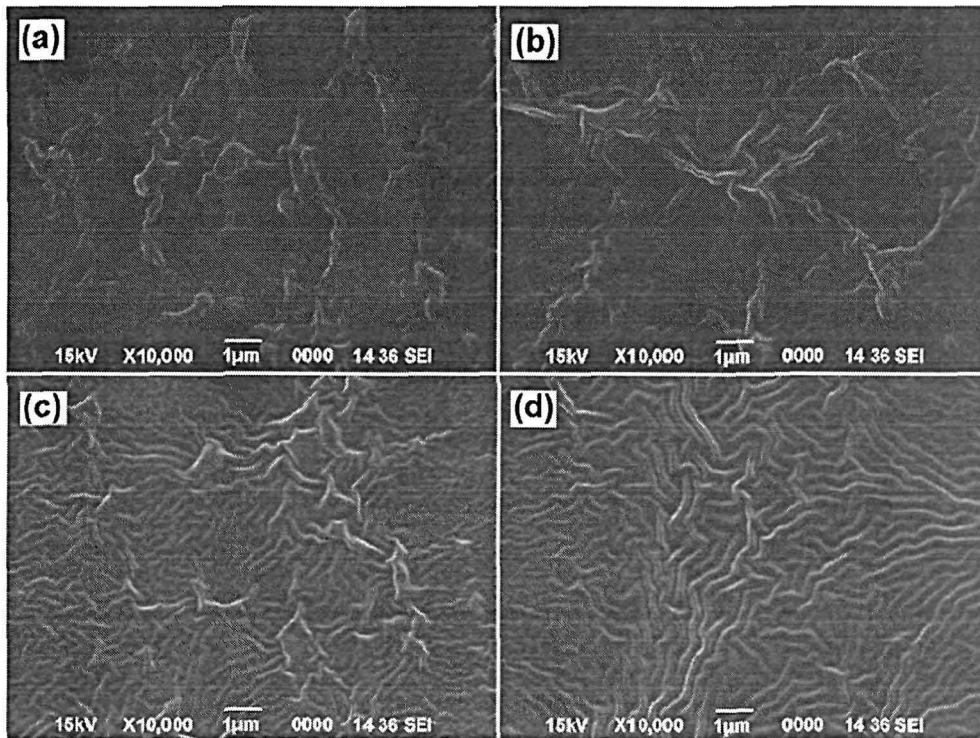


Fig. 4.13: SEM micrographs for (a) PE, (b) PNC1, (c) PNC2.5 and (d) PNC5

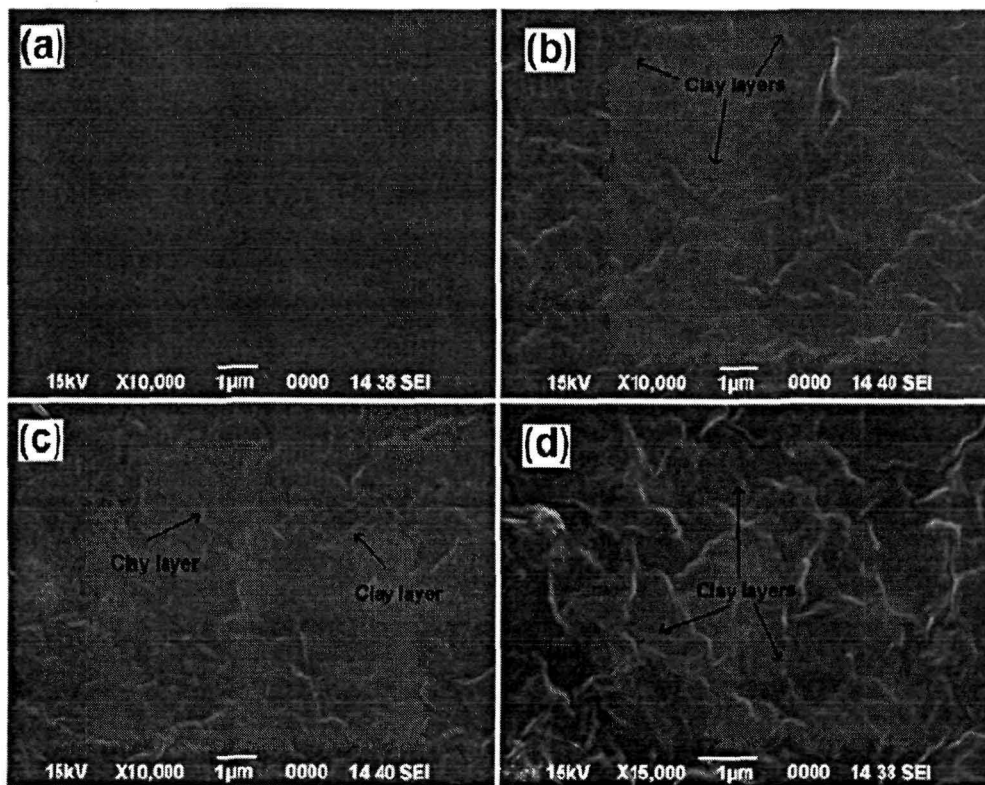
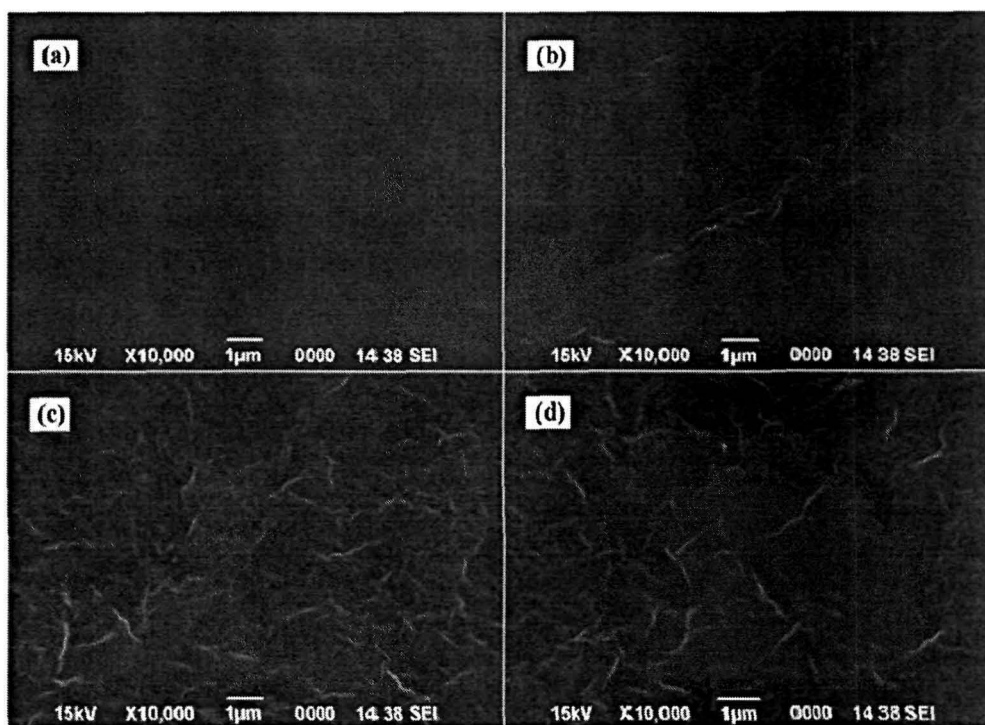


Fig. 4.14: SEM micrographs for (a) PEB1, (b) BNC1, (c) BNC2.5 and (d) BNC5



Fig. 4.15 shows SEM micrographs for the water dispersible HBPE nanocomposites, where smooth surface with expanding layers or lines with systematic pattern or uniform distribution of clay layers in the surface were observed. This indicates that clay layers are well-dispersed and embedded in the polymer matrix. As clay loading increases, the number of clay layers or lines also increases in the nanocomposites.



*Fig. 4.15: SEM micrographs for (a) water dispersible HBPE, (b) WBPENC1, (c) WBPENC2.5 and (d) WBPENC5*

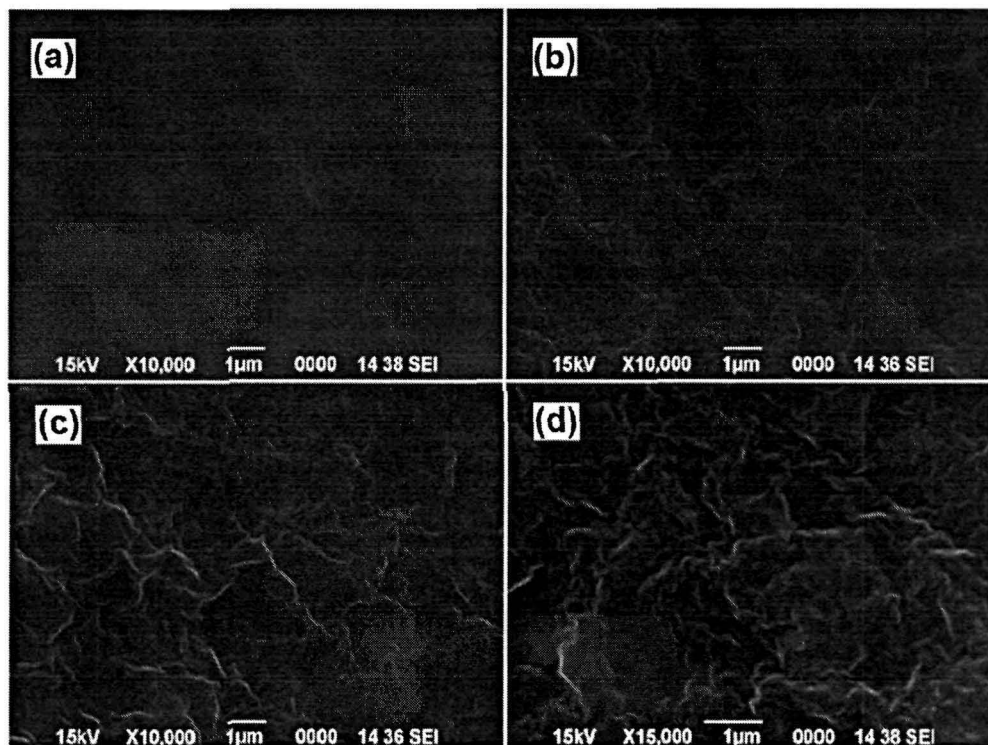
The uniform distribution and well-dispersion of clay layers throughout the polyester matrix was observed from the SEM micrographs (Fig. 4.16) of the acrylate modified HBPE nanocomposite samples with 0-5 wt.% OMMT. This homogeneous distribution of the nanoclay is due to the interaction of the -OH groups of nanoclay with the ester groups of polyester through H-bonding or other secondary polar-polar interactions. The dispersed layers or lines increased in the matrix with the increase of clay loadings in the nanocomposites.

#### 4.3.2.4. TEM Study

To understand the actual pattern of nanoclay layers dispersion and to evaluate visually



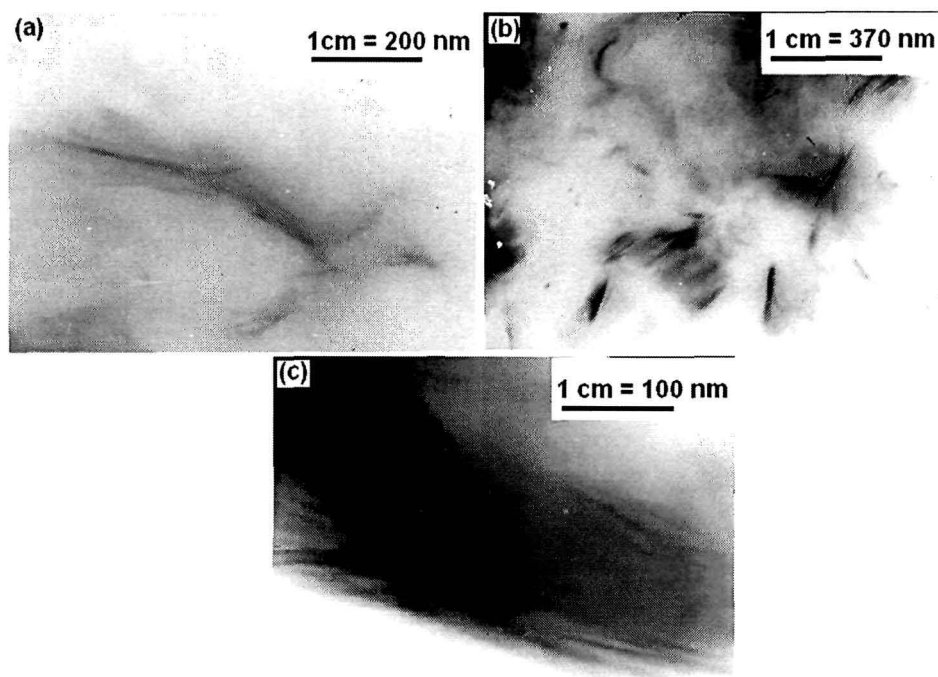
the degree of intercalation, exfoliation and aggregation of the clay clusters and confirm the XRD results in the polymer matrix, TEM micrographs of the nanocomposites were



*Fig. 4.16: SEM micrographs for (a) acrylate modified HBPE, (b) PAN1, (c) PAN2.5 and (d) PAN5*

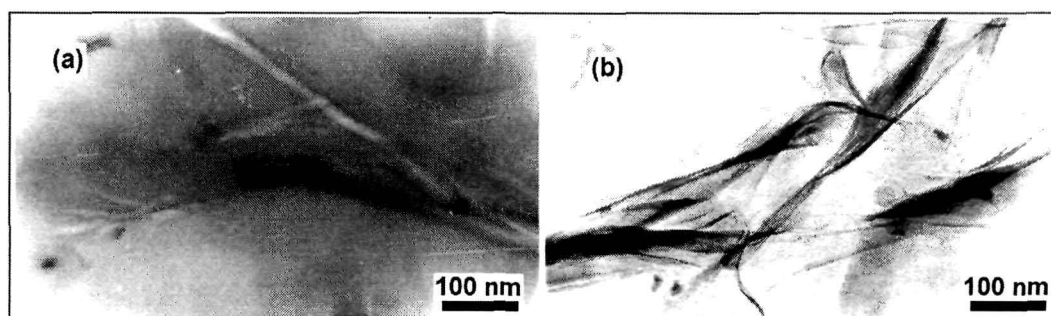
recorded. It has been reported in the literature that raising the nanoclay loading, enhances the ordering of nanoclay platelets, and gradually enervates the exfoliation potential of nanoclay by the polymer. It is ascribed to the increased viscosity that impedes the ease of melt flow and causes stabilization of the flow, hindering the complex flow patterns and agitation necessary to break apart the tactoids. Moreover, in high loadings of organoclay, silicate-silicate interactions, which impede dispersion of the nanoclay layers, become more probable. Representative TEM micrographs of the HBPE, LPE, PE, HBPE/epoxy blend, water dispersible HBPE and acrylate modified HBPE nanocomposites are shown in Fig. 4.17, 4.18, 4.19, 4.20, 4.21 and 4.22 respectively.

The dispersed nanoclay platelets with average layer thickness of 30-40 nm was observed in the TEM micrographs of the HBPE nanocomposites (Fig. 4.17). The clay layers were found to be disintegrated and partially exfoliated by the different components present in the matrix. The TEM micrographs of LPE nanocomposites (Fig. 4.18) showed homogeneous dispersion and a dominant exfoliated structure with clay

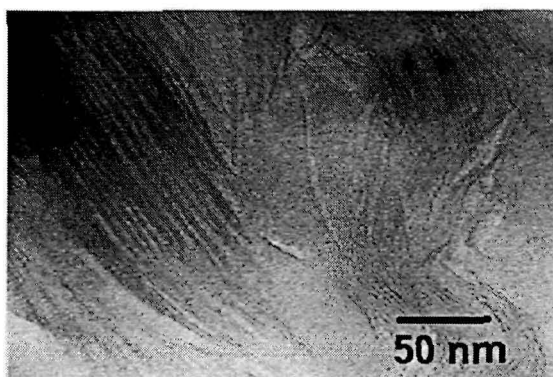


**Fig. 4.17:** TEM micrographs for (a) PENC1, (b) PENC2.5 and (c) PENC5

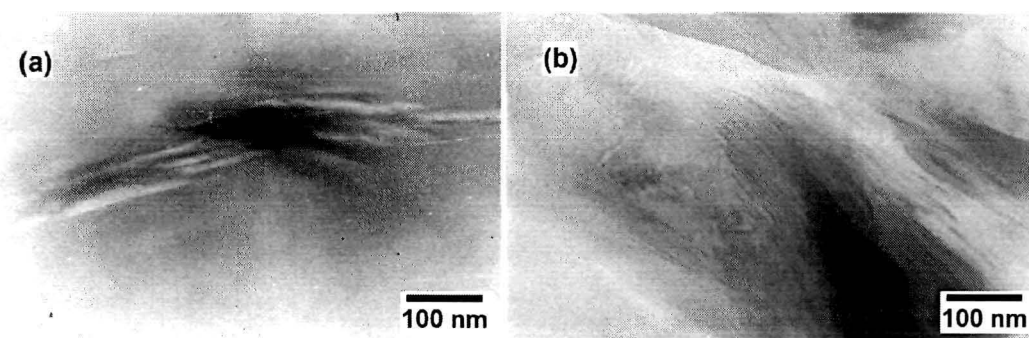
platelets having average thickness in the range of 20-25 nm in the vicinity of the clay boundaries, supporting XRD findings. Representative TEM micrograph (Fig. 4.19) of the PE nanocomposite (PNC2.5) also showed homogeneous dispersion and an exfoliated structure which supported the XRD results. Homogeneous dispersion of clay platelets with average thickness in the range of 25-30 nm was observed in the TEM micrographs (Fig. 4.20) of the HBPE/epoxy blend nanocomposites. Homogeneous dispersion of clay platelets with average thickness in the range of 15-25 nm and several nm in length were observed in the TEM micrographs (Fig. 4.21) of water dispersible HBPE nanocomposites. The representative TEM micrograph of acrylate modified HBPE nanocomposite showed homogeneous dispersion and a partial exfoliation of clay layers by the polymer chains (Fig. 4.22). The average thickness of the OMMT layers was found in the range of 12-20 nm in the TEM micrographs.



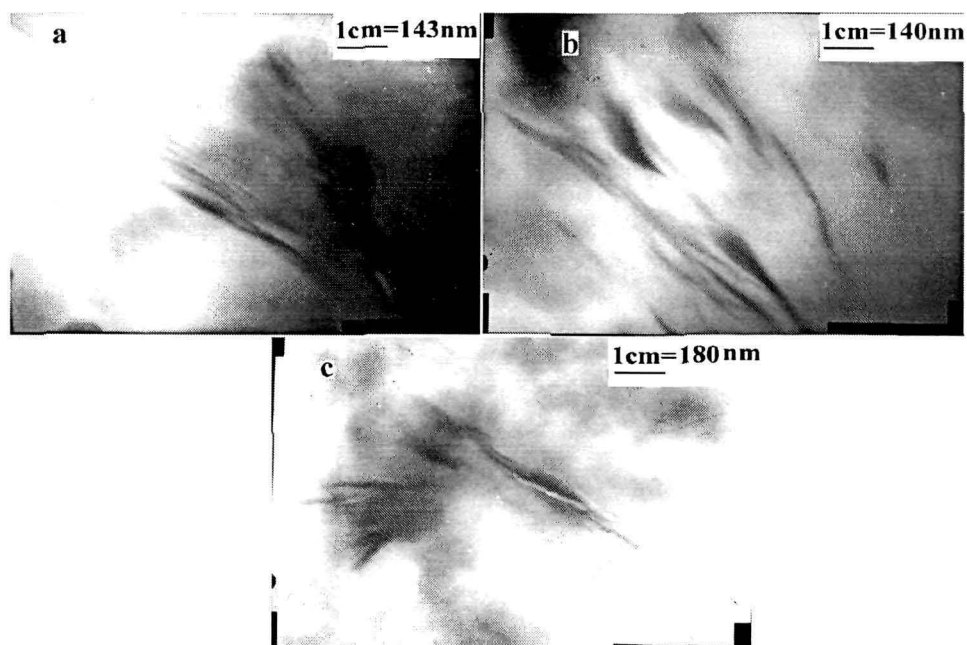
**Fig. 4.18:** TEM micrographs for (a) LPENC1 and (b) LPENC2.5



**Fig. 4.19:** Representative TEM micrograph for PE nanocomposite (PNC2.5)



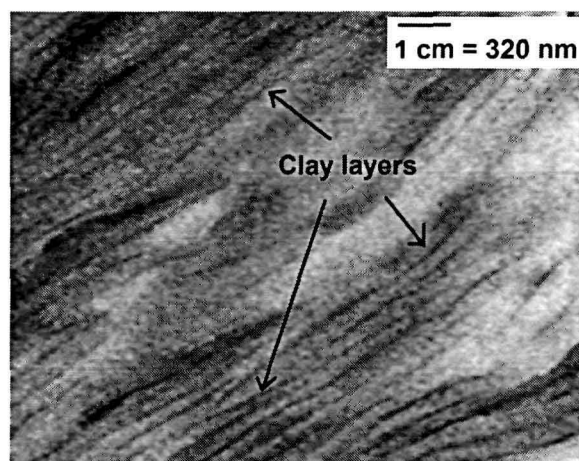
**Fig. 4.20:** TEM micrographs for (a) BNC1 and (b) BNC2.5



**Fig. 4.21:** TEM micrographs for (a) WBPENC1, (b) WBPENC2.5 and (c) WBPENC5

After the formation of nanocomposites, the individual nanoclay layers were found to be disintegrated or partially exfoliated and well-dispersed in the polymer matrix for all the cases. Also the individual clay layers as well as zones with more than one clay layer can be notable in the TEM micrographs. The probable reason for this

excellent distribution is the strong interactions between the polar carboxylic ester groups of the polyesters and the -OH group of nanoclay and hydrophilic character of both the components. Also the highly branched, globular, high surface functionality of the HBPE helps in this strong interactions. The parallel dark lines that were seen are the edges of the clay layers. Since the discrete clay layers were observed so, the exhibited morphology can be classified as exfoliated.



*Fig. 4.22: Representative TEM micrograph for acrylate modified HBPE nanocomposite (PANC2.5)*

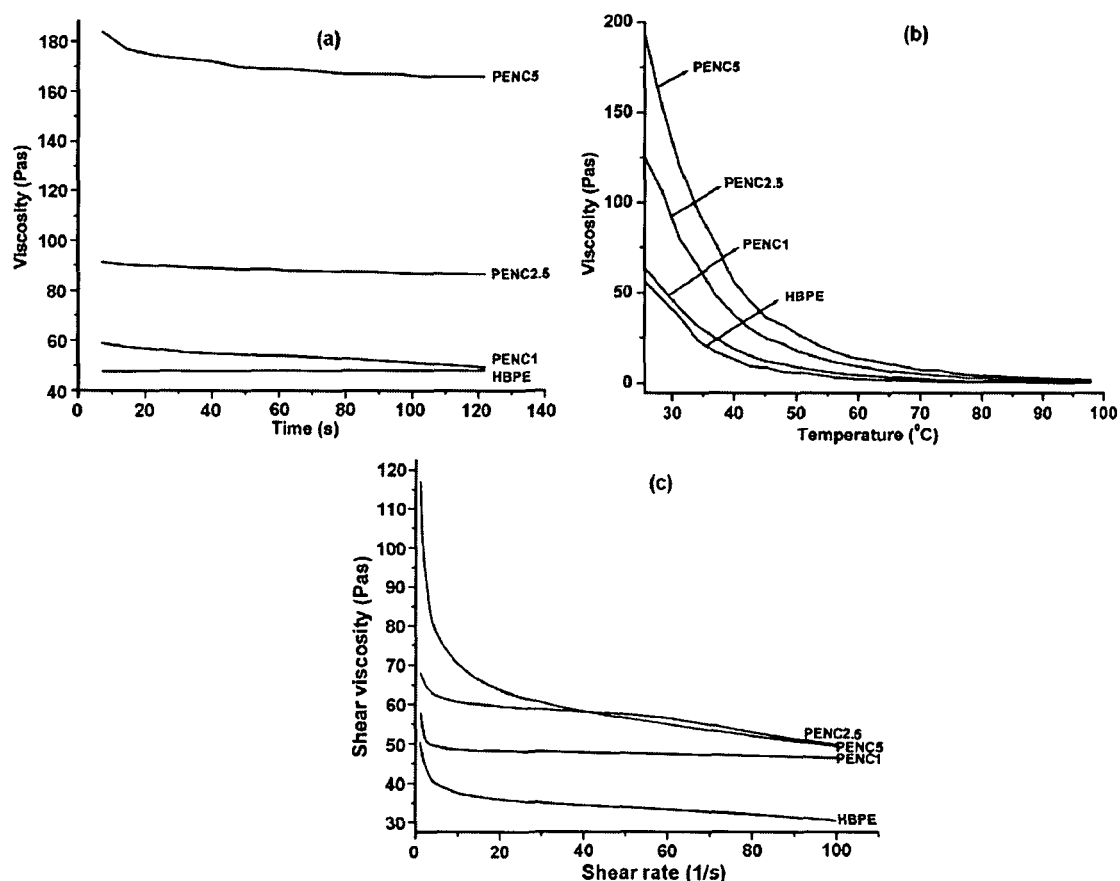
#### **4.3.3. Rheological Behaviors**

Rheological experiments were conducted on a controlled strain rheometer equipped with parallel plate geometry. Oscillatory measurements were performed to compare the rheological behavior of the pristine polyester resins to their nanocomposites.

The variation of viscosity with time at controlled stress and single shear value for HBPE nanocomposites is shown in Fig. 4.23(a), where viscosity remains almost constant with time. However, an overall increase in viscosity of all the nanocomposites was observed with the increase of clay loadings. The melt flow behavior of HBPE nanocomposites was determined by the variation of shear viscosities as a function of temperature in the range of 25-100 °C at shear stress of 70 Pa. [Fig. 4.23(b)]. From this figure it was observed that viscosity decreases with temperature in all the nanocomposite systems. Fig. 4.23(c) shows the shear viscosity as a function of shear rate for the HBPE and its nanocomposites. The shear viscosity of the nanocomposite systems decreased with increasing shear rate showing shear thinning behavior. The shear viscosity also increased substantially with OMMT content over a broad range of shear rates. At low shear rates, the shear viscosity data exhibited a non-Newtonian

plateau of all the HBPE nanocomposites systems. With the increase of shear rate, the HBPE nanocomposites exhibited higher degrees of shear-thinning behavior compared to the pure HBPE.

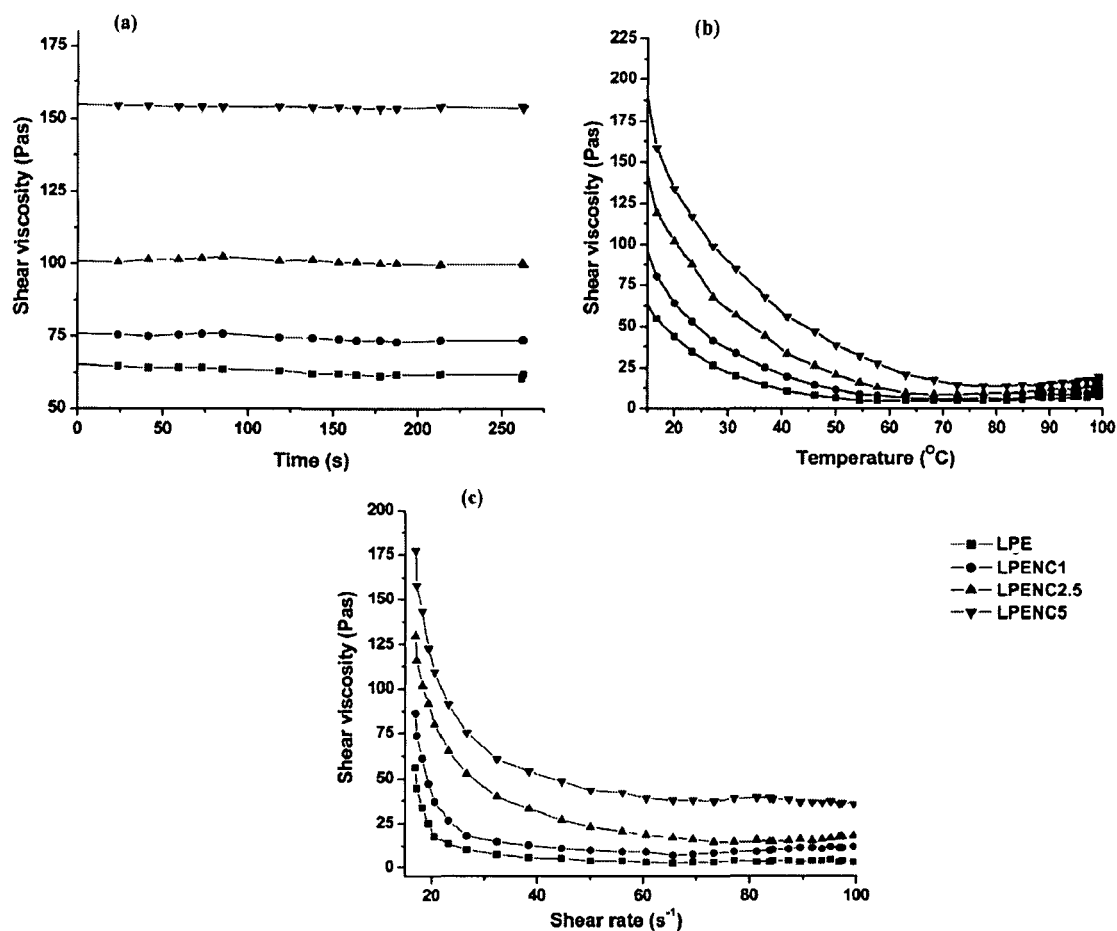
The shear viscosity of all the LPE nanocomposites remained almost constant with time [Fig. 4.24(a)] as measured at controlled stress and single shear value. The overall viscosities of the all the nanocomposite systems were higher than that of the pristine system and increase with clay loading (0-5 wt.%). The shear viscosity in all the LPE nanocomposite systems [Fig. 4.24(b)] was found to decrease with the increase of temperature. The dependence of steady shear viscosity on shear rate for the nanocomposites is shown in Fig. 4.24(c). The shear viscosity of the nanocomposites with 2.5 and 5 wt.% loadings showed significantly higher zero-shear viscosities and an earlier onset of shear thinning compared to that of the unfilled matrix.



*Fig. 4.23: Rheological behaviors of HBPE nanocomposite*

Fig. 4.25(a) showed the effect of time on shear viscosity of all the PE nanocomposites. The shear viscosity remained almost constant with time. The overall viscosities of all nanocomposites were higher than that of the pristine polyester. With

the increases of OMMT loading (0-5 wt.%) the shear viscosity increases. The behavior of shear viscosity with temperature of the pristine polyester and its nanocomposites is shown in Fig. 4.25(b). The shear viscosity decreased with the increase of temperature. The dependence of steady shear viscosity on shear rate for the polyester nanocomposites is shown in Fig. 4.25(c). The shear viscosity of the nanocomposites with 0-5 wt.% loadings showed significantly higher shear viscosities than the pure polyester system.



*Fig. 4.24: Rheological behaviors of LPE nanocomposites*

The shear viscosity of all the water dispersible HBPE nanocomposites slightly decreases with time [Fig. 4.26(a)] as measured at controlled stress and single shear value. This slight decrease may be due to the alignment of clay layers in the direction of flow. However with the increase of amount of the loading (0-5 wt.%) of clay, an overall increase in shear viscosity was noticed for all the nanocomposites. The shear viscosity in all the nanocomposite systems [Fig. 4.26(b)] was found to decrease with temperature. Shear thinning behavior [Fig. 4.26(c)] was observed for all the

nanocomposites where the shear viscosity decreases with the increase of shear rate. The shear viscosity also increased substantially with clay content over a broad range of shear rates. At low shear rates, the shear viscosity data demonstrated a strong pseudo-plastic behavior (non-Newtonian flow) of all the nanocomposites systems, which is characterized by a progressive decline in viscosity as shear rate increases.<sup>28</sup> Above a certain value of shear rate flow curve becomes linear. With the increase of shear rate, the nanocomposites exhibited higher degrees of shear-thinning behavior compared to the pristine polymer.

Fig. 4.27(a) showed the effect of time on the shear viscosity for all the acrylate modified HBPE nanocomposites measured at controlled stress and single shear value. The shear viscosity was found almost constant with time for all the nanocomposites. However, the overall viscosity of the nanocomposites was increased with clay loading (0-5 wt.%) than pristine matrix system. The shear viscosity in all the nanocomposite systems [Fig. 4.27(b)] was found to decrease with temperature. Fig. 4.27(c) showed the dependence of shear viscosity on the shear rate for the nanocomposites. The shear

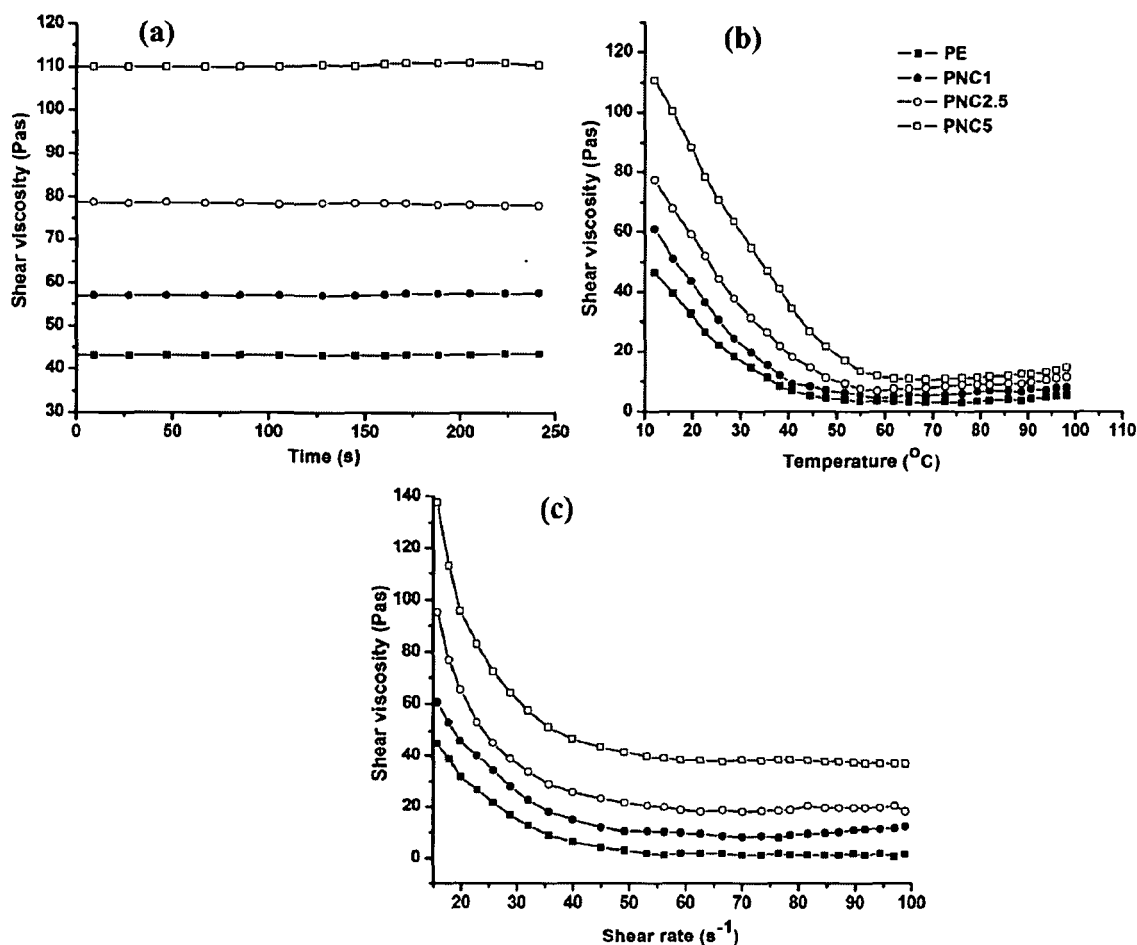
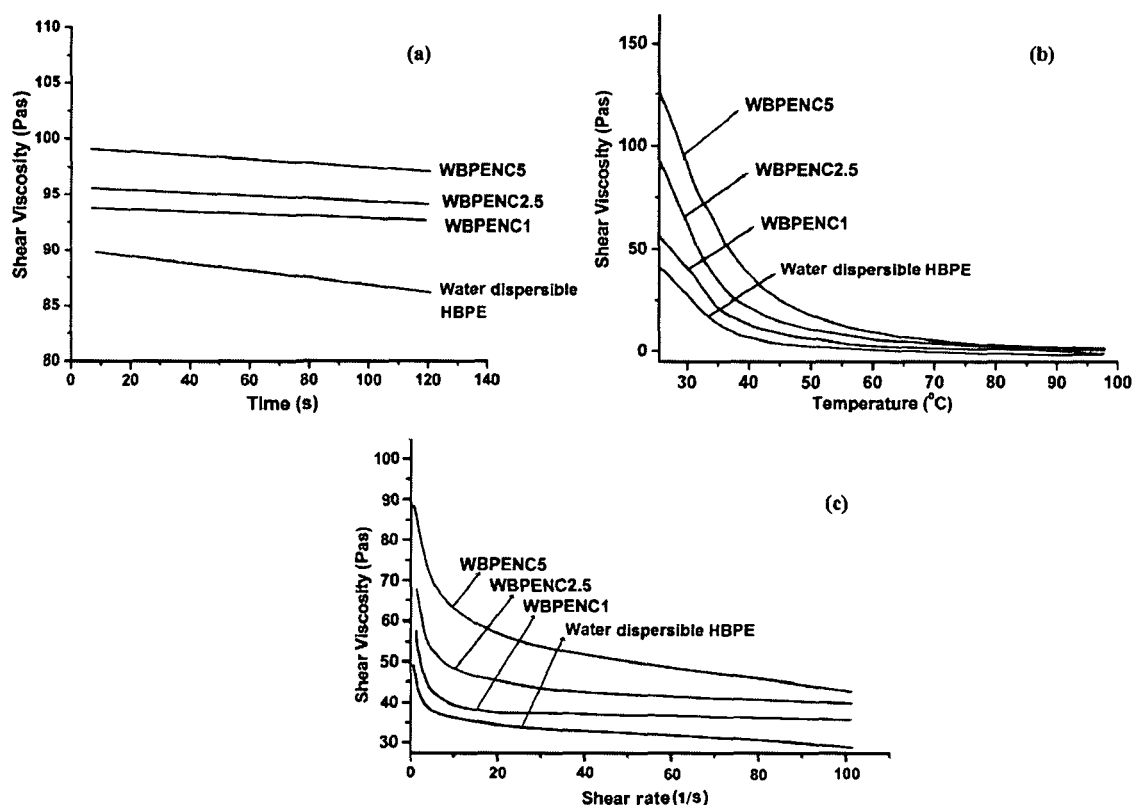


Fig. 4.25: Rheological behaviors of PE nanocomposites

viscosity of the nanocomposites with 0-5 wt.% loadings showed significantly higher zero-shear viscosities and shear thinning compared to that of the pristine system. At low shear rates, the network of dispersed clay layers remains unaffected by the imposed flow. At high shear rates the clay platelets align in parallel and become oriented in the flow direction, contributing to shear thinning behavior of the nanocomposites.<sup>31,32</sup> This alignment of the clay layers causes the viscosity to decrease and approach to that of the pure polyester. At low shear rate, the nanocomposites systems exhibited non-Newtonian flow, which is characterized by a progressive decline in viscosity as shear rate increases.<sup>28</sup> Above a certain value of shear rate flow curve becomes linear.



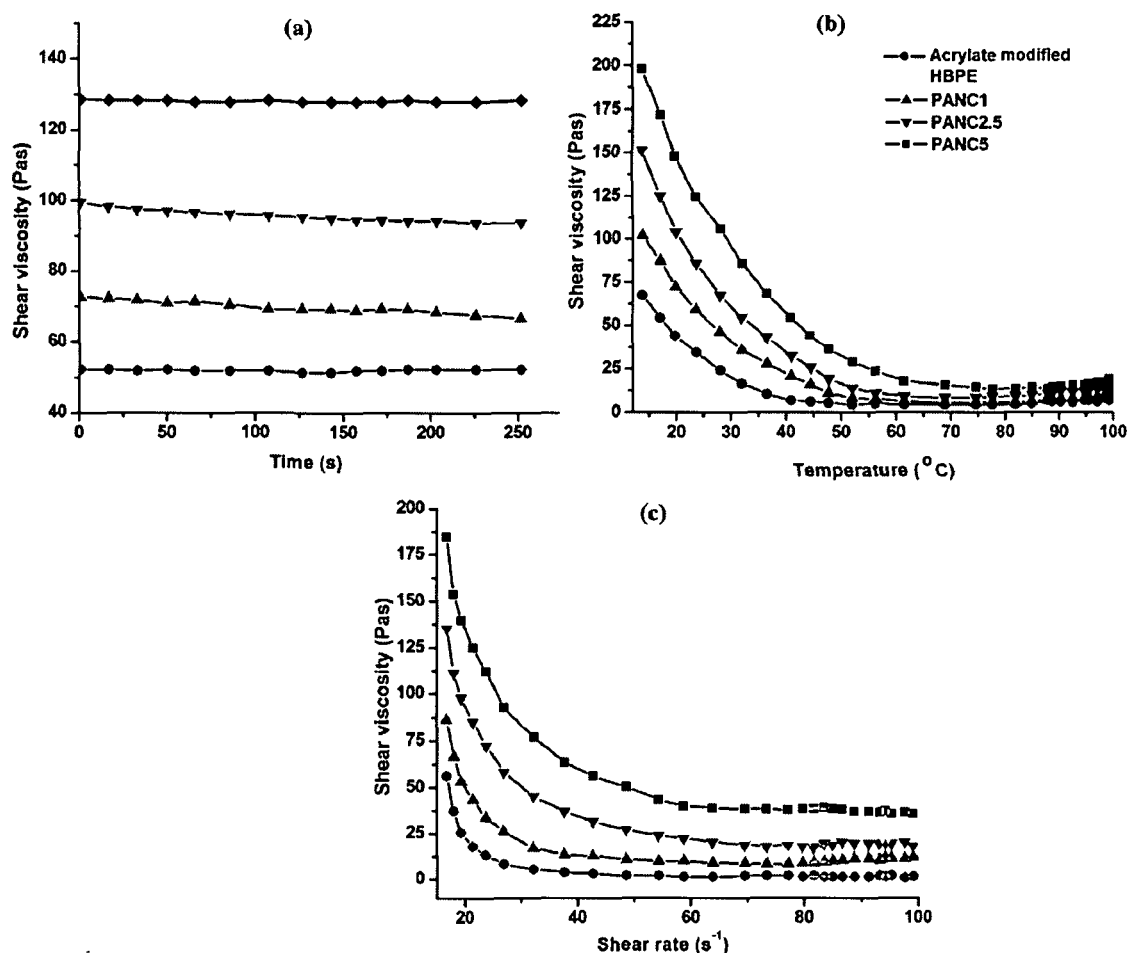
**Fig. 4.26:** Rheological behaviors of water dispersible HBPE nanocomposites

The increased viscosity of all the nanocomposites with nanoclay loading is attributed to increase in interaction level that result in increase in effective clay content and less number of polymer segments participating in the bulk flow process. Also the polyester chain molecules intercalate/partially exfoliate into the OMMT interlayer and high level of interaction occurs between the -OH groups of the clay with the polymer chains. Again due to exfoliation, a high exposed clay surface is generated which resulted high interaction between the polymer chains and clay as a consequence this partially arrests the segmental movements of the pristine polymer. As the clay loadings



increase more and more polymer chains diffused into the relative empty gallery of the silicate and as an outcome the viscosity of the nanocomposites system gradually increased.

The decreased in viscosity of all the nanocomposites with temperature is due to the decreased in intermolecular H-bonding between the clay and the polyester segments, and increased kinetic energy of the molecules present in the nanocomposites.



**Fig. 4.27:** Rheological behaviors of acrylate modified HBPE nanocomposites

Usually the polymers with high molecular weights have a tendency to entangle with their neighboring macromolecules in their three dimensional network at low shear rates. But during the shear process, the molecules are usually oriented in the shear direction by entangling to a certain extent which decrease in their flow resistance. This behavior is attributed to the physical jamming or percolation of randomly distributed silicate layers.<sup>33</sup> The OMMT layers, especially the intercalated or exfoliated ones could support this orientation by alignment of their rigid crystalline lamellar structure towards the direction of flow at high shear rates as similarly reported by other researchers.<sup>34,35</sup>

The high shear viscosity is attributed to the strong interaction between dispersed OMMT layers and polymer chains at low shear rate. Also, the interaction between OMMT layers becomes stronger at higher OMMT contents as the distance between layers becomes smaller. As a consequence, the restricted local environment of the OMMT layers limits the ability of the polymer chains to relax. The high zero-shear viscosities of nanocomposites indicate that at low shear rates the nanostructure of these materials consists of a strong interaction between dispersed clay layers and polymer chains. At lower shear rates, the network of dispersed clay layers remains unaffected by the imposed flow. The high shear rates or prolonged action of slow shear forces result collapse in the network structure that cause a break down in network structure and the platelets do increasingly align in parallel. This results the orientation of the OMMT silicate layers in the flow direction, and contributes shear thinning behavior in the nanocomposites. This alignment of the clay layers causes the viscosity to decrease and approach to that of the virgin polyester. The shear viscosity also increased substantially with clay content over a broad range of shear rates. At low rates of shear, such systems exhibit non-Newtonian flow, which is characterized by a progressive decline in viscosity as shear rate increases.<sup>28</sup> Above a certain value of shear rate flow curve becomes linear. Nevertheless, because of this shear thinning property, the nanocomposites can be processed in the melt state using the conventional equipment available in a manufacturing line. Also pronounced shear thinning has been found to be a characteristic feature of truly nano dispersed composites.

Although the exact mechanism that causes the shear thinning behavior is not very clear, but it can be deduced that the orientation of the silicate layers under shear is the main cause. With the increase of shear rate, the preferential orientation/alignment of the silicate layers and the intercalated chain conformations change as the coils align parallel to the flow.<sup>32</sup> This shear thinning of the materials is an added advantage in application of the coating during spray or brushing and eliminates or minimizes the sagging problem.

#### ***4.3.4. Curing Studies of the Nanocomposites***

Non-drying oil based polyester resin requires long time for hard drying due to the slow crosslinking reaction which occurs through radical reaction by absorbing oxygen from the atmosphere. The drying time of the polyester resin improved significantly by using

epoxy resin and poly(amido amine) hardener as curing agents. This is due to high curing rate of epoxy resin by the hardener and the crosslinking reactions between hydroxyl/epoxide of epoxy resin and amine groups of the hardener with the hydroxyl/ester groups of polyester resin.<sup>36</sup> In the HBPE nanocomposites the cure rate was enhanced with the increase of OMMT loading (Table 4.1). This is ascribed to the restricted mobility of the polymer segments. The OMMT interacts with the polymer chains due to its high surface area and restricts the mobility of the molecular chains, and takes part in the crosslinking reactions via interactions through H-bonding between -OH group of OMMT/polyester with the -OH of epoxy resin as well as -NH of amine hardener (Scheme 4.1). As a result, cure rate of polyester nanocomposites increased with the OMMT loading compared to the pristine resin. Also the alkyl ammonium ions present in the OMMT are most probably responsible for the catalytic acceleration of the curing reaction, which enhances the curing rate.

Again, the curing mechanism associated with the oil modified water dispersible HBPE and MF resins is a complex phenomenon due to the presence of a large number of functionalities such as -OH, -OR, -COOR, -COOH, >NH, -NH<sub>2</sub> etc. in the system. Thus a variety of reactions are possibly occurred between these two resins. The principal reaction occurs during the curing process between the alkoxyethyl or methylol group of amino resin and hydroxyl group of polyester resin, leads to form ether linkages.<sup>37</sup> The cure rate of water dispersible HBPE nanocomposites increased with the increase of nanoclay (bentonite) loading. This increase is ascribed to the restricted mobility of the polymer segments along with the favorable rheological properties, which helps well-dispersion of nanoclay and other components present in the nanocomposite systems. This homogenization of the components helps to strong interactions and thereby increased the rate of cross-linking reaction. The nanoclay interacts with the polymer chains due to its high surface area and restricts the mobility of the molecular chains. The -OH groups of nanoclay layers also participate in the crosslinking reaction via interaction through H-bonding between -OH group polyester and -OH and / or >N-H group of MF resin (Scheme 4.3).

#### ***4.3.5. Performance Characteristics of the Nanocomposites***

The performance characteristics like tensile strength, elongation at break, gloss, impact resistance and scratch hardness of the cured HBPE, LPE, PE, HBPE/epoxy blend,

water dispersible HBPE, acrylate modified HBPE nanocomposites films are shown in Table 4.1, 4.2, 4.3, 4.4, 4.5 and 4.6 respectively.

Although for the most of the polymer systems increase of material tensile strength resulted in decrease of tensile elongation at break (%). However, it was found that both the tensile strength as well as the elongation at break (%) values of HBPE nanocomposites improves to a noticeable degree with the addition of OMMT (Table 4.1). The tensile strength of nanocomposites increased from 2.68 to 7.11 N/mm<sup>2</sup>, whereas the elongation at break (%) changed from 24 to 145% with the increase of OMMT content from 0 to 2.5 wt.%. However, further addition of OMMT i.e. at 5 wt.% the properties decreased. The improvement in tensile strength as well as the elongation at break (%) of the nanocomposites indicates that the HBPE was strengthening by the incorporation of homogeneously dispersed OMMT. The delamination of the aluminosilicate layers of OMMT offers the maximum surface of the silicate layers for strong interaction through H-bonding with the polymer chains. This strong interfacial interaction between polymer chains and nano-level dispersed layers of OMMT forms shear zones when the nanocomposites are under stress and strain.<sup>38</sup> This interaction contributes to the increase in tensile strength and elongation at break of the nanocomposites. Further, increase of crosslinking density (Table 4.1) as supported by swelling with the increase of clay loading enhances tensile strength. However, when relatively high OMMT content (5 wt.%) was used, more and more OMMT aggregates instead of being delaminated, which results in a deterioration of the mechanical properties.

**Table 4.1:** Performance characteristics of HBPE and its nanocomposites

Property	HBPE	PENC1	PENC2.5	PENC5
Gloss at 60°	98	102	105	92.2
Scratch Hardness (kg)	7	9	10	8.7
Impact hardness (cm)	80	90	95	90
Tensile stress (N/mm <sup>2</sup> )	2.68	4.91	7.11	5.82
Elongation at break (%)	24	99	145	140
Curing time (h at 120 °C)	3	2.5	2	2
Swelling (%) in xylene	34.2	32	30.1	31.4

**Table 4.2:** Performance characteristics of LPE and its nanocomposites

Property	LPE	LPENC1	LPENC2.5	LPENC5
Gloss at 60°	78	80	85	97
Scratch hardness (kg)	6	6.4	7.2	8
Impact resistance (cm)	55	62	70	85
Tensile strength (N/mm <sup>2</sup> )	5.66	8.11	10.07	12.04
Elongation at break (%)	31.7	39.4	52.3	64.1
Curing time (h at 120 °C)	4	3.5	3	2.5
Swelling (%) in xylene	36.22	33.5	28.5	25

**Table 4.3:** Performance characteristics of PE and its nanocomposites

Property	PE	PNC1	PNC2.5	PNC5
Gloss at 60°	83	93	96	98
Scratch hardness (kg)	8	8.5	10	10
Impact resistance (cm)	>100	>100	>100	>100
Tensile strength (N/mm <sup>2</sup> )	5.46	7.87	8.99	11.18
Elongation at break (%)	102.21	89.4	57.05	47.75
Curing time (min at 120 °C)	80	60	50	45
Swelling (%) in xylene	35.26	33.16	32	30.5

The tensile strength of the LPE nanocomposites (Table 4.2) was enhanced to a noticeable degree from 5.66 to 12.04 N/mm<sup>2</sup> with the increase of OMMT loading from 0 to 5 wt.%. With the addition of OMMT, surprisingly even the elongation at break (%) of the nanocomposites was also increased to a certain extent from 31.67 to 64.04%. An improvement in tensile strength value of 5.72 N/mm<sup>2</sup> was found in the PE nanocomposite (PNC5) compared to the pristine polyester (Table 4.3). However, the elongation at break (%) of the nanocomposites was decreased from 102.21 to 47.75% with the increases of OMMT loadings from 0 to 5 wt.%. This is due to the restricted motion of the polymer chains by the OMMT layers. In the HBPE/epoxy blend based nanocomposites (Table 4.4) the tensile strength showed an increase in trend to a noticeable degree from 2.7 to 6.42 N/mm<sup>2</sup> with the increase of OMMT loading from 0 to 5 wt.%. The addition of vegetable oil based epoxy resin increased the flexibility of the blends as observed experimentally as enhanced elongation at break (%) with

OMMT loading. The addition of OMMT enhanced the blends flexibility and hence increased the ductility.

**Table 4.4:** Performance characteristics of the HBPE/epoxy blend and its nanocomposites

Property	PEB1	BNC1	BNC2.5	BNC5
Gloss at 60°	82	90	95	103
Scratch hardness (kg)	5	5.5	7	8
Impact resistance (cm)	65	75	80	84
Tensile strength (N/mm <sup>2</sup> )	2.7	3.26	4.92	6.42
Elongation at break (%)	52	79	104	137
Curing time (min at 120 °C)	80	75	60	50

The tensile strength of water dispersible HBPE nanocomposites (Table 4.5) was found to enhance to a noticeable degree from 1.96 to 6.98 N/mm<sup>2</sup> with the increase of nanoclay (bentonite) loading from 0 to 5 wt.%. Surprisingly, it has been found that the elongation at break (%) of the nanocomposites increased with the nanoclay loading.

The tensile strength of the acrylate modified HBPE was enhanced after the formation of nanocomposite (Table 4.6). The PANCS film showed the best tensile strength among the nanocomposites with an increase in the tensile strength from 4.53 to 11.8 N/mm<sup>2</sup> compared to the acrylate modified HBPE matrix. With the addition of OMMT the elongation at break (%) of the nanocomposites increased upto a certain loading and then further decreased with higher loading of OMMT.

**Table 4.5:** Performance characteristics of water dispersible HBPE and its nanocomposite

Property	Water dispersible	WBPE	WBPE	WBPE
	HBPE	NC1	NC2.5	NC5
Gloss at 60°	39	48	55	60
Scratch hardness (kg)	3.7	4	4.3	6
Impact resistance (cm)	40	50	55	70
Tensile stress (N/mm <sup>2</sup> )	1.96	2.42	4.70	6.28
Elongation at break (%)	51.3	64.3	96.9	122.5
Curing time (min at 140 °C)	90	60	50	45
Surface blister	None	None	None	None

**Table 4.6:** Performance characteristics of acrylate modified HBPE and its nanocomposites

Property	Acrylate modified HBPE	PANC1	PANC2.5	PANC5
Gloss at 60°	70	72	76	82
Scratch hardness (kg)	4	4.6	5	6
Impact resistance (cm)	55	60	68	70
Tensile strength (N/mm <sup>2</sup> )	4.53	5.74	6.89	11.8
Elongation at break (%)	47	62.5	31.7	26
Curing time (h at 150 °C)	5.5	5	4.5	4.17
Swelling (%) in xylene	32.6	31.4	30	28.5

The improvement of tensile strength in all the above nanocomposites is attributed to the presence of immobilized or partially mobilized polymer phases as a consequence of interaction of polymer chains with organically modified clays. Further, the silicate layer as well as molecular orientation along the direction of tensile flow has radically contributed to the observed enhancement in tensile strength.<sup>39</sup> The nano dispersed clay with high aspect ratio has a large surface area available for adhesion between the polymer molecules and clay layers. They provide a high stress-bearing capability and efficiency to the reinforcing phase and contribute to the improved tensile strength. Stronger interactions between nanoclay layers and the polymer molecules associated with a larger contact surface result in effective constraint on the motion of the polymer chains.<sup>40</sup> With the increase of the amount of nanoclay, the number of available reinforcing elements increased due to dispersion of clay layers and it improves the load bearing capacity.

Elongation is a property influenced more seriously by chain breakage than chain slippage.<sup>41</sup> The increase of the elongation at break (%) with the increase of clay content is caused by the presence of long hydrocarbon chain of the fatty acid and the internal bond strength rather than crosslink density. With increasing OMMT content, the increase in the elongation at break (%) is mainly attributed in part to the plasticizing effect of the gallery oniums which contributes to the formation of dangling chains. It is also due to conformational effects at the polyester matrix/clay interface and the enhanced stress-bearing capability of the nanocomposites.

## Chapter 4

Gloss refers to specular reflection or the light reflected at the same angle as the angle of incidence. The gloss of the coated surface depends upon the amount of light absorbed or transmitted by the coating material that is influenced by the smoothness or texture of the surface. In HBPE nanocomposites the gloss value increases with the clay content as large amount of light is reflected from the smooth surface. But at higher loading (5 wt.%) the value decreases which may be due to agglomeration of clay particles in the matrix. The gloss values of the LPE, PE, HBPE/epoxy blend, water dispersible HBPE and acrylate modified HBPE nanocomposites were also increased with the increase of clay loading. The improvement of this gloss value reflects the better compatibility of all the components in the nanocomposites like polyester resin, epoxy resin with hardener along with the nanoclay etc. After the formation of nanocomposites as nanoclay loading increases better crosslinking of the cured films occurs. This leads to formation of smooth surface which augment the gloss value of the nanocomposites with nanoclay loading from 0-5 wt.%. Also with the increase of nanoclay content as large amount of light is reflected from the smooth surface, the gloss value increases (Table 4.6).

Scratch hardness arises from the resistance of the materials to the dynamical surface deformation, i.e. ploughing and from the interfacial friction between the indenter surface and the material. Scratch hardness represents the response of the material under serious dynamic surface deformation that involve highly localized strain field and materials failure in plastic and/or brittle manner depending upon the nature of the scratched materials. An increase in scratch hardness value of HBPE nanocomposites was found as compared to the pristine polyester. Uniformly distributed nano sized (30-40 nm layer thickness, Fig. 4.17) clay platelets effectively restrict indentation in the nanocomposites. Due to the presence of porosity in the nanocomposites no further improvement in hardness was noticed at high clay content (i.e. 5 wt.%). During the processing of nanocomposites at high clay contents, it was observed that the viscosity of the resin increases significantly. So, the entrapped air during shear mixing finds very difficult to escape out from the matrix system and vacuum was used before curing.

A significant improvement in scratch hardness was observed in the LPE, PE, HBPE/epoxy blend, water dispersible HBPE and acrylate modified HBPE nanocomposites reinforced with 0-5 wt.% organophilic nanoclay. With the inclusion of



nanoclay, the physical crosslink results an effective network formation. Consequently, uniformly disseminated nanoclay restricts the indentation and enhances the scratch hardness values in all the nanocomposites.

The impact resistance of the prepared HBPE nanocomposites increases as the amount of clay loading increases from 1 to 2.5 wt.% and slightly decreases for the organoclay content of 5 wt.%. However at high clay loading (5 wt.%) there may be agglomeration of clay particles in the matrix which results in deterioration of property. Addition of nanoclay with loadings from 0 to 5 wt.% significantly improved the impact resistance of the LPE polyester nanocomposites. The impact resistance of the PE nanocomposites was also improved significantly with the addition of OMMT. Again, in the blend based nanocomposites the value was observed to increase with the OMMT loading from 0-5 wt.%. The impact resistance of the prepared water dispersible HBPE nanocomposites was also found to increase as the amount of clay loading increases from 1 to 5 wt.%. Addition of 0-5 wt.% OMMT, significantly improved the impact resistance of the acrylate-modified polyester nanocomposites. The nanosize clay platelets play a vital role for the improvement in impact resistance for all the nanocomposites. It acts as crack stoppers and forms a tortuous pathway for crack propagation. Therefore, the stress can be dispersed by those layers having higher stiffness and strength than the matrix resulting in higher impact energy. Also the nanoclay layers interact with the polyester as well as epoxy chains and restrict its mobility which increases the strength of the nanocomposites films.

From the curing time measurement it is observed that curing time of all the nanocomposites decreased with the increase of clay loading from 0-5 wt.%. This increase is due to the interaction the clay layers with the polyester which restricts the mobility of the polymer segments. Due to the high surface area of the nanoclay, it assists the physical crosslinking reaction via interaction through H-bonding between (Scheme 4.1 and 4.2) hydroxyl groups of nanoclay and hydroxyl/carboxyl groups of polyester along with the epoxy group of the epoxy resin (curing agent) and amine groups of the poly(amido amine) hardener.

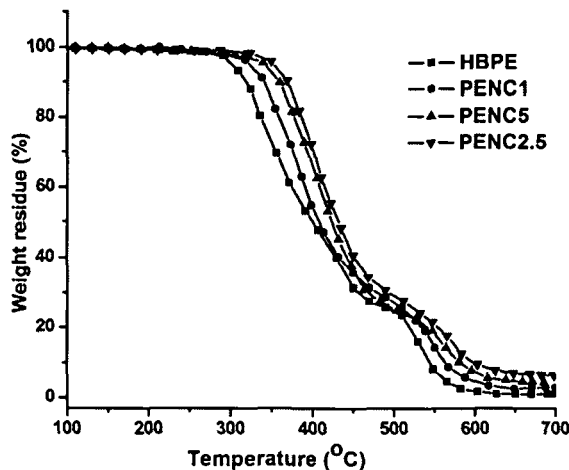
### ***4.3.6. Thermal Properties***

In general, thermal stability of the polymer nanocomposites plays a crucial role in determining their processing and application, because it affects the final properties of

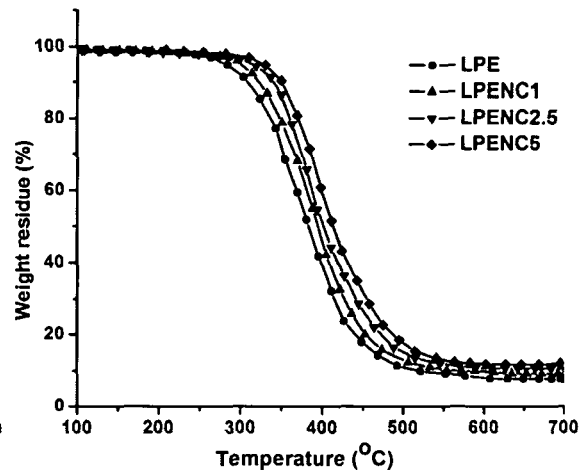
the polymer nanocomposites such as the upper-limit of service temperature and dimensional stability. For the fabrication of advanced nanocomposites with better balance in processing and performance, it is very instructive to characterize the thermal decomposition behavior of the polymer nanocomposites.

Fig. 4.28 elucidates the effect of aluminosilicate layer of OMMT on the thermal degradation of HBPE nanocomposites. A significant increase in the thermal degradation temperature and decrease in thermal degradation rate with an increasing amount of dispersed OMMT clay were observed. Initial thermal degradation temperature ( $T_i$ ) of polyester was remarkably improved from 285 to 340 °C by the formation of nanocomposite.

The thermogravimetric analysis of the LPE nanocomposites showed single step degradation pattern (Fig. 4.29) with an enhanced thermal stability compared to pristine polymer. The onset ( $T_{on}$ ) and the endset ( $T_{end}$ ) thermal degradation temperatures of LPE, LPENC1, LPENC2.5, and LPENC5 were found to be 268, 293, 306 and 321 °C and 473, 487, 501 and 520 °C respectively. Thus with the loading of 5 wt.% OMMT clay the nanocomposite showed an increment of 53 °C thermal degradation temperature compared to the pristine polyester. It is also noticeable that not only the initial decomposition temperature increases but also the weight residue increases (at 650 °C) with the increase in the clay content (0-5 wt.%).



**Fig. 4.28:** TGA thermograms for HBPE nanocomposites



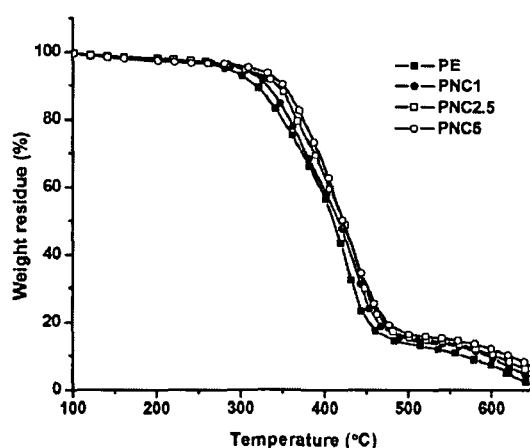
**Fig. 4.29:** TGA thermograms for LPE nanocomposites

The thermal degradation behaviors of the PE nanocomposites are depicted in Fig. 4.30. It is evident that the degradation temperature of the virgin matrix increased with the incorporation of nanoclays. The thermal decomposition of virgin polyester

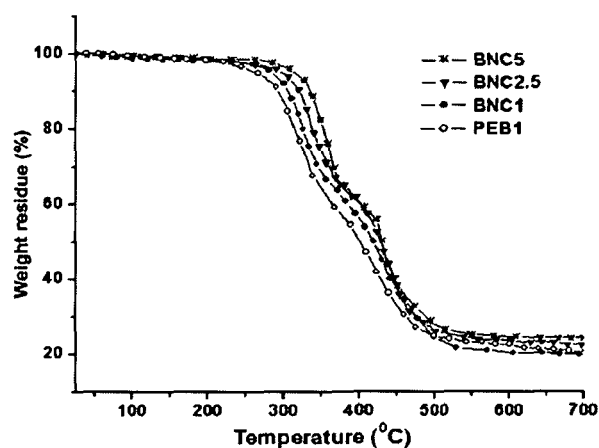
started at a temperature of 300 °C and almost completed at 650 °C. Conversely, in case of nanocomposites PNC1, PNC2.5 and PNC5, the onset of thermal decomposition was observed at 319, 329 and 337 °C respectively. Thus the degradation of the polyester takes place at a higher temperature in the presence of OMMT compared to pristine system. An increment of 37 °C in thermal degradation temperature was observed after 5 wt.% OMMT loadings compared to pristine polyester.

The thermogravimetric traces obtained for the HBPE/epoxy blend based nanocomposites are shown in Fig. 4.31. From this figure it was observed that the HBPE/epoxy blend based nanocomposites degraded by a two step pattern. After formation of nanocomposites the thermal degradation temperature of the blend was found to improved from 273 to 318 °C with 0-5 wt.% of OMMT loading. As observed from Fig. 4.31, the first step  $T_{on}$  and  $T_{end}$  of BNC1, BNC2.5 and BNC5 were found to 287, 300 and 318 °C and 386, 398 and 401 °C respectively. Similarly, in the second step of thermal degradation of the blend nanocomposites, the  $T_{on}$  and  $T_{end}$  values were obtained as 406, 416 and 425 °C and 500, 514 and 529 °C respectively.

TGA thermograms of the water dispersible HBPE nanocomposites are shown in Fig. 4.32. An improvement in the thermal stability of the nanocomposites was found with an increase in the nanoclay content. The onset of the thermal degradation temperatures was enhanced from the pristine polymer by about 5, 12 and 18 °C for the nanocomposites with 1, 2.5 and 5 wt.% of nanoclay content respectively.

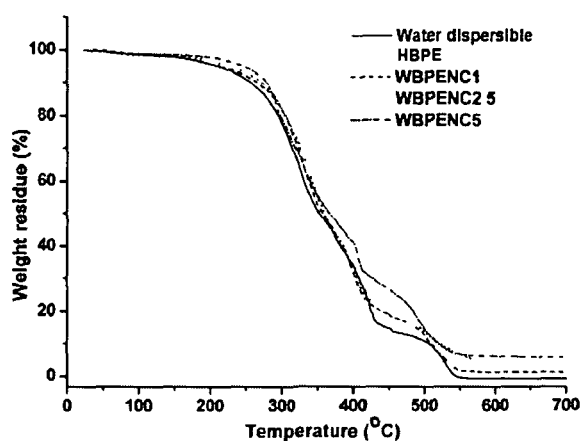


*Fig. 4.30: TGA thermograms for PE nanocomposites*

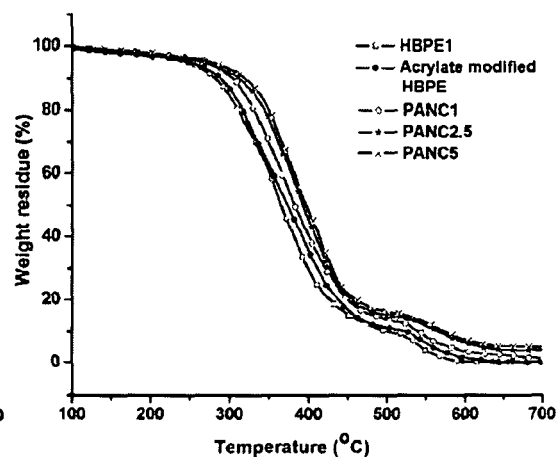


*Fig. 4.31: TGA thermograms for HBPE/epoxy blend nanocomposites*

TGA thermograms of the acrylate modified HBPE nanocomposites are shown in Fig. 4.33. The  $T_d$  of acrylate modified polyester was further enhanced after the formation of nanocomposites with incorporation of 1-5 wt.% OMMT.



*Fig. 4.32: TGA thermograms for water dispersible HBPE nanocomposites*



*Fig. 4.33: TGA thermograms for acrylate modified HBPE nanocomposites*

The nanoclay plays the important role in the enhancement of thermostability of all the nanocomposites. By the incorporation of well-dispersed nanoclay, a diffusion effect occurs which forms char and hinders the emission of the volatile decomposition products.<sup>42</sup> The nanoclay therefore enhances thermal stability by acting as a mass transport barrier to the volatile product generated during decomposition, as a result of a decrease in permeability.<sup>43</sup> Also, the chain kinetics in the region immediately surrounding the nanoclay platelets is altered due to interaction of polymer chains with the nanoclay. The physical and chemical interactions between the polymer chains and the nanoclay surface, restrict the molecular mobility of the affected chains, and modify the conformation and orientation of chain segments in the neighborhood of the surface. The intermolecular attractions among the polymer chains and the layers of nanoclay enhance even at low dose level due to the extremely high specific surface area of nanoclay. The degradation of polymers starts with the formation of free radical at weak bonds and/or chain ends, followed by their transfer to adjacent chains via inter-chain interactions. The degradation behavior is also associated with the morphological changes that occurred in the nanocomposites with clay loading. With the increase of clay concentration (0-5 wt.%), much more exfoliated clay is formed, which results more char formation and consequently promotes the thermal stability of the nanocomposites. The improved thermal stability can also be explained through the reduced mobility of the polyester chains in the nanocomposite. The presence of small amounts of clay in the polyester matrix confined the motion of polymer chains. Because of reduced chain mobility, the chain transfer reaction is suppressed, and consequently the degradation process is hindered.<sup>44</sup>

### 4.3.7. Chemical Resistance

The chemical resistance of all the HBPE, LPE, PE, HBPE/epoxy blend, water dispersible HBPE and acrylate modified HBPE nanocomposites was performed by checking the visual change of the cured nanocomposites films in various chemical environments viz. aqueous sodium hydroxide, aqueous hydrochloric acid, aqueous sodium chloride solutions and distilled water for 15 days at ambient temperature.

The chemical resistance (Table 4.7) indicates that the resistivity of HBPE towards dilute HCl acid and aqueous NaCl solution increases significantly after the formation of nanocomposites, while in distilled water the HBPE and its nanocomposites showed excellent resistance. However, it is affected to varying degrees by alkali. Table 4.8 showed that the alkali resistance of the LPE was enhanced after the formation of nanocomposites with 0-5 wt.% OMMT loading. Also the improvement of chemical resistance towards all other media was found in the LPE nanocomposites with increasing amount of OMMT loading from 0 to 5 wt.%. The poor alkali resistance (Table 4.9) of PE was improved after formation of nanocomposites with 0-5 wt.% OMMT. The improvement of chemical resistance towards all other media was also found in the nanocomposites. The polyester/epoxy blend based nanocomposites showed excellent chemical resistance towards all the media (Table 4.10). The films of water dispersible HBPE nanocomposites (Table 4.11) showed appreciable resistance towards dilute HCl acid, aqueous NaCl solution and distilled water. However, the resistance towards alkali was not so good due to the presence of alkali hydrolyzable ester group. The alkali resistance (Table 4.12) of acrylate modified HBPE was improved after the formation of nanocomposites with 0-5 wt.% clay loading. The chemical resistance was also improved towards all the tested media with the increase of clay loading from 0-5 wt.% in the nanocomposites.

**Table 4.7: Chemical resistance of HBPE and its nanocomposites**

Types of media	HBPE	PENC1	PENC2.5	PENC5
5 wt.% aqueous NaOH	P	A	G	G
25 wt.% aqueous HCl	G	G	E	E
25 wt.% aqueous NaCl	G	E	E	E
Distilled water	E	E	E	E

P=Poor, damage of films, A=Average, loss in gloss; G=Good, slight loss in gloss; E=Excellent, unaffected

**Table 4.8: Chemical resistance of LPE and its nanocomposites**

Types of media	LPE	LPENC1	LPENC2.5	LPENC5
5 wt.% aqueous NaOH	P	G	G	E
25 wt.% aqueous HCl	A	G	E	E
25 wt.% aqueous NaCl	A	E	E	E
Distilled water	G	E	E	E

A=Average, P= Poor, G= Good, E= Excellent

**Table 4.9: Chemical resistances of PE and its nanocomposites**

Types of media	PE	PNC1	PNC2.5	PNC5
5 wt.% aqueous NaOH	P	A	G	E
25 wt.% aqueous HCl	A	G	E	E
25 wt.% aqueous NaCl	G	E	E	E
Distilled water	E	E	E	E

P= Poor, A= Average, G= Good, E= Excellent

**Table 4.10: Chemical resistance of HBPE/epoxy blend and its nanocomposites**

Types of media	PEB1	BNC1	BNC2.5	BNC5
5 wt.% aqueous NaOH	G	E	E	E
25 wt.% aqueous HCl	E	E	E	E
25 wt.% aqueous NaCl	E	E	E	E
Distilled water	E	E	E	E

G= Good, E= Excellent

**Table 4.11: Chemical resistance of water dispersible HBPE and its nanocomposites**

Types of media	Water dispersible HBPE	WPENC1	WPENC2.5	WPENC5
5 wt.% aqueous NaOH	P	A	A	G
25 wt.% aqueous HCl	A	A	G	E
25 wt.% aqueous NaCl	A	A	G	E
Distilled water	G	E	E	E

P= Poor, A= Average, G= Good, E= Excellent

**Table 4.12:** Chemical resistance of acrylate modified HBPE and its nanocomposites

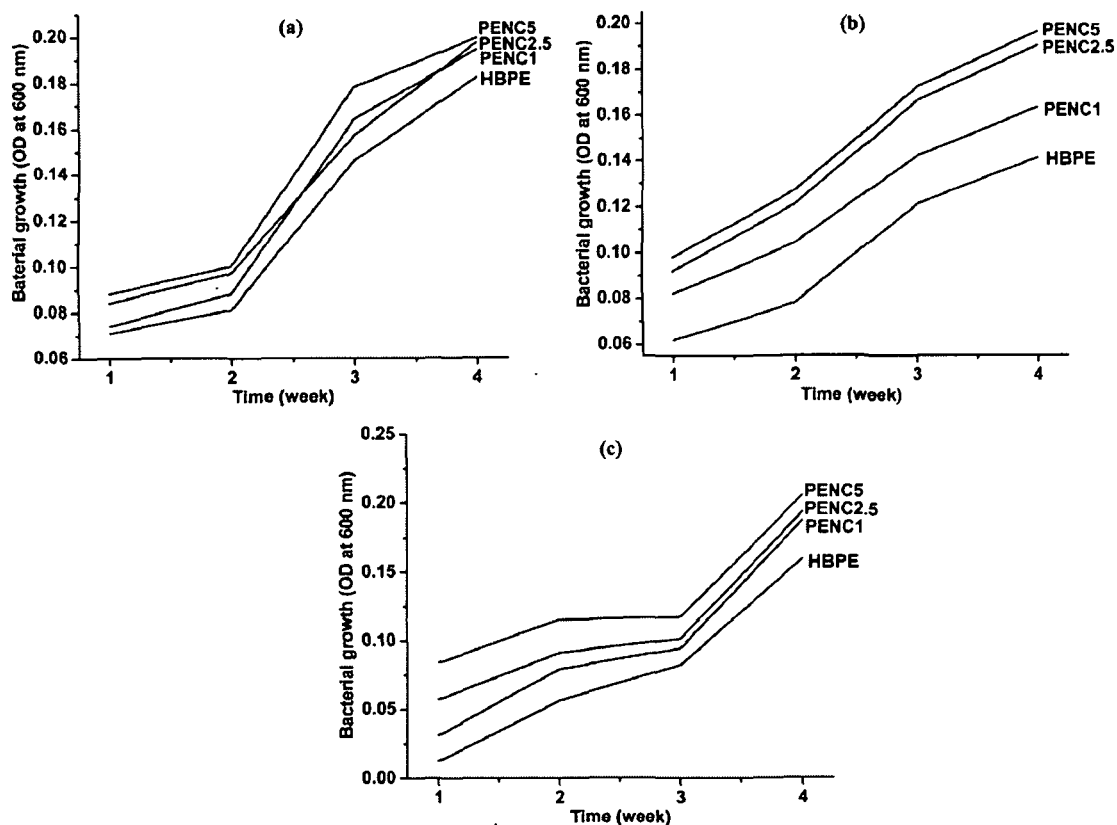
Types of media	Acrylate modified HBPE	PANC1	PANC2.5	PANC5
5 wt.% aqueous NaOH	A	E	E	E
25 wt.% aqueous HCl	G	E	E	E
25 wt.% aqueous NaCl	G	E	E	E
Distilled water	E	E	E	E

A= Average, G= Good, E= Excellent

The poor alkali resistance of all the matrix system is due to the presence of alkali hydrolyzable ester group as mentioned above. But in the nanocomposites with the increase of nanoclay loading, the resistance towards alkali was increased which is due to interaction of clay layers with the polyester chains that results compact and crosslinked structure of the nanocomposites where clay layers are bonded to the polyester matrix. The resistance towards all other chemical media was also enhanced for all the nanocomposites. The permeability of the nanocomposites is reduced by homogeneous dispersion or delamination of the clay layers through insertion of polymer chains and thereby produces a tortuous pathway for diffusion. Due to this the different ions or species present in different media cannot be easily penetrated the surface and thereby increases the chemical resistance. Also, the nanosize clay platelets act as barrier and increase the mean effective path for the molecules to travel. They act as barrier by increasing the mean effective path of the alkali medium to enter inside the polyester matrix which evades the solvent absorption of the polymer system.

#### **4.3.8. Biodegradation Studies**

The polyesters are prone to microbial attack due to the presence of hydrolyzable ester bond in their main chain. Broth culture technique was employed for the biodegradation study of HBPE nanocomposites. The nanocomposite films were directly exposed to different bacterial strains in broth culture media as stated in the experimental section 4.2.2.8. After four weeks, the polyester nanocomposites showed high biodegradation rate as compared to the pristine polymer (Fig. 4.34). The growth of all the bacterial strains increased with the increase of the time of bacterial exposure. The rate of growth was not much significant in nanocomposites as well as on the pristine polymer upon

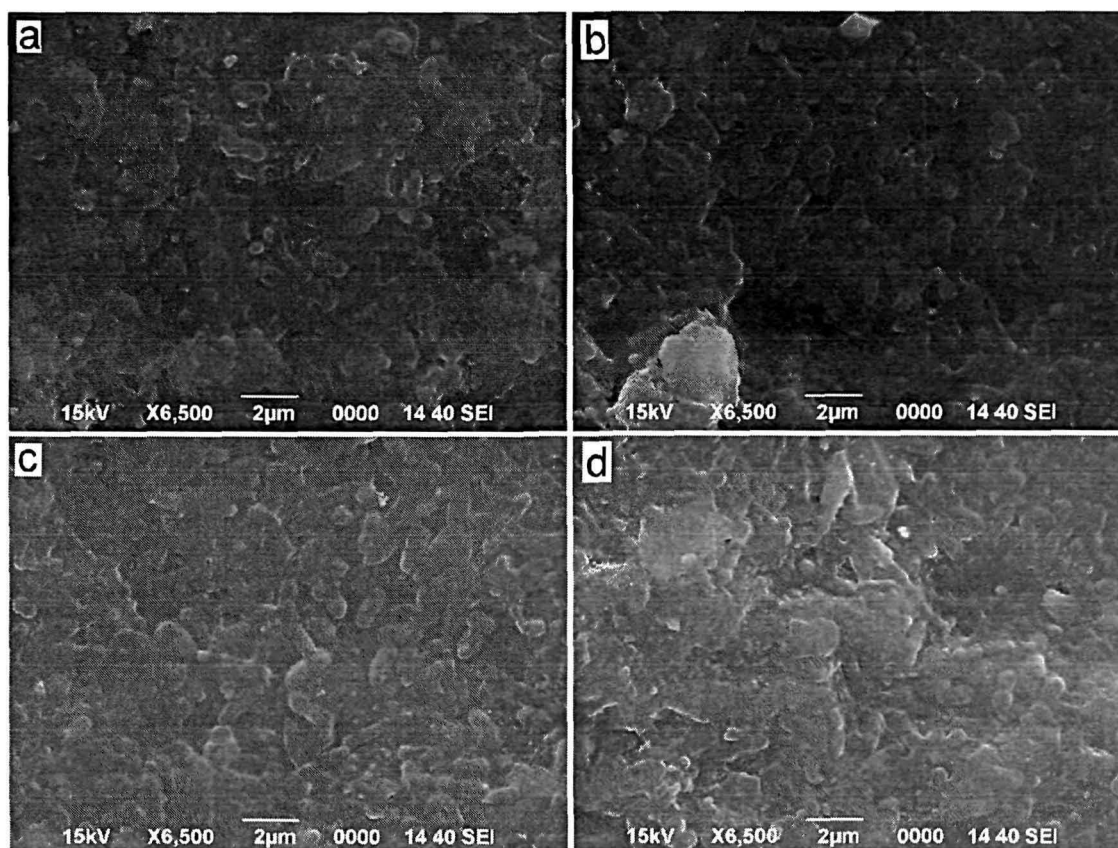


**Fig. 4.34:** Growth of (a) *Pseudomonas aeruginosa*, PN8A1, (b) *Pseudomonas aeruginosa*, vs1 and (c) *Bacillus subtilis*, MTCC73 on HBPE nanocomposites

bacterial exposure up to two weeks. But after two weeks, the bacterial growth increased tremendously which indicates improved biodegradation rate. This is due to the catalytic role of OMMT in hydrolysis of the ester groups.<sup>45</sup> After absorbing water in the presence of microbes the unreacted terminal –OH groups of OMMT can cause heterogeneous hydrolysis which takes a little time for initiation.<sup>46</sup> For this reason, only after two weeks considerable improvement of biodegradation was found. The microbes broke all the nanocomposite films. The SEM micrographs (Fig. 4.35) of the recovered films after four weeks of bacterial exposure further support this.

The biodegradation efficacy of the acrylate modified HBPE nanocomposite films was checked by directly exposing them to microbial attack of different bacterial strains as mentioned in the section 4.2.2.8. The growth of the bacterial strains was monitored by using McFarland turbidity method. Up to 2 weeks the degradation of the nanocomposites as well as polyester was not so noticeable. After exposure of 3 weeks, the pristine polyester as well as nanocomposites was observed to degrade. The bacterial growth was continuously increased up to 5 weeks. However the degradation of the nanocomposites was more than that of the pristine polyester which could be depicted





**Fig. 4.35:** SEM micrographs of (a) HBPE, (b) PENC1, (c) PENC2.5, and (d) PENC5 after biodegradation by *Bacillus subtilis*, MTCC73

from the optical density of the nanocomposites in Fig. 4.36. Also with the increase of nanoclay concentration the degradation was found to increase. The growth of bacteria in the nanocomposites film can also be depicted from the SEM micrographs (Fig. 4.37) of nanocomposites films. Degradation in the present nanocomposites occurs by the ester hydrolysis of the crosslinked polyester resin, as in conventional aliphatic polyesters, with the generation of fragments and respective starting carboxylic acids and diols.<sup>47</sup> Similar to degradation by enzyme, the bacterial degradation takes place chiefly in two stages. In the first stage, polyester chains of high molecular weight hydrolyze to form the oligomers where an acid, base, or moisture can accelerate the reaction. Then the microorganisms consume the low molecular weight oligomers in the last stage to produce CO<sub>2</sub>, H<sub>2</sub>O and humus.<sup>22</sup> The polar groups of the matrix along with the hydroxy groups of the OMMT absorb water which accelerates the first step and thus became the determining step for biodegradation.

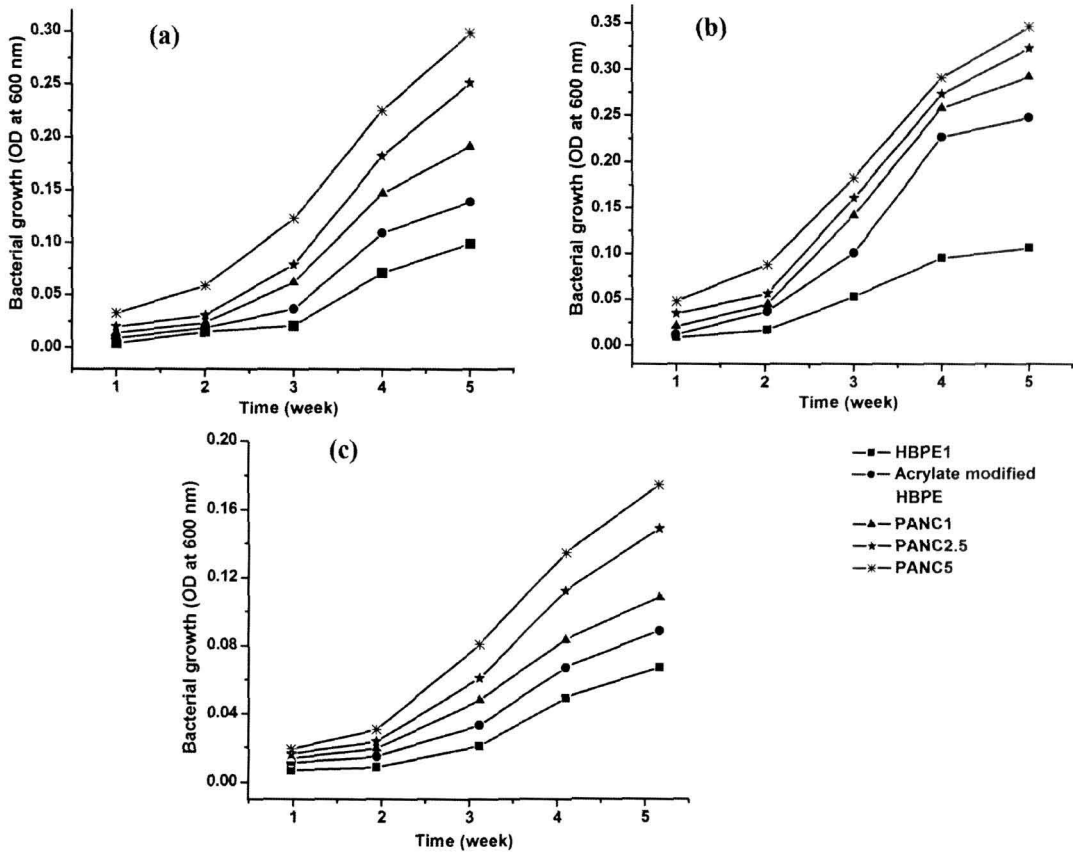


Fig. 4.36: Growth of (a) *Pseudomonas aeruginosa*, SD2, (b) *Pseudomonas aeruginosa*, SD3 and (c) *Bacillus subtilis*, MTCC736 on acrylate modified HBPE nanocomposites

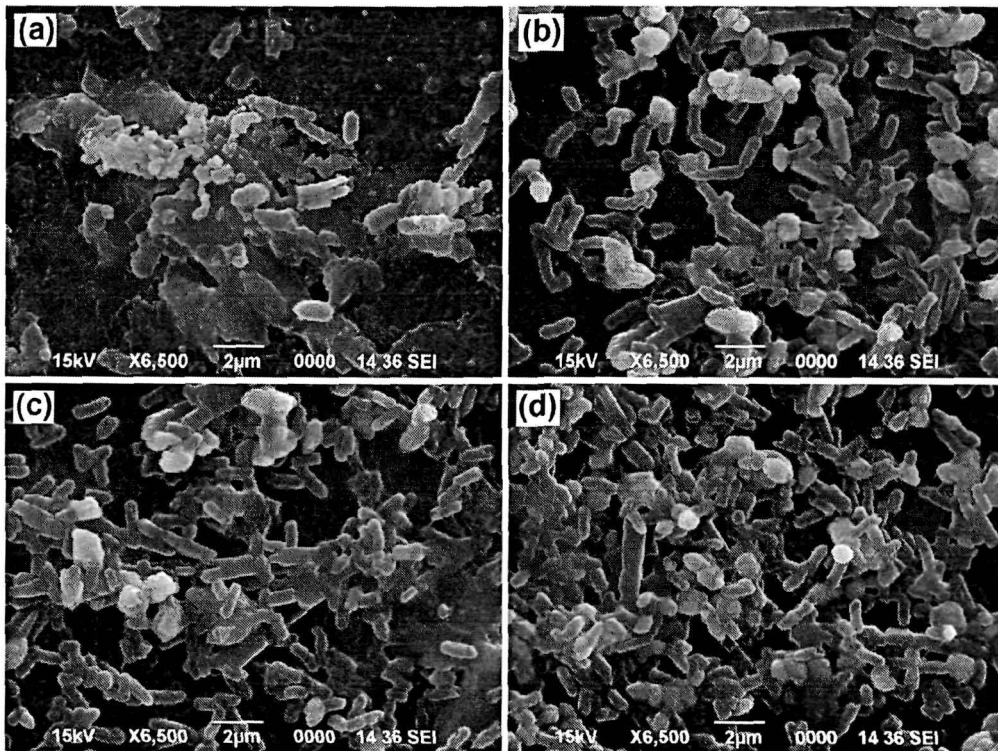


Fig. 4.37: SEM micrographs for (a) acrylate modified HBPE, (b) PANC1, (c) PANC2.5 and (d) PANC5 after biodegradation by *Pseudomonas aeruginosa*, SD3

#### 4.4. Conclusions

Thus the study revealed the successful way of preparing *Mesua ferrea* L. seed oil based HBPE, LPE, PE, HBPE/epoxy blend, water dispersible HBPE and acrylate modified HBPE with clay nanocomposites through *ex-situ* solution technique using high mechanical shear force and ultrasonication. All the prepared nanocomposites showed significant improvement of the performance characteristics like mechanical properties, thermostability, chemical resistance etc. compared to their pristine system. Besides these performance characteristics, the HBPE and acrylate modified HBPE nanocomposites also showed enhancement of biodegradability. The study also evaluated the suitability of the water dispersible HBPE/clay nanocomposite system as a new renewable oil-based environmental friendly aqueous processable material. Thus the resulted nanocomposites have the potentiality as advanced thin film and coating materials in different industrial fields along with some other high performance applications.

#### References

1. Karak, N. *Fundamentals of Polymers: Raw Materials to Finish Products* (PHI Learning Pvt. Ltd., New Delhi, 2009)
2. Pfaendner, R. Nanocomposites: Industrial opportunity or challenge? *Polym. Degrad. Stab.* **95**, 369-373 (2010)
3. Haq, M.; Burgueño, R.; Mohanty, A.K.; Misra, M. Bio-based polymer nanocomposites from UPE/EML blends and nanoclay: Development, experimental characterization and limits to synergistic performance. *Compos. Part A: Appl. Sci. Manufactur.* **42**, 41-49 (2011)
4. Usuki, A.; Hasegawa, N.; Kato, M. Polymer-clay nanocomposites. *Adv. Polym. Sci.* **179**, 135-195 (2005)
5. Calvo, S.; Prolongo, M.G.; Salom, C.; Masegosa, R.M. Preparation and thermal-mechanical characterization of nanoclay-unsaturated polyester composites. *J. Nanosci. Nanotech.* **10**, 2863-2869 (2010)
6. Torre, L.; Chieruzzi, M.; Kenny, J.M. Compatibilization and development of layered silicate nanocomposites based of unsaturated polyester resin and customized intercalation agent. *J. Appl. Polym. Sci.* **115**, 3659-3666 (2010)

## Chapter 4

7. Ahmadi, S.J.; Huang, Y.D.; Li, W. Synthetic routes, properties and future applications of polymer-layered silicate nanocomposites. *J. Mater. Sci.* **39**, 1919-1925 (2004)
8. Karak, N. Polymer (epoxy) clay nanocomposites. *J. Polym. Mater.* **23**, 1-20 (2006)
9. Wang, Z.; Pinnavaia, T.J. Nanolayer reinforcement of elastomeric polyurethane. *Chem. Mater.* **10**, 3769-3771 (1998)
10. Rehab, A.; Salahuddin, N. Nanocomposite materials based on polyurethane intercalated into montmorillonite clay. *Mater. Sci. Eng. A* **399**, 368-376 (2005)
11. Finnigan, B.; Martin, D.; Halley, P.; Truss, R.; Campbell, K. Morphology and properties of thermoplastic polyurethane nanocomposites incorporating hydrophilic layered silicates. *Polymer* **42**, 2249-2260 (2004)
12. Seo, W.J. *et al.* Effects of ultrasound on the synthesis and properties of polyurethane foam/clay nanocomposites. *J. Appl. Polym. Sci.* **102**, 3764-3773 (2006)
13. Haq, M.; Burgueño, R.; Mohanty, A.K.; Misra, M. Hybrid bio-based composites from blends of unsaturated polyester and soybean oil reinforced with nanoclay and natural fibers. *Compos. Sci. Technol.* **68**, 3344-3351 (2008)
14. Pilla, S. *et al.* Microcellular processing of polylactide-hyperbranched polyester-nanoclay composites. *J. Mater. Sci.* **45**, 2732-2746 (2010)
15. Santra, S.; Kaittanis, C.; Perez, J.M. Aliphatic hyperbranched polyester: A new building block in the construction of multifunctional nanoparticles and nanocomposites. *Langmuir* **26**, 5364-5373 (2010)
16. Sangermano, M.; Messori, M.; Galleco, M.M.; Rizza, G.; Voit, B. Scratch resistant tough nanocomposite epoxy coatings based on hyperbranched polyesters. *Polymer* **50**, 5647-5652 (2009)
17. Karak, N.; Maiti, S. *Dendrimers and Hyperbranched Polymers-Synthesis to Applications* (MD Publication Pvt Ltd., New Delhi, 2008)
18. Irfan, M.; Seiler, M. Encapsulation using hyperbranched polymers: From research and technologies to emerging applications. *Ind. Eng. Chem. Res.* **49**, 1169-1196 (2010)
19. Lu, J.; Hong, C.K.; Wool, R.P. Bio-based nanocomposites from functionalized plant oils and layered silicate. *J. Polym. Sci. Part B: Polym. Phys.* **42**, 1441-1450 (2004)

20. Ray, S.S.; Bousmina, M. Biodegradable polymers and their layered silicate nanocomposites: In greening the 21st century materials world. *Prog. Mater. Sci.* **50**, 962-1079 (2005)
21. Miyagawa, H.; Misra, M.; Drzal, L.T.; Mohanty, A.K. Novel biobased nanocomposites from functionalized vegetable oil and organically-modified layered silicate clay. *Polymer* **46**, 445-453 (2005)
22. Maiti, P.; Batt, C.A.; Giannelis, E.P. New biodegradable polyhydroxybutyrate/layered silicate nanocomposites. *Biomacromolecules* **8**, 3393-3400 (2007)
23. Krishnamoorti, R.; Vaia, R.A.; Giannelis, E.P. Structure and dynamics of polymer-layer silicate nanocomposites. *Chem. Mater.* **8**, 1728-1734 (1996)
24. Yu, L.; Petinakis, S.; Dean, K.; Bilyk, A.; Wu, D. Green polymeric blends and composites from renewable resources. *Macromol. Symp.* **249-250**, 535-539 (2007)
25. Wang, J.C.; Chen, Y.H.; Chen, R.J. Preparation of thermosetting polyurethane nanocomposites by montmorillonite modified with a novel intercalation agent. *J. Polym. Sci. Part B: Polym. Phys.* **45**, 519-531 (2007)
26. Ding, Q. *et al.* Synthesis and characterization of polyurethane/montmorillonite nanocomposites by *in-situ* polymerization. *Polym. Int.* **55**, 500-504 (2006)
27. Deka, H.; Karak, N. Shape-memory property and characterization of epoxy resin-modified *Mesua ferrea* L. seed oil-based hyperbranched polyurethane. *J. Appl. Polym. Sci.* **116**, 106-115 (2010)
28. Isci, S.; Ünlu, C.H.; Atici, O.; Gungor, N. Rheology and structure of aqueous bentonite-polyvinyl alcohol dispersions. *Bull. Mater. Sci.* **29**, 449-456 (2006)
29. Uhl, F.M.; Davuluri, S.P.; Wong, S.C.; Webster, D.C. Polymer films possessing nanoreinforcements via organically modified layered silicate. *Chem. Mater.* **16**, 1135-1142 (2004)
30. Ahn, Y.H.; Chang, J.H. Thermotropic liquid crystalline polyester nanocomposites via *in-situ* intercalation polycondensation. *Polym. Adv. Technol.* **19**, 1479-1485 (2008)
31. Wu, D.; Zhou, C.; Hong, Z.; Mao, D.; Bian, Z. Study on rheological behavior of poly(butylene terephthalate)/montmorillonite nanocomposites. *Eur. Polym. J.* **41**, 2199-2207 (2005)

32. Lim, S.T.; Hyun, Y.H.; Choi, H.J. Synthetic biodegradable aliphatic polyester/montmorillonite nanocomposites. *Chem. Mater.* **14**, 1839-1844 (2002)
33. Pavlidou, S.; Papaspyrides, C.D. A review on polymer-layered silicate nanocomposites. *Prog. Polym. Sci.* **33**, 1119-1198 (2008)
34. Kim, T.H.; Jang, L.W.; Lee, D.C.; Choi, H.J.; Jhon, M.S. Synthesis and rheology of intercalated polystyrene/Na<sup>+</sup>-montmorillonite nanocomposites. *Macromol. Rapid Commun.* **23**, 191-195 (2002)
35. Yılmaz, O.; Cheaburu, C.N.; Gülümser, G.; Vasile, C. Rheological behavior of acrylate/montmorillonite nanocomposite latexes and their application in leather finishing as binders. *Prog. Org. Coat.* **70**, 52-58 (2011)
36. Kokane, S.V. Epoxy system- A review. *Paintindia* **52**, 69-81 (2002)
37. Vargha, V.; Kiss, G. Time-temperature-transformation analysis of an alkyd-amino resin system. *J. Therm. Anal. Calorim.* **76**, 295-306 (2004)
38. Pramanik, M.; Srivastava, S.K.; Samantaray, B.K.; Bhowmick, A.K. EVA/clay nanocomposite by solution blending: Effect of aluminosilicate layers on mechanical and thermal properties. *Macromol. Res.* **11**, 260-266 (2003)
39. Mohanty, S.; Nayak, S.K. Effect of clay exfoliation and organic modification on morphological, dynamic mechanical, and thermal behavior of melt-compounded polyamide-6 nanocomposites. *Polym. Compos.* **28**, 153-162 (2007)
40. Tsujimoto, T.; Uyama, H.; Kobayashi, S. Synthesis of high-performance green nanocomposites from renewable natural oils. *Polym. Degrad. Stab.* **95**, 1399-1405 (2010).
41. Zhao, C.X.; Zhang, W.D. Preparation of waterborne polyurethane nanocomposites: Polymerization from functionalized hydroxyapatite. *Eur. Polym. J.* **44**, 1988-1995 (2008)
42. Duquesne, S. *et al.* Elaboration of EVA–nanoclay systems-characterization, thermal behavior and fire performance. *Compos. Sci. Technol.* **63**, 1141-1148 (2003)
43. Alexandre, M.; Dubois, P. Polymer-layered silicate nanocomposites: preparation, properties and uses of a new class of materials. *Mater. Sci. Eng.* **28**, 1-63 (2000)
44. Chou, C.W.; Hsu, S.H.; Chang, H.; Tseng, S.M.; Lin, H.R. Enhanced thermal and mechanical properties and biostability of polyurethane containing silver nanoparticles. *Polym. Degrad. Stab.* **91**, 1017-1024 (2006)

## Chapter 4

45. Pandey, J.K.; Reddy, K.R.; Kumar, A.P.; Singh, R.P. An overview on the degradability of polymer nanocomposites. *Polym. Degrad. Stab.* **88**, 234-250 (2005)
46. Ray, S.S.; Okamoto, M. Polymer/layered silicate nanocomposites: A review from preparation to processing. *Prog. Polym. Sci.* **28**, 1539-1641 (2003)
47. Jayabalan, M.; Shalumon, K.T.; Mitha, M.K.; Ganesan, K.; Epple, M. Effect of hydroxyapatite on the biodegradation and biomechanical stability of polyester nanocomposites for orthopaedic applications. *Acta Biomater.* **6**, 763-75 (2010)

## CHAPTER 5

---

### HBPE/Clay Silver Nanocomposites

---

#### 5.1. Introduction

Antimicrobial assets of surface coating materials are undeniably the priority for the researchers of material sciences in recent days. Antimicrobial polymers that restrain silver captured great attention to the academy and industry due to their novelty in being a long-lasting biocidal material with high thermal stability and low volatility.<sup>1</sup> The large increase in number and occurrence of antimicrobial resistant bacterial strains has impelled a rehabilitated interest in the exploitation of silver as an antimicrobial agent.<sup>2</sup> However, the leaching out tribulations of silver into the environment causes not only an environmental risk but also has serious adverse effects on the durability and useful life of the treated material, though it does not emerge to impact marketability.<sup>3,4</sup> So non-leaching antimicrobial polymeric surfaces, where the antimicrobial agent is enduringly fixed to the surface through strong interaction, is a striking alternative stratagem.<sup>5</sup> Antibacterial coatings that can be easily applied to different types of surfaces to halt harmful microorganisms from proliferating would curtail detrimental situations like formation of biofilms and the spate of infectious diseases by adhesion of bacteria onto the surfaces of materials.<sup>6</sup>

Again, the expanding horizon of nanotechnology is leading to the genesis of a multitude of novel utilities. The preparation of organic-inorganic-metal hybrid materials has been of great curiosity in the field of nanocomposite materials.<sup>7</sup> The inclusion of inorganic nanoparticles is one of the effectual methods that augment the mechanical and thermal properties of the polymer matrix.<sup>8</sup> In recent years, due to inimitable size-induced properties, silver nanoparticles have received immense attention and provided the prospect of new applications or the additional flexibility to the existing systems in many areas, such as catalysis, magnetism, optics, microelectronic, chemical sensor, biomedical and so forth.<sup>9-16</sup> Although the polymer matrix acts as stabilizers, templates, or protecting agents, the nanoparticles get aggregated easily, causing deterioration of their physico-chemical properties even when they are stored at room temperature.<sup>17</sup> However, if nanoparticles are formed in supporting materials, the nanoparticles can not release easily and aggregation of the



nanoparticles can also be prevented. Therefore, the supported nanoparticles would be of great potential for assorted applications.<sup>17</sup> So the present work tried to use organically modified montmorillonite nanoclay (OMMT) as nanofiller for the improvement in mechanical along with thermal properties of the pristine polyester and also as a support material for the stabilization of the silver nanoparticles preventing the aggregation from the solution.

Formation of nanoparticles in polymer matrices have recently emerged as an active field of research.<sup>18-20</sup> This is due to their (a) enhanced stability, (b) difference in physical and chemical properties, (c) film forming ability of the polymer etc. As a new genus of polymers with quasi-spherical highly branched architecture and special solution or melting properties, hyperbranched polymers have received more and more attention.<sup>21</sup> The use of these types of polymers in the field of nanocomposites have special interest as they have better control over size, shape and structure of metal-nanoparticles than that of conventional polymers.<sup>21</sup> The highly functionalized three dimensional globular non-entangled structures of hyperbranched polymers can regulate the size, shape and stability of metal nanoparticles. Although, a number of reports described the utility of hyperbranched polymer as the matrix for metal nanoparticles but the vegetable oil derived matrices are really in scanty. Hyperbranched polyester is one such category that provides more stabilization to the nanodomain via interactions with their various types of active functional group. Another important feature of hyperbranched polyester is its tailor made properties. Therefore the bis-MPA based HBPE as described in Chapter 2, section 2.2.2.1 was used as stabilizer as well as matrix to obtain silver nanoparticles. Due to the presence of large number of easily accessible functional groups, high solubility in different solvents and low viscosity of the HBPE, the silver nanoparticles are easily stabilized by it. Since the reported silver encapsulated polyester nanocomposites possess antimicrobial properties so there will be a mounting demand for them to be used as potential antimicrobial surface coatings ranges from medicine, to the construction as well as food packaging industry.

Therefore in this chapter, preparation and characterization of *Mesua ferrea* L. seed oil modified HBPE/clay silver based nanocomposites that are prepared by *in-situ* technique, are reported. The performance characteristics such as mechanical, thermal and rheological properties of the silver nanocomposites were also investigated. Along with these, the antibacterial efficacy of the prepared silver nanocomposites was also studied.

## 5.2. Experimental

### 5.2.1. Materials

Silver nitrate ( $\text{AgNO}_3$ ) was purchased from Merck, India. It has m.p.  $212\text{ }^\circ\text{C}$ , minimum assay 99.8% and  $M_w$  169.6 g/mol. It was used as received and utilized for preparation of silver nanoparticles.

The required chemicals and solvents such as *Mesua ferrea* L. seed oil, glycerol, PA, MA, bis-MPA, lead mono oxide, DMF, xylene, epoxy resin, poly(amido amine) etc. were of same specifications as described in Chapter 2, section 2.2.1. OMMT was of same specifications as described in Chapter 4, section 4.2.1. All the minerals ( $\text{NH}_4$ )<sub>2</sub>SO<sub>4</sub>, Na<sub>2</sub>HPO<sub>4</sub>, KH<sub>2</sub>PO<sub>4</sub>, MgSO<sub>4</sub>.7H<sub>2</sub>O, CaCl<sub>2</sub>.2H<sub>2</sub>O, FeSO<sub>4</sub>.7H<sub>2</sub>O, CuSO<sub>4</sub>.7H<sub>2</sub>O, MnSO<sub>4</sub>.5H<sub>2</sub>O, ZnSO<sub>4</sub>.7H<sub>2</sub>O, H<sub>3</sub>BO<sub>3</sub>.5H<sub>2</sub>O and MoO<sub>3</sub> used for preparation of bacterial broth culture media during antimicrobial study were of same specifications as described in Chapter 4, section 4.2.1. The bacterial strains *Staphylococcus aureus*, MTCC96; *Bacillus subtilis*, MTCC736; *Escherichia coli*, MG1655; *Pseudomonas aeruginosa*, PN1; and *Candida albicans* (clinical isolate) used for antimicrobial study were obtained from the Department of Molecular Biology and Biotechnology (Department of Biotechnology, DBT Centre, Government of India), Tezpur University. All other reagents were of reagent grade and were used without further purification.

### 5.2.2. Instruments and Methods

The FTIR and TGA analyses were carried out using the same instruments and conditions as mentioned in Chapter 2, section 2.2.2. and Chapter 3, section 3.2.2. respectively. The XRD, SEM and TEM were carried out using the same instruments and conditions as mentioned in Chapter 4, section 4.2.2. The measurements of gloss, impact resistance, scratch hardness and chemical resistance were performed according to the standard methods as mentioned earlier (Chapter 2, section 2.2.2.). The mechanical and rheological properties were evaluated by the similar methods as described in the Chapter 2, section 2.2.2. UV-visible spectra of the silver nanocomposites were recorded by UV-visible spectrophotometer, UV-2550 (Shimadzu, Japan) with a 0.001% solution in DMF at room temperature ( $\sim 27\text{ }^\circ\text{C}$ ). Sonication was done with the same instrument as mentioned in Chapter 3, section 3.2.2 at fixed amplitude and a half cycle for proper dispersion of the OMMT in the HBPE matrix.

*Mesua ferrea* L. seed oil was extracted from the matured seeds by the same method as described in Chapter 2, section 2.2.2. The percent of swelling of the nanocomposites films was determined by the same method as discussed in the Chapter 2, section 2.2.2.

### 5.2.2.1. Preparation of HBPE/Clay Nanocomposites

The *Mesua ferrea* L. seed oil based HBPE was prepared by using the same method as described in the experimental section of Chapter 2, sections 2.2.2.1. After completion of the resinification when the temperature reduces to 150 °C, 2.5 wt.% (with respect to resin) pre-dispersed OMMT was added to the resin and stirred continuously for half an hour under the same condition. The OMMT was dispersed in xylene by mechanical shearing for 30 min followed by ultra-sonication for 10 min before adding into the resin. Then heating was stopped and the mixture was cooled to room temperature followed by sonication for half an hour.

### 5.2.2.2. Preparation of Silver Nanocomposites

Different amount of AgNO<sub>3</sub>, 1, 3 and 5% (w/w) with respect to the HBPE were used for the preparation of silver nanocomposites. 10 g of above HBPE/clay nanocomposite was taken in a round bottom flask. The required amount of AgNO<sub>3</sub> solution dissolved in minimum amount of DMF solvent was added dropwise into it with continuous stirring at room temperature. After complete addition of the solution the reaction mixture was stirred continuously for 24 h. The aliquots were checked for their absorption spectra to ascertain the reduction of the silver time to time during this reduction process. After 24 h the color of the resultant solution turns to greenish black from dark brown mixture.

### 5.2.2.3. Preparation of Nanocomposite Films

40 parts of bisphenol-A based epoxy resin with respect to 60 parts of HBPE and 25% poly(amido amine) of epoxy resin were mechanically mixed into the silver nanocomposites by stirring for 30 min. The mixture was then degassed for about 20 min under vacuum until it was completely bubble free. Then it was cast on different substrates similarly as described in Chapter 2, section 2.2.2. and dried under vacuum in dessicator for overnight at room temperature. The cast films were then allowed to cure at 120 °C for further study. The curing time was measured by the similar method as

described in the Chapter 2, section 2.2.2. The prepared silver nanocomposites were denoted as PENCAg0, PENCAg1, PENCAg3 and PENCAg5 corresponding to the AgNO<sub>3</sub> content of 0, 1, 3, and 5 wt.% respectively.

### 5.2.2.4. Preparation of Culture Media

The mineral salt medium for incubation of microorganism with the composition 2.0 g of (NH<sub>4</sub>)<sub>2</sub>SO<sub>4</sub>, 2.0 g of Na<sub>2</sub>HPO<sub>4</sub>, 4.75 g of KH<sub>2</sub>PO<sub>4</sub>, 1.2 g of MgSO<sub>4</sub>.7H<sub>2</sub>O, 0.5 mg of CaCl<sub>2</sub>.2H<sub>2</sub>O, 100 µg of MnSO<sub>4</sub>.5H<sub>2</sub>O, 70 µg of ZnSO<sub>4</sub>.7H<sub>2</sub>O, 10 µg of H<sub>3</sub>BO<sub>3</sub>.5H<sub>2</sub>O, 100 µg of CuSO<sub>4</sub>.7H<sub>2</sub>O, 1 mg of FeSO<sub>4</sub>.7H<sub>2</sub>O, and 10 µg of MoO<sub>3</sub> was prepared using the same method as described in Chapter 4, section 4.2.2.7.

### 5.2.2.5. Antibacterial Assessment

The samples were individually tested against a panel of microorganisms including *Staphylococcus aureus*, MTCC96; *Bacillus subtilis*, MTCC736; *Escherichia coli*, MG1655; *Pseudomonas aeruginosa*, PN1; and *Candida albicans*. The antibacterial tests were performed as described elsewhere<sup>22</sup> after some modification (use of Mueller Hinton broth as culture medium for bacteria instead of Nutrient broth and use of Sabouraud dextrose broth for culturing *Candida albicans* (30 °C, 48 h) instead of yeast extract peptone dextrose (YEPD) broth at 28 °C). Antimicrobial activity of samples was determined by the agar-well diffusion method. All the microorganisms mentioned above were incubated (37 °C, 24 h) by inoculation into Mueller Hinton broth. *Candida albicans* was incubated in Sabouraud dextrose broth (30 °C, 48 h). The culture suspensions were prepared and adjusted by comparing against 0.4–0.5 McFarland turbidity standard tubes. Mueller Hinton Agar and Sabouraud dextrose Agar (20 mL) were poured into each sterilized Petri dish (10 mm x 90 mm) after injecting cultures (100 µL) of bacteria and yeast and distributing medium in Petri dishes homogeneously. For the investigation of the antibacterial and anticandidal activity, the samples were dissolved in DMSO to a final concentration of 20%. The prepared two samples at various concentrations were introduced into the wells (6 mm) in agar plates directly. Plates injected with the yeast cultures were incubated at 30 °C for 48 h, and the bacteria were incubated at 37 °C for 24 h. At the end of the incubated period, inhibition zones were evaluated (in mm) using antibiotic zone scale (HiMedia). Studies were performed in triplicate and the inhibition zones were compared with those of reference drugs. Inhibitory activity of DMSO was

also tested. Reference drugs used as control were as follows: Nystatin (10 mg/mL) for *Candida albicans* and Ampicillin (1 mg/mL) for the rest.

### 5.3. Results and Discussion

#### 5.3.1. Formation of HBPE/Clay Silver Nanocomposites

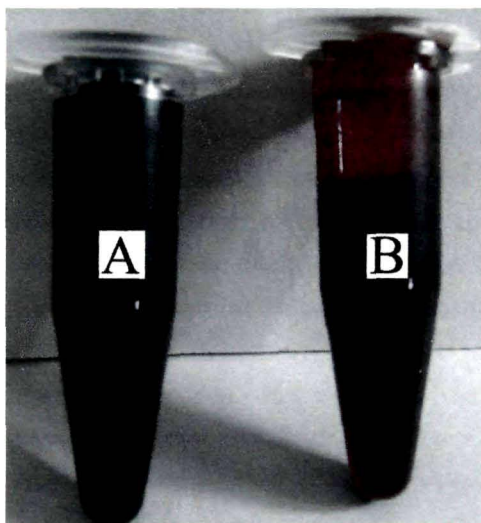
Nanoparticles have very high aspect ratio and possess very high surface energy, therefore have a great tendency to agglomerate. The polymers are frequently used as stabilizer of the nanoparticles in chemical synthesis of metal nanoparticles, since they prevent agglomeration and precipitation of the nanoparticles. The embedding of such nanoparticles in polymer matrix is also advantageous from the viewpoint of film casting.<sup>23</sup> The OMMT was impregnated as the avenue to compensate for the low mechanical and thermal properties of pristine HBPE by forming nanocomposites. The carboxyl groups of the HBPE can easily interact with hydroxyl groups of nanoclay through H-bonding or other polar-polar interaction to form stable and well dispersed nanocomposites as already mentioned in Chapter 4. For uniform dispersion and delamination of the nanoclay layers through insertion of polymer chains, mechanical agitation with high shear force and ultrasonication were employed. The silver nanoparticles were formed *in-situ* in the HBPE/clay nanocomposite systems by reduction of AgNO<sub>3</sub> using DMF as a diluent as well as reducing agent at room temperature for 24 h. It is already reported that the reduction of Ag<sup>+</sup> ions in DMF takes place spontaneously at room temperature.<sup>24</sup> Again the confined geometry of HBPE along with the dispersed OMMT layers helps in stabilization preventing agglomeration of the silver nanoparticles. The used method has some merits like no extra reducing agent was needed, the process was conducted at room temperature under normal pressure, and the obtained silver nanoparticles have several good properties, including long dispersion stability (Fig. 5.1), small particle sizes, and a narrow size distribution along with good antimicrobial efficacy.

#### 5.3.2. Characterization of the Nanocomposites

##### 5.3.2.1. UV-Vis Spectroscopy

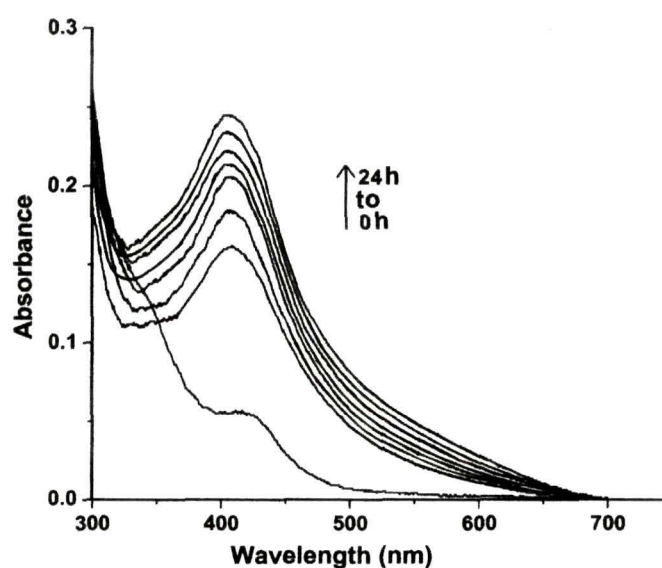
The formation of silver nanoparticles in HBPE/clay nanocomposite system was first observed by UV-visible absorption study (Fig. 5.2). No absorption peak was observed in the UV-visible absorption spectrum of HBPE/clay nanocomposite before reduction of Ag<sup>+</sup> due to its d<sup>10</sup> electronic configuration. However, after reduction of Ag<sup>+</sup> ions to

$\text{Ag}^0$  a strong absorption at about 407 nm was observed which is characteristic of surface plasmon absorption of silver metal as  $\text{Ag}^0$  nanoparticles are known to exhibit intense plasmon absorption band in this region.<sup>25</sup> Further as the nature of the spectrum was

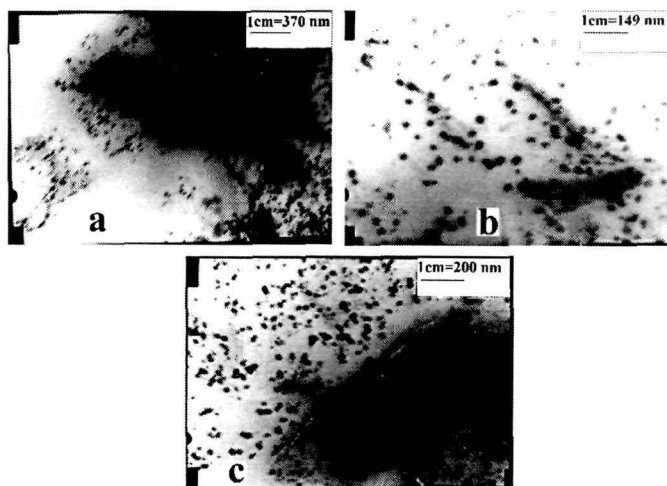


**Fig. 5.1:** Silver nanoparticles (A) and silver salt solution before reduction (B) in nanocomposite

almost symmetrical, so it was expected that the nanoparticles are well-dispersed and spherical in shape. These are further supported by TEM studies (Fig. 5.3). Again, a common confrontation encountered in nanoparticles preparation is that of agglomeration upon storage. However, the retention of the peak sharpness and position at 407 nm indicated the stability of the system even for the samples analyzed after 6 months of preparation and storage at room temperature. This high stability of nanoparticles is due to the unique architectural feature of the HBPE and also the presence of nanoclay with polar hydroxyl groups.



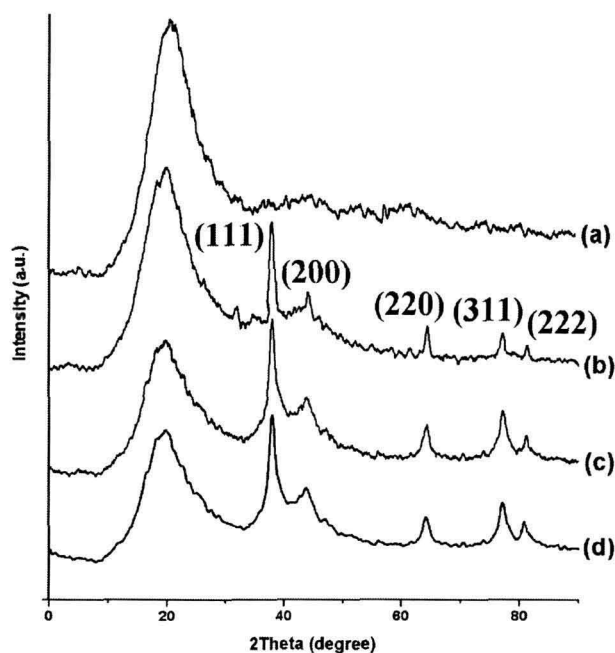
**Fig. 5.2:** UV-visible spectra for silver nanoparticles against time during reduction



**Fig. 5.3:** TEM micrographs for (a) PENCAg1, (b) PENCAg3 and (c) PENCAg5

### 5.3.2.2. XRD Study

Fig. 5.4 illustrates a typical X-ray diffractograms of the silver nanocomposites showing five prominent peaks at  $2\theta$  values of about  $38^\circ$ ,  $44^\circ$ ,  $64^\circ$ ,  $77^\circ$  and  $81^\circ$ , well in agreement with the literature values of silver nanoparticles.<sup>26</sup> These peaks are indexed to the (1 1 1), (2 0 0), (2 2 0), (3 1 1) and (2 2 2) planes representing Bragg's reflections for the face-centered cubic symmetry of silver. The hump at  $2\theta = 19\text{-}20^\circ$  is attributed to the amorphous nature of HBPE. The size of the nano-Ag grains ( $2\theta = 38^\circ$ ) was estimated by using Debye-Scherrer's formula,  $D = 0.9\lambda/\beta\cos\theta$ , where  $D$  is the crystallite size in

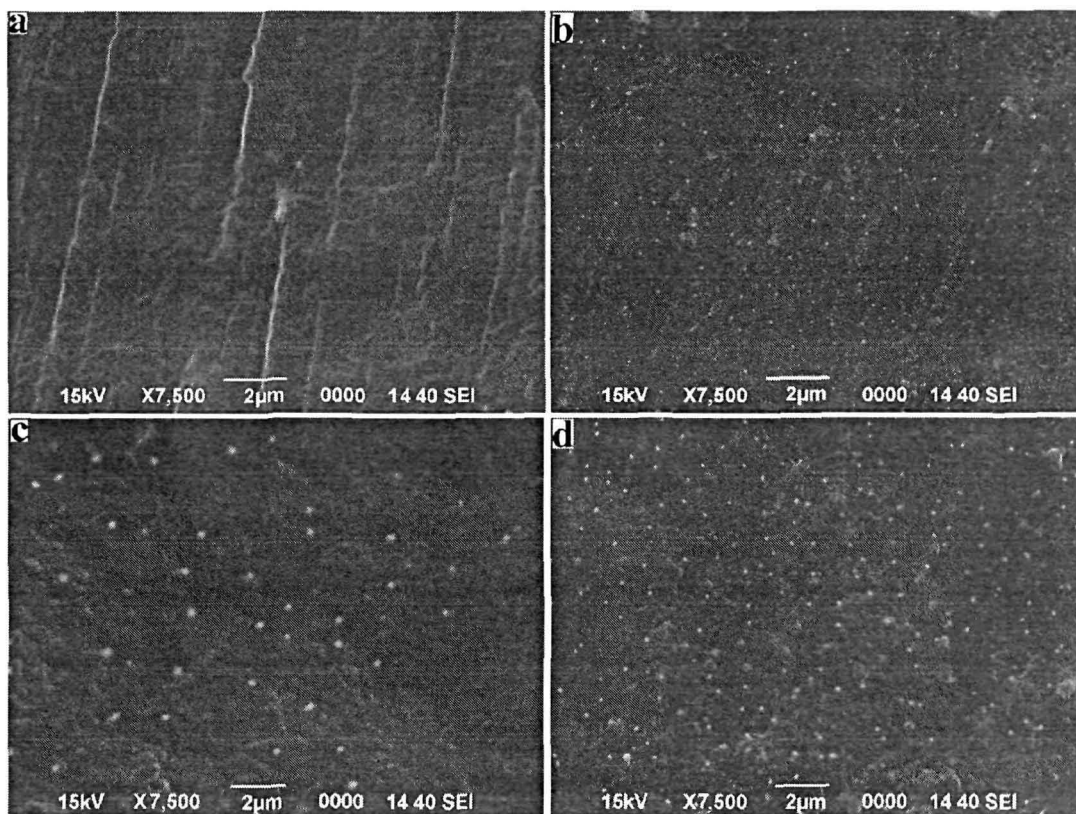


**Fig. 5.4:** XRD diffractograms for (a) PENCAg0, (b) PENCAg1, (c) PENCAg3 and (d) PENCAg5

nm,  $\lambda$  is the radiation wavelength (0.154 nm for Cu K $\alpha$ ),  $\beta$  is the full bandwidth at half-height and  $\theta$  is the diffraction peak angle.<sup>27</sup> The calculated crystallite average size was found to be 14 nm, which is in agreement with average diameter of silver nanoparticles estimated by TEM.

### 5.3.2.3. SEM Study

SEM micrographs were used to evaluate the surface morphology of the silver nanoparticles deposited on the surface. As shown in Fig. 5.5, ultra-fine and disaggregated silver nanoparticles were homogeneously distributed on the surface of HBPE/clay nanocomposite matrix. The silver particles were granular in nature and appeared to be nanosize, typically in the range of < 50 nm, which was in agreement with the XRD and TEM observations.



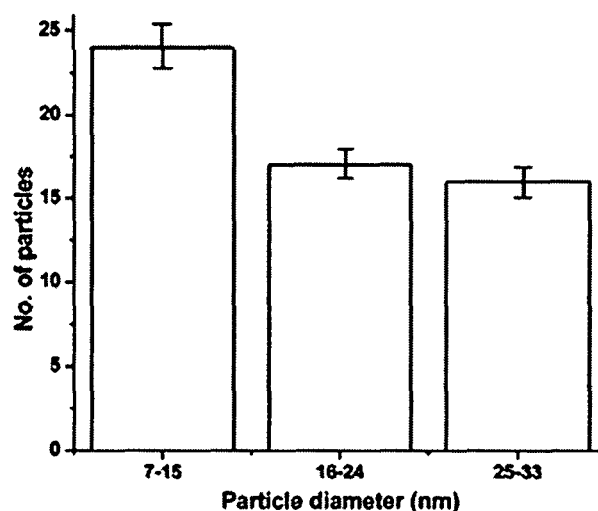
**Fig. 5.5:** SEM micrographs for (a) PENCAg0, (b) PENCAg1, (c) PENCAg3 and (d) PENCAg5

### 5.3.2.4. TEM Study

TEM studies (Fig. 5.3) confirmed that silver nanoparticles were not agglomerated but rather well-dispersed and almost spherical in shape. The histogram of the particles size distributions (Fig. 5.6) indicated that silver nanoparticles size distribution ranged from



7 to 32 nm. Most of the particles had average size of about 15 nm. The size distribution of the particles was also found to be narrow. Some smaller aggregates were also seen in Fig. 5.3, but their diameters were below 50 nm. The reason for this distribution is the strong interactions between the polar carboxylic ester groups of the polymer or the -OH group of clay and the silver nanoparticles. This leads to a good adsorption of the polyester chains on the silver nanoparticles. This means the silver nanoparticles were completely embedded by the polyester chains preventing the growth or agglomeration of the silver nanoparticles.

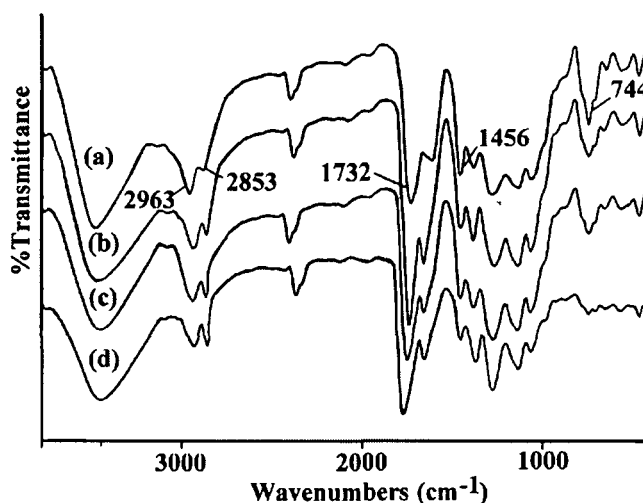


*Fig. 5.6: Bar diagram for size distributions of silver nanoparticles*

#### 5.3.2.5. FTIR Study

Fig. 5.7 shows the infrared spectra for the silver nanocomposites. The analysis showed that the spectral features of nanocomposites with and without silver were not so different. The differences were observed only in the intensity of their peaks. It was observed from Fig. 5.7 that after formation of silver nanocomposites the intensity of  $-\text{CH}_2$  symmetric stretching at  $2857\text{ cm}^{-1}$  increased and asymmetric band at  $2926\text{ cm}^{-1}$  decreased. It is well known that the peak positions for symmetric and asymmetric  $-\text{CH}_2$  stretching vibration can be used as the sensitive indicator of the alkyl chains.<sup>28</sup> This difference in intensity is characteristic of highly ordered conformation. Also the  $\text{C}=\text{O}$  stretching frequency of the carboxylic ester groups of HBPE observed at  $1732\text{ cm}^{-1}$  got slightly increased with the increase in amount of silver content after the formation of nanocomposites. The result indicated a strong interaction between esters and silver nanoparticles. With the increase of silver content it was also seen from the figure that the intensity of  $-\text{CH}_2$  deformation peak ( $1456\text{ cm}^{-1}$ ) of the nanocomposites with silver decreased along with diminishing of peak intensity observed at  $744\text{ cm}^{-1}$ , which is due

to –C-H out of plane deformation of aliphatic hydrocarbon chain of the system. This confirmed the interaction of silver nanoparticles with the matrix as well as nanoclay layers.

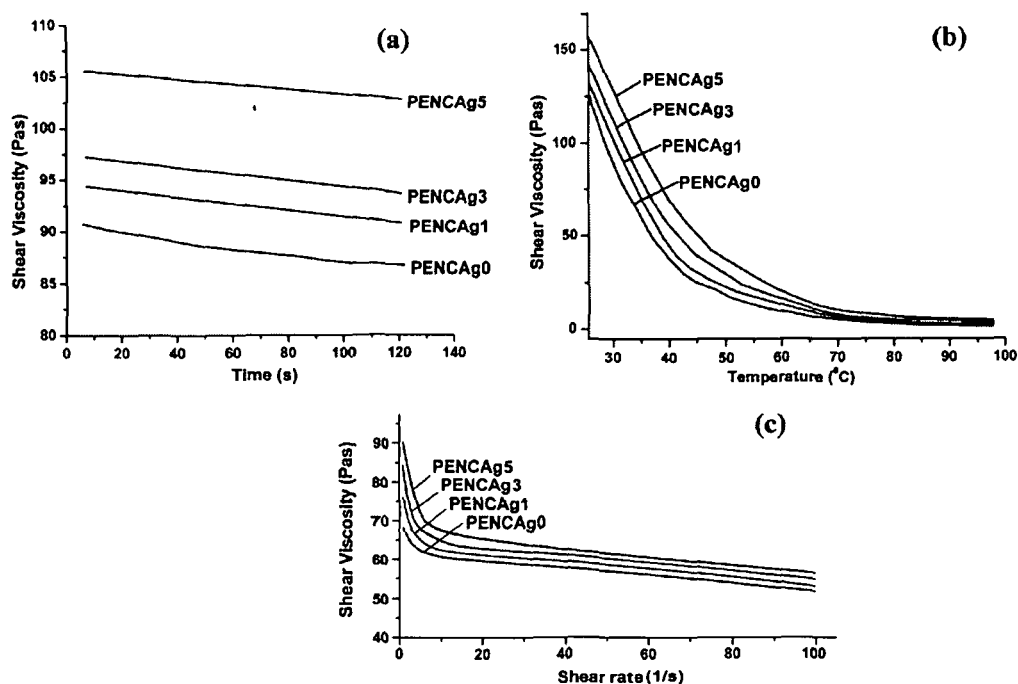


*Fig. 5.7: FTIR spectra for (a) PENCAg0, (b) PENCAg1, (c) PENCAg3 and (d) PENCAg5*

### 5.3.3. Rheological Behaviors

The rheological behaviors of silver nanocomposites were studied utilizing the controlled strain rheometer equipped with parallel plate geometry through oscillatory measurements. At controlled stress and single shear value, an overall enhancement of viscosity in the silver nanocomposites was observed with the increase in amounts of silver, was found to decrease slightly although the viscosity with time [Fig. 5.8(a)]. This enhanced viscosity is ascribed to higher interaction level of silver nanoparticles with the polymer chains and along with the clay which may also partially obstruct segmental movements.<sup>29</sup> Also this interaction results in higher effective silver content and less number of polymer segments partaking in the bulk flow process. From the variation of shear viscosities as a function of temperature in the range of 25-100 °C at shear stress of 70 Pa [Fig. 5.8(b)], the flow behavior of silver nanocomposites was observed. The viscosity was found to decrease in all the silver nanocomposite systems, owing to increase in kinetic energy of the molecules present. Shear thinning behavior was observed in the Fig. 5.8(c), where shear viscosity of the nanocomposite systems decreased with the increase of shear rate. The shear viscosity was also increased with silver content over an extensive range of shear rates. Because of this shear-thinning asset, as already mentioned, the nanocomposites can be processed in the melt state using the conventional equipment available in a manufacturing line. Also, this shear

thinning of the materials is an added advantage in application of the coating during spray or brushing and eliminates or minimizes the sagging problem.



*Fig. 5.8: Variation of shear viscosity of silver nanocomposites against (a) time at constant stress and temperature, (b) temperature under constant stress and (c) shear rate under constant temperature*

#### 5.3.4. Curing Studies of HBPE/Clay Silver Nanocomposites

The cure rate of HBPE/clay silver nanocomposites increased with the silver loading compared to the pristine resin (Table 5.1). This increase is due to the catalytic effect of silver nanoparticles. The basicity of DMF may also influence the crosslinking reaction. Since sizes of the silver particles are small and spherical in shape, their surface areas are high. Thus they strongly interact with the polymer chains and thereby bring resins and clay system in close proximate, which helps in the crosslinking reaction. Further, silver nanoparticles may also act as catalyst in crosslinking reaction due to electropositive character.<sup>30</sup>

#### 5.3.5. Performance Characteristics

The different performance characteristics of the prepared HBPE/clay silver nanocomposites like tensile strength, elongation at break, gloss, impact resistance and scratch hardness were determined and are given in Table 5.1.

The tensile strength of HBPE/clay silver nanocomposites was found to improve to a noticeable degree from 7.10 to 11.6 N/mm<sup>2</sup> with the increase of amount of silver

from 0 to 5 wt.%. This is attributed to the inclusion of homogeneously dispersed silver nanoparticles into the clay layers that are further delaminated by the polymer chains, thereby strengthening the matrix system. Also maximum surface of the silicate layers are available for strong interaction with the polymer chains and silver nanoparticles after delamination of the aluminosilicate clay layers which leads to increase in tensile strength with the silver contents. The increase of crosslinking density as indicated by swelling results (Table 5.1) due to increase of silver loading is also responsible for enhancement of strength property of the nanocomposites films. A smooth surface

**Table 5.1:** Performance characteristics of the HBPE/clay silver nanocomposites

Property	HBPE	PENCAg0	PENCAg1	PENCAg3	PENCAg5
Gloss at 60°	98	104	110	117	130
Scratch hardness (kg)	7	10	11	11.5	12.6
Impact hardness (cm)	80	95	97	100	100
Tensile strength (N/mm <sup>2</sup> )	2.68	7.10	8.5	9.74	11.6
Elongation at break (%)	24	140	134	130	118
Curing time (h at 120 °C)	3	2	2	1.75	1.5
Swelling (%) in xylene	32	30	29.86	24.76	21.37

obtained due to the better crosslinking of the cured films leads to augmentation of gloss characteristics of the films after the formation of nanocomposites. These escalation results are due to better compatibility of silver nanoparticles with the polyester along with clay. The gloss value was found to increase with the silver content as large amount of light is reflected from the smooth surface. The scratch hardness value of the films was found to be increased for the nanocomposites with silver as compared to the nanocomposite without silver. The nanoclay layers along with uniformly disseminated nano sized silver nanoparticles proficiently restrict indentation in the nanocomposites. At high silver contents, it was observed that the viscosity of the resin during the processing of nanocomposites increases significantly and hence the entrapped air cannot escape from the matrix. The impact resistance of the prepared nanocomposites increases as the amount of silver loading increases from 1 to 5 wt.%. The evenly distributed nanosize silver particles have an imperative role for this improvement by interacting with the polyester segments of the matrix along with the nanoclay platelets. The presence of high interactions by small silver nanoparticles resulted high rigidity.

So, they interact with the polymer chains and restrict their mobility which increases the strength of the silver nanocomposites films.

The chemical resistance of the cured nanocomposites films with or without silver was tested by subjecting them in various chemical environments (Table 5.2) for 15 days at room temperature. It was found that the resistivity of silver nanocomposites film towards dilute HCl acid, aqueous NaCl solution and distilled water increases appreciably with increasing silver content without any leaching out of silver nanoparticles. However, due to the presence of alkali hydrolyzable ester group the

**Table 5.2:** Chemical resistance of the HBPE/clay silver nanocomposites

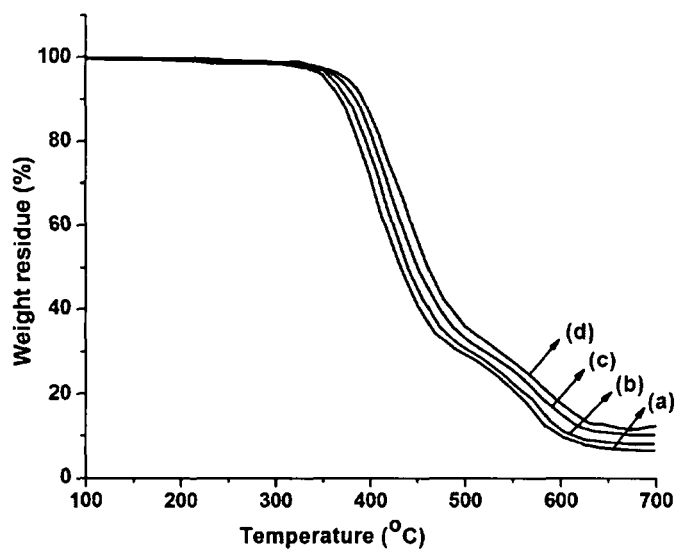
Types of media	Weight loss (%)				
	HBPE	PENCAg0	PENCAg1	PENCAg3	PENCAg5
5 wt % aqueous NaOH	9.16	4.21	3.41	2.17	1.83
25 wt % aqueous HCl	1.20	0.48	0.47	0.37	0.15
25 wt % aqueous NaCl	2.06	0.64	0.58	0.43	0.18
Distilled water	0.90	0.29	0.18	0	0

resistance of the silver nanocomposites towards alkali was not so profound. In presence of alkali it was found that some amount of silver nanoparticles were leached out from the film surface, which was confirmed by observing absorption peak in UV-visible spectrum. As the silver amount increases, enhancement of resistivity towards all the media was observed due to compact and crosslinked structure of the nanocomposites where silver nanoparticles interact with the nanoclay layers along with polyester chains. The permeability of the silver nanocomposites is also reduced by delamination of the clay layers through insertion of silver nanoparticles and the polymer chains. Due to this the different ions or species present in different media cannot easily penetrate the surface and thereby increases the resistance.

### 5.3.6. Thermal Properties

The TGA thermograms of the nanocomposites with different silver contents are shown in Fig. 5.9. The thermal stability of the silver nanocomposites was found to improve with the increase of the amount of silver. The onset of the thermal degradation temperatures was enhanced by about 10, 13 and 20 °C for PENCAg1, PENCAg3 and PENCAg5 nanocomposites respectively. This may be due to enhancement of intermolecular attraction among the polymer chains by the presence of fine spherical

silver nanoparticles. The degradation of polymers starts with free radical formations at weak bonds and/or chain ends, followed by their transfer to adjacent chains via inter-chain reactions.<sup>31</sup> The improved thermal stability can also be explained through the reduced mobility of the polyester chains in the nanocomposite. The presence of small amounts of silver in the HBPE/clay system confined the motion of polymer chains and served as a nucleation site for enhanced crystallization of nanocomposites. Because of reduced chain mobility, the chain transfer reaction will be suppressed and consequently



**Fig. 5.9:** TGA thermograms for (a) *PENCAg0*, (b) *PENCAg1*, (c) *PENCAg3* and (d) *PENCAg5*

the degradation process will be slowed and decomposition will take place at high temperatures.<sup>32</sup> The incorporation of nanoclay into the matrix also acts as a superior insulator and mass transport barrier to the volatile products generated during decomposition which enhances the overall thermal stability.

### 5.3.7. Antibacterial Properties

The antibacterial efficacy of the HBPE/clay silver nanocomposites was tested against the microbes based on zone of inhibition tests. Table 5.3 details the relative retention of activity (zone of inhibition) of HBPE, nanocomposites with and without silver against Gram positive bacteria (*Staphylococcus aureus* and *Bacillus subtilis*), Gram negative bacteria (*Escherichia coli* and *Pseudomonas aeruginosa*) and Fungi (*Candida albicans*). After 24 h of incubation, the zones of inhibition of the nanocomposites with silver against Gram negative and Gram positive bacteria ranged from 10 to 19 mm (Table 5.3), whereas nanocomposite without silver as well as pristine HBPE did not show any zone of inhibition. The nanocomposites with silver exhibited significant

efficacy against bacteria, especially against *Escherichia coli*, and also the efficacy increased with the increase of silver content. These results thus confirmed that the nanocomposites with silver have good antimicrobial efficacy against these bacteria.

However, the mechanism of bactericidal action of silver nanoparticles is still not well understood. The silver nanoparticles bind strongly to electron donor groups in biological molecules containing sulphur, oxygen or nitrogen.<sup>33</sup> This may result in the formation of defects in the bacterial cell wall so that cell contents are lost. It is reasonable to state that the binding of the particles to the bacteria depends on the surface area available for such interactions. The smaller particles with a larger surface-to-volume ratio provided a more efficient means of antibacterial activity than larger particles. A complex formation with proteins may disturb the metabolism of bacterial cells and their power functions, such as permeability and respiration.<sup>34</sup> Both effects lead to death of the bacterial cells. Sulphur-containing proteins in the membrane or inside the cells as well as phosphorus-containing elements, such as DNA, are likely to be the preferential sites for silver nanoparticles interaction and thereby preventing cell reproduction. One more possibility would be the release of silver ions from nanoparticles, which will have an additional contribution to the bactericidal properties of silver nanoparticles. Overall comparison of the microbial reduction rates in the present study revealed Gram-negative bacteria to be more susceptible to the antimicrobial effects of silver than Gram positives, presumably due to their thinner murine wall, which may allow more rapid absorption of silver into the cell.<sup>35</sup>

**Table 5.3: Antimicrobial activity of HBPE/clay silver nanocomposites**

Microbes	Zone of inhibition (mm)						Ampicillin	Nystatin <sup>#</sup>
	HBPE	PENC	PENC	PENC	PENC	PENC		
		Ag0	Ag1	Ag3	Ag5			
<b>Gram (+) bacteria</b>								
<i>S. aureus</i>	0	0	10	14	17	26	-	
<i>B. subtilis</i>	0	0	0	0	14	20	-	
<b>Gram (-) bacteria</b>								
<i>E. coli</i>	0	0	13	17	19	23	-	
<i>P. aeruginosa</i>	0	0	10	12	16	12	-	
<b>Fungi</b>								
<i>C. albicans</i>	0	0	0	0	0	0	18	

<sup>#</sup> Nystatin is used for *Candida*. For all others Ampicillin is used as positive control

Again, the silver nanocomposites were found ineffective against *Candida albicans*. This may be because of the difference in *Candida albicans*'s cell wall composition than that of the bacteria's used, as prokaryotic cell wall differs from that of eukaryotic cell wall.

### 5.4. Conclusions

From the above studies it can be concluded that silver nanoparticles embedded HBPE/clay nanocomposites were prepared using a simple *in-situ* chemical reduction technique using DMF as a reducing agent under ambient conditions. Nanoclay was successfully employed as nanofiller for property improvement of the pristine polymer as well as a supporting material for the stabilization of the silver nanoparticles. The prepared silver nanocomposites exhibited enhanced performance characteristics such as tensile strength, scratch hardness, impact resistance, chemical resistance and thermal properties over the pristine polyester system. The fabricated nanocomposites with silver showed enhanced antibacterial efficacy against Gram negative bacteria (*E. coli* and *P. aeruginosa*). These results suggest that the nanocomposites with silver have the potentiality to be considered as effective and long lasting bactericidal surface coating material in future antibacterial applications.

### References

1. Monteiro, D.R. *et al.* The growing importance of materials that prevent microbial adhesion: Antimicrobial effect of medical devices containing silver. *Int. J. Antimicrob. Agents* **34**, 103-110 (2009)
2. Stobie, N. *et al.* Prevention of Staphylococcus epidermidis biofilm formation using a low-temperature processed silver-doped phenyltriethoxysilane sol-gel coating. *Biomaterials* **29**, 963-969 (2008)
3. Lee, S.B. *et al.* Permanent, nonleaching antibacterial surfaces. 1. Synthesis by atom transfer radical polymerization. *Biomacromolecules* **5**, 877-882 (2004)
4. Pang, X.; Zhitomirsky, I. Electrodeposition of hydroxyapatite-silver-chitosan nanocomposite coatings. *Surf. Coat. Technol.* **202**, 3815-3821 (2008)
5. Murata, J.H.H.; Koepsel, R.R.; Russell, A.J.; Matyjaszewski, K. Antibacterial polypropylene via surface-initiated atom transfer radical polymerization. *Biomacromolecules* **8**, 1396-1399 (2007)



## Chapter 5

6. Lee, D.; Cohen, R.E.; Rubner, M.F. Antibacterial properties of Ag nanoparticle loaded multilayers and formation of magnetically directed antibacterial microparticles. *Langmuir* **21**, 9651-9659 (2005)
7. Luo, N.; Wu, Z.; Mou, N.; Jiang, L.; Wu, D. Preparation and characterization of polyimide/silica/silver composite films. *Front. Chem. Eng. China* **2**, 291-295 (2008)
8. Shao, H.; Zhong, S. Preparation and characterization of supported polyimide-silica-silver hybrid membranes. *Acta Polym. Sin.* **4**, 513-518 (2005)
9. Kim, Y.H.; Lee, D.K.; Cha, H.G.; Kim, C.W.; Kang, Y.S. Synthesis and Characterization of Antibacterial Ag-SiO<sub>2</sub> Nanocomposite. *J. Phys. Chem. C* **111**, 3629-3635 (2007)
10. Chang, L.T.; Yen, C.C. Studies on the preparation and properties of conductive polymers. VIII. Use of heat treatment to prepare metallized films from silver chelate of PVA and PAN. *J. Appl. Polym. Sci.* **55**, 371-374 (1995)
11. Shanmugam, S.; Viswanathan, B.; Varadorojan, T.K. A novel single step chemical route for noble metal nanoparticles embedded organic-inorganic composite films. *Mater. Chem. Phys.* **95**, 51-58 (2005)
12. Lin, W.C.; Yang, M.C. Novel silver/poly (vinyl alcohol) nanocomposites for surface-enhanced Raman scattering-active substrates. *Macromol. Rapid Commun.* **26**, 1942-1947 (2005)
13. Pinchuk, A.; Hilger, A.; von Plessen, G.; Kreibitz, U. Substrate effect on the optical response of silver nanoparticles. *Nanotechnology* **15**, 1890-1896 (2005)
14. Chang, W.C.W.; Nie, S. Quantum dot bioconjugates for ultrasensitive nonisotopic detection. *Science* **281**, 2016-2018 (1998)
15. Kim, Y.; Johnson, R.C.; Hupp, J.T. Gold nanoparticle-based sensing of "spectroscopically silent" heavy metal ions. *Nano Lett.* **1**, 165-167 (2001)
16. Chen, Q. *et al.* Magnetron sputtering synthesis silver and organic PEO nanocomposite. *Surf. Coat. Technol.* **202**, 5576-5578 (2008)
17. Kim, Y.H. *et al.* Bulk like thermal behavior of antibacterial Ag-SiO<sub>2</sub> nanocomposites. *J. Phys. Chem. C* **113**, 5105-5110 (2009)
18. Jones, S.K.; Winter, J.G.; Gray, B.N. Treatment of experimental rabbit liver tumours by selectively targeted hyperthermia. *Int. J. Hyperthermia* **18**, 117-128 (2002)

19. Kim, D.K. *et al.* Superparamagnetic iron oxide nanoparticles for bio-medical applications. *Scripta Mater.* **44**, 1713-1717 (2001)
20. Tomalia, D.A.; Dvornic, P.R. What promise for dendrimers? *Nature* **372**, 617-618 (1994)
21. Zhang, Y. *et al.* Hyperbranched poly(amidoamine) as the stabilizer and reductant to prepare colloid silver nanoparticles in situ and their antibacterial activity. *J. Phys. Chem. C* **112**, 2330-2336 (2008)
22. Turkoglu, A.; Duru, E.M.; Mercan, N.; Kivrak, I.; Gezer, K. Antioxidant and antimicrobial activities of *Laetiporus sulphureus* (Bull.) Murrill. *Food Chem.* **101**, 267-273 (2007)
23. Khanna, P.K. *et al.* Synthesis and characterization of Ag/PVA nanocomposite by chemical reduction method. *Mater. Chem. Phys.* **93**, 117-121 (2005)
24. Pastoriza-Santos, I.; Liz-Marzan, L.M. Formation and stabilization of silver nanoparticles through reduction by *N,N*-dimethylformamide. *Langmuir* **15**, 948-951 (1999)
25. Voronov, A.; Kohut, A.; Vasylyev, S.; Peukert, W. Mechanism of silver ion reduction in concentrated solutions of amphiphilic invertible polyesters in nonpolar solvent at room temperature. *Langmuir* **24**, 12587-12594 (2008)
26. Bakar, N.H.H.A.; Ismail, J.; Bakar, M.A. Synthesis and characterization of silver nanoparticles in natural rubber. *Mater. Chem. Phys.* **104**, 276-283 (2007)
27. Welham, N.J. Formation and characterization of germanium nanoparticles. *J. Mater. Res.* **15**, 2400-2407 (2000)
28. Mahapatra, S.S.; Karak, N. Silver nanoparticle in hyperbranched polyamine: Synthesis, characterization and antibacterial activity. *Mater. Chem. Phys.* **112**, 1114-1119 (2008)
29. Chae, D.W.; Oh, S.G.; Kim, B.C. Effect of silver nanoparticles on the dynamic crystallization behavior of nylon-6. *J. Polym. Sci. Part B: Polym. Phys.* **42**, 790-799 (2004)
30. Murugadoss, A.; Chattopadhyay, A. A "green" chitosan-silver nanoparticle composite as a heterogeneous as well as micro-heterogeneous catalyst. *Nanotechnology* **19**, 015603 (6pp) (2008)
31. Mbhele, Z.H. *et al.* Fabrication and characterization of silver-polyvinyl alcohol nanocomposites. *Chem. Mater.* **15**, 5019-5024 (2003)

## Chapter 5

32. Chou, C.W.; Hsu, S.H.; Chang, H.; Tseng, S.M.; Lin, H.R. Enhanced thermal and mechanical properties and biostability of polyurethane containing silver nanoparticles. *Polym. Degrad. Stab.* **91**, 1017-1024 (2006)
33. Weir, E.; Lawlor, A.; Whelan, A.; Regan, F. The use of nanoparticles in antimicrobial materials and their characterization. *Analyst* **133**, 835-845 (2008)
34. Damm, C.; Münstedt, H.; Rösch, A. The antimicrobial efficacy of polyamide-6/silver-nano-and microcomposites. *Mater. Chem. Phys.* **108**, 61-66 (2008)
35. Rhim, J.W.; Hong, S.I.; Park, H.M.; Ng, P.K.W. Preparation and characterization of chitosan-based nanocomposite films with antimicrobial activity. *J. Agric. Food Chem.* **54**, 5814-5822 (2006)

## CHAPTER 6

---

### *Mesua ferrea* L. Seed Oil Based HBPE/MWCNTs Nanocomposites

#### 6.1. Introduction

Nowadays with the hasty advancement of nanoscience and technology, extensive research and development are implemented on high performance polymeric nanomaterials for targeted applications in various fields.<sup>1</sup> The amalgamation of nanoscale reinforcements into the polymer matrix is also an endeavor to develop polymer nanocomposites in different scientific and industrial fields. After the first report by Iijima in 1991,<sup>2</sup> the carbon nanotubes (CNTs), due to their excellent potentiality in unique nanostructure with inimitable physical characteristics, remarkable electrical and mechanical properties, and high aspect ratios, are ideal advanced reinforcing agents for polymer nanocomposites.<sup>3,4</sup> The reinforcing effects of CNTs in polymer nanocomposites are generally optimized by the degree of dispersion, their alignment and the interfacial adhesion between the CNTs and the polymer matrix. However, due to high aspect ratio and strong van der Waals attractions, CNTs are often tend to bundle together leading to some agglomeration which result an inhomogeneous dispersion in polymer matrices. Also the surface of CNTs provides poor interfacial adhesion to the matrix, which limits effective load transfer from the matrix to the nanotubes.<sup>5</sup> Therefore, to improve the dispersion and interfacial adhesion between CNTs and the polymer matrix, functionalization of CNTs has been done in most of the cases via oxidative method by using surfactant and ultrasonication.

In recent days, the development of biodegradable polymeric materials with desired material's properties is an issue of active research interest to the academia and industrialists. This is due to the concerns over the persistence of polymers in the environment, shortage of landfill space, emissions during incineration, and negative impact on wildlife through ingestion and entrapment.<sup>6,7</sup> Its pertinent to mention that biodegradable polyesters synthesized from diol and dicarboxylic acid through polycondensation reaction are commercially promising high performance materials complemented by low-cost inputs and easy production-processibility.<sup>8,9</sup> The biodegrad

-ability of these polymers is due to the hydrolyzable ester bond present in their main chain, which is susceptible to hydrolysis and microbial attack, and leads to the formation of low molecular weight and eventually to fine chemicals.<sup>10</sup> Other factors revealing the biodegradation include molecular weight, hydrophobic/hydrophilic properties, degree of crystallinity and morphology.<sup>10</sup> Again, the tailor made properties and ease of fabrication make polymers excellent biomaterials. Desirable material properties, biocompatibility and time-frame dependent biodegradability are indispensable requisites for a polymeric biomaterial for specific application in the biomedical niche. In this context, development of CNTs-reinforced biodegradable polymeric biomaterial seems to be an interesting proposition.

These days, “going green” has become the steering guideline in various research domains including material science. This is of significance in the context of dwindling natural resources, global economic set-backs, and the intertwined problems of pollution and biological niche degradation. Exploiting plant based raw materials contributes to global sustainability without diminution of scarce resources.<sup>11</sup> In this perspective *Mesua ferrea* L. seed oil based HBPE is used as the matrix for preparation of modified MWCNTs nanocomposites. The potentiality of this oil based materials in different fields has already been reflected from the earlier reports.<sup>12-15</sup> The unique architecture, large surface functionalities and low viscosity of the highly branched polymer facilitate the dispersion of CNTs in the matrix through different physico-chemical interactions with the nanofillers.<sup>16</sup> To validate the prospects of using the reported nanocomposite as biomaterial with desired material properties, assessments on biodegradability and cytocompatibility are also reported. Thus, the present study stands at the intersection between nanotechnology and biology to develop environmentally benign application-oriented CNTs based polymer nanocomposites.

Therefore, in this chapter the preparation, characterization and properties of the *Mesua ferrea* L. seed oil based HBPE/MWCNTs nanocomposites are described. The effect of MWCNTs on various properties like mechanical, thermal, biodegradation and cytocompatibility of the HBPE matrix are also discussed. Thus the potentiality of HBPE/MWCNTs nanocomposites as biomaterial is primarily focused here.

## **6.2. Experimental**

### **6.2.1. Materials**

## Chapter 6

Multiwalled carbon nanotubes (MWCNTs) with diameter 10-20 nm and length of about 20  $\mu\text{m}$  were obtained from Iiljin Nanotech, Korea. The details about the MWCNTs were described in Chapter 1, section 1.3.1.2.

Potassium permanganate ( $\text{KMnO}_4$ ) was obtained from S.D. Fine Chemical Ltd., Mumbai. It appears as purplish-bronze-gray needles. Its m.p. is 240  $^\circ\text{C}$ ,  $M_w$  is 158.03 g/mol and density is 2.73  $\text{g/cm}^3$ . It was used as an oxidizing agent to modify the MWCNTs.

Cetyltrimethylammonium bromide (CTAB) was purchased from Merck, India. Its melting range is 237-243  $^\circ\text{C}$  and  $M_w$  is 364.45 g/mol. It was used as a surfactant in the modification of MWCNTs.

Acetic acid was obtained from Merck, India. It is a colorless liquid with  $M_w$  60.05 g/mol and density 1.049  $\text{g/cm}^3$ . Its m.p. is 16.5  $^\circ\text{C}$  and b.p. is 118.1  $^\circ\text{C}$

The other required chemicals and solvents such as *Mesua ferrea* L. seed oil, glycerol, PA, MA, bis-MPA, lead mono oxide, DMF, xylene, epoxy resin, poly(amido amine) etc. were of same specifications as described in Chapter 2, section 2.2.1. The necessary minerals used for preparation of bacterial broth culture to study the biodegradation were of same specifications as described in Chapter 4, section 4.2.1. The *Pseudomonas aeruginosa* bacteria with strains PN8A1 and vs1; and *Bacillus subtilis* with strain MTCC73 used for biodegradation study of the nanocomposites, along with all other items used for the RBC hemolysis protection assay were taken from the Department of Molecular Biology and Biotechnology (Department of Biotechnology, DBT Centre, Government of India), Tezpur University. All other reagents employed in the study were of reagent grade and used without further purification.

### **6.2.2. Instruments and Methods**

The FTIR and TGA analyses were carried out using the same instruments and conditions as mentioned in Chapter 2, section 2.2.2. and Chapter 3, section 3.2.2. respectively. The XRD, SEM and TEM were carried out using the same instruments and conditions as mentioned in Chapter 4, section 4.2.2. The measurements of gloss, impact resistance, scratch hardness and chemical resistance were performed according to the standard methods as described earlier in Chapter 2, section 2.2.2. The mechanical properties were evaluated by the similar methods as mentioned in the Chapter 2, section 2.2.2. Sonication was done with the same instrument as mentioned in Chapter 3, section

3.2.2. at fixed amplitude and a half cycle for proper dispersion of the nanotubes in the HBPE matrix.

*Mesua ferrea* L. seed oil was extracted from the matured seeds by the same method as described in Chapter 2, section 2.2.2. The percent of swelling of the nanocomposites films was determined using the same method as discussed in Chapter 2, section 2.2.2.

### 6.2.2.1. Purification and Modification of MWCNTs

The MWCNTs were purified by thermal annealing at 500 °C for 1 h in muffle furnace followed by their functionalization by the similar method as reported by Zhang et al.<sup>17</sup> Briefly, the modification method was as follows. A mixture of 0.12 g of nanotubes and 1.0 g of CTAB in 25 mL of dichloromethane was sonicated for 30 min. 5 g of KMnO<sub>4</sub> powder was then added in small portions over a period of 2 h followed by addition of 5 mL of acetic acid. The whole mixture was then stirred mechanically for 48 h at room temperature. The color of the mixture changed from dark purple to dark brown due to the reduction of Mn<sup>+7</sup> to Mn<sup>+</sup>. The final material was then obtained by post filtration of the mixture through Teflon membrane sheet followed by different washing steps with conc. HCl, water and finally acetone. The purified nanotubes were then dried under vacuum oven at 40-50 °C for 24 h before use.

### 6.2.2.2. Preparation of HBPE/MWCNTs Nanocomposites

The *Mesua ferrea* L. seed oil based HBPE was prepared by using the same method as described in the experimental section of Chapter 2, sections 2.2.2.1. Prior to the preparation of nanocomposites the HBPE was placed in a vacuum oven at 50 °C to remove entrapped volatiles. HBPE was then mechanically mixed with desired dose of modified MWCNTs for 30 min followed by ultrasonication for 30 min. After sonication, calculated amount of bisphenol-A based epoxy resin (polyester: epoxy = 60: 40 in weight ratio) and poly(amido amine) (25% with respect to epoxy resin) hardener were added and stirred mechanically for 30 min. The prepared nanocomposites were coded as PCNTC0.5, PCNTC1 and PCNTC2 corresponding to the amount of 0.5, 1 and 2 wt.% MWCNTs.

### 6.2.2.3. Fabrication of Nanocomposites into Thin Films and Their Curing

## Chapter 6

The prepared nanocomposite was degassed for 30 min under vacuum to make it completely bubble free. Thin films of the nanocomposites were then prepared by drawing the homogeneous mixture on mild steel plates (150 mm × 50 mm × 1.60 mm) and glass plates (75 mm × 25 mm × 1.75 mm) using a micro adjustable thickness gauge under ambient conditions. After removal of sufficient amount of solvent under atmospheric conditions, the coated strips were degassed under vacuum at  $(45 \pm 5)^\circ\text{C}$  for 45 min and kept overnight in a vacuum dessicator. Then the coated nanocomposite films were cured by heating at  $120^\circ\text{C}$  in an oven for a specified time period. The cured nanocomposite films were kept under ambient conditions for 24 h for further processing. Then the dried films were peeled off from the glass plates by immersing them in warm water. The films were kept in a dessicator under vacuum and stored for 7 days prior to testing. The thickness of the completely dried nanocomposite films was measured by the same instrument as described in Chapter 2 and was found to be in the range of 25-35  $\mu\text{m}$ . The curing time was determined similarly as discussed in the Chapter 2.

### *6.2.2.4. Preparation of Bacterial Culture Media*

The mineral salt medium for biodegradation study was prepared with the following composition. 2.0 g of  $(\text{NH}_4)_2\text{SO}_4$ , 2.0 g of  $\text{Na}_2\text{HPO}_4$ , 4.75 g of  $\text{KH}_2\text{PO}_4$ , 1.2 g of  $\text{MgSO}_4 \cdot 7\text{H}_2\text{O}$ , 0.5 mg of  $\text{CaCl}_2 \cdot 2\text{H}_2\text{O}$ , 100 mg of  $\text{MnSO}_4 \cdot 5\text{H}_2\text{O}$ , 70 mg of  $\text{ZnSO}_4 \cdot 7\text{H}_2\text{O}$ , 10 mg of  $\text{H}_3\text{BO}_3 \cdot 5\text{H}_2\text{O}$ , 100 mg of  $\text{CuSO}_4 \cdot 7\text{H}_2\text{O}$ , 1 mg of  $\text{FeSO}_4 \cdot 7\text{H}_2\text{O}$  and 10 mg of  $\text{MoO}_3$  using the similar method as described in Chapter 4, section 4.2.2.7.

### *6.2.2.5. Bacterial Strains*

Pure cultures of the bacterial strains were grown in nutrient broth by the same method as discussed in the Chapter 4, section 4.2.2.8. The growth of the tested bacterial strains was measured spectrophotometrically using the method as described in the Chapter 4, section 4.2.2.8.

### *6.2.2.6. Cytotoxicity by Hemolytic Activity Assay*

Fresh goat blood was collected from the slaughter house. Sodium citrate, dissolved in phosphate buffer saline (PBS), pH 7.4 was used as anticoagulant. The blood samples were immediately placed in an ice bath. Red Blood Cells (RBCs) were separated by centrifugation (3000 g for 10 min at  $25^\circ\text{C}$ ) and re-suspended in PBS. This procedure



was repeated until the supernatant became colorless. The packed cells were suspended in 4 volume of PBS to perform the experiment. The experimental nanocomposite films with uniform thickness were cut to obtain 10 mg sample for each. The films were surface sterilized under ultraviolet light for 30 min in a laminar air flow hood. The experiments were performed according to protocols described by Dutta et al.<sup>18</sup> and Hassan et al.<sup>19</sup> after slight modifications. 2 mL of erythrocyte suspension was treated with 10 mg of each type of film. H<sub>2</sub>O<sub>2</sub> solution with concentration of 100 μM and PBS (pH 7.4) was taken as positive and negative control respectively. The RBC suspensions were incubated for 30 min at 37 °C and then 200 μL of the suspensions was diluted to eight times using PBS solution. The samples were then centrifuged at 3000 g for 5 min at 25 °C and the absorption of the supernatant in each case was measured at a wavelength of 540 nm against PBS as the blank solution.

### **6.3. Results and Discussion**

#### ***6.3.1. Purification and Modification of MWCNTs***

Most of the production processes of CNTs, generate a range of carbonaceous particles such as amorphous carbon, fullerenes, nanocrystalline graphites, transition metal catalysts etc. Hence, it is indispensable to eliminate these effluents before using CNTs as nanofillers. Otherwise proper dispersion as well as interfacial adhesion of the nanotubes with the polymer matrix will not be proper. So, to remove these unwanted by-products thermal annealing in air or oxygen was done at 500 °C in furnace for selective etching of the amorphous carbons. Besides this other techniques like mechanical centrifugal separation, size exclusion chromatography and microfiltration may also be applied as well.

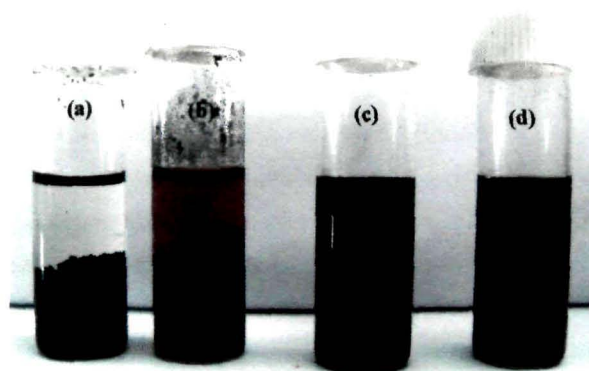
Functionalization of the thermally annealed MWCNTs, as described in the experimental section, generates carboxylic or hydroxyl groups on the sidewalls of the nanotubes.<sup>17</sup> These reactive groups facilitate the dispersion as well as interfacial adhesion of MWCNTs with the polyester matrix. CTAB acts as phase transferring agent which extracts the KMnO<sub>4</sub> into the organic medium (dichloromethane) containing the suspended nanotubes. The modification was done at ambient temperature as CTAB substantially decreases the activation energy and hence increases the rate of reaction. The acetic acid used in the reaction neutralizes the hydroxide ions and hence promotes the reaction further.<sup>20</sup>

### 6.3.2. Preparation of HBPE/MWCNTs Nanocomposites

Relatively lower stiffness and strength of polymers as compared to ceramics or metals limit the former's engineering or industrial applications. Impregnation with nanoscale materials is viewed as one of the many routes to overcome the challenge of poor mechanical attributes of vegetable oil based polyester resin. For this the modified MWCNTs were incorporated into HBPE matrix by *ex-situ* technique by intense mechanical mixing and ultrasonication. The presence of carboxyl/hydroxyl groups on the modified MWCNTs facilitates the dispersion of the nanotubes. The unique architecture and high surface functionality of the matrix along with its low viscosity help to enhance the interfacial adhesion between the ester groups of the matrix and the carboxyl/hydroxyl groups of MWCNTs through H-bonding. The use of high speed mechanical stirring and ultrasonication also aids in the de-agglomeration and proper dispersion of MWCNTs in the polyester matrix.<sup>21,22</sup>

### 6.3.3. Solvent Dispersibility

The modified MWCNTs were dispersed in different organic solvents such as ethanol, methanol, DMF, toluene, dichloromethane etc. The nanotubes tend to agglomerate due to their nanoscale dimensions, high surface energy and strong van der Waals interactions.<sup>23</sup> However, the functionalization of the MWCNTs and the formation of acidic groups dramatically improve the dispersibility in various solvents. Fig. 6.1 shows the dispersibility of neat-MWCNTs, modified MWCNTs and HBPE/MWCNTs nanocomposites in DMF post 15 days storage. In DMF, neat-MWCNTs agglomerated and sedimented at the bottom of the container, but the modified MWCNTs as well as the HBPE/MWCNTs were well-dispersed. The improved dispersion of HBPE/MWCNTs nanocomposites is due to the strong interactions of



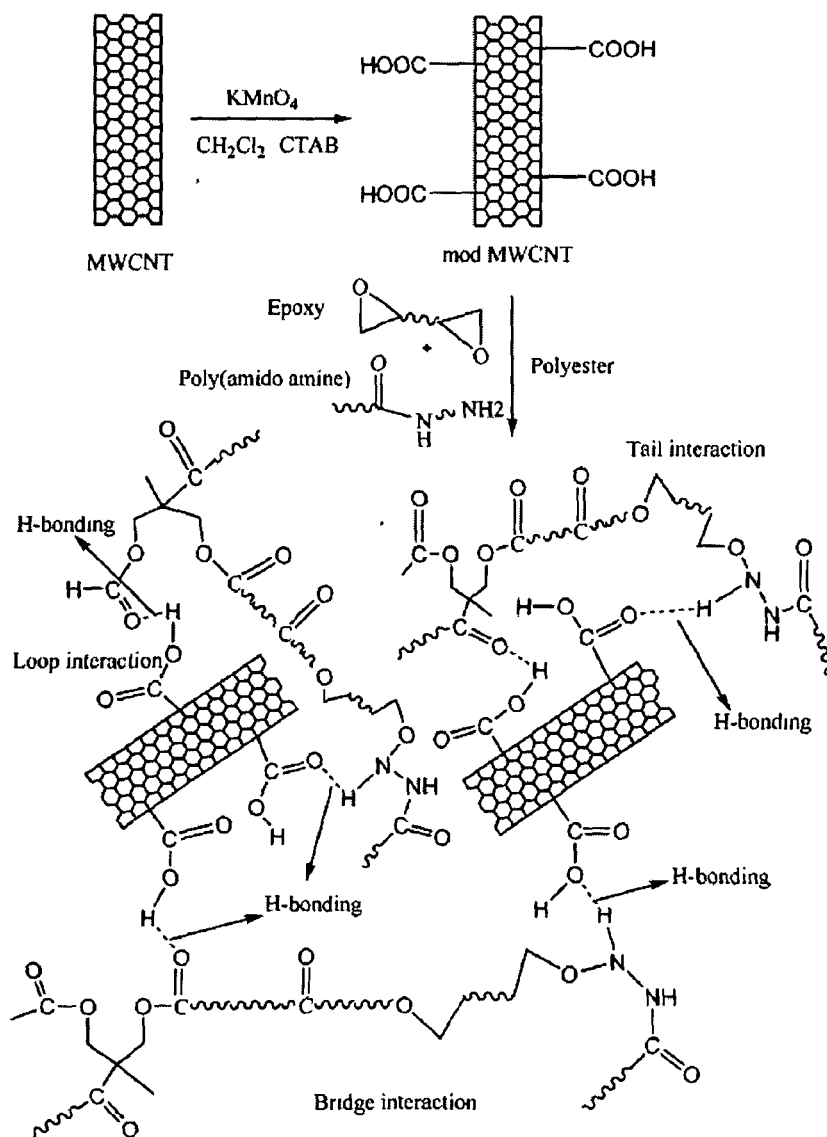
**Fig. 6.1:** Stability of neat MWCNTs in (a) DMF (b) HBPE, and modified MWCNTs in (c) DMF (d) HBPE nanocomposites

carboxyl/hydroxyl groups attached on the MWCNTs with the HBPE matrix through H-bonding (Scheme 6.1).

### 6.3.4. Characterization of Nanocomposites

#### 6.3.4.1. FTIR Study

FTIR spectra of neat and modified MWCNTs are shown in Fig. 6.2. For the neat MWCNTs, the band at  $3400\text{ cm}^{-1}$  is attributed to the presence of the hydroxyl groups ( $-\text{OH}$ ) on the surface of the MWCNTs. This could have appeared either from ambient moisture bound to the MWCNTs or during the purification of the raw material.<sup>24</sup> For modified MWCNTs, the characteristic band observed at  $1720\text{ cm}^{-1}$  corresponds to the stretching vibrations of carboxylic acid groups indicating the effective modification. The relative increase in intensity of the band at around  $3400\text{ cm}^{-1}$  suggests the presence



**Scheme 6.1:** Possible interactions of MWCNTs with polyester, epoxy and hardener system

of more -OH groups on the surface of the MWCNTs after oxidation and water treatment.<sup>25</sup>

Fig. 6.3 shows the FTIR spectra of the nanocomposites. The carboxylic groups on the MWCNTs are expected to enhance the interfacial interactions between the HBPE and MWCNTs. The broad band at  $3430\text{ cm}^{-1}$  is the result of overlapping of hydrogen bonded -OH stretching of polyester and -OH stretching of modified MWCNTs. Further, with the increase of MWCNTs loading the shifting of C=O band from  $1730$  to  $1710\text{ cm}^{-1}$  was observed. This is attributed to the interaction between the host polymer and nanofillers.

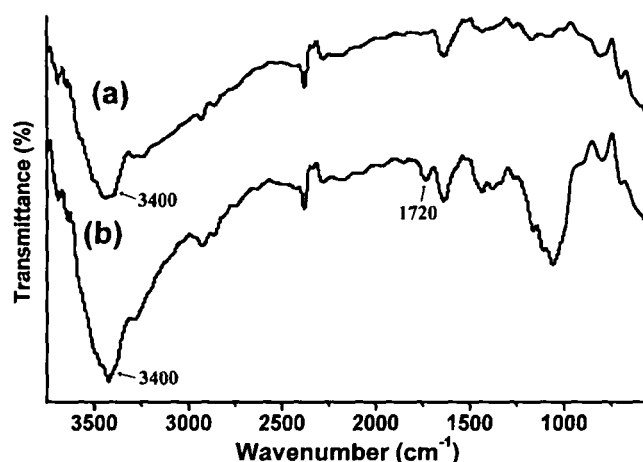


Fig. 6.2: FTIR spectra of (a) MWCNTs and (b) modified MWCNTs

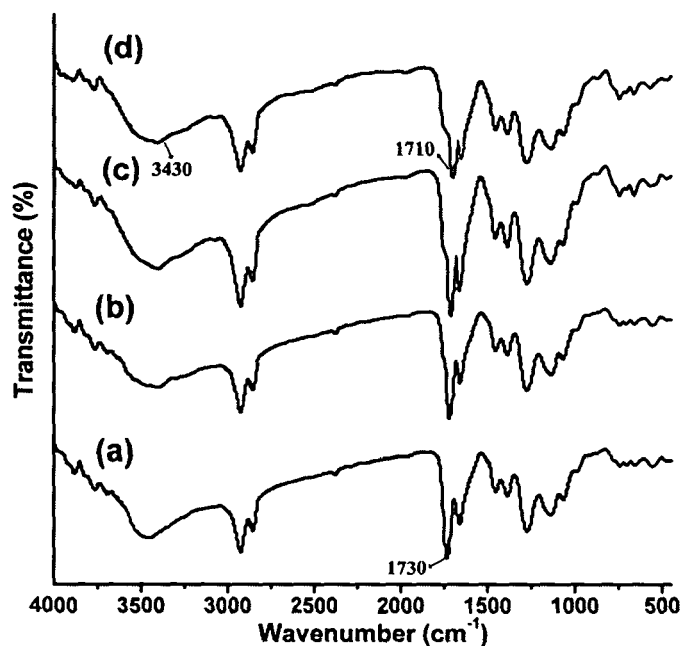
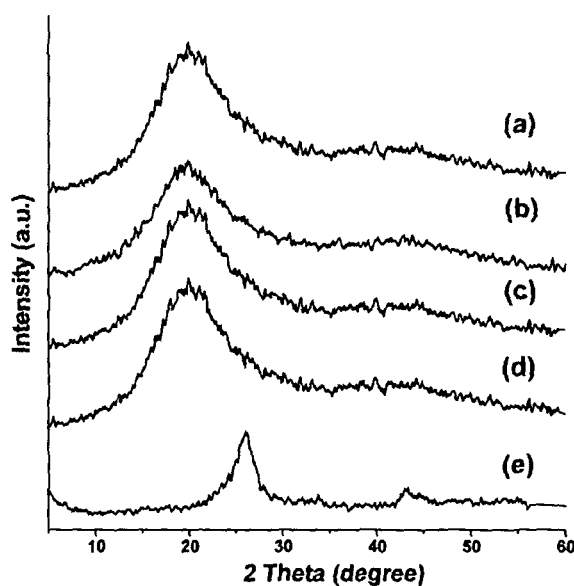


Fig. 6.3: FTIR spectra of (a) HBPE, (b) PCNTC0.5, (c) PCNTC1 and (d) PCNTC2

#### 6.3.4.2. XRD Study

Fig. 6.4 illustrates the XRD patterns of modified MWCNTs, HBPE and its nanocomposites with the addition of 0.5, 1 and 2 wt.% of MWCNTs. The pure HBPE showed a characteristic broad peak at around  $2\theta = 20^\circ$  which confirmed the amorphous nature of the polymer. The X-ray diffraction pattern of the MWCNTs revealed the presence of two crystalline peaks at  $2\theta = 25.9^\circ$  and  $43.1^\circ$ , corresponding to the inter-layer spacing of 0.34 nm and 0.21 nm attributed to (002) and (100) planes of the carbon atom, respectively. It was noticed that incorporation of MWCNTs does not significantly affect the structure of HBPE, as supported by the XRD pattern of the HBPE/MWCNTs nanocomposites. In this study, as low amounts of MWCNTs (up to 2 wt.%) were used to prepare the nanocomposites, so no noticeable X-ray diffraction peak appeared for MWCNTs in the nanocomposites (Fig. 6.4). The nanocomposites with high MWCNTs content may show significant diffraction peaks due to the presence of MWCNTs.



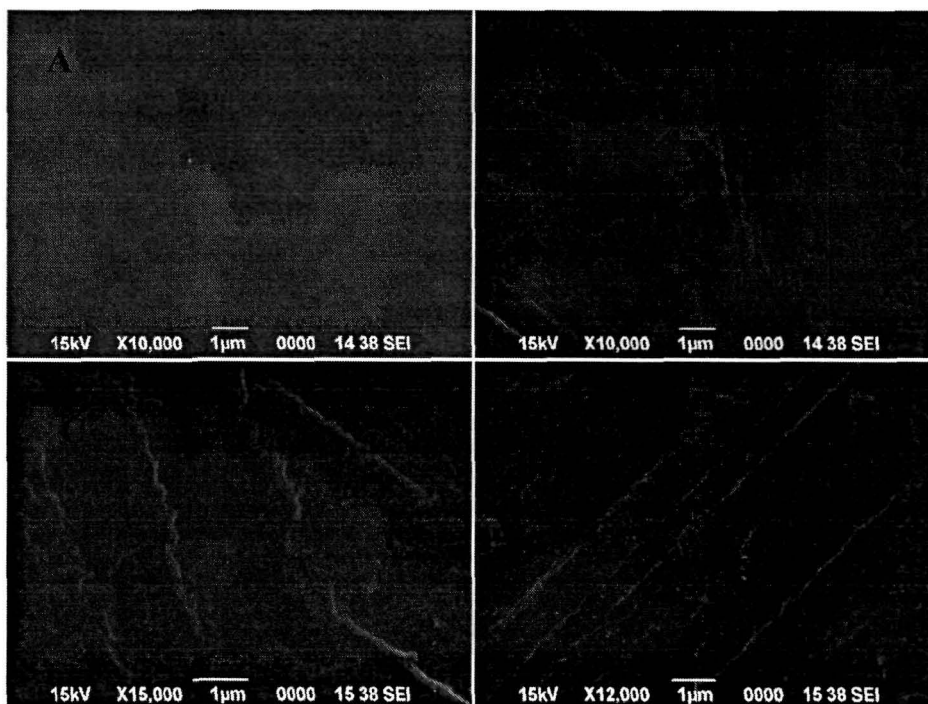
**Fig. 6.4:** XRD diffractograms for (a) HBPE, (b) PCNTC0.5, (c) PCNTC1, (d) PCNTC2 and (e) MWCNTs

#### 6.3.4.3. SEM Study

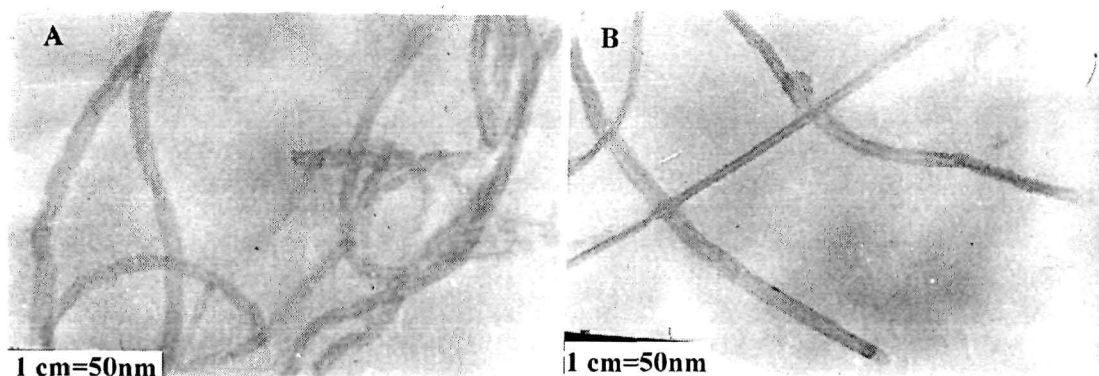
The surface morphology and distribution of the modified MWCNTs in the HBPE matrix can be visualised in the SEM micrographs (Fig. 6.5). For the nanocomposites with 0.5-2 wt.% MWCNTs, the individual MWCNTs are well dispersed throughout the polyester matrix. It is pertinent to mention that chemical functionalization of the MWCNTs assists good wetting by the matrix and enhanced interfacial adhesion between them through interactions of -OH/-COOH groups of MWCNTs with the ester groups of polyester by H-bonding or other polar-polar interactions (Scheme 6.1).

## 6.3.4.4. TEM Study

The representative TEM images of the nanocomposites are shown in Fig. 6.6. The TEM images of the nanocomposites were illustrative to the degree of intercalation, exfoliation and aggregation of the individual MWCNTs. The TEM micrographs showed the disintegration or exfoliation and homogeneous dispersion of the individual MWCNTs with average outer diameter in the range of 15-20 nm. The reason for this excellent distribution and exfoliation is again due to strong interactions between the polar carboxylic ester groups of the polymer and the -OH/-COOH groups of modified MWCNTs attached on the sidewalls (Scheme 6.1).



**Fig. 6.5:** SEM micrographs for A. HBPE, B. PCNTC0.5, C. PCNTC1 and D. PCNTC2



**Fig. 6.6:** TEM micrographs for A. PCNTC1 and B. PCNTC2

## 6.3.5. Performance Characteristics of the Nanocomposites

The different performance characteristics of HBPE/MWCNTs nanocomposites are shown in Table 6.1. The mechanical properties of a nanofiller-reinforced polymer mainly depend on the state of dispersion, distribution and orientation, high aspect ratio of the nanofillers, size and shape of domain and degree of compatibility. Good interfacial adhesion and high load transferring efficiency between the MWCNTs and polymer matrix are the key factors for improvements of mechanical properties of the nanocomposites. The tensile strength of HBPE/MWCNTs nanocomposites enhanced significantly from 2.68 to 27.78 N/mm<sup>2</sup> with the increase of MWCNTs loading from 0.5 to 2 wt.%. This is due to the nano-reinforcing effect of the MWCNTs with high aspect ratio. After functionalization of the MWCNTs the carboxylic acid groups are attached on the defect sites on sidewalls of MWCNTs. As illustrated in Scheme 6.1, possible interactions between the carboxylic acid groups of the modified MWCNTs and the ester groups in polyester macromolecular chains through hydrogen bonding result in enhance interfacial adhesion between them. This also leads to good dispersion of the nanotubes in the HBPE matrix. This improved dispersion of MWCNTs in the HBPE matrix was supported by the SEM and TEM images. This favors effective load transfer from the polymer matrix to the nanotubes that leads to substantial improvement in tensile strength of the nanocomposites.<sup>26</sup> Again, the elongation at break of the nanocomposites increased at 0.5 wt.% loading. However, the value decreased at high loading of MWCNTs. This may be attributed to the formation of more stiff nanocomposites by the MWCNTs and the generation of micro-voids around the nanotubes.<sup>27</sup> However, the value was still higher than pristine matrix system.

It was observed that the curing time (Table 6.1) of the nanocomposites decreased with the increase of MWCNTs loading from 0.5 to 2 wt.%. The interaction of the homogeneously dispersed MWCNTs in the matrix restricts the mobility of the polymer segments. The high aspect ratio of MWCNTs favors the H-bonding mediated crosslinking reaction between -OH or -COOH groups of MWCNTs and hydroxyl/carboxyl groups of polyester along with the epoxy group of the epoxy resin (curing agent) and amine groups of the poly(amido amine) hardener (Scheme 6.1).

Smoothness or surface texture influences the gloss of coated material. The gloss values of the nanocomposites (Table 6.1) improve with the increase in loading of MWCNTs, indicating the improved compatibility of the various components in the system. The crosslinking density increases as the amount of MWCNTs increases as

supported by swelling value (Table 6.1). The smoothed surface augments the gloss value of the nanocomposites with MWCNTs loading from 0.5-2 wt.%.

Scratch hardness represents the response of the material under serious dynamic surface deformation. A significant improvement in scratch hardness was observed in the nanocomposites reinforced with 0.5-2 wt.% MWCNTs (Table 6.1). The inclusion of MWCNTs with uniform dissemination enhances the crosslinking reaction resulting in an effective network formation. This prevents the indentation and enhances the scratch hardness.

Addition of MWCNTs with loadings from 0.5 to 2 wt.% significantly improves the impact resistance of the nanocomposites (Table 6.1). The nanofillers act as crack stoppers. The homogeneous dispersion of the MWCNTs and good crosslinking play vital role for this improvement in impact resistance.

**Table 6.1:** Performance characteristics of HBPE/MWCNTs nanocomposites

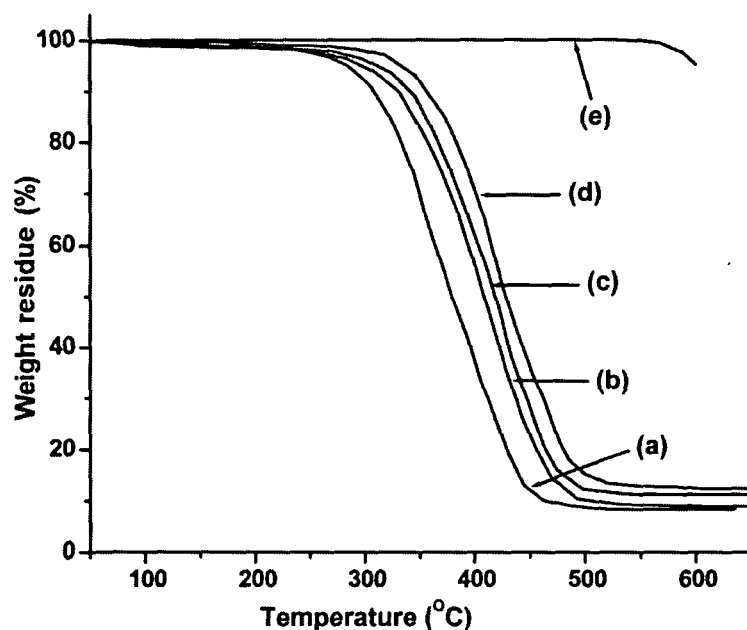
Property	HBPE	PCNTC0.5	PCNTC1	PCNTC2
Gloss at 60°	98	102	106	110
Scratch hardness (kg)	7	9	10	10
Impact resistance (cm)	80	85	95	100
Tensile strength (N/mm <sup>2</sup> )	2.68	13.84	16.24	27.78
Elongation at break (%)	24	129.26	92.16	65.95
Curing time (h at 120 °C)	3	2	1.75	1.5
Swelling in xylene (%)	32	30	28	27.6

### 6.3.6. Thermal Properties

The thermal degradation behavior of the nanocomposites can provide useful information to determine the optimum processing conditions and can identify the potential applications of the final products.<sup>28</sup> Thermal degradation behavior of the HBPE/MWCNTs was investigated by employing thermogravimetric analysis (TGA) under the nitrogen atmosphere. TGA thermograms of the nanocomposites are presented in Fig. 6.7. The pristine MWCNTs have no weight loss below 600 °C, as shown in Fig. 6.7(e). From the TGA thermographs of the nanocomposites it was observed that even very low amount of nanofiller contributed considerably to the increase in initial thermal degradation temperature ( $T_i$ ). The addition of 0.5 wt.% of MWCNTs into the HBPE matrix increases the  $T_i$  of the nanocomposites by 14 °C in comparison to the pristine HBPE. The  $T_i$  increases further with the increase of MWCNTs amount and



enhancement of 44 °C at 2 wt.% loading. The well-dispersed MWCNTs hinder the flux of degradation product and thereby delay the onset of degradation.<sup>3,29</sup> The presence of carboxylic groups on the nanotubes surface leads to the strong interfacial interactions between the polymer matrix and the nanotubes in the nanocomposites. Since thermal degradation of a polymer starts with chain cleavage and radical formation, the modified MWCNTs in the nanocomposite might act as radical scavengers to delay the onset of thermal degradation and hence improved the thermal stability of polyester. Another reason of this improved thermal stability is the high thermal conductivity of the nanotubes that facilitates heat dissipation within the nanocomposite.<sup>29</sup>



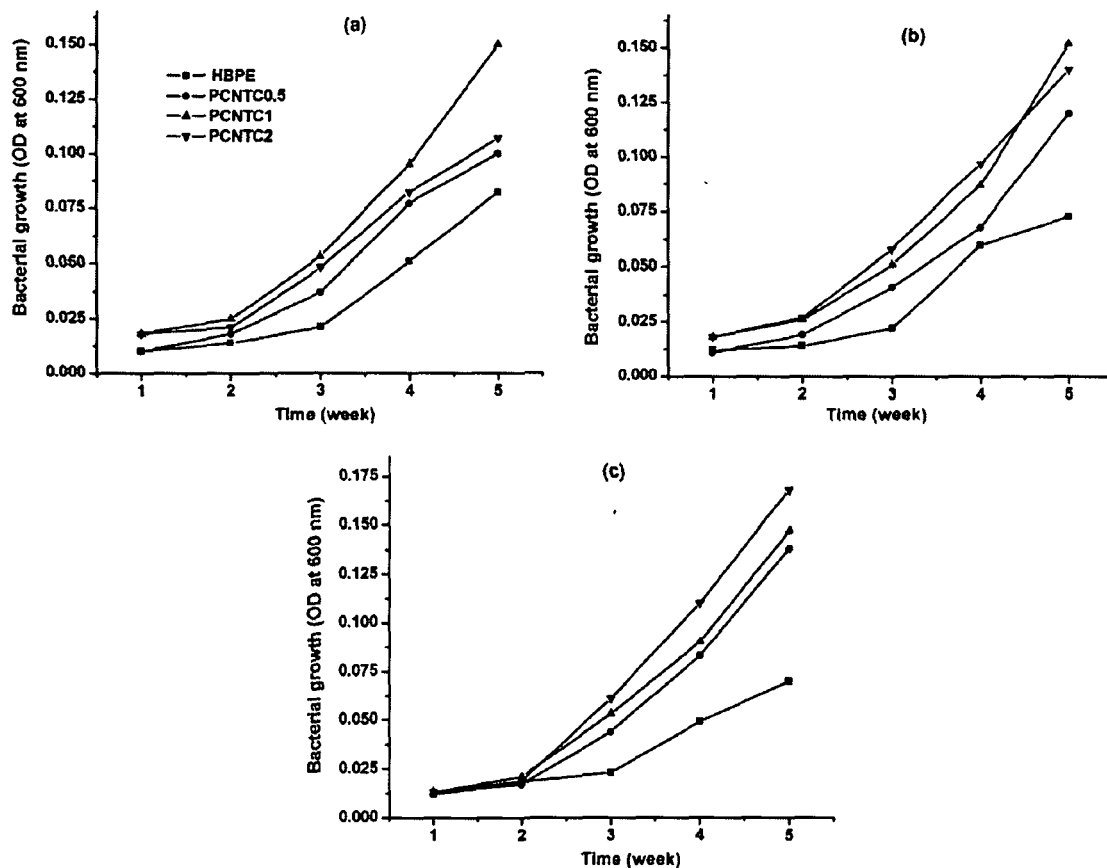
*Fig. 6.7: TGA thermograms for (a) HBPE, (b) PCNTC0.5, (c) PCNTC1, (d) PCNTC2 and (e) modified MWCNTs*

### 6.3.7. Biodegradation Study

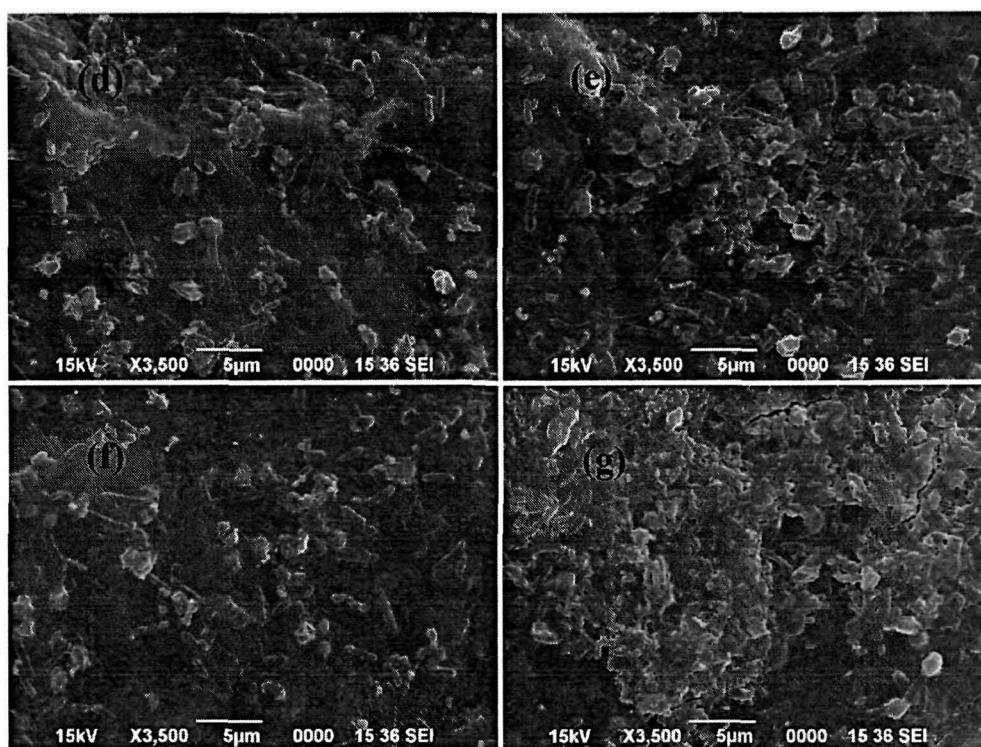
Biodegradation of the HBPE/MWCNTs nanocomposite films was assessed by their direct exposure to the microbial attack by different bacterial strains. McFarland turbidity method<sup>18</sup> was used to monitor the growth of the bacterial strains. The degradation of the nanocomposites as well as neat polyester was not so noticeable upto 2 weeks. However, the bacterial growth started to increase from the 3<sup>rd</sup> week onward [Fig. 6.8 (a), (b), (c)] implying a direct correlation of time with the gradual increase in the extent of biodegradation. The degradation of the nanocomposites was more than that of the pristine system which can be evaluated from the time-course dependent optical density of the culture media containing the nanocomposites. The degradation was found to increase with the increase of MWCNTs concentration which may due to

the formation of exfoliated structure. The growth of bacteria in the nanocomposites film was also observed in the SEM micrographs [Fig. 6.9 (d), (e), (f)].

Degradation of the nanocomposites occurs by the ester hydrolysis of the crosslinked polyester resin with generation of fragments and respective monomeric carboxylic acids and diols.<sup>30</sup> Similar to degradation of polymers by enzyme, the bacterial degradation takes place chiefly in two stages. In the first stage, polyester chains with high molecular weight are hydrolyzed to form oligomers. An acid, base, or moisture can accelerate the reaction. The micro-organisms then consume the low molecular weight oligomers in the last stage to produce CO<sub>2</sub>, H<sub>2</sub>O and humus.<sup>6</sup> The absorption of water by the polar ester groups of the matrix along with the -COOH/-OH groups of the MWCNTs is the rate determining step for biodegradation.



**Fig. 6.8:** Bacterial growth of *Pseudomonas aeruginosa* with strains (a) PN8A1 and (b) vs1, and *Bacillus subtilis* with strain (c) MTCC73 on nanocomposites



**Fig. 6.9:** SEM micrographs for (d) HBPE, (e) PCNTC0.5, (f) PCNTC1 and (g) PCNTC2 after biodegradation

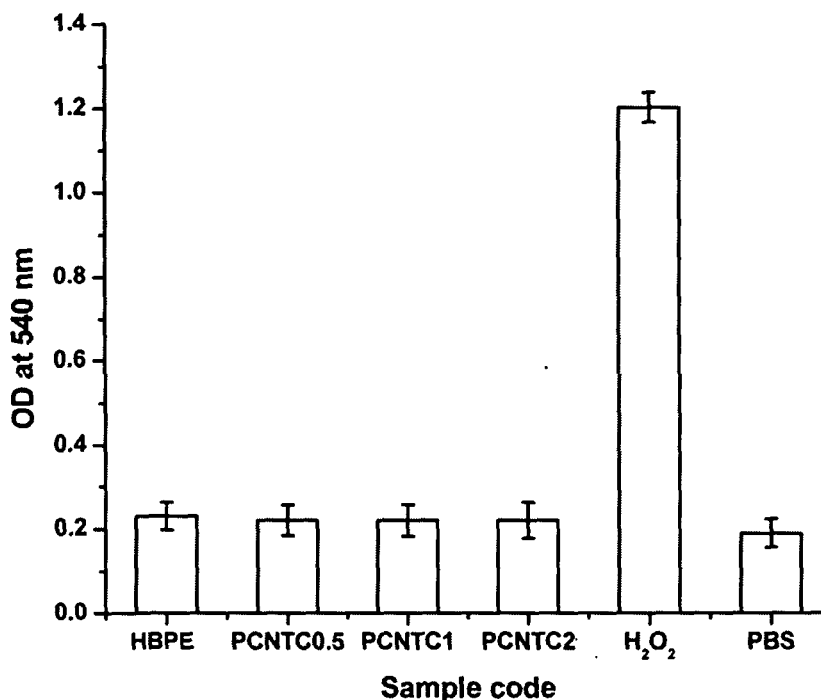
### 6.3.8. Cytotoxicity Study

Evaluating the events at the bio-nano interface is indispensable. Although CNTs are becoming increasingly studied new materials of emerging technology particularly for controlled drug delivery, there is paucity of information on their toxicological attributes. In parallel lines, establishing the biocompatibility of a biodegradable polymeric material under a specified environment is pre-requisite.

In the present report, the cytotoxicity of the HBPE/MWCNTs nanocomposites was studied by RBC hemolysis protection assay. Fig. 6.10 shows the non-cytotoxic nature of the nanocomposites films. The hemolytic activity of the nanocomposites was checked by measuring absorptions of the suspensions containing the RBC at 540 nm against 100  $\mu\text{M}$   $\text{H}_2\text{O}_2$  as the positive control and PBS as the negative control. The absorption value (OD at 540 nm) was found almost constant with MWCNTs loading from 0.5 to 2 wt.% in the HBPE matrix.

Hemolysis assay indicates the nature of particle/membrane interactions and which detects direct damaging interactions between particle surfaces and membranes, which can be driven by oxidative stress for some particles. By hemolysis assay we can also measure the direct membranolytic or membrane-perturbing action of any substance.<sup>30</sup> As hemolysis was found to be negligible in case HBPE/MWCNTs

nanocomposites, it may be concluded that the nanocomposites were almost non-toxic in nature.



*Fig. 6.10: Bar diagram showing cytotoxicity test results for the nanocomposites*

#### 6.4. Conclusions

Renewable resource based HBPE/MWCNTs nanocomposites were prepared by *ex-situ* technique with high shearing force and ultrasonication. The HBPE displayed suitable matrix properties for dispersion of the modified MWCNTs as evident from the XRD, SEM and TEM results of the nanocomposites. The mechanical and thermal properties of the nanocomposites unveiled that a small amount of MWCNTs loading can substantially reinforce the HBPE matrix. The incorporation of the modified MWCNTs improved the biodegradability of the nanocomposites to a great extent. Assessment of the toxicity at the cellular level revealed the cytocompatible attribute of the prepared nanocomposite material. Thus, the *Mesua ferrea* L. seed oil based HBPE/MWCNTs nanocomposites have a good prospect of serving as polymeric biomaterial for applications in the biomedical niche.

#### References

1. Kim, J.Y.; Kim, S.H. Influence of multiwall carbon nanotube on physical properties of poly(ethylene 2,6-naphthalate) nanocomposites. *J. Polym. Sci. Part B: Polym. Phys.* **44**, 1062-1071 (2006)

## Chapter 6

- Iijima, S. Helical microtubules of graphitic carbon. *Nature* **354**, 56-58 (1991)
- Koval'chuk, A.A. *et al.* Synthesis and properties of polypropylene/multiwall carbon nanotube composites. *Macromolecules* **41**, 3149-3156 (2008)
- Wang, S.F.; Shen, L.; Zhang, W.D.; Tong, Y.J. Preparation and mechanical properties of chitosan/carbon nanotubes composites. *Biomacromolecules* **6**, 3067-3072 (2005)
- Kim, J.Y.; Han, S.I.; Hong, S. Effect of modified carbon nanotube on the properties of aromatic polyester nanocomposites. *Polymer* **49**, 3335-3345 (2008)
- Maiti, P.; Batt, C.A.; Giannelis, E.P. New biodegradable polyhydroxybutyrate/layered silicate nanocomposites. *Biomacromolecules* **8**, 3393-3400 (2007)
- Ray, S.S.; Yamada, K.; Okamoto, M.; Ogami, A.; Ueda, K. New polylactide/layered silicate nanocomposites. 3. High-performance biodegradable materials. *Chem. Mater.* **15**, 1456-1465 (2003)
- Furth, M.E.; Atala, A.; Dyke, M.E.V. Smart biomaterials design for tissue engineering and regenerative medicine. *Biomaterials* **28**, 5068-5073 (2007)
- Shih, Y.F. Thermal degradation and kinetic analysis of biodegradable PBS/multiwalled carbon nanotube nanocomposites. *J. Polym. Sci. Part B: Polym. Phys.* **47**, 1231-1239 (2009)
- Lim, S.T.; Hyun, Y.H.; Choi, H.J. Synthetic biodegradable aliphatic polyester/montmorillonite nanocomposites. *Chem. Mater.* **14**, 1839-1844 (2002)
- Uyama, H.; Kuwabara, M.; Tsujimoto, T.; Kobayashi, S. Enzymatic synthesis and curing of biodegradable epoxide-containing polyesters from renewable resources. *Biomacromolecules* **4**, 211-215 (2003)
- Dutta, S.; Karak, N. Synthesis, characterization of poly(urethane amide) resins from Nahar seed oil for surface coating applications. *Prog. Org. Coat.* **53**, 147-152 (2005)
- Deka, H.; Karak, N.; Kalita, R.D.; Buragohain, A.K. Biocompatible hyperbranched polyurethane/multi-walled carbon nanotube composites as shape memory materials. *Carbon* **48**, 2013-2022 (2010)
- Deka, H.; Karak, N. Bio-based hyperbranched polyurethane/clay nanocomposites: adhesive, mechanical, and thermal properties. *Polym. Adv. Technol.* (doi:10.1002/pat.1603) (2010)

15. Das, G.; Karak, N. Epoxidized *Mesua ferrea* L. seed oil-based reactive diluent for BPA epoxy resin and their green nanocomposites. *Prog. Org. Coat.* **66**, 59-64 (2009)
16. Rana, S.; Karak, N.; Cho, J.W.; Kim, Y.H. Enhanced dispersion of carbon nanotubes in hyperbranched polyurethane and properties of nanocomposites. *Nanotechnology* **19**, 495707 (8pp) (2008)
17. Zhang, N.; Xie, J.; Varadan, V.K. Functionalization of carbon nanotubes by potassium permanganate assisted with phase transfer catalyst. *Smart Mater. Struct.* **11**, 962-965 (2002)
18. Dutta, S.; Karak, N.; Saikia, J.P.; Konwar, B.K. Biocompatible epoxy modified bio-based polyurethane nanocomposites: Mechanical property, cytotoxicity and biodegradation. *Bioresour. Technol.* **100**, 6391-6397 (2009)
19. Hassan, S.M. *et al.* Haemolytic and antimicrobial activities of saponin-rich extracts from guar meal. *Food Chem.* **119**, 600-605 (2010)
20. Lee, D.G.; Chang, V.S. Oxidation of hydrocarbons. 8. Use of dimethyl polyethylene glycol as phase transfer agent for the oxidation of alkenes by potassium permanganate. *J. Org. Chem.* **43**, 1532-1536 (1978)
21. Seyhan, A.T.; Tanoglu, M.; Schulte, K. Tensile mechanical behavior and fracture toughness of MWCNT and DWCNT modified vinyl-ester/polyester hybrid nanocomposites produced by 3-roll milling. *Mater. Sci. Eng. A* **523**, 85-92 (2009)
22. Seyhan, A.T.; Gojny, F.H.; Tanoglu, M.; Schulte, K. Critical aspects related to processing of carbon nanotube/unsaturated thermoset polyester nanocomposites. *Eur. Polym. J.* **43**, 374-379 (2007)
23. Grujicic, M.; Sun, Y.P.; Koudela, K.L. The effect of covalent functionalization of carbon nanotube reinforcements on the atomic-level mechanical properties of poly-vinyl-ester-epoxy. *Appl. Surf. Sci.* **253**, 3009-3021 (2007)
24. Ramanathan, T.; Fisher, F.T.; Ruoff, R.S.; Brinson, L.C. Amino-functionalized carbon nanotubes for binding to polymers and biological systems. *Chem. Mater.* **17**, 1290-1295 (2005)
25. Cho, J.W.; Kim, J.W.; Jung, Y.C.; Goo, N.S. Electroactive shape-memory polyurethane composites incorporating carbon nanotubes. *Macromol. Rapid Commun.* **26**, 412-416 (2005)

## Chapter 6

26. Kim, J.Y.; Kim, D.K.; Kim, S.H. Effect of modified carbon nanotube on physical properties of thermotropic liquid crystal polyester nanocomposites. *Eur. Polym. J.* **45**, 316-324 (2009)
27. Kim, J.Y.; Han, S.I.; Hong, S. Effect of modified carbon nanotube on the properties of aromatic polyester nanocomposites. *Polymer* **49**, 3335-3345 (2008)
28. Kim, H.S.; Chae, Y.S.; Kwon, H.I.; Yoon, J.S. Thermal degradation behavior of multi-walled carbon nanotube-reinforced poly(L-lactide) nanocomposites. *Polym. Int.* **58**, 826-831 (2009)
29. Moniruzzaman, M.; Winey, K.I. Polymer nanocomposites containing carbon nanotubes *Macromolecules* **39**, 5194-5205 (2006)
30. Lu, S. et al. Efficacy of simple short-term in vitro assays for predicting the potential of metal oxide nanoparticles to cause pulmonary inflammation. *Environ. Health Perspect.* **117**, 241-247 (2009)

## CHAPTER 7

---

### HBPE Modified Epoxy Based Industrial Paint

---

#### 7.1. Introduction

Paint is a compounded liquid, liquefiable, or mastic composition which after application on a desired surface of substrates in a thin layer is converted to a continuous opaque solid film.<sup>1</sup> This is chiefly utilized for the protection of objects from devastation caused by exterior assault and for embellishment purpose. The basic constituents of paints are binder, solvent, additive and pigment. Among these constituents the binder is the key component of the paint. The binder commonly referred to as the vehicle, is the actual film forming component of paint which comprises synthetic or natural resins such as acrylics, polyurethanes, polyesters, melamine resins, epoxies, or vegetable oils and natural fats. It is the only component that must be present; other components are included optionally, depending on the desired properties of the cured film.<sup>2</sup> The binder imparts adhesion, binds the pigments and other additives together, and strongly influences the basic assets of paints such as gloss, drying, hardness, exterior durability, flexibility, toughness, abrasion resistance, impact resistance, chemical resistance, adhesion etc. The behavior of the binders in paints was tested by looking at the transparency, the blocking resistance, the hardness development, drying time and gloss of the paint. The various kinds of additives used in modern paints are dispersing agents, wetting agents, viscosity controlling agents, anti-settling agents, anti-skinning agents, antioxidants, antifoaming agents, adhesion promoters, desiccants, driers, biocides, light stabilizers etc. The pigment is a fine powder, whose functions are to provide required aesthetic appearance i.e. color and hiding to the paint, protect the paint from ultra-violet (UV) light and corrosion, and increase the elasticity, hardness and abrasion resistance. The efficacy of a pigment depends on its particle size distribution and the dispersion in the binder system.<sup>3</sup> The solvent is used to facilitate the ease of processing and wetting of pigment by reducing the viscosity of the binder which helps in application, and flow level. The solvent system may either be a single or a mixture of solvents which should be sufficiently volatile so that no trace of it should remain after finishing of the paint.<sup>3</sup> With the ever-increasing necessity to prevent the environment from low level atmospheric pollution and the enforcement of the strict legislature and legal procedures,

---

This work is communicated.



the use of volatile organic compounds (VOC) in paint systems is under constant pressure.<sup>4,5</sup> These factors have been driving the coating industry to look for and accelerate research work for developing eco-friendly coating formulations. So, the development of products processed with reduced amounts of organic solvents, or even without solvents, is a great challenge.<sup>3</sup> Epoxy resins are viscous, tacky materials which are difficult to handle. This is minimized by dissolving them in organic solvents, which evaporate into the atmosphere as VOC, and that is against the regulations for such applications. This is a most important problem with epoxy resins as binders for paint along with its brittleness character.

Nowadays, intensive research is being conducted on the development of new binders, which is driven by the need for performance improvements as well as for sustainable development. In this regards different researchers have tried to reduce VOC in the paints through the use of acrylic dispersion, alkyd emulsion or high solid alkyd resin.<sup>4,6</sup> The use of reactive diluent is an alternative for increasing the solid contents of conventional paints in addition to reduce VOC.<sup>7</sup> The high solids commercial paints have been available for long times on the decorative market that meet the requirements for reduced VOC emissions.<sup>8</sup> Among the different existing binder systems, vegetable oil modified polyester resins are the most extensively used binders for different paints including automotive finishing, sewing machines, fans, equipment machines finishes etc.<sup>9</sup> In Chapter 2 the satisfactory performance characteristics of *Mesua ferrea* L. seed oil based HBPE as a surface coating material is already explained. Several other reports are also found on the development of vegetable oil based highly branched polyester resin with desired performance characteristics including flexibility.<sup>10-12</sup> Coatings made from these resins have advantages in terms of drying time and their properties fulfill the service demands for decorative paints. In addition to the above, large numbers of functionality, unique structural architecture, low viscosity and high reactivity of highly branched such polyesters assist in processing and wetting of pigments and other additives and thereby improve performance of the prepared paints. The aforementioned HBPE was therefore used as reactive diluent for the commercial epoxy resin in the formulations of a commercial epoxy based industrial paint.

Thus, the current chapter deals with the potentiality of *Mesua ferrea* L. seed oil based HBPE as reactive diluent for a commercial epoxy resin to formulate an easily processable low VOC high solid epoxy paint. The prospective of the HBPE in

combination with the commercial epoxy resin as binder material was also investigated. The various physical properties and performance characteristics of the resulting test paint were compared with an industrially used standard commercial epoxy paint used for protective coating applications.

### **7.2. Experimental**

#### **7.2.1. Materials**

The required chemicals and solvents such as *Mesua ferrea* L. seed oil, glycerol, PA, MA, bis-MPA, lead mono oxide, DMF, xylene etc. were of same specifications as described in Chapter 2, section 2.2.1. Commercially available epoxy paint used for protective coating application was used as the standard paint. All other materials related to paint formulations such as titanium dioxide (TiO<sub>2</sub>), n-butanol, barytes, silica, epoxy resin [70% non-volatile content (NVC) in xylene], poly(amido amine), urea-formaldehyde (UF) resin (60% NVC in n-butanol) were of commercial grade and obtained from Shalimar Paints India Ltd., Kolkata, India.

#### **7.2.2. Instruments and Methods**

The particle size of the crushed particles was checked by using Hegman Gauge (Sheen Instrument Ltd., UK) during the preparation of paint. The SEM and TGA analyses of both the test and the standard paints were carried out using the same instruments and conditions as mentioned in Chapter 3, section 3.2.2. The coating performance characteristics like gloss, impact resistance and scratch hardness of both the test and standard paints were measured using the same instruments according to the standard methods as mentioned earlier (Chapter 2, section 2.2.2.). The rheological behavior of both the paints was studied by using the same instrument and method with similar conditions as described in Chapter 2, section 2.2.2.

*Mesua ferrea* L. seed oil was extracted and purified by the same method as described in Chapter 2, section 2.2.1. The physical properties such as acid value, hydroxy value, viscosity, specific gravity and non-volatile matter content of both the test and standard paints were determined by using the standard IS methods.<sup>13-17</sup> The salt spray test, protection against corrosion and UV exposure test for both the paints coated on mild steel panels were performed by using the standard IS methods.<sup>18-20</sup>

### 7.2.2.1. Preparation of HBPE

The HBPE was prepared by the same method as described in Chapter 2, section 2.2.2.1.

### 7.2.2.2. Preparation of Paints

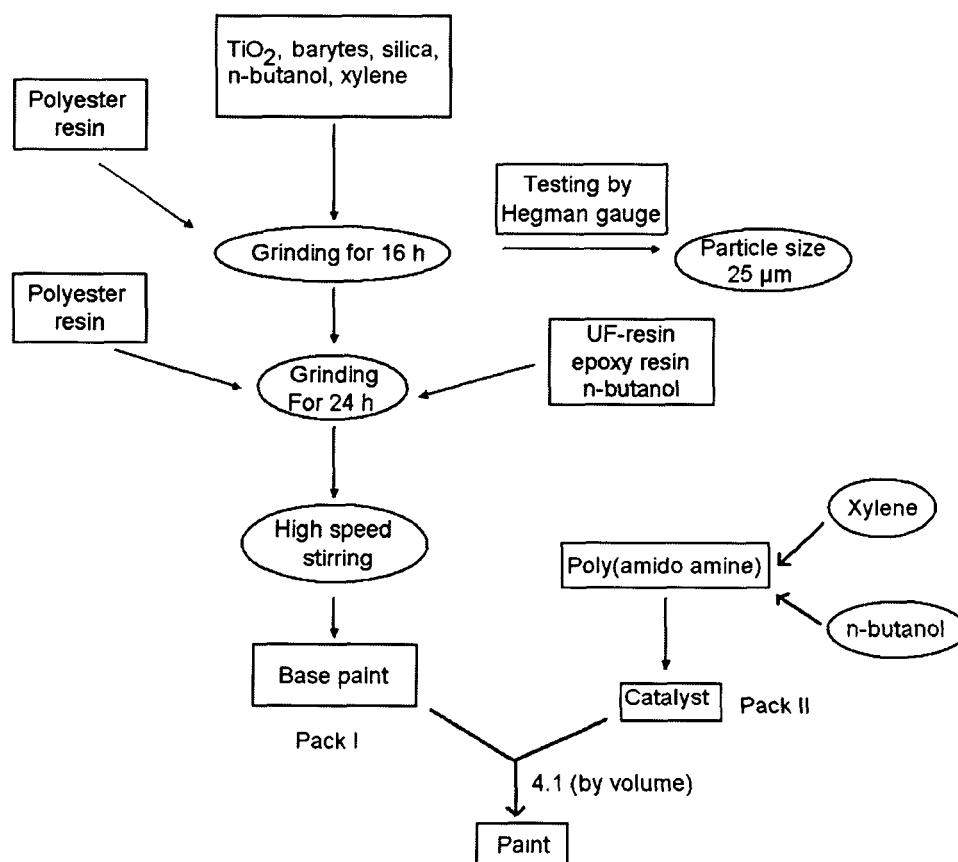
The flow sheet diagram for the manufacturing process of the paint is shown in Scheme 7.1. The prepared polyester modified epoxy resin based paint was two-pack paint system, one pack was epoxy resin containing paint usually called base and the other pack was poly(amido amine) called as catalyst. The base paint (Pack I) formulation recipe is given in Table 7.1. The base paint was prepared in porcelain ball mill using HBPE as binder in the grinding stage. At first, the ingredients like pigment  $\text{TiO}_2$ , extenders, HBPE and around 20% of solvent were charged in the ball mill. The grinding of the pigments and extenders was done for around 16 h to make the particle size of about 25  $\mu\text{m}$ , as measured by Hegman gauge. After attaining the required grinding size, the materials were dropped into different containers and mixed with epoxy resin and finally adjusted with the remaining solvents and other additives to achieve required amount of viscosity of paint (30-40 s in Ford cup, FC4 at 30 °C). Finally, the prepared paint was kept for 24 h for wetting. The standard paint has the same formulation with 100% epoxy binder without HBPE.

**Table 7.1: Formulations for the test paint**

Ingredients	Amount (wt.%)	Function
<b>(a) Pack I</b>		
$\text{TiO}_2$	10	Pigment
Barytes	12	Filler
Silica	15	Filler
Test HBPE	25	Binder/reactive diluent
Xylene	14	Solvent
n-butanol	7	Co-solvent
UF resin (60% NVC in n-butanol)	1	Flow promoter
Epoxy resin (70% NVC in xylene)	16	Binder
<b>(b) Pack II</b>		
Poly(amido amine)	40	Curing agent
Xylene	52	Solvent
n-butanol	8	Co-solvent

## 7.2.2.3. Preparation of Test Panels

The base paint and the catalyst or curing agent (Pack II of Table 7.1) were mixed in the ratio of 4:1 by volume before application of paint on mild steel panels. The prepared paint mixture was diluted to 46% solid content by adding xylene. The paint solution was then sprayed with the help of specific gravity type spray gun from a distance of 15-20 inch on the mild steel plates (150 mm × 100 mm × 1.25 mm) placed on spray booth. The prepared panels were then kept in open air for complete drying. The thin films of both the paints were also prepared by drawing a homogeneous mixture of the components on glass plates by the similar method as described in Chapter 2, section 2.2.2. After removal of sufficient amount of solvent under atmospheric conditions, the coated strips were degassed under vacuum at (45±5) °C for 45 min to remove the last trace of solvent and volatile compounds. Then the coated plates were cured at room temperature for specified time period. The cured paint films were kept under ambient conditions for 24 h before further studies. The dried films from the glass plates were peeled off by immersing the plates in warm water followed by drying in a dessicator



**Scheme 7.1:** Flow sheet diagram for the manufacturing process of the paint

under vacuum and were stored for 7 days before taking SEM micrographs. The thickness of the dried coating films was measured by using the same instrument and method as mentioned in Chapter 2, section 2.2.2. and found in the range of 30-35  $\mu\text{m}$ .

### **7.3. Results and Discussion**

#### **7.3.1. Paint Preparation**

The *Mesua ferrea* L. seed oil based HBPE possesses the optimal performances as a surface coating material which is already discussed in Chapter 2. The low viscosity and large surface functionality of HBPE helped in processing and wetting of pigment that results improvement of flow level, gloss and wetting of the substrate. So, this resin was utilized as the reactive diluent for the epoxy paint to reduce the VOC emissions and to prepare a high solid paint. Along with the reactive diluent, this HBPE modified commercial epoxy resin was used as binder for the production of the high solid low VOC epoxy paint.

The pigment particles exist largely in the form of clusters or aggregates<sup>21</sup> in dry condition. So, these clusters should be broken for proper dispersion of individual pigment particles in the paint medium. The pigment was pulverized and dispersed in the vehicle (binder) along with all other additives to obtain a fine dispersion of the pigment particles in the medium.<sup>22</sup> The pulverization process was continued until the degree of dispersion became acceptable for the paint as determined by the Hegman gauge (average particle size of 25  $\mu\text{m}$ ). Stable dispersion of the dispersed particles was obtained through wetting of the dispersed phase in the binder medium. At last, high-speed stirring was executed to descent the dispersion with additional vehicle to get the final paint composition with optimum level of performance characteristics.<sup>23</sup>

#### **7.3.2. Physical Properties**

The different physical properties like viscosity, specific gravity, non-volatile content, acid value and hydroxyl value of the test HBPE resin as well as for the paints are given in Table 7.2.

The viscosity of the test resin was low which is due to the highly branched globular structure as described in Chapter 2. The viscosity of the test paint was found to lower than the analogous standard paint. This low value of viscosity helps in the processing, storage, and film formation of the paint. The acid value of the test HBPE

resin was also low. The specific gravities of both the paints were comparable. The test paint has slightly higher non-volatile content as compared to the standard paint. From these results it can be anticipated that the test paint has the requisite physical properties to be used as an industrial paint.

**Table 7.2:** Physical parameters of the HBPE and paints (standard and test)

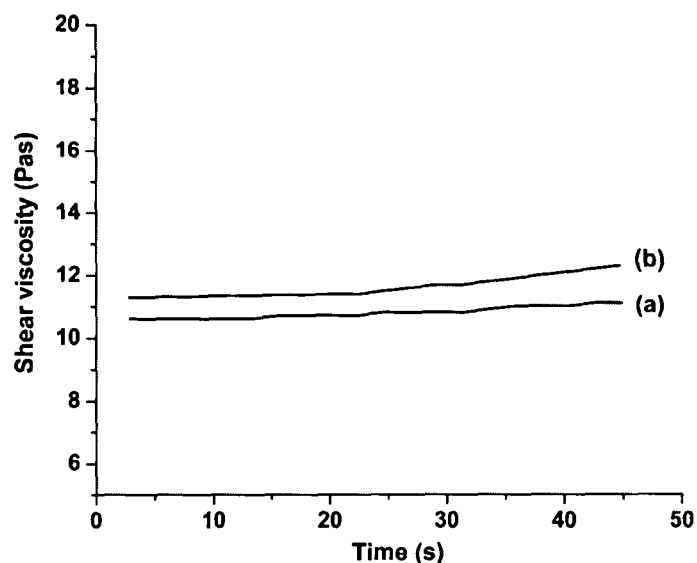
Parameters	HBPE	Paint	
		Standard	Test
NVC (wt.%)	61.20	68.70	72.76
Specific gravity <sup>a</sup>	1.01	1.41	1.42
Viscosity (30 °C, min) <sup>b</sup>	2.5	40	30
Acid value (mg KOH/g, base paint)	10.66	3.23	11.31
Hydroxyl value (mg KOH/g, base paint)	102.3	172.6	186.6

<sup>a</sup> Unit less, relative to standard medium, <sup>b</sup> Measured by Ford cup method

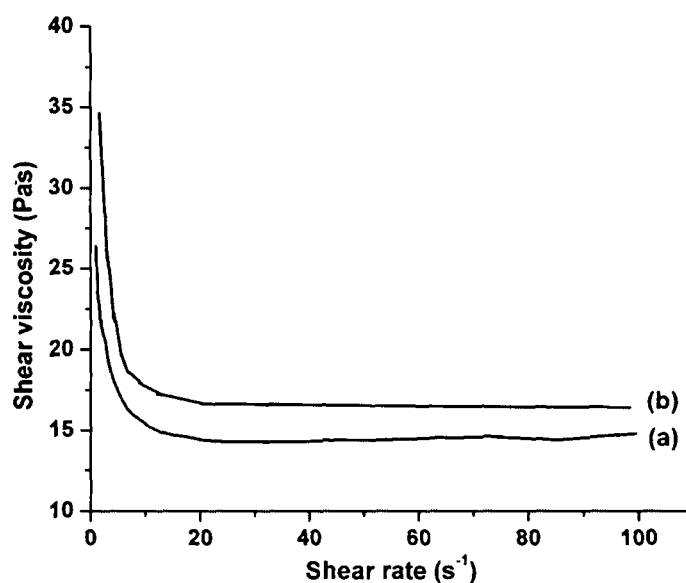
### 7.3.3. Rheological Behaviors

The viscosity is the most important rheological property for paint. To achieve good application characteristics and improve the manufacturing process, paints have to be non-Newtonian liquids, which are highly shear dependent.<sup>24</sup> The variation of viscosity with time at controlled stress and single shear value is shown in Fig. 7.1, where viscosity remained almost constant with time for both the paints. However an overall viscosity of the test paint was found to be lower compared to the standard paint. This is due to the highly branched globular structure of the binder of the test paint (Chapter 2).

Fig. 7.2 shows the shear viscosity as a function of shear rate for both the paints. Viscosity at high shear rates must be controlled in a narrow range to give sufficient film buildup and coverage without extreme brush or roller drag, or too high pressure in spray painting.<sup>25</sup> The low shear rate viscosity must be high enough to prevent in-can settling and sagging after painting. As a result, shear-thinning behavior is needed. The shear viscosity of both the paint systems decreased with the increase of shear rate showing shear thinning behavior. At low shear rates, the shear viscosity data exhibited a strong pseudoplastic behavior for both the paints.



*Fig. 7.1: Variation of shear viscosity against time at constant stress and temperature for (a) test and (b) standard paints*

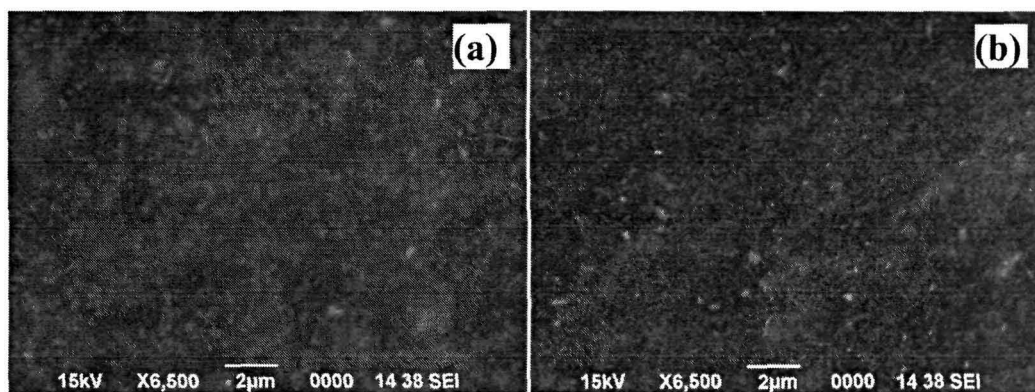


*Fig. 7.2: Variation of shear viscosity against shear rate at constant temperature for (a) test and (b) standard paints*

#### 7.3.4. Morphological Study

The SEM micrographs of the test and standard paints are shown in Fig. 7.3. The uniform distribution of the dispersed phases was observed in the SEM micrograph of the test paint which is comparable to the standard paint (Fig. 7.3). The nature and composition of the binder system, evaporation rate of solvent and viscosity influences the morphology of the paint.<sup>26</sup> The domain sizes of dispersed phases in the test paint were smaller than the standard paint which is due to the better compatibility of the

components with the HBPE. This is due to the confined geometry and low viscosity of the HBPE. Furthermore, the high mechanical stress during ball milling had broken the dispersed phase into smaller particles in the matrix. So, all the ingredients are homogeneously disintegrated in both the paint systems that are observed from the SEM micrographs (Fig. 7.3).



*Fig. 7.3: SEM micrographs for (a) test and (b) standard paints*

### **7.3.5. Performance Characteristics**

The different performance characteristics of both the paints are given in Table 7.3. The test paint showed comparable gloss value with the industrially used standard epoxy paint for protective coating application. This gloss of the paints is due to smooth surface of the paint films which comes from good dimensional stability by the formation of dense network structure<sup>27</sup> as supported by swelling value (Table 7.3). Also the resin HBPE itself possesses high gloss. Although the touch dry and handleable dry times of the test paint were higher compared to the relevant standard epoxy paint, still they meet the requirements for protective coating applications and hence could be a focus for the customers. These comparable drying times are mainly due to the high surface functionality of the HBPE that takes part in the crosslinking reaction with the epoxy resin. The possible reaction occurs between the hydroxyl/ester group of HBPE and hydroxyl/epoxide group of epoxy resin via H-bonding or other polar-polar interactions (Scheme 7.2). Self life is the competence of the paint to remain stable without phase separation that is occurring in the stored container for a particular duration and can be used without any detrimental effect to its application properties or ultimate performance. The test paint as well as the standard paint possessed a pot life of 8 h without loss of homogeneity, which indicates their excellent storage availability. This is due to their low tendency towards skinning and appropriate viscosity of the



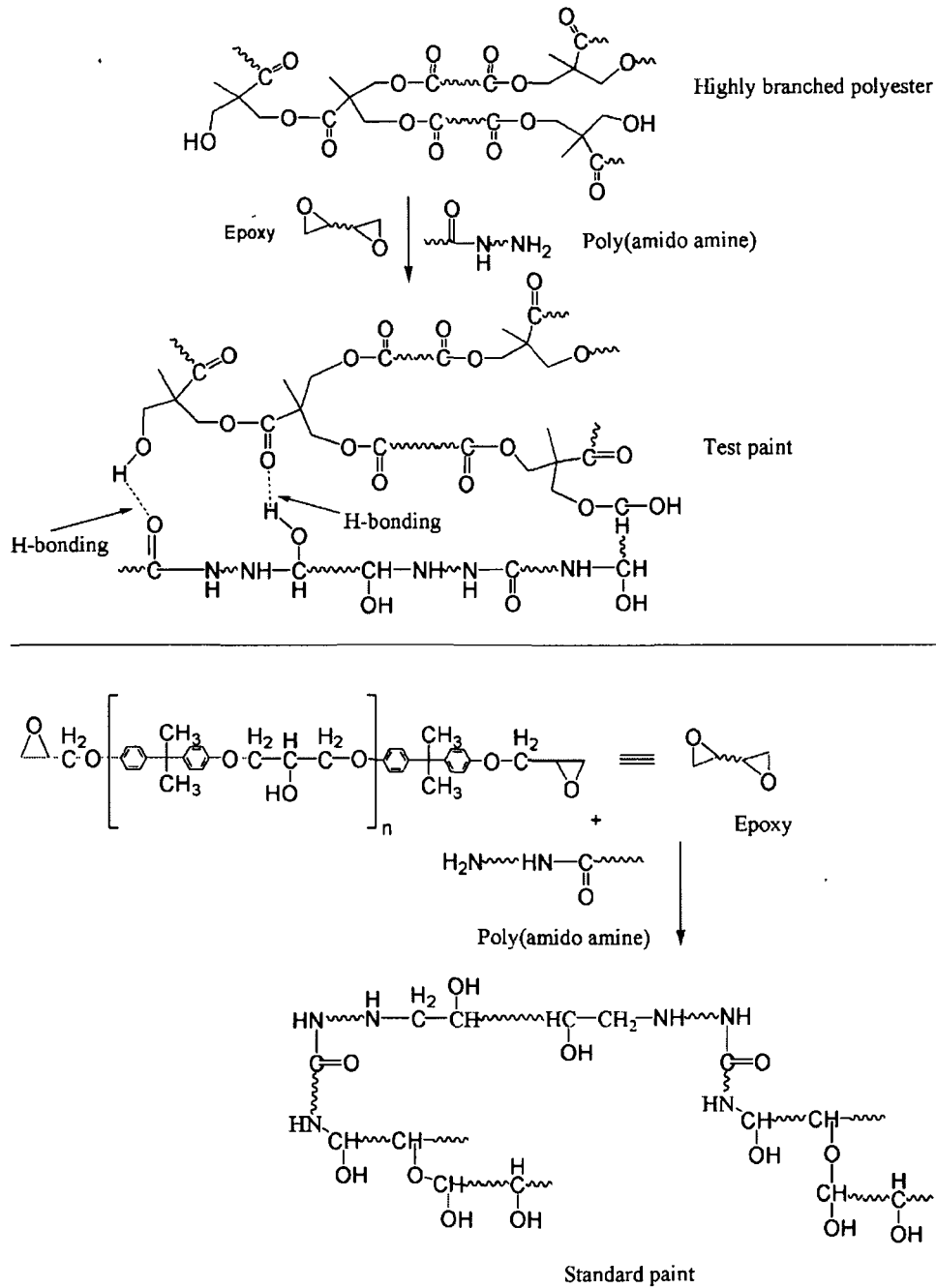
binder systems. The scratch hardness value of the test paint was also comparable to the standard paint which fulfill service requirement for paint applications. The impact resistance of the test paint was quite satisfactory which may be due to good mechanical strength obtained from optimum crosslinking density and good flexibility<sup>28</sup> of the hydrocarbon chains of the fatty acids of the oil.

The protection against corrosion for both the paints was assessed by exposing them to various chemical environments for a specified time of exposure. Both the test and the standard paints were resistant to corrosion upto 25 days. The corrosion resistance test is important as it reflects the actual field performance of the paints. Initial damage of the paint was indicated by color fading. It is mainly due to the attack of moisture through oxidation or rust formation on the metal surface. To evaluate the resistance of the paint samples to corrosive chemicals environment the salt spray test was performed. In this test, the samples were kept in the environment of corrosive chemicals such as moisture, NaCl etc. Both the test and standard paints were found to possess excellent salt spray resistance of greater than 15 days. Such good chemical resistance of the paints is due to the low penetration rate of the corrosive chemicals through the paint films.<sup>9</sup> The strong three-dimensional networks and the presence of rigid aromatic moieties in the networks prevent the chemicals to pass through the paint films. The stability of both the paints towards harmful UV rays was checked by exposing them under UV rays for 544 h. According to IS 8662:2004, the durability of any painted panel under UV exposure of 250 h can withstand 1 year under normal environmental condition. So UV exposure of 544 h is sufficient time for durability study. Both the paints showed good resistance towards the UV rays for this specified period of time. However it was found that after the exposure to UV rays the gloss of the paint films was reduced and percent gloss reduction of the test paint was comparable to the standard paint. Generally, gloss retention of epoxy based paint under UV exposure is not very good and that is why epoxy based paint is not used for top coat application. This reduction of gloss after exposure may be due to the degradation of epoxy resin by the exposure of UV light.

Although most of the properties of the test paint were comparable to the standard industrial paint, yet there are added advantages of the *Mesua ferrea* L seed oil based HBPE due to its low viscosity, high solubility and highly branch globular structure with freely expose groups, which helps in the processing, storage, application

## Chapter 7

and film formation of paints. Also it acts as a reactive diluent for the epoxy resin, reduces the VOC emissions and forms high solid epoxy paint.



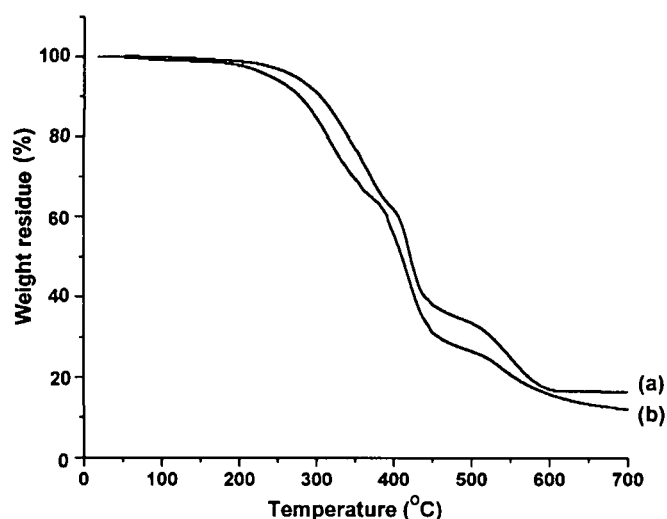
**Scheme 7.2:** Possible curing reaction mechanisms of the paints

**Table 7.3: Performance characteristics of test and standard paints**

Properties	Standard paint	Test paint
Protection against corrosion (after 25 days)	Pass	Pass
UV exposure (after 544 h)	Pass	Pass
Salt spray (after 15 days)	Pass	Pass
Initial gloss (60°)	55.6	60.4
Percent gloss reduction exposure (544 h)	84	86
Pot life (8 h)	Pass	Pass
Scratch hardness (kg)	1.2	1.3
Impact resistance (100 cm)	Pass	Pass
Touch dry (h, at room temperature)	3	4
Handleable dry (h, at room temperature)	8	10
Swelling (% in xylene, after 7 days)	29	23

### 7.3.6. Thermal Study

TGA curves for the test and standard paints are shown in Fig. 7.4. From the figure two-step degradation patterns were observed and found that the test as well as standard paints were thermally stable upto 240 °C. However, the overall thermal decomposition temperature of the test paint was found to be higher than the standard paint. This higher



**Fig. 7.4: TGA thermograms for (a) test and (b) standard paints**

thermostability of the test paint is due to the presence of various thermostable units present in the renewable natural oil based binder system. Also, from the figure it can be seen that 50% decomposition of both the paints was occurred at 410-421 °C. Again the

weight residue for the test paint was found to be comparable to the standard paint (weight residue 8.2% and 6.2% for test and standard paints respectively at 700 °C).

### 7.4. Conclusions

From this chapter it is concluded that the *Mesua ferrea* L. seed oil based HBPE modified epoxy resin was successfully utilized as a binder for the preparation of an industrial paint. The various physical properties, performance characteristics of the test paint are found to be comparable to that of the standard industrial epoxy paint. *Mesua ferrea* L. seed oil may be used potentially as an alternative raw material since it is renewable and easily available at a very low cost. Moreover, the low viscosity of *Mesua ferrea* L. seed oil based HBPE acts as a reactive diluent of epoxy resin and results to high solid content of the paint and low VOC emission which can serve as a remedial step to maintain clean environment, an important aspects of eco-friendly coating. Due to excellent resistance towards salt spray, corrosion, UV-light of the test paint it would gain many perspectives as high performance industrial paint in the automotive and wood industries.

### References

1. Karak, N. *Fundamentals of Polymers: Raw Materials to Finish Products* (PHI Learning Pvt. Ltd., New Delhi, 2009)
2. Dutta, N. *Development of Polyester Resins from Mesua ferrea L. Seed Oil* (PhD Thesis, Tezpur University, India, 2006)
3. Dutta, S. *Development of Mesua ferrea L. Seed Oil Based Polyurethane Resins* (PhD Thesis, Tezpur University, India, 2009)
4. Geurts, J.; Bouman, J.; Overbeek, A. New waterborne acrylic binders for zero VOC paints. *J. Coat. Technol. Res.* **5**, 57-63 (2008)
5. Sastry, N.V.; Thakor, R.R. Synthesis and evaluation of functional polymeric additives with urethane linkage as dispersing agents for preparation of pigment concentrates with high solid loading, low-VOC content, and usefulness for industrial coatings. *J. Coat. Technol. Res.* **6**, 11-25 (2009)
6. Heiskanen, N.; Jämsä, S.; Paaanen, L.; Koskimies, S. Synthesis and performance of alkyd-acrylic hybrid binders. *Prog. Org. Coat.* **67**, 329-338 (2010)

7. Biermann, U.; Butte, W.; Holtgreffe, R.; Feder, W.; Metzger, J.O. Esters of calendula oil and tung oil as reactive diluents for alkyd resins. *Eur. J. Lipid Sci. Technol.* **112**, 103-109 (2010)
8. Zabel, K.H. *et al.* Design and incorporation of reactive diluents for air-drying high solids alkyd paints. *Prog. Org. Coat.* **35**, 255-264 (1999)
9. Dutta, N.; Karak, N.; Dolui, S.K. Stoving paint from *Mesua ferrea* L. seed oil based short oil polyester and MF resins blend. *Prog. Org. Coat.* **58**, 40-45 (2007)
10. Johansson, M. *et al.* Design of coating resins by changing the macromolecular architecture: solid and liquid coating systems. *Prog. Org. Coat.* **48**, 194-200 (2003)
11. Bat, E.; Gündüz, G.; Kısakürek, D.; Akhmedov, İ.M. Synthesis and characterization of hyperbranched and air drying fatty acid based resins. *Prog. Org. Coat.* **55**, 330-336 (2006)
12. Manczyk, K.; Szewczyk, P. Highly branched high solids alkyd resins. *Prog. Org. Coat.* **44**, 99-109 (2002)
13. IS 548 : Indian Standard Methods of Sampling and Test for Oils and Fats, 548 (Part I), p. 29, 1964.
14. IS 101: Indian Standard Methods of Sampling and Test for Paints, Varnishes and Related Products, vol. 101 (Part 1/Sec. 5), p. 1. 1989.
15. IS 101: Indian Standard Methods of Sampling and Test for Paints, Varnishes and Related Products, vol. 101 (Part 1/Sec. 7), p. 1.1987.
16. IS 101: Indian Standard Methods of Sampling and Test for Paints, Varnishes and Related Products, vol. 101 (Part 2/Sec. 2), p. 1.(1986).
17. IS 101: Indian Standard, Methods of Sampling and Test for Paints, Varnishes and Related Products, vol. 101 (Part 5/Sec. 3), p. 1, 1988.
18. IS 101: Indian Standard Methods of Sampling and Test for Paints, Varnishes and Related Products, vol. 101 (Part 6/Sec. 1), p. 2, 1988.
19. IS 101: Indian Standard Methods of Sampling and Test for Paints, Varnishes and Related Products, vol. 101 (Part 6/Sec. 3), p. 1, 1990.
20. IS 101: Indian Standard Methods of Sampling and Test for Paints, Varnishes and Related Products, vol. 101 (Part 6/Sec. 5), p. 1, 1997.
21. Veselý, D.; Kalendová, A.; Němec, P. Properties of organic coatings depending on chemical composition and structure of pigment particles. *Surf. Coat. Technol.* **204**, 2032-2037 (2010)

## Chapter 7

22. Sreeram, K.J. *et al.* Use of mixed rare earth oxides as environmentally benign pigments. *Dyes Pigm.* **76**, 243-248 (2008)
23. Morgan, W.M. *Outlines of Paint Technology* (Charles Griffin and Company Ltd., London, 1969)
24. Iribarren, J.I.; Armelin, E.; Liesa, F.; Casanovas, J.; Aleman, C. On the use of conducting polymers to improve the resistance against corrosion of paints based on polyurethane resins. *Mater. Corros.* **57**, 683-688 (2006)
26. Dutta, S.; Karak, N.; Jana, T. Evaluation of *Mesua ferrea* L. seed oil modified polyurethane paints. *Prog. Org. Coat.* **65**, 131-135 (2009)
25. Armelin, E. *at al.* A simple model to describe the thixotropic behavior of paints. *Prog. Org. Coat.* **57**, 229-235 (2006)
27. Odian, G. *Principles of Polymerization*, 3<sup>rd</sup> edn. (John Wiley and Sons Inc., New York, 1991)
28. Stoye, D. (Ed.) *Resins for Coatings* (Hanser, New York, 1996)

## CHAPTER 8

---

### Conclusions and Future Directions

---

#### 8.1. Summary and Conclusions

The thesis highlights the synthesis, characterization, properties evaluation and application of *Mesua ferrea* L. seed oil based highly branched polyesters, modified HBPEs and their various nanocomposites with different types of nanofillers. The first chapter of the thesis describes a general introduction and a brief review on the vegetable oil based polyester nanocomposites giving emphasis on the importance, general techniques of preparation, characterization, properties and applications. The scopes, objectives and plans of work for the present investigation are also focused in this chapter. The entire technical work of the present investigation is divided into six parts in six consecutive chapters.

In the first part, i.e. in second chapter, the synthesis, characterization and properties evaluation of *Mesua ferrea* L. seed oil based three highly branched polyesters using polyfunctional carboxyl or polyol compounds like trimellitic anhydride (TMA), 2,2-bis(hydroxymethyl) propionic acid (bis-MPA) and hyperbranched polyol along with other conventional anhydrides were described. The linear analog of the highly branched polyester was also synthesized without using tri/multifunctional compounds for comparison purpose and reported in this chapter.

In the second part, enhancement of various performance characteristics of the bis-MPA based highly branched polyester resin (HBPE) was reported through the modification by different methods such as blending with vegetable oil based epoxy, neutralization with triethylamine to form water dispersible polyester and grafting with methyl methacrylate. The characterizations and properties evaluations of these modified HBPEs are also discussed in this part, i.e. in chapter three.

The third part of the technical work deals with the preparation, characterization and performance characteristics of nanocomposites reinforced with organically modified montmorillonite (OMMT) and unmodified bentonite using the bis-MPA and hyperbranched polyol based highly branched polyester resins, and all the modified HBPEs as matrices through an *ex-situ* technique. The rheological characterization also provides some insights about the dispersion state of the nanofillers in the matrices. Further the bis-MPA based HBPE and acrylate modified HBPE nanocomposites

showed biodegradation behavior as tested by laboratory broth culture technique. All the above reports are described in chapter four.

The preparation, characterization, properties evaluation and applications of silver nanoparticles based nanocomposites using the aforementioned HBPE as the matrix with silver were reported in the fourth part of the technical work, i.e. in chapter five. The results showed that the silver based nanocomposites exhibited the high potential as an antimicrobial surface coating materials.

The fifth part of the technical work, i.e. chapter six described the preparation, characterization and properties of the HBPE/MWCNTs nanocomposites as biodegradable non-cytotoxic biomaterials. Along with the mechanical and thermal properties, rheological characteristics, biodegradability, cytotoxicity etc. were also studied in details to evaluate the suitability of the nanocomposites for the possible advanced applications.

The final part of the technical work is on utilization of the *Mesua ferrea* L. seed oil modified bis-MPA based HBPE as binder materials for the preparation of an industrial paints. The results, which showed the suitability of the tested binder system in the industrial paint by comparing with the standard system, are described in chapter seven.

The summary and conclusions along with the future directions of the whole thesis are described in the last chapter that is the present chapter of the thesis.

Thus, from the present investigation the following conclusions are drawn.

- (i) A highly potential non-edible vegetable oil, *Mesua ferrea* L. seed oil was successfully utilized for the first time to prepare highly branched polyesters. The linear analogue of the HBPE was also prepared for comparison purpose.
- (ii) The synthesized highly branched polyesters were characterized by the conventional analytical and spectroscopic techniques. The various properties such as physical, mechanical and thermal confirmed the suitability of this polymer as matrix for nanocomposite preparation.
- (iii) The modification of the HBPE by different methods such as blending with vegetable oil based epoxy, neutralization with triethylamine to form water reducible polyester and grafting with methyl methacrylate significantly



improved the properties especially mechanical properties, thermal stability and chemical resistance.

- (iv) The nanocomposites of highly branched polyester resins, the modified HBPE resins and nanoclay (OMMT and bentonite) were successfully prepared by *ex-situ* techniques. The prepared nanocomposites exhibited noticeable improvements in performance characteristics
- (v) The HBPE/clay nanocomposite system is good template for the preparation of silver nanoparticles. The well dispersed and highly stable silver nanoparticles based nanocomposites showed better performance properties than the pristine system. The silver nanocomposites also exhibited adequate antimicrobial activity.
- (vi) The HBPE/MWCNT nanocomposites showed excellent improvements in the properties like mechanical, thermal and rheological. They also showed higher biodegradation and improved cytocompatibility nature compared to the pristine HBPE.
- (vii) The different nanocomposites have the high potential to be used as advanced surface coating materials, highly thermo-stable materials, antimicrobial surface coating materials and biodegradable biomaterials.
- (viii) The HBPE showed high potentiality to be used as a binder for an industrial paint.

Thus in a nut shell, the prime achievement of the present investigation is the successful exploitation of a less significant renewable raw material to scientifically important products with great impact.

## 8.2. Future Directions

Although a systematic and comprehensive study was made in the present investigation but still there are a few future scopes of *Mesua ferrea* L. seed oil based polyester nanocomposites to be worth mentioned for further studies.

- (i) The comprehensive study with theoretical modeling on the reinforcement action of the nanofillers could be carried out to deduce the exact mechanism of the nanofillers.

- (ii) *Mesua ferrea* L. seed oil based HBPE nanocomposites could be evaluated by *in-vitro* and *in-vivo* tests for different biomedical applications.
- (iii) To develop flame retardant HBPE and its nanocomposites using different types of nanofillers.

### List of Publications

#### In Journals

1. **Konwar, U.;** Karak, N. *Mesua ferrea* L. Seed Oil Based Highly Branched Polyester Resins. *Polym. Plast. Technol. Eng.* **48**, 970-975 (2009)
2. **Konwar, U.;** Karak, N.; Mandal, M. *Mesua ferrea* L. Seed Oil Based Highly Thermostable and Biodegradable Polyester/Clay Nanocomposites. *Polym. Degrad. Stab.* **94**, 2221-2230 (2009)
3. **Konwar, U.;** Karak, N.; Mandal, M. Vegetable Oil Based Highly Branched Polyester/Clay Silver Nanocomposites as Antimicrobial Surface Coating Materials. *Prog. Org. Coat.* **68**, 265-273 (2010)
4. **Konwar, U.;** Karak, N. *Mesua ferrea* L. Seed Oil Based Highly Branched Environment Friendly Polyester Resin/Clay Nanocomposites. *J. Polym. Environ.* (DOI 10.1007/s10924-010-0242-8, **Online, 2010**)
5. **Konwar, U.;** Das, G.; Karak, N. *Mesua ferrea* L. Seed Oil Based Highly Branched Polyester and Epoxy Blends and Their Nanocomposites. *J. Appl. Polym. Sci.* (DOI: 10.1002/app.33743, **Online, 2010**)
6. **Konwar, U.;** Karak, N.; Hyperbranched Polyether Core Containing Vegetable Oil Modified Polyester and Its Clay Nanocomposites. *Polym. J.* (DOI: PJ.2011.19, **Online, 2011**)
7. **Konwar, U.;** Karak, N. Epoxy Modified *Mesua ferrea* L. Seed Oil Based Polyester/Clay Nanocomposites. *Int. J. Polym. Mater.* (**Accepted**)
8. **Konwar, U.;** Karak, N.; Jana, T. Vegetable Oil-based Highly Branched Polyester Modified Epoxy Based Low VOC High Solid Industrial Paint. (**Communicated**)
9. **Konwar, U.;** Karak, N.; Mandal, M. Structural, Mechanical, Biodegradable and Biocompatible Characteristics of *Mesua ferrea* L. Seed Oil Based Highly Branched Polyester/Functionalized MWCNT Nanocomposites. (**Communicated**)

10. **Konwar, U.;** Karak, N.; Mandal, M. Acrylate-Modified *Mesua ferrea* L. Seed Oil Based Highly Branched Polyester Resin/Clay Nanocomposites (**Communicated**)

**In Book**

1. **Konwar, U.;** Karak, N. *Developments in Nanocomposites*, edited by Kar K. K.; Hodzic, A. ISBN: 978-981-08-3711-2, (Research Publishing Services, Innovative Partners for Publishing Solutions, Singapore, 2011) (**Accepted**)

**Conference Presentations (Published as Proceeding)**

1. **Konwar, U.;** Karak, N. “*Mesua ferrea* L. seed oil based waterborne polyester resin/clay nanocomposites for coating applications” National Seminar On Emerging Trends In Polymer Science and Technology (POLY-2009), Saurashtra University, Rajkot, Gujarat, October **2009**.
2. **Konwar, U.;** Karak, N. “Fluorescence characteristic of renewable oil based polyester/clay silver nanocomposites” National Seminar on Photonics and Quantum Structures (NSPQS 2009) Tezpur University, Assam, November **2009**.
3. Karak, N.; Mahapatra, S.S.; Dutta, S.; Deka, H.; **Konwar, U.;** Das, G.; Konwar, R. “Polymer nanocomposites-multifaceted advanced materials for today’s society” National Seminar on Photonics and Quantum Structures (NSPQS 2009) Tezpur University, Assam, November **2009**.
4. **Konwar, U.;** Karak, N. “Hyperbranched polyether modified vegetable oil based polyester/clay nanocomposites” National Conference on Smart Nanostructures (NCSN 2011) Tezpur University, Assam, January **2011**.